Identification and Characterisation of proteins interacting with the melanoma associated adaptor protein RaLP/ShcD

Thesis submitted for the degree of

Doctor of Philosophy

at the University of Leicester

by

Dal-Hee Chung MSc

Department of Biochemistry

University of Leicester

2013

Statement

The thesis entitled *"Identification and Characterisation of proteins interacting with the melanoma associated adaptor protein RaLP/ShcD"* is submitted for the degree of Doctor of Philosophy. Unless otherwise acknowledged by references or in the text, the thesis based on the experimental work has been fulfilled by the author in the Department of Biochemistry at the University of Leicester between Janunary 2009 and December 2012. The work has not been submitted for any other degree at this or any other university.

Signed:

Date:

Department of Biochemistry

Henry Wellcome Building

Lancaster Road

Leicester

LE1 9HN

Identification and Characterisation of proteins interacting with the melanoma associated adaptor protein RaLP/ShcD

Abstract

Dal-Hee Chung

Cell signalling by Receptor Tyrosine Kinases (RTKs) is widely known to regulate several cellular processes. Activated RTKs can associate with many cellular transducer proteins containing PTB (phosphotyrosine-binding) domains and/or SH2 (Src homology 2) domains. The Shc (Src Homology and Collagen) family of adaptor proteins contain both of these critical domains and bind to many growth factor receptors. Four Shc family members have been identified including Shc/ShcA, Sli/ShcB, Rai/ShcC, and the latest member, RaLP/ShcD. Although all the family members share a similar domain modularity, their tissue expression and biological roles are different. As the most recently identified Shc protein, RaLP/ShcD remains poorly characterised. RaLP/ShcD has been shown to have a migratory role in melanoma cells in humans, to interact with Muscle-Specific Kinase (MuSK) receptor in mice, and to regulate cell differentiation during stem cell development. In order to further understand its role in these or other processes, this study aimed to identify novel interacting partners of RaLP/ShcD. The SH2 domain of RaLP/ShcD was shown to interact with another signalling scaffold protein, Gab1, through phosphorylated tyrosine 183, as revealed by GST pull-down and co-immunoprecipitation experiments. Notably, a Gab1Y183F mutant was unable to recruit RaLP/ShcD to the cell membrane in ruffles upon growth factor stimulation. By screening a yeast two-hybrid library, Peg3/Pw1 and HP1α were isolated as novel binding partners for the collagen homology domain 1 (CH1 domain) of RaLP/ShcD. The ability of RaLP/ShcD to interact with both Peg3/Pw1 and HP1α was confirmed by GST pull-down and co-immunoprecipitation assays using transfected human cell lines. Interestingly, a small portion of RaLP/ShcD co-localised with Peg3/Pw1 in the nucleus. Finally, using an affinity column comprising purified CH1 domain coupled to sepharose beads, vimentin was purified from melanoma cell extracts.

Acknowledgements

"Go ye therefore, and teach all nations, baptizing them in the name of the Father, and of the Son, and of the Holy Ghost:

Teaching them to observe all things whatsoever I have commanded you: and, lo, I am with you alway, even unto the end of the world. Amen."

(Matthew 28:19-20)

Firstly, I am sincerely grateful to my supervisor Dr. Sally Prigent. Without her guidance, encouragement and the numerous informative discussions, it would have been much more difficult me to ahieve this point.

I would like to take this opportunity to thank the lab 2/38 who has helped me during my Ph.D. I feel fortunate to have had such friendly lab people including Juhwan, Eva, Samrein, and Naif and am also grateful to the lab 2/42 for great help. I will always remember the enjoyable and great experience in the lab 2/38. Also, thank to my committees Dr. Raj Patel, Dr. Martin Dickens, and Dr. Peter Moody who offered me great discussions during my Ph.D.

Finally, I would like to thank my wife and family members, pastors and remnants for their prayer and encouragement and endless love and support. I am sure I would not have reached this point without them. I am honestly grateful to them.

Contents

Statement II

Abstract III

Acknowledgements IV

Contents V

Figures and Tables XII

Abbreviations XVII

CHAPTER 1:INTRODUCTION 1

1.1. Overview 2

1.2. The Src Homology and Collagen (Shc) family 3

1.2.1. Domain Structure of Shc Family members 6

1.2.1.1. The Src Homology 2 (SH2) domain of Shc 6

1.2.1.2. The Phosphotyrosine-Binding (PTB) domain of Shc 7

1.2.1.3. The Collagen Homology 1 (CH1) domain of Shc 9

1.2.1.4. The Collagen Homology 2 (CH2) domain of Shc 11

1.2.2. Biological function of the Shc family members in tumour Progression 11

1.3. Critical signalling pathways in melanoma progression to metastasis 12

1.3.1. Shc and the mitogen activated protein kinase (MAPK) cascade 12

1.3.2. Association of Shc with the survival pathway (PI3K/AKT) 13

1.3.3. Integrin Pathway and Shc proteins 17

1.4. Shc and Pro-apoptotic Function 18

1.5. The newest member of Shc family of RaLP/ShcD or Shc4 22

1.5.1. Discovery of RaLP (Rai-like protein)/ShcD/Shc4 22

1.5.2. The significance of the CH1 domain 24

1.5.3. The Biological function of RaLP/ShcD 26

1.5.4. RaLP/ShcD and Migration Role in Melanomas 28

1.5.5. RaLP/ShcD associates with Muscle-Specific Kinase Receptor (MuSK) 30

1.5.6. RaLP/ShcD is involved in cell differentiation during embryonic stem cell development 31

1.6. Grb2-associated binder 1 (Gab1) protein 33

1.6.1. The PH (Plecstrin-Homolgy) domain of Gab1 35

1.6.2. The PRD (Proline-Rich) domain of Gab1 36

1.6.3. Functional Roles of Gab1 38

1.6.3.1. Gab1 and migration in melanoma 38

1.6.4. Gab1-mediated Signalling Pathways by the RTKs in melanoma 38

1.6.4.1. c-Met receptor signalling pathway 38

1.6.4.2. EGF receptor signalling pathway 41

1.7. General understanding of Melanoma 43

1.8. Aims and Objectives of this Project 45

CHAPTER 2: MATERIALS AND METHODS 47

2.1. Materials 48

2.2. Composition of standard Solutions 48

2.2.1. Western Blot Analysis 48

2.2.2. Immunoprecipitation 49

2.2.3. Bacterial Cloning and Transformation 49

2.2.4. Agarose Gel Electrophoresis 50

2.2.5. GST-pull down assay 50

2.2.6. SDS-PAGE Gel Staining 51

2.2.7. Yeast Two-Hybrid screen 51

2.2.8. Plasmid Minipreparations by Alkaline Lysis/LiCl Method 52

2.2.9. Preparation of SDS-PAGE Gels 53

2.2.10. Primary and Secondary Antibodies 54

2.2.10.1. Primary antibodies 54

2.2.10.2. Secondary antibodies 55

2.2.11. Materials for Yeast-Two Hybrid (Y2H) Screen 55

2.2.11.1. Materials for Y2H screen 55
2.3. Methods 57
2.3.1. Molecular Biology Methods 57
2.3.1.1. Preparation of competent *E.coli* BL21(DE3) and DH5α cells 57
2.3.1.2. Preparation of HB101 (Leu-) electrocompetent cells 57
2.3.1.3. Bacterial Cell transformation 58
2.3.1.4. Mini Plasmid DNA purification using QIAGEN spin columns 58
2.3.1.5. Plasmid DNA purification using QIAGEN Plasmid Maxi kit 59
2.3.1.6. Plasmid Minipreparations by Alkaline Lysis/LiCl Method 60
2.3.1.7. Measurement of DNA concentration 61
2.3.1.8. DNA separation by Agarose gel electrophoresis 61
2.3.2. Site-Directed Mutagenesis 62
2.4. Cell culture 63
2.4.1. Cell lines 63
2.4.2. Maintenance of Cell lines 64
2.4.3. Cell culture 64
2.4.4. Freezing of Cell lines 64
2.4.5. Transfection of Cells 65
2.4.6. Cell line Stimulation 65
2.4.6.1. EGF or PDGF stimulation 65
2.4.6.2. Camptothecin (CPT) treatment 65
2.4.6.3. Cisplatin (CIS) treatment 66
2.4.6.4. Leptomycin B (LMB) treatment 66
2.5. SDS-PAGE and Western blotting 66
2.5.1. SDS-PAGE 66
2.5.2. Western blot Analysis 67
2.5.3. Stripping of Nitrocellulose Transfer Membranes 68
2.6. GST (Glutathione S-transferase) pull-down experiment 68
2.6.1. GST-fusion protein preparation 68

2.7. Expression and Purification of the CH1 domain of RaLP/ShcD 69

2.7.1. Further purification by Gel filtration chromatography 70

2.8. Preparation of beads for Immunoprecipitation (IP) Assays 71

2.9. Preparation cell lysates for IP or GST-pull downs 71

2.10. Immunofloresence Microscopy 72

2.10.1. Preparation of Coverslips and Immunofluorecence Staining 72

2.10.2. Localisation study using Confocal Microscopy technique 73

2.10.3. BCA Protein Assay 73

2.10.4. Metal binding study 74

2.10.5. Purification and identification of proteins interacting with the RaLP/ShcD-CH1 domain 74

2.10.5.1. Coupling of CH1 domain protein to NHS-activated sepharose beads 74

2.10.5.2. Coupling of $NiCl_2$ to Chelating sepharose beads 75

2.10.5.3. Purification of Proteins binding to the CH1 domain for analysis by Mass Spectrometry 75

2.10.5.4. Matrix-Assisted Laser Desorption/Ionisation Time-Of-Flight Mass Spectrometry (MALDI-ToF MS) 76

2.11. Yeast-Two Hybrid Screen 76

2.11.1. Constructs for Yeast two-hybrid screen 76

2.11.2. Small-Scale Test Transformation 76

2.11.3. Test HIS3 Transcriptional Activation using 3-AT 78

2.11.4. Large-Scale Library Transformation 78

2.11.5. β-Galactosidase Filter Assay 80

2.11.6. Library Plasmid Recovery from Positive Colony 80

2.11.7. Electroporation of HB101 (Leu-) electrocompetent cells 81

2.11.8. Quantitative assay for β-Galactosidase with ONPG substrate 82

2.12. *Renilla* Luciferase Assay 83

2.13. siRNA knock down experiments 83

CHAPTER 3: INVESTIGATION OF THE INTERACTION BETWEEN RaLP/ShcD AND Gab1 IN MELANOMA CELL LINES

..... 85

3.1. Introduction 86

3.2. Results 88

3.2.1. Association of RaLP/ShcD and Gab1 88

3.2.1.1. Demonstration of interaction between the SH2 domain of RaLP/ShcD and Gab1 88

3.2.1.2. Determination of Gab1 expression in Melanoma cell lines 90

3.2.1.3. Expression of Receptor Tyrosine Kinases in Melanoma cell lines 92

3.2.1.4. Co-immunoprecipitation of RaLP/ShcD and wild-type Gab1 from 518 melanoma cells 92

3.2.1.5. Determination of Subcellular Localisation of RaLP/ShcD and Gab1 in transfected Melanoma cells 98

3.2.2. Identification of the phosphorylation site on Gab1 responsible for the interaction with RaLP/ShcD 100

3.2.2.1. Demonstration of interaction between the SH2 domain of RaLP/ShcD and two Gab1 tyrosine mutants 100

3.2.2.2. Co-immunoprecipitation of RaLP/ShcD and Y183F mutant expressed in 518 melanoma cells 103

3.2.2.3. Determination of the Subcellular localisation of RaLP/ShcD and Gab1Y183F mutant in 518 melanoma cells 105

3.2.2.4. Determination of Gab1 knock-down by siRNA 107

3.3. Discussion 110

3.3.1. RaLP/ShcD can directly associate with Gab1 110

3.3.2. Pak4 is a novel potential linker for the association between RaLP/ShcD and Gab1? 113

3.3.3. Future Investigations 115

CHAPTER 4: IDENTIFICATION AND CHARACTERISATION OF PROTEINS INTERACTING WITH THE CH1 DOMAIN OF RaLP/ShcD BY USING A YEAST TWO-HYBRID SYSTEM 116

4.1. Introduction 117

4.2. Results 119

4.2.1. A Yeast two Hybrid screen of mouse embryo library with CH1 domain of RaLP/ShcD as bait 119

4.2.1.1. Small-Scale Test transformation 119

4.2.1.2. Suppression of background HIS3 Transcriptional Activation using 3-amino triazole (3-AT) 121

4.2.1.3. Large-Scale Library Transformation 123

4.2.1.4. Isolation and characterisation of library plasmids from positive yeast clones 125

4.2.1.5. BLAST analysis of Clones illustrates novel binding partners for the CH1 domain of RaLP/ShcD 125

4.2.1.6. Confirmation that isolated library plasmids encode proteins that interact specifically with RaLP/ShcD 129

4.2.1.7. Quantitative Analysis of β-Galactosidase activity 129

4.2.2. The investigation of RaLP/ShcD and Peg3/Pw1 interaction 132

4.2.2.1. Precipitation of Peg3/Pw1 and Znic Finger domains using GST-RaLP/ShcD-CH1 fusion protein in HEK293 cells 132

4.2.2.2. Co-immunoprecipitation of RaLP/ShcD and Peg3/Pw1 expressed in HEK293 cells 135

4.2.2.3. Effect of Peg3/Pw1 and Camptothecin on RaLP/ShcD protein in HEK293 cells stably expressing FLAG-RaLP/ShcD (F4) or GFP-RaLP/ShcD (G5) 137

4.2.2.4. Renilla Luciferase Assay 141

4.2.2.5. Determination of endogenous levels of RaLP/ShcD in B16-F10 Melanoma cells and the effect of Peg3/Pw1 transfection 141

4.2.2.6. Determination of Subcellular localisation of RaLP/ShcD and Peg3/Pw1 in HEK293 cells 144

4.2.3. Investigation of RaLP/ShcD and HP1α interaction 151

4.2.3.1. Precipitation of HP1α using GST-RaLP/ShcD-CH1 fusion protein in HEK293 cells 151

4.2.3.2. Co-immunoprecipitaion of RaLP/ShcD and HP1α expressed in HEK293 cells 153

4.2.3.3. Determination of Subcellular localisation of RaLP/ShcD and HP1α in 518 melanoma cells 153

4.3. Discussion 157

4.3.1. A nuclear role for RaLP/ShcD 157

4.3.2. Peg3/PW1 as a novel binding partner of RaLP/ShcD 158

4.3.3. HP1α (heterochromatin protein 1) is a novel binding partner for RaLP/ShcD 163

CHAPTER 5: CHARACTERISATION OF THE CH1 DOMAIN OF RaLP/ShcD 167

5.1. Introduction 168

5.2. Results 170

5.2.1. Expression and Purification of GST-RaLP/ShcD-CH1domain 170

5.2.2. Purification of GST-RaLP/ShcD CH1 domain 172

5.2.3. Further Purification by Gel-filtration chromatography 174

5.2.4. Investigation of the CH1 domain of RaLP/ShcD as a metal binding domain 176

5.2.5. Further investigation of the CH1 domain as a Metal binding domain using Cobalt ions 178

5.2.6. Affinity purification of proteins interacting with the CH1 domain of RaLP/ShcD and identification by Mass Spectrometry 180

5.2.7. Determination of Subcellular localisation of RaLP/ShcD and Vimentin 182

5.3. Discussion 185

5.3.1. The interaction between RaLP/ShcD and Vimentin which may have migratory functions 185

5.3.2. Is the CH1 domain of RaLP/ShcD a Metal-binding or Zinc finger-like domain? 187

CHAPTER 6: DISCUSSION 189

6.1. Discussion 190

REFERENCES 195

APPENDIX 214

Figures and Tables

List of Figures

CHAPTER 1

Figure 1.1. Domain structure of members of the Shc family in mammals..... 5

Figure 1.2. The role of ShcA in coupling RTK activation to the MAPK pathway..... 14

Figure 1.3. Schematic representation of Shc protein mediated activation of the PI3K/PTEN/mTOR signalling pathway 15

Figure 1.4. Schematic representation of domain structures of three isoforms of ShcA protein 19

Figure 1.5. The schematic illustrations of the pro-apoptotic function of p66ShcA 21

Figure 1.6. Amino acids sequence alignment of the members of the Shc protein family 25

Figure 1.7. Proposed function of RaLP/ShcD in the major signalling cascades which are deregulated in human melanoma 27

Figure 1.8. Schematic illustration of the domain structure of mammalian Gab1 protein 34

Figure 1.9. A schematic model of the signalling molecules recruited to activate the Met-mediated signalling pathway..... 39

Figure 1.10. Schematic illustration of the EGFR-mediated signalling pathways involving Shc and Gab1 42

CHAPTER 2

Figure 2.1. Vector maps of transformed bait plasmid including LexA DNA binding domain and PDGFR tyrosine kinase (A) and VP16 library plasmid encoding DNA activation domain (B) 56

CHAPTER 3

Figure 3.1. β-galactosidase filer assay to demonstrate interaction between RaLP/ShcD SH2 domain and wild-type Gab1 89

Figure 3.2. Precipitation of Gab1 from melanoma cell lines using GST-RaLP/ShcD-SH2 fusion protein 91

Figure 3.3. Expression of receptor tyrosine kinases (EGF receptor, PDGF receptor β, and Met receptor) in melanoma cell lines 93

Figure 3.4. GFP-RaLP/ShcD can co-immunoprecipitate with GFP-Gab1 in 518 melanoma cells 95

Figure 3.5. mCherry-RaLP/ShcD can co-immunoprecipitate with GFP-Gab1 in 518 melanoma cells 97

Figure 3.6. Determination of subcellular localisation of mCherry-RaLP/ShcD and GFP-Gab1 in 518 melanoma cells 99

Figure 3.7. Schematic diagram indicating the domain structure of mammalian Gab1.. 101

Figure 3.8. Y2H β-galactosidase filer assay to demonstrate interation between the SH2 domain of RaLP/ShcD and Y162F and Y183F mutant of Gab1 102

Figure 3.9. mCherry-RaLP/ShcD can only co-precipitate with wild-type GFP-Gab1 in 518 melanoma cells 104

Figure 3.10. Determination of subcellular localisation of mCherry-RaLP/ShcD and GFP-Gab1Y183F in 518 melanoma cells 106

Figure 3.11. Attempted inhibition of Gab1 and Lamin expression by RNA interference in HeLa cells 108

Figure 3.12. Model illustrating possible involvement of RaLP/ShcD and Gab1 in RTK signalling pathways 112

CHAPTER 4

Figure 4.1. β-galactosidase filter assay to demonstrate interaction between RaLP/ShcD-CH1 domain and Grb2 120

Figure 4.2. Test transformations to determine for the ability of bait plasmids to self-activate *HIS3* reporter gene 122

Figure 4.3. β-galactosidase filter assays on select yeast clones isolated from large-scale yeast library screen 124

Figure 4.4. Digestion of plasmids isolated from positive yeast clones by *Not*I restriction enzyme 126

Figure 4.5. BLAST analysis of Clones 7 and 29 revealed that they encode Peg3/Pw1 protein 127

Figure 4.6. BLAST analysis of clone 3 indicates that it is a fragment of HP1α protein.. 128

Figure 4.7. β-galactosidase filter assay on positive plasmids from library screen with negative controls 130

Figure 4.8. Quantitative assay of β-Galactosidase activity of yeast transformants.. 131

Figure 4.9. Precipitation of Peg3/Pw1 and a deletion encoding only the ZnF domains from transfected HEK293 cell lines using GST-RaLP/ShcD-CH1 fusion protein.. 133

Figure 4.10. GFP-RaLP/ShcD can co-precipitate with HA-Peg3/Pw1 and HA-ZnF in HEK293 cells 136

Figure 4.11. Effect of Peg3/Pw1 and Camptothecin on RaLP/ShcD protein in HEK293 cells stably expressing FLAG-RaLP/ShcD (F4) 138

Figure 4.12. Effect of Peg3/Pw1 and Camptothecin on RaLP/ShcD protein in HEK293 cells stably expressing GFP-RaLP/ShcD (G5) 140

Figure 4.13. Determination of the activity of the CMV promoter by performing *Renilla* Luciferase assays in HEK293 cells 142

Figure 4.14. The endogenous level of RaLP/ShcD is increased following transfection with Peg3/Pw1 in B16-F10 melanoma cells 143

Figure 4.15. Determination of the subcellular localisation of HA-Peg3/Pw1 and GFP-RaLP/ShcD in HEK293 cells 145

Figure 4.16. Determination of the efficiency of CPT treatment and anti-HA staining.. 147

Figure 4.17. Determination of subcellular localisation of GFP-p49RaLP/ShcD in HEK293 cells with and without CPT treatment 149

Figure 4.18. Determination of subcellular localisation of HA-Peg3/Pw1 and GFP-p49RaLP/ShcD in HEK293 cells with and without CPT treatment 150

Figure 4.19. Precipitation of HP1α from transfected HEK293 cell lines using GST-RaLP/ShcD-CH1 fusion protein. HEK293 cells were transfected with GFP-HP1α 152

Figure 4.20. mCherry-RaLP/ShcD can precipitate with GFP-HP1α in HEK293 cells.. 154

Figure 4.21. Determination of Subcellular localisation of mCherry-RaLP/ShcD and GFP-HP1α in 518 melanoma cells 156

Figure 4.22. Schematic illustration of human and mouse Peg3/Pw1 protein 159

Figure 4.23. Schematic illustration of domain structure of HP1α 164

CHAPTER 5

Figure 5.1. Expression of GST-RaLP/ShcD-CH1 in the soluble or insoluble fraction of BL21(DE3) 171

Figure 5.2. Purification of the GST-RaLP/ShcD-CH1 domain 173

Figure 5.3. Purification of GST-RaLP/ShcD-CH1 domain by Gel-filtration chromatography 175

Figure 5.4. Preliminary characterisation of the CH1 domain as a metal binding domain.. 177

Figure 5.5. Assay to measure Co^{2+} binding to the CH1 domain of RaLP/ShcD.. 179

Figure 5.6. Large-scale *in vitro* pull-down assay using the CH1 domain of RaLP/ShcD and 518 melanoma cell extracts 181

Figure 5.7. Determination of cellular localisation of Vimentin in 518 melanoma cells.. 183

Figure 5.8. Determination of cellular localisation of RaLP/ShcD and Vimentin in 518 melanoma cells 184

CHAPTER 6

Figure 6.1. A diagram illustrating the possible interaction partners for different domains of RaLP/ShcD 191

List of Tables

CHAPTER 2

Table 2.1. The list of primary antibodies was employed for Western blot (W.B), Immunoprecipitaion (I.P) and immunofluorescence (I.F) experiments 54

Table 2.2. Western blotting (W.B) and immunofluorescence (I.F) experiments 55

Table 2.3. Primers for the point-mutation of tyrosine (Y) 183 to phenylalanine (F) on Gab1 62

Table 2.4. The sequence of Oligonucleotide primers for Gab1 siRNA 84

Table 2.5. The sequence of Oligonucleotide primer for Lamin A/C siRNA 84

Abbreviations

BCA: Bicinchoninic acid

BDNF: brain-derived growth factor

bp: base pairs

BSA: bovine serum albumin

CAM: cell adhesion molecule

CDK: cyclin dependent kinase

CDKN: cyclin dependent kinase inhibitor

CMV: cytomegalovirus

cDNA: complemetray DNA

CIS: cisplatin

CPT: camptothecin

Cyto *c*: cytochrome *c*

DMEM: Dulbecco's modified Eagle's medium

DMSO: dimethyl sulphoxide

DNA: deoxyribonucleic acid

DOS: daughter of sevenless

DTT: dithiothreitol

ECL: enhanced chemiluminescence

ECM: extracellular matrix

EDTA: diaminoethanetera acetic acid

EGF: epidermal growth factor

EGFR: epidermal growth factor receptor

EMT: epithelial-mesenchymal transition

Eps8: epidermal growth factor receptor pathway substrate 8

ERK: extracellular-signal-regulated kinase

ET: endothelin

FACS: fluorescence-activated cell sorting

FAK: focal adhesion kinase

FBS: foetal bovine serum

GPCR: G-protein coupled receptor

Grb2: growth factor receptor-bound protein 2

GSK3: glycogen synthase kinase 3

GST: glutathione S-transferase

h: hour

HCl: hydrogen chloride

HGF: hepatocyte growth factor

H_2O_2: hydrogen peroxide

IL: interleukin

IMM: inner mitochondrial membrane

IMS: inter-membrane space

IGF: insulin-like growth factor

IPTG: Isopropyl β-D-1-thiogalactopyranoside

IR: insulin receptor

IRS: insulin receptor substrate

Kb: kilo base pairs

kDa: kilodalton

LMB: leptomycin B

MAPK: Mitogen-activated protein kinase

mRNA: messenger RNA

mTOR: mammalian target of rapamycin

MuSK: muscle-specific kinase

MW: molecular weight

NaF: sodium fluoride

Na_3VO_4: sodium orthovanadate

NMJ: neuromuscular junction

NGF: nerve growth factor

OD: optical density

ONPG: ortho-nitrophenyl-β-D-galactopyranoside

PBS: phosphate buffered saline

PCR: polymerase chain reaction

PDGF: platelet-derived growth factor

PEG: polyethylene glycol

PI3K: phosphatidylinositide 3-kinase

PIP2: Phosphatidylinositol 4,5-bisphosphate

PIP3: Phosphatidylinositol-3,4,5-bisphosphate

PMSF: phenylmethanesulphonylfluoride

PTEN: phosphatase and tensin homolog

PTP: permeability transition pore

RNA: ribonucleic acid

ROCK: Rho-associated, coiled-coil containing protein kinase

ROS: reactive oxygen species

rpm: revolution per minute

RTK: receptor tyrosine kinase

SCF: stem cell factor

SDS: sodium dodecyl sulfate

Shc: Src Homology and Collagen

shRNA: short hairpin RNA

Siah: seven in absentia homolog

siRNA: small interfering RNA

SOS: son-of-sevenless

TAE: tris-acetate-EDTA buffer

TBS: tris buffered saline

TEV: tobacco etch virus

TLB: triton lysis buffer

UV: ultra-violet

VEGF: vascular endothelial growth factor receptor

VEGF-R2 (Flk-1): vascular endothelial growth factor receptor 2

WT: wild type

YPD: yeast extract-peptone-dextrose

2xYT: Yeast Extract Tryptone broth

Chapter 1

Introduction

1.1. Overview

Signalling from cell surface receptors to intracellular targets usually involves a diverse set of modular protein-protein interactions which are initiated by the binding of phosphotyrosine-containing motifs on activated receptor tyrosine kinases (RTKs) to proteins containing SH2 (Src homology 2) or PTB (phosphotyrosine-binding) domains. The members of the Shc (Src Homology and Collagen) family of adaptor proteins share two significant phosphotyrosine-binding domains; the PTB domain at the N-terminus, and the SH2 domain at the C-terminus which are able to interact with several Receptor Tyrosine Kinases (RTKs) and signalling transducer proteins such as G-protein coupled receptors (GPCRs) in cells, resulting in the regulation of several cellular signalling pathways including the mitogen activated protein kinase (MAPK) and the AKT pathways. There are four members of this protein family that have been identified as Shc/ShcA (p46, p52 and p66), ShcB/Sli (p68), ShcC/Rai (p52 and p64) and the newest member of RaLP/ShcD (p69).

RaLP/ShcD was identified at nearly the same time by two distinct research groups by employing the Basic Local Alignment Search Tool (BLAST) technique to screen mouse and human genomic databases for sequences related to ShcA (p66), ShcB/Sli and ShcC/Rai (Fagiani *et al*., 2007, Jones *et al*., 2007). Although there is some structural similarity between the Shc family members, Shc proteins have non-redundant roles in intracellular signalling pathways (Pelicci *et al*., 2002; Migliaccio *et al*., 1999). Until now, there are only a few biological roles of RaLP/ShcD that have been characterised by different research groups. It has been shown to be involved in the regulation of the migration of melanomas in mammals (Fagiani *et al*., 2007), to interact with specific RTKs such as Muscle-Specific Kinase (MuSK) through its PTB domain (Jones *et al*.,

2007), and is involved in cell differentiation during the embryonic stem cell (ESC) to the primed epiblast stem cell (EpiSC) transition (Turco *et al*., 2012).

Since the function of an adaptor protein, such as RaLP/ShcD is mainly to be involved in protein complexes, a key to understanding its biological role will be to characterise interacting proteins. For that reason, this project will firstly aim to investigate novel binding partners of RaLP/ShcD which could be involved in either upstream or downstream in signalling pathways. Also, the least well conserved CH1 domain, which contains six cysteines and two histidines, will be characterised to determine whether it functions as a metal-binding domain.

1.2. The Src Homology and Collagen (Shc) family

Signalling from cell surface receptors to intracellular targets involves a diverse set of modular protein-protein interactions which are initiated by the binding of phosphotyrosine-containing motifs on activated receptor tyrosine kinases (RTKs) to proteins containing SH2 (Src homology 2) or PTB (phosphotyrosine-binding) domains. The family of Shc (Src homology and collagen) adaptor proteins are a model of the evolutionary success of signal transduction adaptor proteins which possess both the SH2 and PTB domains. In mammals, the Shc family comprises at least seven members encoded by four different genes, namely Shc/ShcA/Shc1, Sli/ShcB/Shc2, Rai/ShcC/Shc3 and RaLP/ShcD/Shc4 which, arise through alternative initiation codon usage and splicing patterns, as described in Figure 1.1 (Luzi *et al*., 2000). RaLP/ShcD/Shc4 is the most recent family member to be identified (Rai-like protein) through TBLASTn searches of both the human and mouse genome using Shc/ShcA, Sli/ShcB, and Rai/ShcC sequences (Fagiani *et al*., 2007; Jones *et al*., 2007). It is

implicated in melanoma. Cell migration and is associated with a muscle-specific kinase receptor (MuSK).

The proteins belonging to the Shc family share a common protein domain structure as shown in Figure 1.1. They are characterised by an N-terminal PTB domain, a central region rich in proline and glycine residues termed the collagen homology (CH) 1 domain, and a C-terminal SH2 domain in the presented order. An N-terminal collagen homology 2 (CH2) region is present in p66-ShcA, p64-Rai/ShcC (Pelicci *et al*., 2002) and p68-Sli/ShcB (Kojima *et al*., 2001; Migliaccio *et al*., 1997) and in p69-RaLP/ShcD. The (CH2)-PTB-CH1-SH2 modularity is unique to the Shc family members.

The Shc family members show distinct patterns of expression, with Shc expressed in all adult tissues except the central nervous system. However, Rai/ShcC and Sli/ShcB proteins are expressed only in the nervous system. Furthermore, Rai/ShcC expression slowly replaces ShcA expression during brain development. This indicates that Rai/ShcC functions specifically in mature neuron survival (Cattaneo and Pelicci, 1998; Nakamura *et al*., 1998). On the other hand, RaLP/ShcD seems to be overexpressed in advanced stage melanomas and expressed mainly in the melanocytic lineage (Fagiani *et al*., 2007). It has been recently shown that RaLP/ShcD is also expressed in muscle and neuronal tissue (Hawley *et al*., 2011).

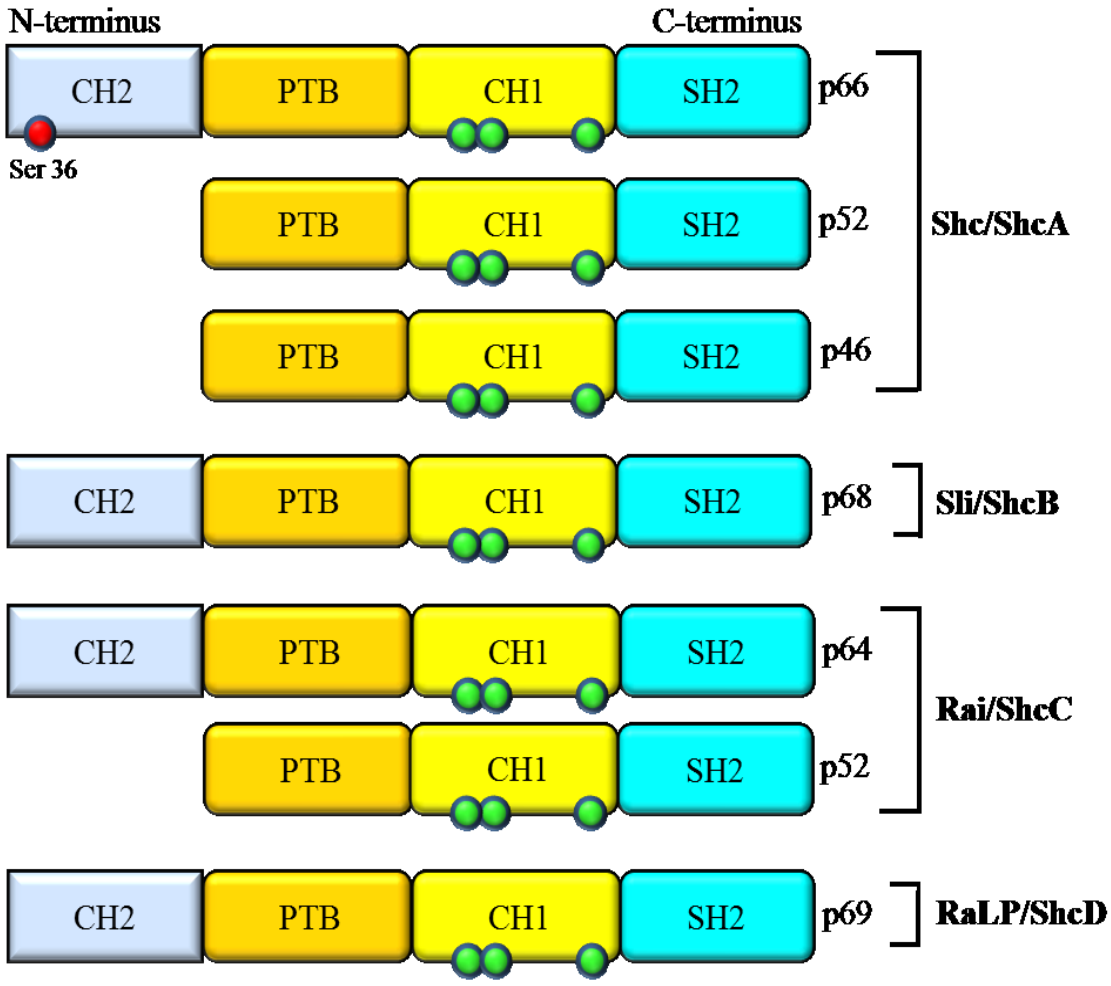

(Modified from Wills and Jones 2012)

Figure 1.1. Domain structure of members of the Shc family in mammals. All the members of Shc proteins share the modular domain structure (CH2)-PTB-CH1-SH2. Three important tyrosine residues on the CH1 domain of all the members are phosphorylated by RTKs and are required for Shc association with Grb2 (green circles). Among all the family members, only four members so far; p66-ShcA, p68-ShcB, p64-ShcC and RaLP/ShcD possess an additional unique CH2 domain at the N-terminus. p66-ShcA has a unique serine residue at position 36 (Ser 36) (red circle) which contributes to its pro-apoptotic role.

Knock-out mouse studies show that mice lacking Rai/ShcC or Sli/ShcB show a decrease in the numbers of certain neuronal populations (Sakai *et al*., 2000), while mice lacking Shc isoforms die during embryogenesis with defects in cardiovascular development (Lai and Pawson, 2000). However, mice in which only the 66-kDa ShcA isoform has been knocked out display increased life span (Migliaccio *et al*., 1999). The biological specificity of Shc proteins may be caused by coordinated expression through adult life and embryonic development, in addition to the association with unique subsets of upstream receptors and downstream targets.

1.2.1. Domain Structure of Shc Family members

1.2.1.1. The Src Homology 2 (SH2) domain of Shc

The C-terminal SH2 domain of Shc was originally discovered as a critical mediator of epidermal growth factor (EGF) receptor signalling (Pelicci *et al*., 1992). In proteins, the SH2 domain only associates with phosphotyrosine residues not phosphoserine or phosphothreonine. The residues carboxy terminal to the phosphotyrosine determines specificity (Pascal *et al*., 1994). The SH2 domain was shown to be involved in almost all Shc-mediated signal transduction cascades, especially the MAPK signalling pathway. The significant function of the SH2 domain in promoting cellular signalling by receptor tyrosine kinases (RTKs) is widely understood.

Upon stimulation with growth factors such as platelet-derived growth factor (PDGF) or epidermal growth factor (EGF), RTKs undergo dimerisation and tyrosine phosphorylation and recruit cellular signalling proteins such as Ras-GAP (GTPase (guanosine trisphosphatase)-activating protein) and phospholipase C-γ (PLC-γ), which contain SH2 domains (Ellis *et al*., 1990; Margolis *et al*., 1990). Isolated SH2 domains

were used in binding assays to show that the SH2 domains of different proteins interact with specific motifs containing phosphotyrosine (Felder *et al*., 1993).

In addition, the tyrosine phosphorylated EGFR was employed in bacterial expression library screens, and various cellular signalling proteins possessing the SH2 domain were identified (Skolnik *et al*., 1991). The SH2 domain of Shc proteins specifically engages tyrosine phosphorylated receptors/peptides having leucine or isoleucine at the (+3) position (Mikol *et al*., 1995). The Grb2-SH2 domain, for instance, associates with a pYXN where pY represents phosphotyrosine, X corresponds to any amino acid and N represents an asparagine residue. This motif is found in numerous cellular proteins such as the family of Shc adaptor proteins and the SHP2 tyrosine phosphatase protein. Alternatively, the SH2 domain of p85 associates specially with a pYMXM or pYXXM where pY is phosphotyrosine, M is methionine, and X is any amino acid. This motif is found in many cellular proteins, PDGF receptor, and Gab1 as well as insulin receptor substrate IRS-1 and IRS-2. Upon phosphorylation, RTK and docking proteins provide tyrosine phosphorylation sites which recruit many signalling proteins (via the SH2 domain) leading to activation of multiple cascades. Therefore, SH2 domains have a significant aspect role in controlling RTK signalling pathways (Schlessinger, 2000).

1.2.1.2. The Phosphotyrosine-Binding (PTB) domain of Shc

The phosphotyrosine binding (PTB) domain was primarily discovered in the family of Shc adaptor/scaffold proteins. Shc was identified as a binding partner for the cytoplasmic domain of insulin receptor (IR) when it is phosphorylated (Sasaoka *et al*., 1994). It was shown that an NPXpY sequence (where N represents asparagine, P refers to proline, X is any amino acid and pY is a tyrosine phosphorylated residue) in the

insulin receptor (IR) is important for associating with the docking protein IRS-1 via its PTB domain (White *et al*., 1988). The PTB domain of Shc has been revealed to have two functions, in both receptor binding and membrane localisation (Howell *et al*., 1999).

In addition, PTB domain binding to an NPXpY motif on the cytoplasmic tail of receptors leads to tyrosine-phosphorylation of Shc proteins within the CH1 domain (Borg and Margolis, 1998). After discovery of the PTB domain of Shc, many studies have identified phosphopeptides and proteins that contain the NPXpY motif and interact with the PTB domain of Shc (Zhou *et al*., 1996). It is interesting to note that the SH2 domain of Shc is not always necessary for interacting with phosphoproteins, suggesting that the PTB domain of Shc has a critical function in targeting tyrosine-phosphorylated proteins (Margolis, 1999).

The PTB domain is also structurally comparable to the PH (Plekstrin Homology) domain which is well-known to bind charged phospholipids such as PI(3,4,5)P3, PI(4,5)P2, and PI(4)P (Rameh *et al*., 1997). Therefore, the domain has evolved to permit its localisation in the cell membrane (Ravichandran *et al*., 1997). The PTB domain of Shc has a high affinity for phosphotyrosine residues contained which the NPXpY motif however not all PTB domains bind tyrosine phosphorylated molecules (Kavanaugh and Williams, 1994; Margolis *et al*., 1999). Many structural studies have elucidated that all of the PTB domains share a PH domain form but their amino acid sequences are not obviously comparable. On the other hand, many PTB domains are not associated with phospholipids such as the PTB domain of IRS-1 (Eck *et al*., 1996). Interestingly, many cellular signalling proteins have a PH domain as well as the SH2 or

PTB domain, such as IRS-1, in which both the PH and PTB domains in the protein play a significant role in its function (Dhe-Paganon *et al*., 1999).

It has been recently reported that the PTB and SH2 domains of RaLP/ShcD interact with TrkB, leading to induction of Brain-Derived growth Factor (BDNF)-associated MAPK signalling (You *et al*., 2010). TrkB is one of the members of tropomyosin-related kinase (Trk) family of RTKs which generally regulates BDNF and nerve growth factor (NGF) signalling (Reichardt *et al*., 2006). RaLP/ShcD is overexpressed in the brain of the adult mouse, indicating that RaLP/ShcD may have a role in neuronal signalling (Smith *et al*., 2006). In a yeast two-hybrid screen, it was confirmed that both the PTB and SH2 domains can associate with TrkB. Upon BDNF stimulation, the phosphorylated PTB domain binds to the NPQY motif on TrkB at tyrosine (Y) 516. Therefore, the interaction between RaLP/ShcD and TrkB leads to increase BDNF-induced MAPK activation (You *et al*., 2010).

1.2.1.3. The Collagen Homology 1 (CH1) domain of Shc

The Shc-CH1 is located in between the PTB and SH2 domains. Because it is rich in glycines and prolines, the region was termed a collagen homology (CH) domain (Pelicci *et al*., 1992) as shown in Figure 1.1. Nevertheless, the CH domains of Shc proteins do not show the unique collagen-like repeats found in collagen. The CH1 domains are the least conserved domains among all the family of Shc proteins. The CH1 domain of ShcA possesses three critical conserved tyrosine (Y) residues, twin tyrosines Y239/240 and Y317 which are conserved in all family members. They are phosphorylated by activated cell surface receptors such as EGF and PDGF following association with the PTB and/or SH2 domain of Shc proteins.

It has been published that the Y317 and Y239/240 of ShcA are phosphorylated by various tyrosine kinases (Walk *et al*., 1998). Furthermore, it has been recently noted that the Y239/240 is phosphorylated and recruited by Src proteins, unlike the Y317 which is tyrosine phosphorylated by other RTKs (Blake *et al*., 2000). Many studies reveal that mutation of these tyrosines (Y239/240 and Y317) either alone or in combination has a negative effect on signalling (Gotoh *et al*., 1997; Pratt *et al*., 1999), suggesting that they are all significant. Both tyrosines (Y239 and Y317), share the asparagine residue at the (+2) position C-terminal to the phosphotyrosine which is important for associating with the SH2 domain of Grb2 (Walk *et al*., 1998).

Upon phosphorylation, Y317 associates with the Grb2-SH2 domain, consequently this tyrosine is involved in mediating Shc-Grb2-SOS-Ras-MAPK signalling pathways (Velazquez *et al*., 2000). However, it has been noted that many other proteins interact individually with these tyrosines other than Grb2 (van der Geer *et al*., 1996). In addition, the twin tyrosines Y239/Y240 have been shown to initiate c-Myc activation, whereas Y317 can activate the MAPK pathway (Gotoh *et al*., 1997). The CH1 domain of Shc possesses a number of PXXP residues which may interact with many proteins containing the SH3 domain, for instance, the SH3 domain of Src and Fyn have been shown to associate with Shc proteins (Weng *et al*., 1994). Furthermore, *in vitro* assays have illustrated that fusion proteins such as the CH1 domain with PTB domain, or CH1 with SH2 domain have better association than the PTB domain or SH2 domain alone (Ravichandran *et al*., 2001).

1.2.1.4. The Collagen Homology 2 (CH2) domain of Shc

p66-ShcA, p68-Sli/ShcB, p64-Rai/ShcC and the most recently identified Shc protein, RaLP/ShcD possess an additional CH2 domain at the N-terminus (Migliaccio *et al*., 1997; Fagiani *et al*., 2007). The CH2 domain is different from the CH1 domain of ShcA and has not been shown to be tyrosine phosphorylated, but it has a novel pro-apoptotic function in ShcA (p66-ShcA), involving serine phosphorylation (Ser 36) on the CH2 domain as seen in Figure 1.5 (Migliacchio *et al*., 1999). It has also been reported that overexpression of the CH2 domain may play a role in inhibiting c-Fos expression (Migliaccio *et al*., 1997). Furthermore, Shc adaptor proteins interact with proteins possessing the SH3 domain such as Src kinase (Weng *et al*., 1994) through their CH2 and CH1 domains, which could play a role in cell migration and cytoskeleton rearrangement.

1.2.2. Biological function of the Shc family members in tumour Progression

Despite some structural similarity, Shc proteins control intracellular functions as various as, apoptosis (p66-ShcA), cell proliferation (p52-ShcA), cell survival (p64-Rai/ShcC), and cell migration (p69-RaLP/ShcD) demonstrating that they have non-redundant functions (Pelicci *et al*., 2002; Migliaccio *et al*., 1999; Fagiani *et al*., 2007). Biochemically, they are all targets of activated RTKs and control diverse downstream signalling pathways. For instance, p52-ShcA protein triggers the Ras/MAPK pathway, after growth factor stimulation, resulting in cell proliferation and p64-Rai/ShcC regulates PI3K activation either following hypoxic/oxidation insult or after growth factor stimulation, leading to enhanced cell survival (Troglio *et al*., 2004) and p66-ShcA regulates stress-induced apoptosis and reactive oxygen species (ROS) metabolism

(Trinici *et al*., 2002). No unique cellular signalling pathways have yet been attributed to p68-Sli/ShcB and p46-ShcA. All the Shc family members are identified in the cytoplasm of cells, which accounts for their role in coupling extracellular signals to downstream signalling pathways. Regulation of their phosphorylation and/or expression status may in sequence be associated with malignancy. Clinical studies have previously indicated that activation of the Shc signalling cascades is correlated with poor patient diagnosis in breast cancer (Ursini-Siegel and Muller, 2008).

1.3. Critical signalling pathways in melanoma progression to metastasis

1.3.1. Shc and the mitogen activated protein kinase (MAPK) cascade

The MAPK pathway is a well-characterised signalling cascade which is essential for the transduction of extracellular signals, originating at the cell surface. This cascade results in cell proliferation, survival, and migration (Yoon and Seger, 2006). In almost all metastatic melanomas, the MAPK pathway is over-activated (Fecher *et al*., 2008).

The crucial regulator of the MAPK signalling pathway is the RAS GTPase which is activated downstream of RTKs, such as epidermal growth factor receptor (EGFR) as well as integrins and also GPCRs, thus comprising the interaction point of complex signalling networks (Mc Kay and Morrison, 2007). Dimerisation of RTKs is activated upon binding of growth factors, resulting in autophosphorylation of the receptor and recruitment of proteins containing SH2 or PTB domains. Among the recruited proteins are Shc family members, which are critical mediators of RAS activation (Hubbard and Miller, 2007).

The role of ShcA in coupling RTK activation to the MAPK pathway is well understood as shown in Figure 1.2. Basically, upon growth factor stimulation such as Epidermal Growth Factor (EGF) and Platelet-Derived Growth Factor (PDGF), Shc proteins associate with activated RTKs through their SH2 and/or its PTB domains and then tyrosine phosphorylation occurs in the CH1 domain of Shc proteins. The phosphorylated CH1 domain is able to interact with the Grb2-SH2 domain, which is constitutively associated with Son-of-Sevenless (SOS), a Ras guanine nucleotide exchange factor. The complex of Grb2-SOS accumulates at the cell membrane and stimulates the Ras-mediated MAPK signalling pathway leading to cellular events such as cell survival, differentiation, invasion, migration and proliferation (Yoon and Seger, 2006).

1.3.2. Association of Shc with the survival pathway (PI3K/AKT)

The phosphatidylinositol-3-kinase (PI3K) pathway has been studied extensively and its alteration is very common in human tumours. Basically, upon the activation of RTKs, the PI3K is stimulated followed by phosphorylation of phosphatidylinositol-4,5-biphosphate (PIP2) to produce phosphatidylinositol-3,4,5-triphosphate (PIP3), which leads to the activation of the AKT signalling pathway. Furthermore, PTEN (phosphatase and tensin homolog), a well-known tumour suppressor gene, negatively regulates the PI3K signalling pathway, by PIP3 dephosphorylation, as shown in Figure 1.3.

The PI3K signalling cascade can be directly/indirectly stimulated by many growth factors. PI3K can associate with a number of proteins, promoting cell migration, differentiation, proliferation, and survival (Hennessy *et al*., 2005).

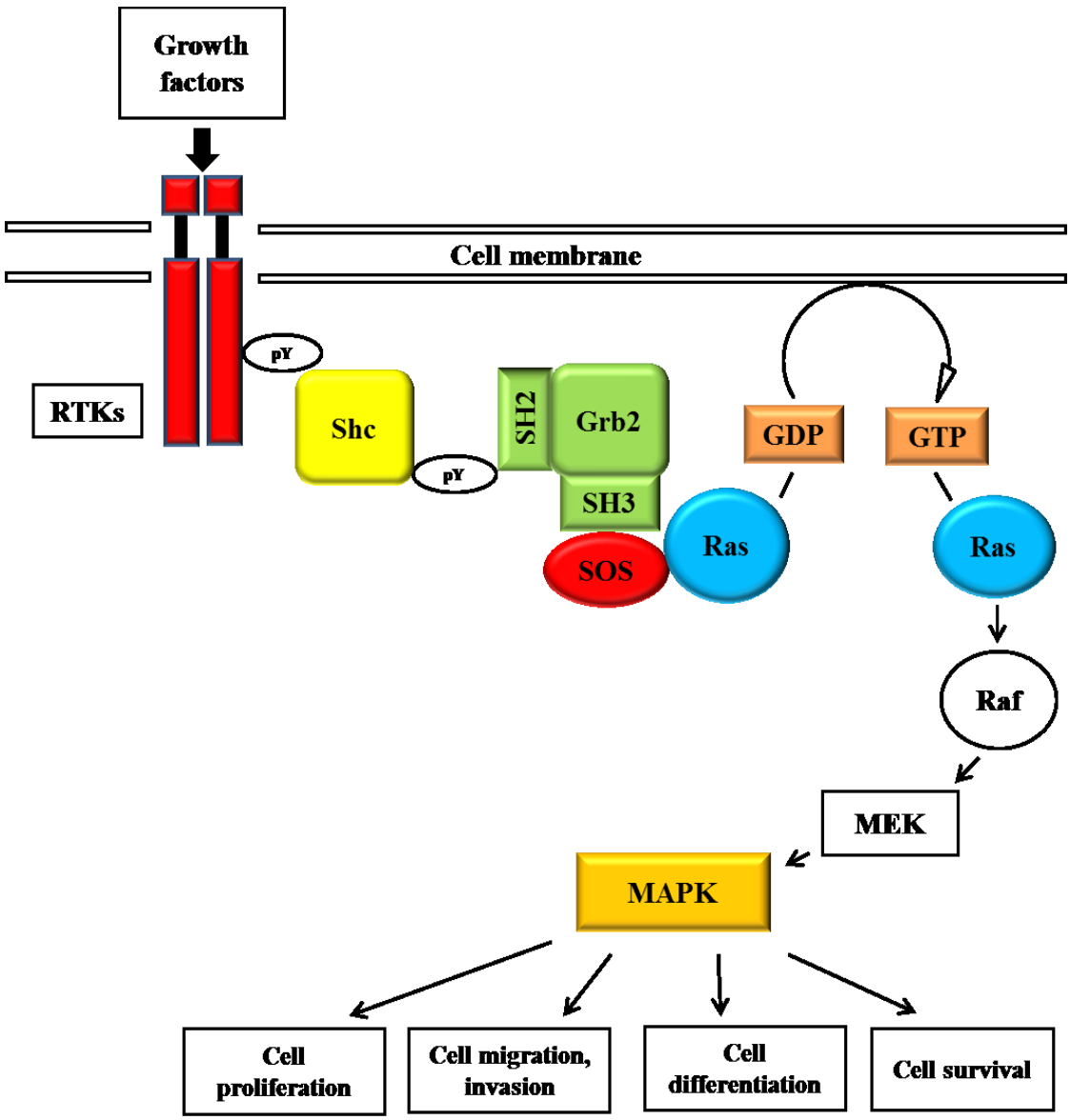

Figure 1.2. The role of ShcA in coupling RTK activation to the MAPK pathway. Upon growth factor stimulation, Shc proteins associate with activated RTKs through their SH2 and/or its PTB domains. Shc is quickly phosphorylated in the CH1 domain. The phosphorylated CH1 domain is able to interact with the Grb2-SH2 domain, which is constitutively associated with SOS, a Ras guanine nucleotide exchange factor. The complex of Grb2-SOS accumulates at the cell membrane and stimulates the Ras-mediated MAPK signalling pathway leading to cellular events such as cell survival, differentiation, invasion, migration and proliferation.

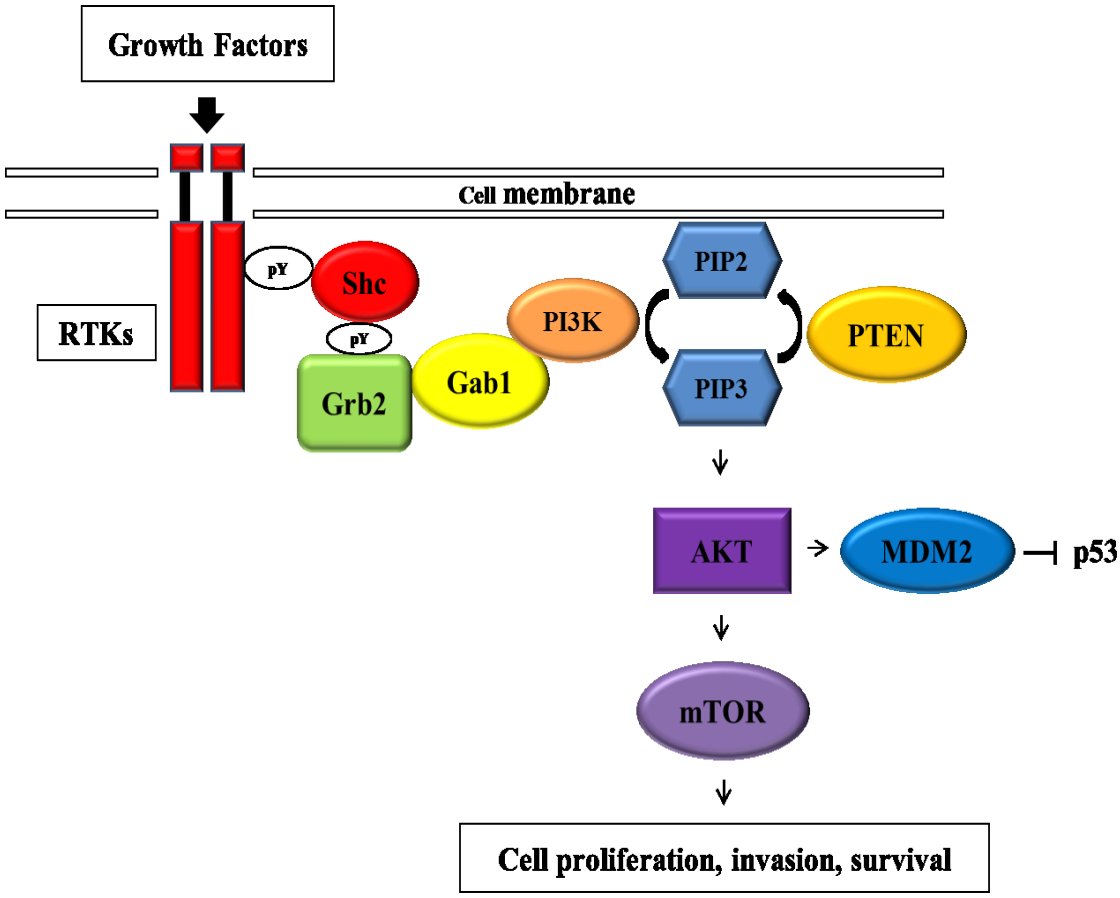

Figure 1.3. Schematic representation of Shc protein mediated activation of the PI3K/PTEN/mTOR signalling pathway. Shc is able to bind to phosphotyrosine residues on the cytoplasmic tail of a RTK. There are several signalling transducers such as Grb2 and Gab1 that are involved in activating the PI3K/AKT signalling pathways. PTEN protein negatively regulates this crucial cascade. MDM2 acts as a negative regulator of p53, disrupting its transcriptional initiation.

As described in Figure 1.3, upon growth factor stimulation, dimerised RTKs recruit Shc proteins which become phosphorylated and interact with Gab1 via Grb2, leading to activation of the PI3K and AKT signalling pathways. Once AKT is activated it can phosphorylate many substrates such as mammalian target of rapamycin (mTOR), and MDM2 leading to promote cell proliferation, invasion, and survival (Figure 1.3).

Many researchers have reported high levels of AKT expression in melanoma. In one report, 71% of primary melanomas, 70% of melanoma metastases, and 53% of nevi expressed high levels of AKT (Slipicevic *et al*., 2005). Also, it was shown that expression was higher in metastatic melanomas than benign nevi and severe dysplastic nevi (Stahl *et al*., 2004). When the expression of phospho-AKT is increased in melanoma, it is associated with tumour development and very poor survival.

The phosphatase and tensin homolog (PTEN) protein is a phosphatase protein which has multiple functions, but its main function is to dephosphorylate PIP3 to PIP2, resulting in negative regulation of the PI3K/AKT pathway (Stambolic *et al*., 1998; Di Cristofano and Pandolfi, 2000). It was previously reported that PTEN is downregulated in 30% ~ 50% of melanoma cells (Wu *et al*., 2003).

PTEN can regulate cell migration, invasion, and adhesion by inactivation of focal adhesion kinase (FAK), causing failure in focal adhesion organisation (Simpson and Parsons, 2001). Interestingly, the ShcA adaptor protein is dephosphorylated by PTEN, thus leading to suppression of the MAPK signalling pathway (Gu *et al*., 1998). Therefore, a reduction of PTEN will lead to increased phosphorylation of Shc and FAK

resulting in induced cell proliferation, invasion, and migration (Pasini *et al*., 2009). However, it is still doubtful what role PTEN plays in melanoma progression.

1.3.3. Integrin Pathway and Shc proteins

Integrins play a significant role in controlling cell migration, survival, stable cell adhesion, proliferation, differentiation and mediating angiogenesis and invasion (Wiesner *et al*., 2005; Eliceiri and Cheresh, 2001). Integrins are well-studied cell surface receptors which are a subgroup of the cell adhesion molecule (CAM) family. Integrins are heterodimers made up of α and β subunits and there are at least 18 α and 8 β subunits which have been identified in humans (Hynes, 1992; Desgrosellier and Cheresh, 2010).

Integrins have an important role in cell signal transduction as well as forming associations with the extracellular matrix (ECM) (Hynes, 1999). They form a bridge between the ECM and actin cytoskeleton. A large group of proteins are recruited to the cytoplasmic tails of integrins at cell junctions which engage with the cytoskeleton. Signalling proteins (and also their ligands) are able to organise cytoskeletal dynamics and modulate the cell junctions' stability. Many receptors such as receptor tyrosine kinases (RTKs), G-protein-coupled receptors, cytokine receptors associate with integrins, leading to activate integrin-involved signalling pathways. In addition, the disruption of integrin regulation allows tumour cell invasion and migration by stimulating changes in the gene expression modifications, and the reorganization of cytoskeleton (Huveneers *et al*., 2007).

Integrins, during melanoma development, control the MAPK and AKT pathways via direct docking to proteins which possess the PTB and/or the SH2 domains, such as Shc and Src proteins (Kuphal *et al*., 2005). A subgroup of integrins directly triggers the MAPK signalling pathways via Shc modulation, they also associate and activate particular integrin-regulated kinases such as focal adhesion kinase (FAK). FAK induces the Rho-associated, coiled-coil containing protein kinase (ROCK) pathway, which is particularly essential in cancer cells for acquiring invasive ability. Furthermore, FAK regulates survival and proliferation, by the interaction with Shc, which provides a binding site for Grb2 (growth factor receptor bound protein 2), causing the formation of the Shc-Grb2-SOS complex and resulting in the induction of the MAPK signalling pathway (Guo and Giancotti, 2008).

1.4. Shc and Pro-apoptotic Function

The Shc family of adaptor proteins has a crucial role in cellular signalling and as well as having a role in cell proliferation, also regulating cellular stress and apoptosis in the cell. Among the members of adaptor proteins, ShcA is the best characterised. There are three isoforms of ShcA proteins encoded by the ShcA gene, referred to as p46-ShcA, p52-ShcA, and p66-ShcA to indicate the molecular weight of the protein product. p66-ShcA is the longest isoform among the ShcA members. They commonly share the phosphotyrosine-binding (PTB) domain, collagen homology 1 (CH1) domain in the middle, and the C-terminal Src-homology 2 (SH2) domain. Among three isoforms of ShcA, only p66-ShcA has a unique collagen homology 2 (CH2) domain at the N-terminus. Also, p66-ShcA and p52-ShcA possess an additional cytochrome *c* binding (CB) domain as shown in Figure 1.4.

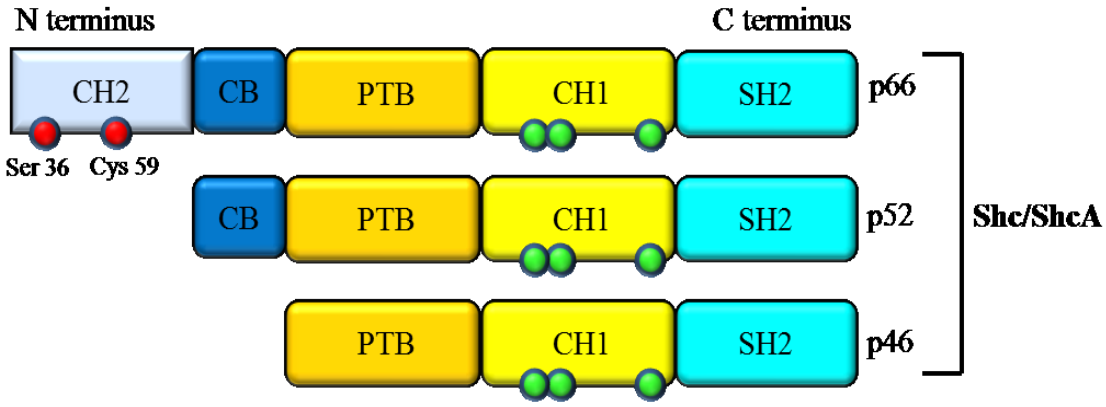

Figure 1.4. Schematic representation of domain structures of three isoforms of ShcA protein. There are three isoforms of the ShcA protein; p66-ShcA, p52-ShcA and p46-ShcA. All the isoforms share the PTB, CH1 and SH2 domains. The N-terminal CH2 domain is only present on the p66-ShcA isoform. p66-ShcA and p52-ShcA proteins contain the cytochrome *c* binding (CB) domain near the N-terminus. The CH2 domain of p66-ShcA possesses a ROS-mediated phosphorylation site at serine residue 36 (Ser 36). The cysteine residue at site 59 (Cys 59) forms disulphide bonds to act as a thiol-based redox sensor that controls the inhibition of apoptosis. There are three important tyrosine residues in the CH1 domain indicated as green circles, which are tyrosine phosphorylated by RTKs.

Upon UV light stimulation, p66-ShcA is phosphorylated and activated via phosphorylation of the CH2 domain of p66-ShcA at Serine 36 (Ser36). Also, it was shown that p66-ShcA is upregulated by p53 (Pellegrini *et al*., 2005). As seen in Figure 1.5, p66-ShcA protein generally exists in the reduced form in the cytoplasm under normal conditions. However, p66-ShcA forms a tetrameric protein in response to oxidative conditions via disulphide bond formation. This tetrameric form is targeted by the prolyl isomerase PIN1, which is a regulator of mitochondrial import, by recognition of Ser 36 on the CH2 domain of p66-ShcA (Wulf *et al*., 2005). After conformational modification of p66-ShcA by PIN1, phosphatase PP2A may dephosphorylate p66-ShcA. It is then transported into the inner mitochondrial membrane (IMM) through the mitochondrial inter-membrane space (IMS) with the help of the TIM/TOM protein complex (Giorgio *et al*., 2007).

In conditions of oxidative stress, p66-ShcA adopts the active tetrameric form and produces ROS, leading to opening of the mitochondrial transition pore, and apotosis. This illustrates that p66-ShcA activates apoptosis via production of ROS, but it can be stimulated by ROS as well (Giorgio *et al*., 2005). It is noted that, in mouse embryonic fibroblasts (MEFs), p66-ShcA overexpression caused enhanced sensitivity to oxidative stress, whereas p66-ShcA knock-out increased resistance to oxidative stress (Migliaccio *et al*., 1999).

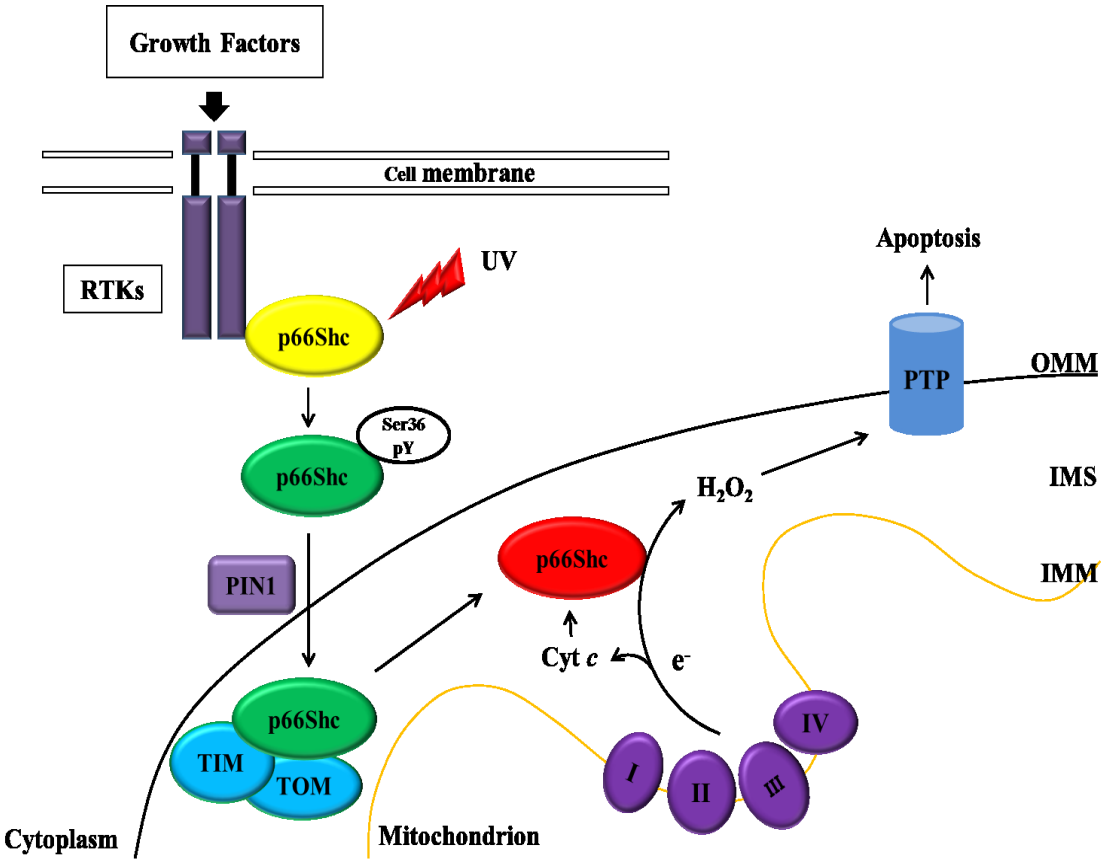

(Modified from Giorgio *et al.*, 2007)

Figure 1.5. The schematic illustrations of the pro-apoptotic function of p66-ShcA. After UV stimulation, p66-ShcA becomes phosphorylated at residue Ser 36 on its CH2 domain. The reduced form of p66-ShcA (in green) is then switched to the activate form. The activated p66-ShcA is targeted by PIN1 which helps mitochondrial import and then the complex is released from the TIM/TOM import machinery in the IMS. The activated p66-ShcA oxidizes reduced Cyt *c* and catalyses the reduction of O_2 to H_2O_2. For this, p66-ShcA recruits electrons (e^-) from the respiratory chain (I-IV) and then H_2O_2 activates the PTP resulting in apoptosis. OMM, outer mitochondrial membrane; IMM; inner mitochondrial membrane; IMS, inter-membrane space; PTP, permeability transition pore.

1.5. The newest member of Shc family of RaLP/ShcD or Shc4

1.5.1. Discovery of RaLP (Rai-like protein)/ShcD/Shc4

RaLP/ShcD is the newest member of the Shc family to be discovered (Fagiani *et al*., 2007; Jones *et al*., 2007) and the protein is situated on the long arm of Chromosome 15 (15q21.1-q21.2) in humans and on Chromosome 2 in mouse (Fagiani *et al*., 2007). The RaLP/ShcD cDNA comprises an Open Reading Frame (ORF) that encodes a protein of 626 or 630 amino acids in mouse and humans respectively, producing a protein of approximately 69-kDa in molecular weight. The CH2 domain of RaLP/ShcD possesses a number of potential start codons therefore it is possible that shorter isoforms of RaLP/ShcD such as p49 and p59 exist (Jones *et al*., 2007).

RaLP/ShcD is predominantly localised in the cytoplasm and roughly 5% of the protein is localised in the cell membrane without stimulation (Fagiani *et al*., 2007). Basically, RaLP/ShcD has the same domain structure as the other Shc family members. There are three critical tyrosine residues corresponding to Y239/240 and Y317 of ShcA with an additional tyrosine residue (Y424) in the CH1 domain of RaLP/ShcD. RaLP/ShcD, among the human Shc homologues, is the most different family member at the protein level showing 45% sequence identity with ShcA, 41% with ShcC/Rai and 37% with ShcB/Sli. The PTB and SH2 domains of RaLP/ShcD are the most conserved domains.

In addition, the CH2 domain of RaLP/ShcD at the N-terminus possesses several PXXP sequences, which may possibly provide binding sites for proteins containing the SH3 domain (Jones *et al*., 2007). Also, a number of serines (Ser) and threonines (Thr) such as Ser 37, Ser 76 and Thr 142 in the CH2 domain, may be phosphorylation sites for kinases (Fagiani *et al*., 2007). The PTB domain of RaLP/ShcD is not able to associate

with PIP2 and PIP3 due to the absence of positively charged amino acids conserved in other family members.

RaLP/ShcD was shown to be expressed at high levels in metastatic and aggressive human melanomas (Fagiani *et al*., 2007). Originally, melanoma initiates from natural melanocytes and progresses to a benign nevus. In some cases a benign nevus can develop into the RGP (radial growth phase) melanoma and subsequently the RGP melanoma may expand into the epidermis and can develop into the VGP (vertical growth phase) melanoma. These stage melanomas are capable of attacking the dermis, and ultimately, developing into metastatic melanoma. The expression of RaLP/ShcD is only observed in more severe stage melanomas such as VGP melanoma and metastatic melanoma, indicating that RaLP/ShcD is a good molecular marker of neoplastic development. RaLP/ShcD has been shown to associate with active EGF and IGF-1 (Insulin-like Growth Factor 1) receptors in IGR-37 metastatic melanoma cells, and when RaLP/ShcD was overexpressed in IGR-39 melanoma cells, which express low levels of endogenous RaLP/ShcD and ShcA, RaLP/ShcD expression resulted in increased MAPK activation (Fagiani *et al*., 2007).

On the other hand, *in vitro* knock-down of RaLP/ShcD expression by siRNA in metastatic melanoma cells resulted in lower cell migration, but did not affect cell proliferation (Fagiani *et al*., 2007). RaLP/ShcD down-regulation, *in vivo*, also prevents tumour metastasis of melanoma cells injected into the tail vein of mice. RaLP/ShcD knock-down, unexpectedly, did not affect MAPK signalling pathway. This indicates that RaLP/ShcD in melanoma can stimulate both Ras-dependent and Ras-independent migratory cascades (Fagiani *et al*., 2007). These results reveal that RaLP/ShcD may

possibly play a significant role in regulating the transition from the VGP stage to metastatic melanoma by regulating melanoma cell migration. Additionally, RaLP/ShcD could represent a special marker for metastatic melanomas, and a possible target for a novel therapeutic strategy to target melanoma.

1.5.2. The significance of the CH1 domain

RaLP/ShcD is the most distinctive member among the human Shc family members. The PTB (69 to 76% identitiy) and SH2 (55 to 69% identity) domains of RaLP/ShcD are the most conserved between ShcA and RaLP/ShcD, but the CH1 domain of RaLP/ShcD is the least conserved (18 to 24% identity) (Fagiani *et al*., 2007). Three important tyrosine residues corresponding to Y239/240 and Y317 of ShcA in the CH1 domain are conserved in all the Shc protein members as well as in RaLP/ShcD.

Also, Jones and colleagues (2007) have mutated these three tyrosines on the CH1 domain of RaLP/ShcD and shown that additional phosphorylation sites exist as the mutant lacking the three sites is still phosphorylated following EGF treatment (Jones *et al*., 2007). Y424 on the CH1 of RaLP/ShcD was identified as an additional binding site for Grb2, leading to activation of the MAPK signalling pathway. In addition, the domain contains six cysteines and two histidines conserved between mouse and humans (in red circles in Figure 1.6B) which is quite different from the other Shc family members and could potentially bind metal ions such as zinc.

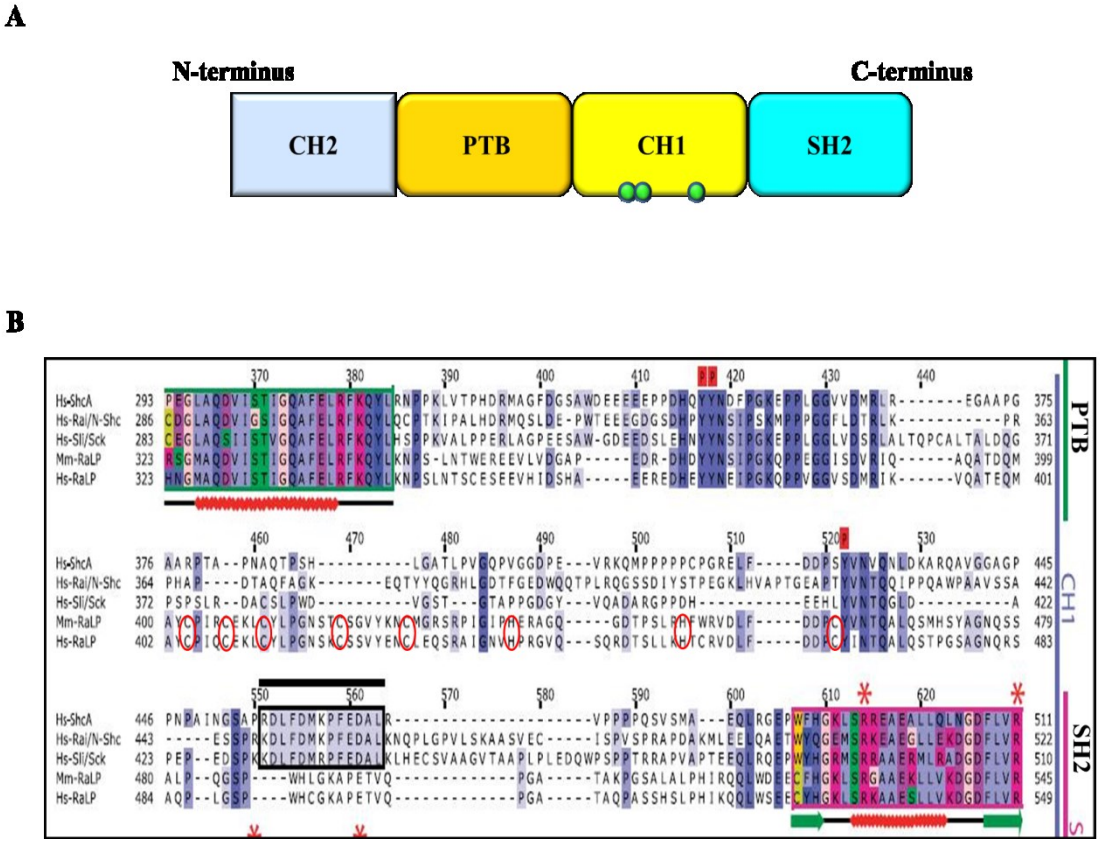

(Acquired from Fagiani *et al*., 2007)

Figure 1.6. Amino acids sequence alignment of the members of the Shc protein family. A, The domain modularity of RaLP/ShcD. B, The CH1 domain of RaLP/ShcD protein in both human and mouse are aligned with the human sequences of p66-ShcA, p68-Sli/ShcB, and p64-Rai/ShcC. The CH1 region is the least conserved among all Shc proteins. A unique region with six cysteine and two histidine residues are highlighted in red circles in the CH1 region of RaLP/ShcD.

Metal-binding domains including Zinc finger domains and LIM domains are commonly involved in DNA binding and mediating protein-protein interaction while the CH1 domain of RaLP/ShcD has no striking homology with either of these domains. It is feasible that it can bind metal ions and thus create a novel interaction interface. The subcellular localisation of RaLP/ShcD is predominantly in the cytoplasm (Fagiani *et al*., 2007), however more intriguingly, based on an unpublished work in this lab, it has been proposed that RaLP/ShcD is able to translocate to the nucleus (Ahmed and Prigent, unpublished). This finding could reveal a novel function of RaLP/ShcD, especially in the nucleus due to its CH1 domain.

1.5.3. The Biological function of RaLP/ShcD

The involvement of RaLP/ShcD in melanoma development and its biological function in the background of nevocytic nevus has not been fully identified. The key cascades implicated in the signal transduction of metastatic human melanoma and the role of RaLP/ShcD, are schematically illustrated in Figure 1.7. According to Pasini *et al*., 2009, RaLP/ShcD could be phosphorylated directly upon stimulation by a number of ligands of cell surface receptors, including hepatocyte growth factor (HGF), epidermal growth factor (EGF), insulin-like growth factor (IGF), and stem cell factor (SCF), or indirectly for example by endothelin-1 (ET-1) associating with GPCRs and subsequent activation of tyrosine kinases. Even if these receptors do not directly interact with the SH2 domain, or PTB domain of RaLP/ShcD, they may form complexes with activated RTKs leading to activation of the Ras/MAPK signalling pathway.

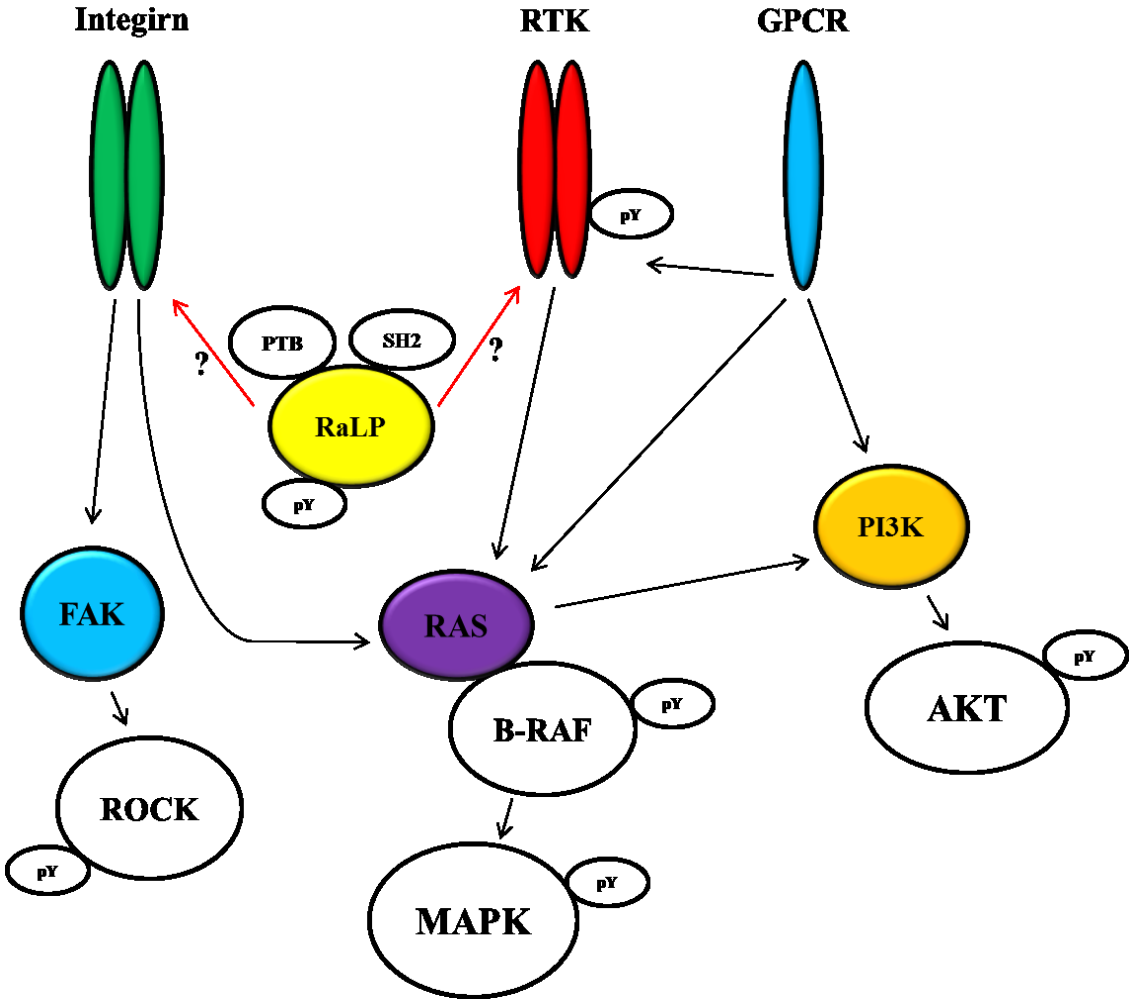

(Modified from Pasini *et al*., 2009)

Figure 1.7. Proposed function of RaLP/ShcD in the major signalling cascades which are deregulated in human melanoma. The three main signalling pathways engaged in the development of metastatic melanoma are illustrated with their significant kinase inducers. Black arrows illustrate the functional activation of signalling pathways. Upon growth factor stimulation, RaLP/ShcD is able to be phosphorylated. Red arrows indicate candidates for the activation of RaLP/ShcD at the cell membrane by RTKs and melanoma-specific integrins. RaLP/ShcD downstream effectors are still unidentified and actively studied. FAK: Focal Adhesion Kinase; GPCR: G-protein coupled receptor; ROCK: Rho-associated, coiled-coil containing protein kinase.

RaLP/ShcD protein possesses a PTB domain and this domain may provide an opportunity of integrin binding by either phosphotyrosine-dependent or independent mechanisms. For instance, it has formerly revealed that integrin was associate with epidermal growth factor receptor pathway substrate 8 (Eps8), talin and tensin (Schlessinger and Lemmon, 2003). RaLP/ShcD would then be a component of a multi-protein complex involved in initiation of intracellular signalling pathways. Actually, knock-down of RaLP/ShcD in metastatic melanoma cells led to reduced cell migration, without affecting the activation of MAPK pathway. This indicates its participation in other migratory signalling cascades, such as the integrin pathway.

1.5.4. RaLP/ShcD and Migration Role in Melanomas

The expression level of RaLP/ShcD mRNA was investigated in human tissue by performing *in situ* hybridization (ISH) with a series of tissue microarrays (TMAs) including both normal tissue and tumour specimens (Fagiani *et al*., 2007). RaLP/ShcD was found to be selectively expressed in melanoma, in particular during VGP stage, where 50% of tumours expressed high levels, and metastatic melanomas, where 47% expressed high levels, meaning that expression of this protein is associated with advanced stages of melanoma. Western blotting confirmed high levels of RaLP/ShcD protein expression in metastatic melanoma cell lines.

RaLP/ShcD can become tyrosine phosphorylated upon stimulation by EGF in metastatic melanoma cell lines. The phosphorylation of RaLP/ShcD increased up to five minutes following EGF stimulation (Fagiani *et al*., 2007). When RaLP/ShcD is overexpressed in melanoma cell lines producing low levels of RaLP/ShcD, it can enhance the activation

of EGF-mediated MAPK and melanoma cell migration. On the other hand, the PI3K/AKT signalling pathway is not induced after EGFR stimulation, not like MAPK. For instance, the AKT phosphorylation level was not significantly increased by EGF, or IGF-1 stimulation, and RaLP/ShcD did not associate with IRS-1, which is a significant adaptor protein linking to Gab1, PI3K, and the p85 in the IGF-1 signalling pathway (Fagiani *et al*., 2007).

Fagiani and colleagues (2007) have also demonstrated a number of biological roles for RaLP/ShcD by performing siRNA (small interfering RNA) studies. First of all, deficiency of RaLP/ShcD did not affect apoptosis or cell proliferation in metastatic melanoma cell lines as measured by anti caspase-3 staining, FACS analysis, and cell counting assays. Additionally, RaLP/ShcD protein was not found to be significantly involved in any morphological changes. However, knock-down of RaLP/ShcD did have an effect on metastatic melanoma cell migration and decreasing tumour development considerably. This may indicate that RaLP/ShcD has a critical function in cell migration and tumour progression of metastatic melanomas.

RaLP/ShcD knock-out assays have shown that this protein has other biological roles *in vitro*. RaLP/ShcD knock-down in metastatic melanoma cells did not affect the MAPK (also the AKT) basal levels, or ability of melanoma cells to migrate upon growth factor stimulation, although both RaLP/ShcD expression and MAPK activation are high in metastatic melanomas. Also, this finding may provide a hint that RaLP/ShcD could regulate melanoma cell migration *in vivo* through other signalling pathways which are downstream to Ras or Ras-independent.

1.5.5. RaLP/ShcD associates with Muscle-Specific Kinase Receptor (MuSK)

RaLP/ShcD was also characterised by another group that identified a totally distinct function for the protein via *in vivo* assays (Jones *et al.*, 2007). RaLP/ShcD was found to be highly expressed in skeletal muscle and brain cells in the adult mouse, and in the brain, expression was mostly restricted to the brain cerebellum. The PTB domains of Shc family members bind to NPXY (Asn-Pro-X-pTyr) sequences on phosphorylated receptors. The RaLP/ShcD, PTB domain, but not that of ShcA, was shown to associate with the phosphorylated NPXY juxtamembrane sequence in MuSK by performing pull-down assays. Taken together with the expression data, it appears that RaLP/ShcD has a role in skeletal muscle.

MuSK is a RTK, which is a receptor for agrin. Upon agrin activation, MuSK becomes tyrosine phosphorylated and regulates clustering of acetylcholine receptors (AChRs) in the neuromuscular junction (NMJ), which is important for the function of the NMJ and synaptic gene expression (Glass *et al.*, 1997). The Dok-7 adaptor protein is a known substrate for MuSK, but according to Jones *et al.*, 2007, RaLP/ShcD also links to MuSK. By performing immunoprecipitation assays, RaLP/ShcD was shown to associate with tyrosine phosphorylated MuSK upon agrin treatment. However, the mutated form of MuSK which is unable to be activated, failed to associate with RaLP/ShcD.

RaLP/ShcD interacts specifically with an NPXY motif on MuSK through its PTB domain. This was shown by replacing the asparagine, or tyrosine residue in the NPXY motif on MuSK for alanine. Mutants showed greatly reduced binding to RaLP/ShcD when these sites were mutated either individually, or combined. Interestingly,

inactivating mutants of either the SH2 domain or PTB domain mutant were still able to interact with MuSK. However, when both the SH2 and PTB domains were inactivated RaLP/ShcD was unable to bind MuSK or become phosphorylated on tyrosine, suggesting that the SH2 and PTB domains together are significantly involved in the association between RaLP/ShcD and MuSK. Despite these findings, the PTB domain of RaLP/ShcD appears to be primarily responsible for association with MuSK, while interaction with the SH2 domain may be synergistic. GST pull-down studies using isolated SH2 and PTB domains revealed that the PTB domain is able to precipitate endogenous, active MuSK from agrin stimulated C2C12 cells, while the SH2 domain is not. Mutation of the PTB domain in the phosphotyrosine binding pocket sites abolishes binding to MuSK in pull-down assays with GST-PTB domain. As it mentioned earlier, tyrosine phosohorylated MuSK occurs following argin stimulation which events can regulate clustering AChRs' tyrosine phosphorylation. Therefore, RaLP/ShcD is required for promoting AChRs' tyrosine phosphorylation in an early stage, even though RaLP/ShcD is not able to stimulate AChRs' clustering.

1.5.6. RaLP/ShcD is involved in cell differentiation during embryonic stem cell development

It has very recently been reported that RaLP/ShcD is regulated in cell differentiation during embryonic stem cell progression (Turco *et al*., 2012). Turco and colleagues (2012) determined that RaLP/ShcD were rapidly upregulated in the transition of Embryonic stem cell (ESC) to Epiblast stem cells (EpiSCs) when ESCs differentiated to neural lineages. Also, RaLP/ShcD was re-expressed after they become neural stem cells. In addition, they have shown that knock-out of RaLP/ShcD in ESCs results in a slight

impairment of progression of cell differentiation. Therefore, a role for RaLP/ShcD in regulating the EpiSC transition pathway was proposed.

Understanding of the broad range of potential *in vivo* roles of RaLP/ShcD is still at an early stage. RaLP/ShcD is so far only associated with melanoma cell migration, synaptic transmission at the neuromuscular junction (NMJ), and embryonic stem (ES) cell differenciation (Fagiani *et al*., 2007; Jones *et al*., 2007; Turco *et al*., 2012). These roles are related to the RaLP/ShcD *in vivo* tissue expression pattern. Also, there are still undiscovered putative serine and possible tyrosine phosphorylation residues in both RaLP/ShcD-CH1 and -CH2 domains (Jones *et al*., 2007) that could link RaLP/ShcD to other cascades involved in tumorigenesis. Furthermore, a preliminary yeast two-hybrid screen identified Gab1 as a potential binding partner for the SH2 domain of RaLP/ShcD.

1.6. Grb2-associated binder 1 (Gab1) protein

Previously, Gab1 was isolated as a potential interacting partner for RaLP/ShcD by screening a mouse embryo yeast-two hybrid library, using the RaLP/ShcD-SH2 domain as a bait protein (Prigent, unpublished data). The family of adaptor proteins of Grb2-associated binder (Gab) are scaffolding adaptor molecules. A Gab-like protein was firstly identified in Drosophila called the Daughter of Sevenless (DOS) (Liu and Rohrschneider, 2002). So far, in mammals, three members of the Gab family of adaptor proteins have been identified as Gab1, Gab2, and finally Gab3. All Gab proteins possess an amino terminal PH (pleckstrin-homology) domain and a proline-rich domain (PRD) in the middle which has binding sites for SH3 (Src homology 3) domain-containing proteins.

The tyrosine phosphorylation of Gab1 can be mediated by several growth factors and phosphorylated Gab1 can directly interact with various signal transduction proteins including SHP2 phosphatase, PLC-γ and PI3K (Weidner *et al*., 1996; Nishida *et al*., 1999). Multiple tyrosine phosphorylation sites have been identified that may recruit SH2 or PTB domain-containing molecules as shown in Figure 1.8. *In vitro/in vivo* and mutagenesis assays have characterised several molecules which interact with Gab family proteins. Functional analyses in a number of cell systems have indicated that these interacting proteins are engaged in several signal transduction cascades. Among the Gab proteins, Gab1 is the best characterised. Gab1 has a crucial function regulating signal transduction pathways with various cell surface receptors and is involved in cell differentiation, migration and proliferation.

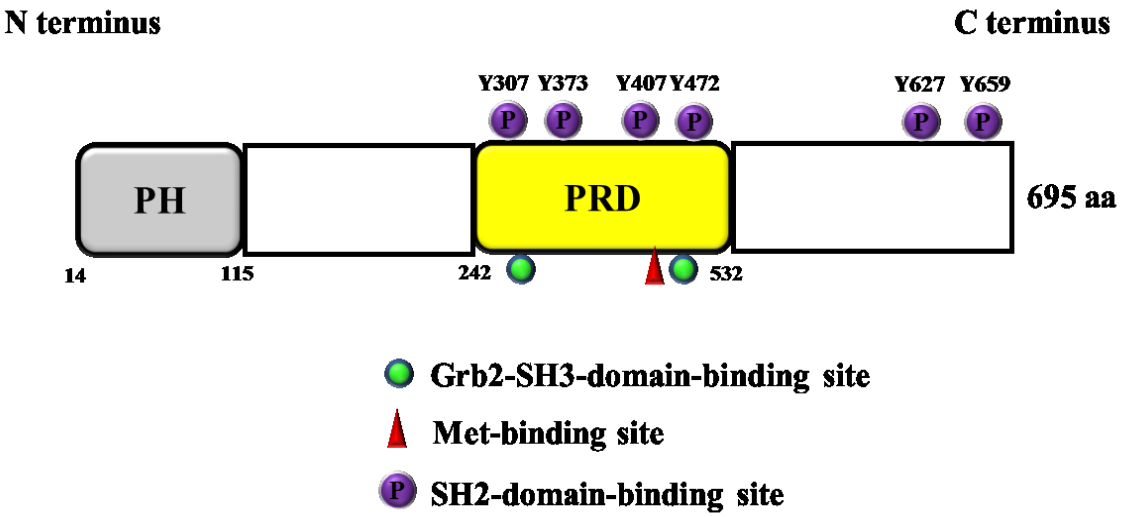

Figure 1.8. Schematic illustration of the domain structure of mammalian Gab1 protein. Gab1 protein comprises an N-terminal PH domain, a proline rich domain (PRD) in the middle and various tyrosines (Y307, Y373 and Y407 for PLCγ; Y472 for p85 PI3 kinase; Y627 and Y659 for SHP2) which can become phosphorylated and are represent possible binding sites favoured by many proteins containing SH2 domains (purple dots). Also, the specific docking site for Met receptor and Grb2 is also shown by the red triangle and green dots, respectively.

1.6.1. The PH (Plecstrin-Homolgy) domain of Gab1

The PH domain of Gab proteins is the most conserved region. PH domains of Gab proteins are able to interact with cell membrane complexes, particularly phosphoinositides such as PIP3, a product of PI3K (Maroun *et al.*, 1999; Rodrigues *et al.*, 2000). Thus it is involved in targeting to the membrane. In addition, the PH domain of Gab1 has a vital role in determining the subcellular localisation of Gab1 upon RTK stimulation, especially by Met. Mutagenesis studies have proved that Gab1 mutants lacking the complete PH domain, or point mutants which fail to bind phospholipid, were unable to regulate tubulogenesis upon Met stimulation (Maroun *et al.*, 1999), indicating that the subcellular localisation is critical in regulating this process. In addition, PH domains of Gab proteins have a common role in all kinds of species.

It has been reported that Gab1 is able to be recruited to PIP3 or to the EGFR in the cell membrane, depending on the strength of the EGF signal (Sampaio *et al.*, 2007). For instance, Gab1 binds to receptor directly via Grb2 after strong EGF stimulation, while PIP3 recruits Gab1 to the cell membrane upon weak EGF stimulation. Recently, it has been shown that interleukin-6 (IL-6) induced translocation of Gab1 to the cell membrane requires PI3K basal activity and requires MAPK activity (Eulenfeld and Schaper, 2009). Basically, the localisation of PH domain containing proteins such as Gab1 to the cell membrane depends on the product of PI3K activity, PIP3. Eulenfeld and Schaper showed that in addition to the PI3K/MAPK activation was required to phosphorylate full-length Gab1 and enable to it to be recruited to the cell membrane. Mutagenesis studies confirmed that when Grb2, SHP2 or PI3K binding sites in Gab1 were mutated, this did not affect the recruitment of Gab1 in the membrane, indicating that Gab1 cell membrane localisation is an upstream mechanism and that when Gab1 is

recruited to the membrane it can become phosphorylated to enable it to associate with these proteins.

1.6.2. The PRD (Proline-Rich) domain of Gab1

The central proline rich domains of Gab proteins possess several PXXP residues which represent potential binding sites for molecules containing SH3 domains (Feng *et al*., 1994). All the members of the Gab protein family interact constitutively with the SH3 domain of the Grb2 adaptor protein (Gu *et al*., 1998; Wolf *et al*., 2002). There are two significant docking sequences for Grb2 that have been identified as the PXXPXR and the PX3RX2KP motifs on Gab1. All Gab proteins share these sites plus a number of other binding sites for signal transduction proteins such as SOS, via Grb2 adaptor protein (Lock *et al*., 2000; Lewitzky *et al*., 2001).

The PRD domain of Gab1 possesses a fragment which is a very unique site for the binding of activated Met receptor (named Met binding site; MBS) as illustrated in Figure 1.8. This unique region was initially identified as thirteen amino acids containing the sequence GMQVPPPAHMGFR of Gab1. This region can directly bind to the Met receptor using a yeast two-hybrid assay, and is distinct from the binding sites of Grb2 (Schaeper *et al*., 2000). Several RTKs such as EGFR were tested for direct interaction with Gab1, however association with this region of Gab1 appears to be unique to the Met receptor (Lock *et al*., 2000).

Unlike Gab2 and Gab3, Gab1 only possesses this unique region for direct binding to the Met receptor. An indirect cascade accounts for the association of Gab proteins and other

RTKs, as the Grb2 protein is a well-known partner to mediate interactions. For instance, Gab proteins constitutively interact with the SH3 domain of Grb2, which allows association with various RTKs such as Met and EGF receptors via the SH2 domain of Grb2 specifically. Consequently, upon growth factor stimulation, Gab proteins with bound Grb2, can be recruited to the activated RTKs. Mutagenesis experiments supported this hypothesis as mutants of Gab1 that did not bind Grb2 failed to be recruited to receptors (Lock *et al*., 2000; Rodrigues *et al*., 2000). Also, Gab1 is not able to become tyrosine phosphorylated upon EGF stimulation of fibroblasts expressing the Gab1 mutant unable to bind Grb2 (Saxton *et al*., 2001), indicating that Grb2 has an important role for association between Gab1 and EGF receptor.

Gab1 is able to associate either directly or indirectly with the Met receptor, but with the EGF receptor it only can interact indirectly. It is interesting to speculate whether Gab1 has different biological functions when associated with two different RTKs such as EGF and Met receptors. Upon hepatocyte growth factor (HGF) stimulation, slow Gab1 tyrosine phosphorylation leads to stimulation of morphological changes in the Madin Darby Canine Kidney (MDCK) cell lines. However, upon EGF stimulation, rapid phosphorylation of Gab1 was observed, and it was not able to promote a morphogenic event (Maroun *et al*., 1999). In addition, the delayed phosphorylation of Gab1 upon HGF stimulation induces MAPK and AKT activation (Gual *et al*., 2000).

1.6.3. Functional Roles of Gab1

1.6.3.1. Gab1 and migration in melanoma

It has been noted that following stimulation of HGF, EGF, VEGF, insulin and PDGF cell surface receptors, Gab1 becomes tyrosine phosphorylated (Holgado-Madruga *et al*., 1996; Laffargue *et al*., 1999). Gab1 is also tyrosine-phosphorylated by oncoproteins such as Tpr-Met and v-Src. Phosphorylated Gab1 may play a role downstream of RTKs, cytokine receptors and maybe other receptor pathways. Although Grb2 constitutively interacts with Gab1, the interaction is enhanced upon stimulation (Nishida *et al*., 1999). Gab1, upon phosphorylation, interacts with SHP2, PI3K, and PLC-γ (Holgado-Madruga *et al*., 1996; Takahashi-Tezuka *et al*., 1998). The HGF/c-Met signalling pathway has been reported to induce various cellular responses, especially the invasive development of the cells in melanomas.

1.6.4. Gab1-mediated Signalling Pathways by the RTKs in melanoma

1.6.4.1. c-Met receptor signalling pathway

The Met receptor possesses two vital tyrosines Y1349 and Y1356 which are well-known binding sites for Gab1. When both tyrosines Y1349 and Y1356 of Met are mutated, it is not able to interact with Gab1. In the case of the single Y1356F mutant of Met, association with Grb2 was abolished but the mutant did not completely lose the ability to bind Gab1 (Bardelli *et al*., 1997; Maroun *et al*., 1999; Nguyen *et al*., 1997). These results indicate that Gab1 possibly prefers to interact with Met receptor through Grb2 using Y1356, but can bind in a direct manner using Y1349 as shown in Figure 1.9.

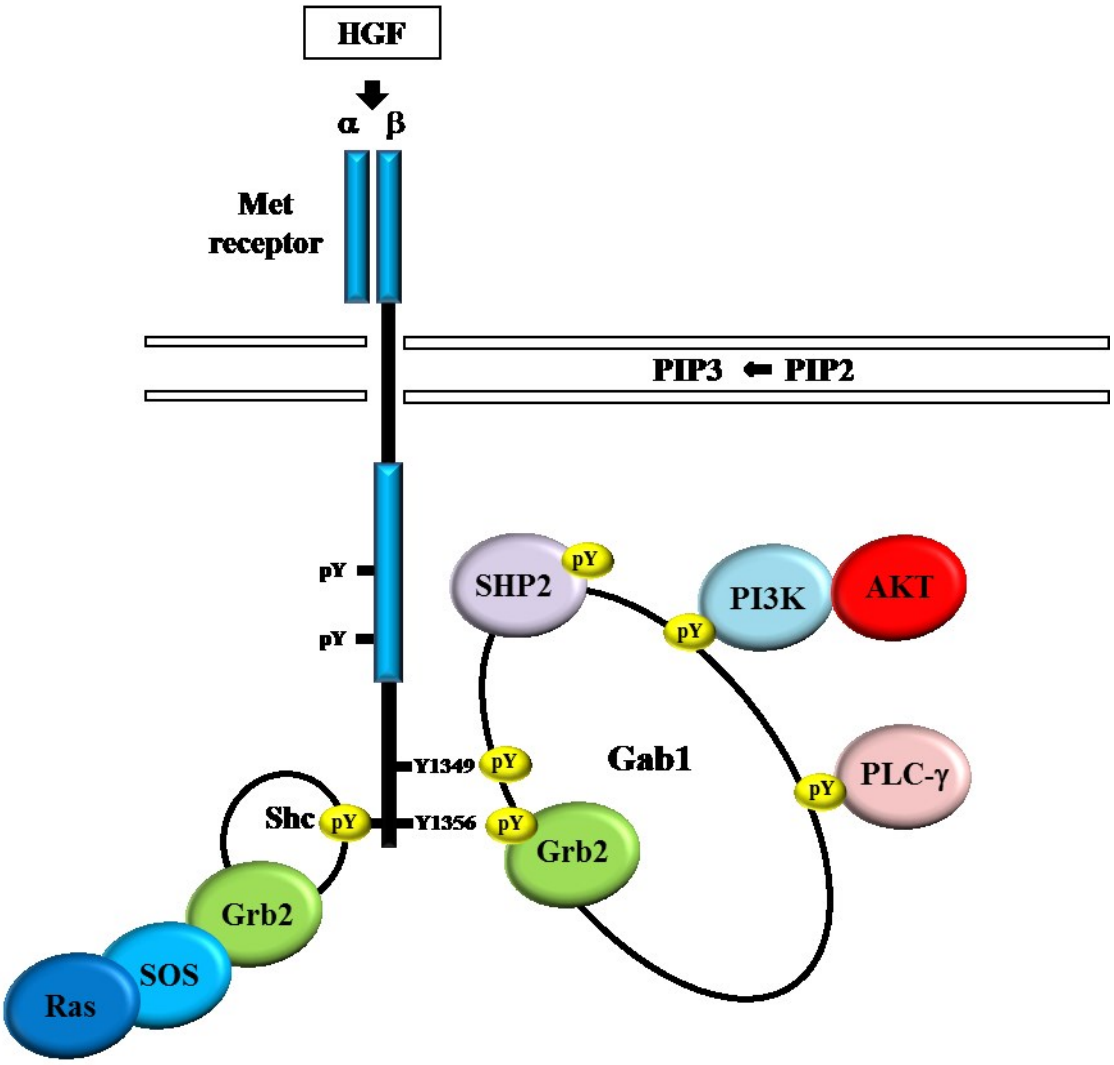

Figure 1.9. A schematic model of the signalling molecules recruited to activate the Met-mediated signalling pathway. Both α and β chains of Met are illustrated. Upon HGF stimulation, Met receptor undergoes dimerisation and phosphorylation then recruits several critical intracellular signalling effectors such as Shc, and Gab1 via its multiple phosphorylation sites, specifically tyrosine 1349 and 1356 residues which are binding sites for Gab1 and Grb2, respectively. These various signalling pathways regulate the HGF-Met induced cellular responses such as cell proliferation, invasion, and survival.

Upon HGF stimulation, Gab1 is recruited and tyrosine phosphorylated which mediates cell branching morphogenesis in several cell lines. This suggests that both tyrosines (Y1349 and Y1356) on Met receptor are an essential effector of the Met signalling pathways with Gab1 (Bardelli *et al*., 1997; Niemann *et al*., 1998).

It has been noted that HGF-Met mediated signalling pathways could require the prolonged activation of Gab1, which leads to enhanced invasion or cell branching morphology. Gab1 can associate with PLC-γ, SHP2 phosphatase, and PI3K as mentioned previously. The association between Gab1 and PLC-γ is abolished by substitution of three tyrosine residues in Gab1 at Y307F, Y373F, and Y407F. Mutation of these three tyrosines also eliminates HGF mediated cell branching tubulogenesis, implicating PLC-γ in this event. However, using selective PLC-γ inhibitors, Gab1-mediated signalling such as branching morphogenesis was incompletely diminished, suggesting that these Gab1 phosphorylation sites may recruit other signal transduction molecules as well as PLC-γ, which have a significant role in cell invasion (Gual *et al*., 2000). In addition, PLC-γ can associate directly, but weakly with the Met receptor (Ponzetto *et al*., 1994), although the preferred mechanism of recruitment is via Gab1 (Figure 1.9).

Furthermore, PI3K activation in association with Gab1 can play a critical part in signal transduction. Mutant Gab1 that fails to bind PI3K is not able to induce branching (Royal and Park, 1995; Niemann *et al*., 1998). Similarly, inhibitors of PI3K including wortmannin and LY294002 prevent HGF induced branching, suggesting that a role for both Gab1 and PI3 kinase in this process. Although the p85 regulatory subunit of PI3K

is able to directly interact with the Met receptor (Ponzetto *et al*., 1994), the activity of PI3K is more elevated when it associates via the Gab1 adaptor, suggesting that PI3K and PLC-γ may bind primarily to the Gab1 adaptor (Bardelli *et al*., 1997; Maroun *et al*., 1999).

1.6.4.2. EGF receptor signalling pathway

EGF receptor stimulation is critical for a number of cellular signalling pathways including cell proliferation, differentiation, apoptosis and cell cycle progression (Hunter, 2000; Schlessinger, 2004). Upon growth factor stimulation, RTKs such as EGF receptor undergo dimerisation and phosphorylation causing the activation of the tyrosine kinase. Consequently, the cytoplasmic tail of EGFR becomes phosphorylated on tyrosine at multiple sites which can recruit a number of proteins with SH2 and PTB domains, leading to activation of many cellular signalling pathways such as the MAPK and the PI3K/AKT signalling cascades as illustrated in Figure 1.10.

Shc and Grb2 adaptor proteins act as crucial adaptors in the EGFR signalling pathways. Grb2 binds directly to activated EGFR or indirectly via phosphorylated Shc (Schlessinger, 2000). This event is regulated by the Grb2 SH2 domain which associates with particular binding sites on Shc or EGFR. The Grb2 adaptor protein interacts with SOS (Cheng *et al*., 1998; Raabe *et al*., 1995) which translocates to the cell membrane and is essential for the activation of the MAPK cascade (Haugh and Lauffenburger, 1997; Kholodenko *et al*., 2000). SOS binds to Ras-GDP (inactive form), promoting the nucelotide exchange to Ras-GTP (active form).

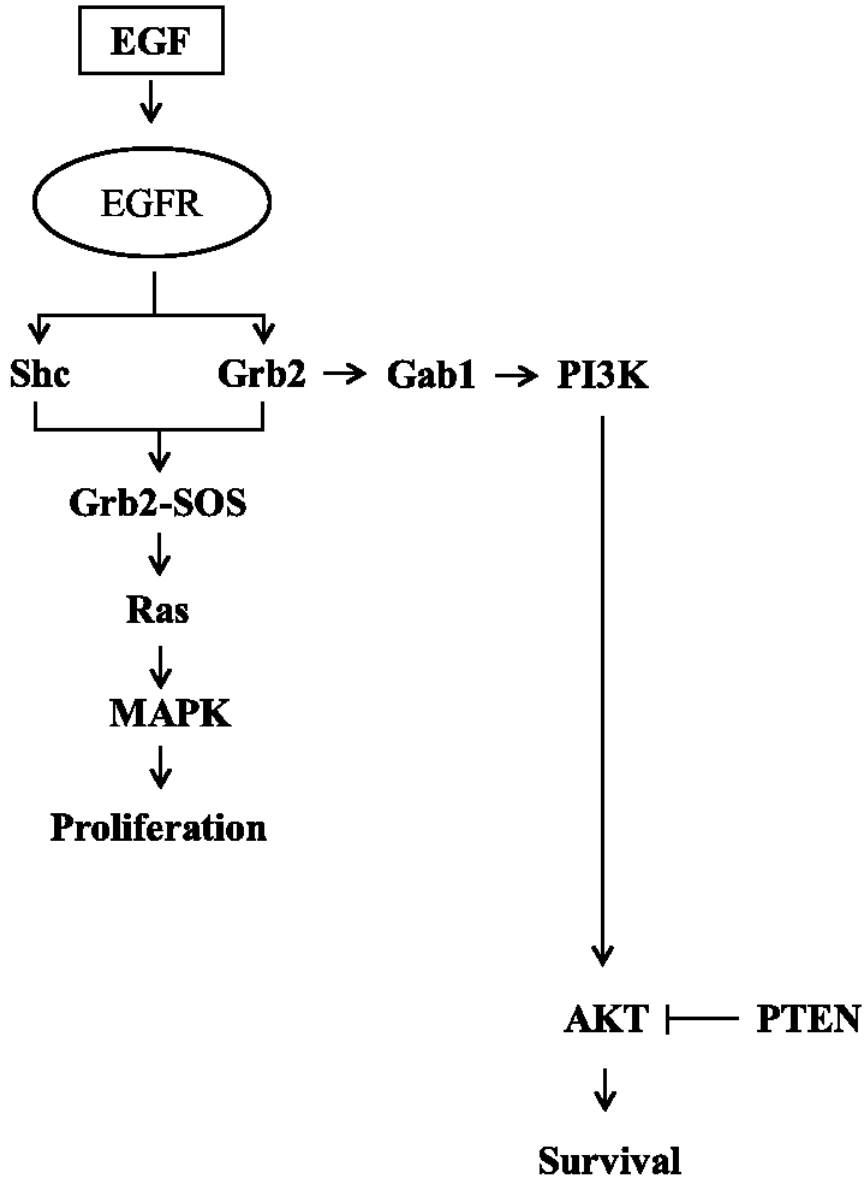

Figure 1.10. Schematic illustration of the EGFR-mediated signalling pathways involving Shc and Gab1. Upon ligand stimulation by EGF, EGF receptor dimerisation and phosphorylation occur and signal transduction molecules such as Shc and Grb2 are recruited. Grb2 is either directly recruited, or indirectly by binding to specific phosphotyrosines on Shc resulting in initiation of the RAS/MAPK pathway leading to cell proliferation. Grb2 also regulates the PI3K/AKT pathway via the Gab1 adaptor protein and leads to cellular survival. PTEN protein acts as a negative regulator of AKT by dephosphorylation of PIP3.

Ras acts as a switch of the MAPK pathway and also various other cellular signalling pathways (Cullen, 2001; Markevich *et al*., 2004). Gab1 is well-understood as an adaptor protein which has a crucial role in the activation of PI3K/AKT pathway by EGFR activation (Rodrigues *et al*., 2000; Mattoon *et al*., 2004).

The interaction between Gab1 and EGFR occurs mostly via Grb2 (Mattoon *et al*., 2004), leading to Gab1 becoming tyrosine phosphorylated allowing binding to the SH2 domains of p85, SHP2, and Ras-GAP. Gab1-p85 complex results in the activation of PI3K at the cell membrane. Also, the location of Gab1 in the plasma membrane induces the Ras/MAPK signalling cascade in various ways. The Grb2 and SOS bound to Gab1 leads to activation of Ras. Phosphorylated Gab1 can also interact with Ras-GAP leading to down-regulation of Ras activity. In addition, SHP2 protein phosphatase, interestingly, can associate with Gab1 which results in the regulation of the MAPK cascade (Agazie and Hayman, 2003; Montagner *et al*., 2005).

1.7. General understanding of Melanoma

Melanocytes originate from the neural crest. They are present in the normal skin and generate the melanin pigment which is responsible for skin colour, and is commonly expressed in the skin but also hair, and the iris of the eye in humans. Following strong exposure to environmental radiation such as UV radiation and ionising radiation (IR), normal melanocytes can develop into melanomas as a result of DNA damage (Rass and Reichrath 2008). Consequently, these radiations can disrupt a number of essential cellular signalling cascades such as the MAPK and the AKT pathways, controlling cell proliferation, survival, invasion, and differentiation that can generate the various types of cancers.

Melanomas are exceptionally aggressive cancers which can arise from different types of tissue such as the eye choroids, and the intestinal mucosa, however, over 90% of melanomas occur in the skin (Liu and Mihm, 2003). Skin melanomas normally originate from benign nevi then progress to the RGP stage and then can expand to the VGP stage in which the malignant melanoma cells can acquire the ability to invade and metastasise (Millar and Mihm, 2006). Basically, melanoma patients with early-stage melanoma may commonly be treated by surgery (Chudnovsky *et al*., 2005). However, patients with late-stage metastatic melanomas are difficult to treat (Gogas *et al*., 2007; Tawbi and Kirkwood, 2007). For instance, melanoma patients with stage IV survive on average 9 months, and five year survival of patients is 5 to 15 % depending on the level of metastasis (Jemal *et al*., 2008).

Genetic alternations have an important role in the progression of melanoma (Bennett, 2008; Hayward, 2003). For example, two genes including the cyclin-dependent kinase inhibitor 2A (CDKN2A) gene, which encodes tumour suppressor proteins p14ARF and p16INK4a, and also the cyclin dependent kinase 4 (CDK4) gene have been found to be mutated in patients with a family history of melanoma. These proteins are involved in regulation of the cell cycle via effects on the retinoblastoma protein, Rb (Giacinti and Giordano, 2006; Fargnoli *et al*., 2006). During the transition of metastatic melanoma from early to late-phase, additional molecular mutations that result in activation of the MAPK and AKT cascades occur. Mutations of N-RAS, B-RAF and PTEN genes are widely involved in these two signalling pathways, and have a vital function in the melanoma development (Polsky and Cordon-Cardo, 2003; Haluska *et al*., 2007). In

addition, the integrin signalling pathway is thought to be involved in metastatic melanoma as upregulation of αvβ3 is often observed (Guo and Giancotti, 2004).

Melanoma is one of the most severe cancers in the skin. Intriguingly, RaLP/ShcD is predominantly expressed in aggressive melanomas which are in the VGP and metastatic stages, but expressed at very low levels in benign nevi and the RGP stage melanomas. Therefore, it is important to elucidate the functions of RaLP/ShcD at this critical phase (Fagiani *et al*., 2007). RaLP/ShcD has a critical role in promoting the migratory mechanisms (both Ras-dependent and -independent) in metastatic melanomas, indicating that the most important role of RaLP/ShcD may be the key mediator of cell migration and invasion. Moreover, RaLP/ShcD overexpression could be associated with the mutations of N-Ras and/or B-Raf in melanoma cells (Fagiani *et al*., 2007).

1.8. Aims and Objectives of this Project

RaLP/ShcD was discovered in 2007 by two different groups, but this protein remains poorly characterised. Based on the structure, and the tissue expression pattern of RaLP/ShcD, there are a lot of possible *in vivo* functions of the protein. Published data indicate a role for RaLP/ShcD is in the migration of melanoma cells (Fagiani *et al*., 2007), in the function of the NMJ (Jones *et al*., 2007), and in embryonic stem cell differentiation (Turco *et al*., 2012). RaLP/ShcD possesses a number of uncharacterised tyrosine phosphorylation sites and putative serine phosphorylation sites in the CH1 and CH2 domains which may promote interactions with other signalling transducer proteins in cellular signalling pathways (Jones *et al*., 2007).

Since RaLP/ShcD is an adaptor protein whose role is to form protein complexes, a key to understanding its function will be to identify interacting proteins. Therefore, the first priority of this project is to determine novel interacting partners of RaLP/ShcD involved in both upstream and downstream signalling pathways, focusing particularly on the SH2 and CH1 domains of RaLP/ShcD in this project.

Gab1 has been characterised as a novel binding partner for the SH2 domain of RaLP/ShcD by a yeast two-hybrid screening and the isolated sequences possess two potential tyrosine phosphorylation sites for RaLP/ShcD. Thus, one aim of this project will be identify the tyrosines on Gab1 responsible for interaction with RaLP/ShcD and to investigate its role in cell migration.

The CH1 domain of RaLP/ShcD, which is the least conserved domain among the other Shc family members, contains unique sequences (six cysteines and two histidines) which could function as a metal binding domain. The second aim of this project will be characterise the CH1 domain of RaLP/ShcD, to determine whether it has the ability to bind metal ions, and to identify novel binding partners that might provide a clue to its role, in particular in melanoma progression.

Chapter 2

Materials and Methods

2.1. Materials

All the materials used during this project were provided from Fisher Scientific, unless otherwise stated.

2.2. Composition of standard Solutions

2.2.1. Western Blot Analysis

10x Tris-Buffered Saline (TBS): 0.1 M Tris (pH 7.4) and 1.5 M NaCl.

SDS-PAGE Running Buffer (50x): 150.15 g Tris Base, 720 g Glycine, 50 g SDS and then made up to 1 litre with dH_2O.

SDS Laemmli Sample Buffer (3x): 0.075 M Tris (pH 6.8), 15% Glycerol, 3% SDS with 0.002% Bromophenol Blue.

Transfer Buffer: 5.82 g Tris Base, 2.93 g Glycine, 200 ml Methanol, 1.875 ml 20% SDS made up to 1 litre with dH_2O.

Blocking Buffer: 5% Dried-skimmed milk powder in 1x Tris-buffered Saline with 0.1% Tween-20.

ECL Detection Reagents: 0.1 M Tris-HCl (pH 8.0), 1.25 mM Luminol 5-amino-2, 3-dihydro-1, 4-pthlazinedione (Sigma), 0.2 mM p-Coumaric acid (Sigma) and 0.03% H_2O_2 (Sigma).

Blot Strip Buffer: 62.5 mM Tris-Base (pH 7.4) containing 2% SDS.

PBS (50x): 400 g NaCl (pH 7.4), 10 g KCl, 72g Na_2HPO_4, 12g KH_2PO_4 made up to 1 litre with dH_2O (autoclaved).

2.2.2. Immunoprecipitation

Triton Lysis Buffer (TLB): 0.05 M Tris-HCl (pH 7.5), 0.005 M EGTA, 0.15 M NaCl, 0.025 M Benzamidine (Sigma), 1% Triton X-100, 0.001 M PMSF, 0.05 M NaF, 0.001 M Na_3VO_4 containing Protease inhibitor cocktail (Sigma) (1/100).

Wash buffer: 0.1% Triton X-100, 0.15 M NaCl and 0.05 M Tris (pH 7.4).

2.2.3. Bacterial Cloning and Transformation

Luria Bertani (LB) Broth: 10 g bacto-tryptone (Melford), 5 g yeast extract (Sigma), 10 g NaCl, made up to 1 litre with dH_2O. The solutioin was autoclaved prior to use. To prepare solid medium, 15 g bacto-agar (Sigma) was added per litre of LB and was autoclaved.

2x YT medium: 16 g bacto-tryptone, 5 g NaCl, 10 g bacto-yeast extract, made up to 1 litre with dH_2O, then autoclaved.

SOC broth: 2% bacto-tryptone, 2.5 mM KCl, 10 mM NaCl, 0.5% bacto-yeast extract (autoclaved). In addition, 0.02 M glucose (filter-sterilised) and 2 M sterile $MgCl_2$ was added immediately prior to use to give a final concentration 20 mM and 10 mM, respectively.

NZY^+ broth: 5 g NZ amine (casein hydrolysate), 2.5 g NaCl and 2.5g yeast extract, made up to 500 ml with dH_2O and was autoclaved before use. Also the following filter-sterilised components were added just before use; 5 ml 2 M glucose, 6.25 ml 1 M $MgCl_2$ and 6.25 ml $MgSO_4$.

1x TE (Tris-EDTA) solution: 10 mM Tris (pH 8.0) and 1 mM EDTA.

$Ca^{2+}Mn^{2+}$ solution: 2x stock solution - 70 mM $MnCl_2.4H_2O$ (pH 5.5), 40 mM $NaOAc.3H_2O$, and 100 mM $CaCl_2.2H_2O$ (filter-sterilised). $Ca^{2+}Mn^{2+}$ solution (filter-sterilised) containing 15% glycerol was prepared by adding 3 ml of 50% v/v glycerol and 2 ml of dH_2O to 5 ml of 2x stock solution.

2.2.4. Agarose Gel Electrophoresis

10x TAE (Tris/Acetate/EDTA) Buffer: 48.4 g Tris-Base (pH 7.0), 11.42 ml Glacial acetic acid with 7.44 g Ethylenediaminetetraacetic acid (EDTA) and made up to 1 litre with dH_2O.

6x Orange G loading dye: 0.01 M Tris-HCl (pH 7.6), 0.06 M of EDTA, 60% Glycerol and 0.15% Orange G.

2.2.5. GST-pull down assay

Extraction Buffer: 0.05 M Tris-HCl (pH 7.5), 0.005 M DTT (Melford), 0.15 M NaCl, 0.001 M PMSF, 0.002 M EDTA, 0.005 M Benzamidine, 10 µg/ml PAL inhibitors (pepstatin, aprotinin and leupeptin), 1% Triton X-100 and 10% glycerol.

Lysis Buffer: 0.05 M Tris-HCl (pH 7.5), 0.15 M NaCl, 0.01 M Benzamidine, 0.002 M EDTA, 1% Triton X-100, 0.001 M PMSF, 0.001 M Na_3VO_4, 0.01 M DTT, 0.05 M NaF, 10% glycerol and protease inhibitor cocktail (Sigma) (1/100).

Wash Buffer: 0.05 M Tris-HCl (pH 7.5), 10% glycerol, 1% Triton X-100, 0.15 M NaCl and 0.001 M DTT.

Hi-LO buffer: 0.05 M Tris (pH 7.4), 0.825 M NaCl and 1% (v/v) NP-40.

2.2.6. SDS-PAGE Gel Staining

Coomasie Blue Stain solution: 0.625 g Brilliant Blue R-250 (Sigma) was dissolved in a mixture of 25 ml Glacial acetic acid, 112.5 ml Methanol and 250 ml dH_2O and then filtered.

Destain Solution: 125 ml Methanol, 35 ml Glacial acetic acid made up to 500 ml with dH_2O.

2.2.7. Yeast Two-Hybrid screen

YPD broth: 5 g Yeast Nitrogen base lacking amino acids (Sigma), 10 g bacto-peptone, made up to 500 ml with dH_2O and adjusted to pH 5.8 to 6.0 and autoclaved prior to use. Also, 25 ml 40% glucose (filter-sterilized) was added before use. For YPD agar plate, 9g bacto-agar was added per 500 ml and autoclaved.

Selective drop-out (-Leu-Trp-Ura) plates: 3.35 g Yeast Nitrogen base lacking amino acids, 0.3 g drop-out mix (CMS-HIS-TRP-LEU-URA) supplied by Q-Biogene containing 25 mg L-Histidine (Sigma).

Selective drop-out (-Leu-Trp-His-Ura) plates: as above, without addition of histidine.

Z-buffer (pH 7.0): 8.05 g $Na_2HPO_4.7H_2O$, 0.375 g KCl, 2.75 g $NaH_2PO_4.H_2O$, 0.125 g $MgSO_4.7H_2O$, made up to 500 ml with dH_2O.

Z-buffer/X-gal substrate solution: 25 ml Z-buffer, 0.0675 ml β-mercaptoethanol and 0.4175 ml X-gal stock solution

X-gal stock: 5-Bromo-4-chloro-3-indolyl-β-D-galactopyranoside (X-Gal), 20 mg/ml dissolved in dimethylformamide (DMF), stored at -20°C freezer (sealed with aluminium foil).

Yeast Lysis Buffer: 0.01 M Tris-HCl (pH 8.0), 2% Triton X-100, 100 mM NaCl, 1% SDS, and 0.001 M EDTA.

M9 Minimal medium (10x): 58 g Na_2HPO_4, 30 g KH_2PO_4, 5 g NaCl, 10 g NH_4Cl, made up to 1 litre with dH_2O then adjusted to pH 7.2 ~ 7.6 and autoclaved. 2 ml sterile filtered Thiamine (2 mg/ml) was also added per litre. For M9 agar plates, 10 g bacto-agar was dissolved in 1x M9 minimal medium (autoclaved) then cooled to 60°C, 5 ml strile filtered 0.01 M $CaCl_2$, 0.5 ml 1 M $MgSO_4$, 5 ml 20% glucose and 0.5 ml Thiamine (from 2 mg/ml stock) were added.

ONPG (ortho-nitrophenyl-β-D-galactopyranoside): freshly prepared and dissolved in Z-buffer (4 mg/ml) by shaking for 1 to 2 hours.

2.2.8. Plasmid Minipreparations by Alkaline Lysis/LiCl Method

Solution 1: 0.01 M EDTA (pH 8.0), 0.025 M Tris-HCl (pH 8.0) and 0.05 M Glucose followed by autoclaving before use.

Solution 2: 0.2 M NaOH, 1% SDS freshly prepared every time before use.

Solution 3: 29.44 g Potassium acetate, 11.5 ml Glacial acetic acid made up to 100 ml with dH_2O.

2.2.9. Preparation of SDS-PAGE Gels

SDS-PAGE Resolving Composition:

Gel / Reagent (ml)	8%	10%	15%
30% Acrylamide	5.34	6.67	10
1 M Tris-HCl, pH 8.8	7.5	7.5	7.5
10% APS (Sigma)	0.15	0.15	0.15
10% SDS	0.1	0.1	0.1
TEMED (Sigma)	0.02	0.02	0.02
dH_2O	6.9	5.6	2.2

SDS-PAGE Stacking Gel:

	3% Gel
30% Acrylamide	1
1 M Tris-HCl, pH 6.8	1.2
10% APS	0.075
10% SDS	0.1
TEMED	0.012
dH_2O	7.6

2.2.10. Primary and Secondary Antibodies

2.2.10.1. Primary antibodies

Company	**Name**	**Type**	**Dilution in W.B/I.P/I.F**
Abcam	anti- RaLP/ShcD (Shc4)	Mouse Monoclonal	1:1000 (W.B)
Sigma	anti-GFP	Mouse Monoclonal	1:1000 (W.B) 5 µg (I.P)
Sigma-Aldrich	anti-FLAG M2	Mouse Monoclonal	1:1000 (W.B) 5 µg (I.P)
Custom made Cambridge Biosciences	anti-RaLP (serum)	Rabbit Polyclonal	1:1000 (W.B)
Cell Signalling	anti-Met	Mouse Monoclonal	1:1000 (W.B)
Santa Cruz	anti-EGFR	Rabbit Polyclonal	1:1000 (W.B)
Santa Cruz	anti-PDGFRβ	Rabbit Polyclonal	1:1000 (W.B)
Millipore	anti-Gab1	Rabbit Polyclonal	1:1000 (W.B) 5 µg (I.P)
Made in Leicester (Dr. Sally Prigent)	anti-GST	Rabbit Polyclonal	1:1000 (W.B)
BD Transduction Laboratories	anti-βCatenin	Mouse	1:2000 (W.B)
Santa Cruz	anti-HA	Rabbit Polyclonal	1:1000 (W.B) 1:100 (I.F) 5 µg (I.P)
Sigma	anti-Vimentin	Mouse Monoclonal	1:1000 (W.B)
Santa Cruz	Flt-1 (VEGF receptor 1)	Rabbit Polyclonal	5 µg (I.P)
Serotec	anti-PK Tag	Mouse	5 µg (I.P)
Santa Cruz	anti-Caveolin	Rabbit	5 µg (I.P)
Sigma	anti-Flotillin 2	Rabbit	5 µg (I.P)
Sigma	mouse IgG	Mouse	5 µg (I.P)

Table 2.1. The list of primary antibodies employed for Western blot (W.B), Immunoprecipitaion (I.P) and immunofluorescence (I.F) experiments.

2.2.10.2. Secondary antibodies

Company	Name	Dilution in W.B/I.F
Invitrogen	Alexa Fluor 594 Goat anti-Rabbit IgG (H+L)	1:1000 (I.F)
Invitrogen	Alexa Fluor 594 Goat anti-Mouse IgG (H+L)	1:1000 (I.F)
Jackson ImmunoResearch	anti-Mouse HRP	1:10,000 (W.B)
Jackson ImmunoResearch	anti-Rabbit HRP	1:10,000 (W.B)

Table 2.2. Western blotting (W.B) and immunofluorescence (I.F) experiments.

2.2.11. Materials for Yeast-Two Hybrid (Y2H) Screen

2.2.11.1. Materials for Y2H screen

The L40 yeast strain (Invitrogen), *S. cerevisiae* strain {MATa *his*3Δ200 *trp*1-901 *leu*2-3112 *ade*2 LYS:: (4*lexA*op-HIS3) URA3:: (8*lexAop-lacZ*)}, was employed as host. This yeast strain additionally carries the *HIS3 and LacZ* reporter genes (Denisenko *et al*., 1996). The pBTM116/PDGFR vector encodes the LexA DNA binding domain and *TRP1* gene as a selection marker as well as the PDGFR kinase sequence (Liouben *et al*., 1996). The pVP16 contains the *LEU2* gene as a selection marker, it also contains *Bam*HI and *Not*I restriction sites for cloning as described in Figure 2.1.

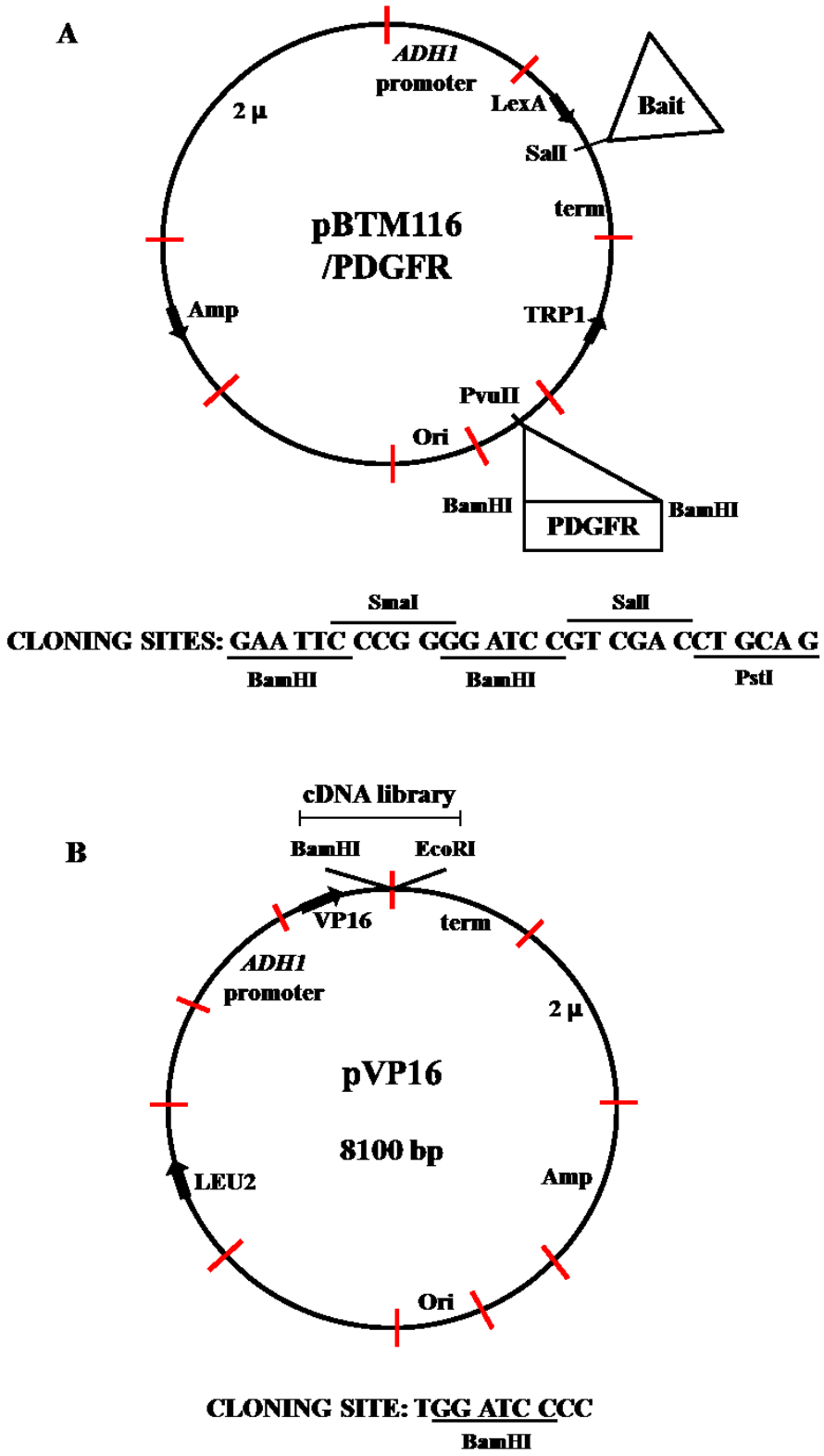

Figure 2.1. Vector maps of transformed bait plasmid including LexA DNA binding domain and PDGFR tyrosine kinase (A) and VP16 library plasmid encoding DNA activation domain (B). The pBTM116/PDGFR and pVP16 vectors were obtained from Jonathan Cooper (Liouben *et al*., 1996) and Stan Hollenberg (Hollenberg *et al*., 1995), respectively.

2.3. Methods

2.3.1. Molecular Biology Methods

2.3.1.1. Preparation of competent E.coli BL21(DE3) and DH5α cells

Either a single colony of BL21(DE3) or DH5α competent cells was inoculated into 10ml of 2x YT followed by incubation at 37°C overnight with shaking. 2 ml of a small scale overnight culture was inoculated into 200 ml of 2x YT (pre-warmed), incubated at 37°C in a shaking incubator until the OD_{600} reached 0.2 (~ 2 hours) and 1 M $MgCl_2$ was added to give a final concentration of 20 mM. The bacterial cells were incubated for approximately 50 minutes until the OD_{600} reached 0.45 to 0.55 and then transferred into 4x 50 ml Falcon tubes. The tubes was incubated on ice for 2 hours and centrifuged at 3,000 rpm for 5 minutes at 4°C. The bacterial pellets were resuspended in 25 ml chilled $Ca^{2+}Mn^{2+}$ solution and left on ice for 45 minutes. The bacterial cells were pelleted by centrifugation for 5 minutes at 3,000 rpm and pellets were then resuspended in a total of 5 ml $Ca^{2+}Mn^{2+}$ solution containing 15% glycerol. The cells were aliquoted into fresh 1.5ml pre-chilled eppendorf tubes (100 µl/tube) and frozen quickly in liquid nitrogen then stored at -80°C until needed.

2.3.1.2. Preparation of HB101 (Leu-) electrocompetent cells

From 5 ml of small scale overnight culture, 2x 0.5 ml of culture was transferred into two 250 ml flasks containing 150 ml of LB medium, then incubated at 37°C with shaking for a couple of hours until the OD_{600} reached 0.6 to 0.8 and then cells were placed onto ice for 20 minutes. Cells were pelleted in six 50 ml Falcon tubes by centrifugation at maximum speed. The each pellet was resuspended in 20 ml of 10% pre-chilled glycerol and combined into two 50 ml Falcon tubes and centrifugation was repeated. The cell pellets were washed three times in 40 ml of pre-chilled 10% glycerol

and centrifuged. The bacterial pellets were resuspended in 1.05 ml of pre-chilled 10% glycerol and then cells were aliquoted into fresh eppendorf tubes (50 µl/tube). The aliquots of cells were frozen rapidly on liquid nitrogen and stored at -80°C.

2.3.1.3. Bacterial Cell transformation

Competent cells used for routinely for plasmid preparation (DH5α) or BL21(DE3) used for protein expression were used for bacterial cell transformation. The competent cells were thawed gently on ice. 50 µl of DH5α or BL21(DE3) competent cells were transferred into a fresh pre-chilled eppendorf tube, and 50 ng of DNA was carefully added to the cells. The transformation mixture was mixed by gently flicking of the tube and incubated on ice for 30 minutes. Bacteria were then incubated at 37ºC in a water bath for 5 minutes. The mixtures were left for two minutes on ice and 500 µl of LB medium (sterilised and autoclaved) was then added. Bacteria were then incubated for 1 hour in a shaking incubator at 220 rpm at 37ºC, and 500 µl of mixture was plated out on LB agar plates containing appropriate antibiotic. The plates were incubated in an incubator overnight at 37ºC. The following day, a single colony from the plate was inoculated into a universal tube containing 5 ml of LB medium with appropriate antibiotic, and the culture was then incubated in a shaking incubator at 37ºC at 220 rpm overnight.

2.3.1.4. Mini Plasmid DNA purification using QIAGEN spin columns

2 ml of an overnight culture of *E.coli* containing the desired plasmid was transferred into a fresh eppendorf tube followed by centrifuging at maximum speed for 1 minute. The supernatant was removed and the pellet was re-suspended in 250 µl of buffer P1 containing RNase. 250 µl of buffer P2 was added and mixed thoroughly by inverting the

tube 6 to 8 times. 350 µl of buffer N3 was added, mixed immediately by inverting the tube 6 to 8 times. The tubes were centrifuged for 10 minutes at maximum speed and the supernatant containing plasmid DNA was transferred to a QIAprep spin column in a collection tube. The column was centrifuged for 1 minute at maximum speed, the flow through was discarded and then it was rinsed with 500 µl of buffer PB and centrifuged at maximum speed for 1 minute, again discarding the flow through.

To wash the column, 750 µl of buffer PE was applied and centrifuged once, the flow through was discarded and an additional centrifugation was performed to remove remaining wash buffer. The spin column was placed in a fresh eppendorf tube and the DNA was eluted by addition of 50 µl buffer elution buffer (EB). The sample was left for 1 minute at room temperature and centrifuged for 1 minute at maximum speed. The eluted plasmid was stored at -20ºC.

2.3.1.5. Plasmid DNA purification using QIAGEN Plasmid Maxi kit

0.5 ml of small scale bacterial culture was inoculated into 500 ml LB containing appropriate antibiotic and grown overnight. The culture was transferred into 250 ml centrifuge bottles followed by centrifugation in a Sorvall Evolution centrifuge (SLA-1500 rotor) at 6,000 rpm at 4ºC for 20 minutes.

The supernatant was discarded and the pellet was resuspended in 10 ml of buffer P1 containing RNase, 10 ml of buffer P2 was added and the contents was thoroughly mixed by inverting the tube 6 to 8 times, followed by an incubation at room temperature for 5 minutes. 10 ml of pre-chilled buffer P3 was added, and mixed by inverting vigorously 6

to 8 times, and incubated for 20 minutes on ice. The bacterial lysates were transferred into a centrifuge tube and centrifuged using a Sorvall SS-34 rotor at 13,000 rpm for 30 minutes at 4ºC. The supernatant was removed into fresh centrifuge tube and centrifuged once more at 4ºC at 13,000 rpm for 15 minutes to remove particulate material. The clear supernatant was transferred into a QIAGEN-tip 500, which had been pre-equilibrated with 10 ml of buffer QBT, and allowed to attach to the resin via gravity flow. The QIAGEN-tip was rinsed twice with 30 ml of buffer QC.

To elute the DNA, 15 ml of buffer QF was added into the tip, and then the eluted DNA was precipitated by addition of 10.5 ml of isopropanol (room-temperature), with thoroughly mixing. The precipitated material was immediately centrifuged at 14,000 rpm for 30 minutes at 4ºC and the supernatant was gently removed. To wash the DNA pellet, it was resuspened in 5 ml of 70% ethanol (room-temperature) and centrifuged once again at 14,000 rpm for 10 minutes at 4ºC. The supernatant was carefully removed and the pellet left to air-dry for 10 to 20 minutes at room temperature. The DNA was dissolved in 500 µl of TE (pH 8.0). Finally, the concentration of the DNA was then measured as described in *2.3.1g* and stored at -20ºC.

2.3.1.6. Plasmid Minipreparations by Alkaline Lysis/LiCl Method

1.5 ml of an overnight culture was centrifuged for 2 minutes at maximum speed at room temperature and the supernatant discarded. To lyse the cells, the pellet was vigorously vortexed by adding 100 µl of pre-chilled Solution 1 and left for 5 minutes at room temperature. 200 µl of Solution 2 was added and the cell lysates were inverted 10 times followed by incubation for 5 minutes at room temperature. To precipitate insoluble materials 150 µl of pre-chilled Solution 3 was added and inverted 10 times, and

incubated for 5 minutes at room temperature. 600 µl of 5 M Lithium chloride (LiCl) was then added and lysates were centrifuged at maximum speed for 5 minutes at room temperature. 1 ml of supernatant was transferred into a fresh eppendorf tube containing 600 µl of isopropanol, the solution was mixed thoroughly and centrifuged at maximum speed for 5 minutes at room temperature. The pellet was washed once with 1 ml 70% ethanol and air-dried for 5 to 10 minutes at room temperature. Finally the plasmid DNA was dissolved in 40 µl of sterile TE (pH8.0).

2.3.1.7. Measurement of DNA concentration

In order to measure DNA concentration, 5 µl of the purified DNA was diluted in 1 ml of dH_2O (1:200 dilution) and absorbance was measured at 260 nm using a spectrophotometer. DNA concentration was calculated based on the knowledge that a 50µg/ml solution of DNA has an OD_{260} of 1.

2.3.1.8. DNA separation by Agarose gel electrophoresis

DNA was analysed on 1% to 2.5% agarose gels prepared in 1x TAE buffer. Agarose was dissolved by microwaving for about 2 minutes. The gel solution was left it to cool (about 60ºC) on the bench and 10 mg/ml of ethidium bromide (EB) was added to a final concentration of 2 µg/ml and then the gel solution was poured into the gel tank. 6x Orange G loading buffer was added to DNA samples prior to loading on the gel. The DNA was run at 120 Volts until the loading dye reached 70 % of the length of the gel, and then the DNA was visualised using a UV transilluminator with the GeneSnap software. 1Kb DNA ladder (Invitrogen) was run alongside samples.

2.3.2. Site-Directed Mutagenesis

Site-directed mutagenesis was performed using the QuikChange® II Site-Directed Mutagenesis Kit from Stratagene. Forward and reverse oligonucleotide primers were used as indicated in Table 2.3 (Invitrogen). Mutation mixtures were set up following manufacturer's recommendation using 50 ng of template, 5 µl of 10x reaction buffer, 125 ng of each of the forward and reverse primer, 1 µl of dNTP mix and ddH_2O to a final volume of 50 µl. 1 µl of *PfuUltra* HF DNA Polymerase (2.5 Unit/µl) was added. Oligonucleotides indicated in Table 2.3 were used to generate the Y183F mutation in full-length GFP-Gab1.

Gene	Primer Sequence (5'→3')
Gab1Y183F Forward	GAG GAT CCT CAA GAC TTC CTG TTG CTC ATC AAC
Gab1Y183F Reverse	GTT GAT GAG CAA CAG GAA GTC TTG AGG ATC CTC

Table 2.3. Primers for the point-mutation of tyrosine (Y) 183 to phenylalanine (F) on Gab1

After the PCR reaction was completed, 1 µl of *Dpn I* restriction enzyme (10 Unit/µl) was immediately added to the amplification product. The reaction mixture was mixed gently and thoroughly by pipetting up and down a couple of times and then the reaction was incubated for 1 hour at 37°C to allow digestion of the parental methylated dsDNA. A 50 µl aliquot of XL1-Blue supercompetent cells was gently thawed on ice. Cells were gently transferred into a pre-chilled 14 ml of BD Falcon polypropylene round-bottom tube from Stratagene. 1 µl of the *Dpn* I-treated DNA was transferred to the aliquot of cells and the tube was incubated for an additional 30 minutes on ice. The transformation

reaction was then heat-pulsed for 45 seconds in a 42°C water bath and it was placed on ice for 2 minutes.

After the incubation, 0.5 ml of preheated NZY^+ broth pre-warmed to 42°C was transferred to the tube followed by incubation in a shaking incubator at 225 rpm at 37°C for 1 hour. Roughly 250 µl of transformation mixture was then plated out on a LB agar plate containing appropriate antibiotic and the plate was incubated at 37°C overnight. The following day, transformed colonies were picked from the plate and inoculated into universal tubes containing 5 ml of LB with appropriate antibiotic, and then the tubes were incubated in a shaking incubator at 37°C at 220 rpm overnight.

2.4. Cell culture

2.4.1. Cell lines

Cell lines employed in these studies included 518.A2 (from now on referred as to 518) (Dunnion *et al*., 1999), DAUV (Moreau-Aubry *et al*., 2000), MDA-MB 435, Mel17, Gerl43 and 1361, which are all human melanoma cell lines, that were a gift from Dr. Mike Browning from the Department of Infection, Immunity and Inflammation. B16F10 mouse melanoma cell lines were a gift from Dr. Christine Pullar from the department of Cell Physiology and Pharmacology. HeLa (cervical carcinoma cell line) and HEK293 (Human Embryonic Kidney) cell line were also used. F4 (HEK293 cells stably expressing FLAG-RaLP/ShcD) and G5 (HEK293 cells stably expressing GFP-RaLP/ShcD) cell lines were generated by Dr. Samrein Ahmed.

2.4.2. Maintenance of Cell lines

All the reagents used for cell culture, including DMEM (Dulbecco's Modified Eagles Medium), Trypsin-EDTA, Penicillin/Streptomycin and FBS (Fetal Bovine Serum) were supplied by GIBCO. All the cell lines were maintained in DMEM containing 1% of Penicillin/Streptomycin antibiotics and 10% of FBS and then they were grown at 37ºC with 5% CO_2 under humidified conditions. Once the cells were grown in a range of 80 ~ 90% of confluence in T75 flasks or 10 cm tissue culture dishes, the cells were split by adding 1x trypsin-EDTA (under sterile conditions).

2.4.3. Cell culture

Frozen cells, which were stored in liquid nitrogen, were thawed quickly and added to 10ml of pre-warmed fresh DMEM containing 10% of FBS and 1% of Penicillin/Streptomycin antibiotics. Cells were then centrifuged for 5 minutes at 1,100rpm in a bench top centrifuge. The supernatant was discarded and the cells were resuspended in 10 ml of fresh medium, then seeded in a 10 cm tissue culture dish or a T75 flask (75 cm^2). The cells were grown in an incubator at 37ºC with 5% CO_2.

2.4.4. Freezing of Cell lines

The cell lines were stored in a liquid nitrogen tank for long-term storage purpose. First of all, when the cell lines were approximately 90% confluent, a flask was washed twice with PBS. 2 ml of 1x trypsin-EDTA was added, allowed to cover the entire cell surface and then discarded. The flask was incubated for 2 to 3 minutes at 37ºC and the cells were resuspended with 2 ml of filtered FBS followed by transferring into a fresh universal tube. An equal volume of filtered freezing medium (DMEM and DMSO in a 4:1 ratio) was added drop-wise to the tube. Finally, 1 ml of cell suspension was

aliquoted into cryovials and slowly frozen to -80ºC for a couple of days before being transferred to a liquid nitrogen tank for long-term stroge.

2.4.5. Transfection of Cells

An appropriate amount of DNA (as recommended in the manufacturer's protocol) was used for transfection with a cell density of about 50 to 70%. Either ExGen500 *in vitro* transfection reagent or Turbofect *in vitro* Transfeciton Reagent from Fermentas, or Lipofectamine 2000 from Invitrogen were used for transfection followed by manufacturer's protocol.

2.4.6. Cell line Stimulation

2.4.6.1. EGF or PDGF stimulation

Cells were washed twice with 1x PBS and pre-warmed fresh medium was then added containing 100 ng/ml EGF or PDGF from Pepro Tech. The Cells were incubated for 5 minutes (EGF) or 2 minutes (PDGF) at 37ºC in a 5% of CO_2 incubator.

2.4.6.2. Camptothecin (CPT) treatment

Cells were rinsed twice with 1x PBS. After that fresh pre-warmed medium was added with a final concentration of 50 µM CPT from Sigma and then incubated for 24 hours in a 5% CO_2 incubator at 37ºC.

2.4.6.3. Cisplatin (CIS) treatment

Cells were washed twice with 1x PBS and then fresh pre-warmed medium was added containing a final concentration of 100 μM cisplatin and cells were incubated for 24 hours at 37 ºC in a 5 % of CO_2 incubator.

2.4.6.4. Leptomycin B (LMB) treatment

Cells were serum starved for 4 hours and then treated with LMB (5 ng/ml) from Sigma for 3 hours. The cells were subsequently fixed and visualised using a confocal microscope.

2.5. SDS-PAGE and Western blotting

2.5.1. SDS-PAGE

Samples were boiled in a heating block at 100ºC for 5 to 10 minutes and were then loaded onto an SDS polyacrylamide gel alongside an appropriate protein Molecular Weight Marker, and gels were run at 120 to 150 Volts. Depending on the molecular weight of the protein of interest, 8%, 10% and 15% gels were employed (Laemmli., 1970). Various molecular weight markers were used including pre-stained protein molecular weight markers; SDS7B2 from Sigma, Precision Plus Protein™ Standards from BIO-RAD (Catalog #161-0373), PageRuler Prestained Protein Ladder from Thermo Scientific and unstained marker from Sigma (SDS7).

2.5.2. Western blot Analysis

After SDS-PAGE, gels were soaked in transfer buffer for 10 to 15 minutes at room temperature prior to transfer. A transfer sandwich was assembled by applying 6 sheets of 3MM Whatman paper pre-soaked in transfer buffer, the Whatman protran nitrocellulose transfer membrane, the SDS-PAGE gel and 6 sheets of 3MM Whatman paper.

Transfer was carried out using a Bio-Rad Trans-blot SD Semi-dry transfer cell for 90 minutes at 22 Volts. To block non-specific binding sites, the nitrocellulose membrane was incubated in blocking buffer containing 5% (w/v) of skimmed milk powder dissolved in 1x Tris-buffered Saline with 0.1% (v/v) Tween-20 for 1 hour at room temperature. After the incubation, the membrane was incubated with primary antibody which was diluted in blocking buffer at 4ºC overnight.

The next day, the membrane was rinsed 4 times for 10 minutes each with 1x Tris-buffered Saline with Tween-20 (0.1% v/v). Then it was incubated with secondary antibody coupled to horseradish peroxidase for 1 hour at room temperature. Again, the membrane was washed 4 times for 10 minutes each in 1x Tris-buffered Saline with 0.1% Tween-20. Bound secondary antibody was detected by developing with ECL detection solution for 1 minute. Finally, the proteins of interest were visualised on X-ray films from Fuji developed in the Compact X4 developer from X-ograph Imaging Systems.

2.5.3. Stripping of Nitrocellulose Transfer Membranes

When nitrocellulose transfer membranes were to be re-probed, bound antibodies were removed by incubating in 50 ml of blot strip buffer containing 350 µl of β-mercaptoethanol in a sealed container. The membrane was then incubated at 55ºC for 50 minutes in a water bath. The membrane was rinsed with dH_2O then washed 4 times for 10 minutes each using Tris-buffered Saline with 0.1% Tween-20. The membrane was then blocked with blocking buffer for 1 hour at room temperature before addition of antibodies.

2.6. GST (Glutathione S-transferase) pull-down experiment

2.6.1. GST-fusion protein preparation

Either the GST-RaLP/ShcD-SH2 or GST-RaLP/ShcD-CH1 plasmid DNA, which were previously prepared by ProTex (Department of Biochemistry, Leicester University), were transformed into BL21(DE3) competent bacterial cells, and plated on LB/Agar plates containing appropriate antibiotic in a 37ºC incubator overnight.

A colony was inoculated into 5 ml of LB containing appropriate antibiotic, and cells were grown with shaking overnight at 37ºC at 220 rpm. The overnight cultures were inoculated (1:50 to 1:100 ratio) into 500 ml of LB broth containing appropriate antibiotic and grown in a shaking incubator at 30ºC at 220 rpm for an additional 1 hour. A final concentration of 0.2 mM IPTG (isopropyl-β-D-thio-galactopyranoside) was then added to the 500 ml of culture and incubated for 6 hours at 30ºC in a shaking incubator. The bacterial culture was centrifuged at 6,000 rpm at 4ºC for 20 minutes. The pellet was extracted with 10 ml of extraction buffer, a French press was then employed four times

to break the bacterial cell walls.

To aid solubilisation of the protein 10% of Triton X-100 was added to give a final concentration of 1% and the solubilised pellet was incubated, tumbling for a further 1 hour at 4ºC. The sample was then centrifuged at 10,000 rpm for 20 minutes at 4ºC. The supernatant was incubated with 500 µl of pre-washed Glutathione-Sepharose beads (50% slurry, GE Healthcare), with tumbling, at 4ºC. The GST-CH1 and GST-SH2 bound beads were rinsed four times with 1 ml of wash buffer (See Standard solutions).

To estimate the amount of protein bound to the beads, samples of 2, 5 and 10 µl were analysed on an SDS-PAGE gel along with BSA standards. To determine the presence of protein, the gel was stained using Coomassie Blue staining solution. The remaining GST-CH1 and GST-SH2 bound beads were stored at -80ºC in wash buffer containing 20% glycerol. For use as a negative control, the GST was prepared by exactly the same method as described for the production of GST-CH1 and GST-SH2 fusion proteins.

2.7. Expression and Purification of the CH1 domain of RaLP/ShcD

To produce the CH1 domain of RaLP/ShcD, the GST-CH1 construct was transformed into competent *E.coli* BL21(DE3) cells. A 10 ml overnight culture of transformant was used to inoculate (1:50 to 1:200 dilution) seven flasks each containing 1 litre LB/ appropriate antibiotic. The culture was grown to reach OD_{550} of 0.6 to 0.8 at 37°C in a shaking incubator and then the GST-CH1 expression was induced with 0.1 mM IPTG at 15°C in a shaking incubator overnight at 220 rpm.

After overnight incubation, bacteria were harvested by centrifugation at 6,000 rpm at 4°C for 20 minutes, and bacterial pellets were then resuspended in 105 ml of buffer containing 20 mM Tris-HCl (pH 7.4), 100 mM NaCl and 2 mM DTT. The cells were disrupted using the French Press and then centrifuged at 15,000 rpm for 10 min to remove the cell debris. The GST-CH1 containing supernatant was then incubated with 10 ml of Glutathione Separose beads (50% of slurry) for about 4 hours at 4 °C with tumbling. The GST-CH1 bound beads were loaded onto a 20 ml column, and the column was washed in 200 ml 1x TBS buffer to remove unbound protein. After washing, the protein was eluted in 36x 1 ml fractions applying elution buffer containing 20 mM Tris (pH 8.0), 100 mM NaCl, 2 mM DTT and 10 mM reduced glutathione 5 µl from each sample was analysed by SDS-PAGE and Coomassie staining to determine which samples contained the eluted proteins.

The GST-CH1 protein was combined from appropriate fractions, and was dialysed to remove reduced glutathione against 2 litre dialysis buffer containing 20 mM Tris-HCl (pH 7.4), 100 mM NaCl and 2 mM DTT for 4 hours, then buffer was replaced and dialysed further overnight at 4°C. 100 µl of GST-TEV (7.5 Unit/µl) protease from Dr. Xiaowen Yang (ProTex, Department of Biochemistry, University of Leicester) was added to the purified GST-CH1 prior to dialysis. The purity of the RaLP/ShcD-CH1 domain was determined by SDS-PAGE on a 15% gel.

2.7.1. Further purification by Gel filtration chromatography

The CH1 domain of RaLP/ShcD was further purified to remove GST and other contaminants by employing gel filtration chromatography on a Superdex 75 column. The column was equilibrated in 0.02 M Tris-HCl (pH 7.4), 0.1 M NaCl with 0.002 M

DTT at room temperature. The sample was applied to the column and 2 ml fractions were collected. Fractions containing protein eluting at the appropriate molecular weight were analysed by SDS-PAGE to confirm the presence of the CH1-domain protein.

2.8. Preparation of beads for Immunoprecipitation (IP) Assays

For each immunoprecipitation, 25 µl of protein G-sepharose (Sigma) was transferred into a fresh eppendorf tube. Beads were washed twice with 1ml ice-cold PBS to remove traces of ethanol. 5 µg of antibody was applied to the beads and the tubes were incubated at 4ºC overnight. The following day, the beads were left for further 2 to 3 hours at room temperature and washed twice with 1 ml of ice-cold PBS to remove unbound antibody. Beads were incubated with cell lysate overnight at 4ºC with rotation.

2.9. Preparation cell lysates for IP or GST-pull downs

Immunoprecipitation or GST pull-down assays were performed using 10 cm dishes of cell lines such as HEK293, 1361, 518, MDA-MB 435, B16F10, Mel17, DAUV, and Gerl43. When precipitating endogenous protein, or protein from transfected cells to over express the protein of interest, cells were incubated for 24 hours in a 37ºC incubator. Cells were washed twice with ice-cold 1x PBS, and lysed by adding 1 ml of Triton lysis buffer and incubating on ice for 2 minutes. The cells were scraped off and transferred into fresh eppendorf tubes and then centrifuged at maximum speed, at 4ºC for 5 minutes. For analysing whole cell lysate, 70 µl of cell lysate was retained whereas the rest of cell lysate was divided into two tubes for incubation with either GST fusion protein and GST control, or 5 µg antibody bound to protein G-sepharose and appropriate negative control. Beads were tumbled overnight at 4ºC, and then washed

four times with wash buffer. Sample buffer and DTT were added to whole cell lysate samples, which were boiled for 10 minutes at 100ºC then stored at -20ºC until needed. After the final wash 100 µl Sample buffer and 10 µl 1 M DTT were added to beads and then the samples were boiled for 10 minutes at 100ºC in a heating block.

2.10. Immunofloresence Microscopy

2.10.1. Preparation of Coverslips and Immunofluorecence Staining

To study the subcellular co-localisation of two different proteins, indirect immunofluorescence analysis was carried out. Initially, the cells were grown on coverslips and on the next day plasmid encoding the two different proteins were transfected into the cells which were incubated for 24 hours at 37ºC in a 5% CO_2 incubator.

Cells were then rinsed twice with 1x PBS and fixed with 3.7% formaldehyde for 10 minutes at room temperature and the cells were then washed gently three times with 1x PBS. To block non-specific binding sites, coverslips were incubated with 1% BSA in 1x PBS for 1 hour and rinsed three times with 1x PBS. 100 µl of primary antibody (diluted in 1x PBS containing 3% BSA) was incubated for 1 hour at room temperature and the cells were carefully washed three times with 1x PBS. 100 µl of fluorophore conjugated secondary antibody (diluted in 1x PBS containing 3% BSA) was incubated for 1 hour at room temperature in the dark. The cells were gently rinsed three times with 1x PBS and stained with Hoechst 33342 dye (1:500 dilution) for 5 minutes in the dark at room temperature and the cells were washed three times with 1x PBS. The coverslips were mounted on glass slides using mounting solution. To prevent and protect the coverslips

from drying out, the edges of the coverslips were sealed using clear nail varnish. To visualise the cells and the localisation of proteins, Confocal Laser Scanning microscopy was employed.

2.10.2. Localisation study using Confocal Microscopy technique

Microscopy was carried out using the Leica TCS SP5 Confocal Laser Scanning Microscope. The fixed cell samples were exposed to an Argon Laser (488 nm), a UV Diode laser (405 nm) and a HeNe 594 laser (594 nm) depending on the fluorophore, using a magnification power of 63x/1.40 oil UV immersion objective. All the captured images were analysed using Leica LAS AF software.

2.10.3. BCA Protein Assay

BCA solution was prepared by mixing together BCA protein assay reagent (A) from Thermo Scientific and 4% copper sulphate solution (B) at a 50:1 ratio. BSA was diluted from a 2 mg/ml stock to give final concentrations of 1, 2, 4, 6, 8, 10, 12, 15, 18, 20, 25 and 30 µg/ml tubes containing 500 µl of the BCA solution with 1x PBS. The same buffer (5 µl) that was used for the cell lysis was added to each tube. For analysing protein concentration, 10 µl of the CH1 protein was added to a tube containing 500 µl of BCA solution with 490 µl of 1x PBS. The samples of BSA standards and the CH1 protein were incubated in a heating block at 60ºC for 15 minutes and allowed to cool for 5 minutes to room temperature. Their OD was measured at 562 nm and these values used to create a BSA standard curve by plotting BSA concentration against absorbance. The protein concentration in each sample was calculated from the BSA standard curve.

2.10.4. Metal binding study

Metal-binding assays were performed as described by employing a Cary® 50 UV-Vis Spectrophotometer (Varian). The CH1 protein was dialysed into buffer containing 20mM of Tris (pH 7.4) with 100 mM of NaCl. The same buffer was used for dissolving $CoCl_2$. To correct the baseline, the same buffer without protein was used. $CoCl_2$ was added into the CH1 domain protein sample with increasing concentration of $CoCl_2$ up to 1 mM and the absorbance of the sample was recorded over the range 250 to 800 nm.

2.10.5. Purification and identification of proteins interacting with the RaLP/ShcD-CH1 domain

2.10.5.1. Coupling of CH1 domain protein to NHS-activated sepharose beads

100 µl of NHS-activated sepharose beads (GE Healthcare) were rinsed 15 times with 1ml ice-cold 1 mM HCl. The protein (3.4 mg/ml) was then mixed with the beads and incubated with tumbling for 4 ~ 6 hours at 4ºC. After coupling, the beads were centrifuged and incubated with tumbling in solution containing 500 mM Ethanolamine (pH 8.3) with 500 mM NaCl for 2 hours at 4ºC. Then the beads were washed with high pH buffer (100 mM Tris-HCl, pH 8.5) and low pH buffer (100 mM Acetate buffer, pH 4.5, with 500 mM NaCl): this step was repeated three times with high pH buffer followed by three washes with low pH buffer for 5 times in total. Washed beads were incubated with 1x PBS containing a final concentration of 20 mM Sodium azide. For a negative control, 100 µl of NHS-activated sepharose beads were prepared following the same protocol in the absence of protein.

2.10.5.2. Coupling of $NiCl_2$ to Chelating sepharose beads

1 ml of chelating sepharose beads (GE Healthcare) was washed twice with 10 ml 1x PBS followed by centrifugation for 2 minutes at 2,000 rpm at room temperature. The supernatant was aspirated and 4 ml $NiCl_2$ was added followed by incubation for 2 hours at room temperature with rolling. After incubation, the beads were washed four times with 1 ml 1x PBS then resuspended in 2 ml 1x PBS containing 20% (v/v) ethanol for storage.

2.10.5.3. Purification of Proteins binding to the CH1 domain for analysis by Mass Spectrometry

518 melanoma cells were seeded in twenty, 10 cm tissue culture dishes. The cells were lysed in Hi-LO buffer containing 50 mM Tris (pH 7.4), 825 mM NaCl with 1% v/v NP-40. 1 ml of ice-cold lysis buffer was added to each dish and incubated for 2 minutes on ice. The cells were scraped off and then transferred to a fresh 50 ml Falcon tube. To shear DNA, the cell lysates were sonicated at 4ºC for 3 bursts, each for 15 seconds followed by 45 seconds incubation at 4ºC, and suspensions were centrifuged at 13,000 rpm for 20 minutes at 4ºC to remove the cell debris.

After centrifugation, the lipid layer was present on the top of the aqueous lysate. To avoid contamination, the cell lysates were carefully removed into a syringe via a 25G needle and transferred to a fresh 50 ml Falcon tube. Finally the cell lysates were divided into two tubes of about 10 ml each followed addition of 100 µl CH1 domain protein conjugated to NHS-activated beads to one tube, and 100 µl of NHS sepharose prepared without protein as a negative control. The samples were tumbled for 5 hours at 4ºC. After incubation, the samples were centrifuged at 2,500 rpm for 20 seconds and the

beads were then transferred into fresh eppendorf tubes.

To remove any unbound or non-specifically bound proteins, the beads were washed 3 times with Hi-Lo buffer followed by 3 times with wash buffer. To elute any bound proteins from the beads, 200 µl of elution buffer containing 50 mM of Sodium Acetate (pH 2.5) with 100 mM of Glycine was added, incubated for 5 minutes on ice and removed to a fresh eppendorf tube. The elution solution was then analysed on a 15% SDS-PAGE gel followed by staining with Instant Blue (Expedeon).

2.10.5.4. Matrix-Assisted Laser Desorption/Ionisation Time-Of-Flight Mass Spectrometry (MALDI-ToF MS)

Bands that were found only in the purification using the CH1 domain of RaLP/ShcD-conjugated to sepharose and not in the negative control were excised and subjected to MALDI-ToF Mass spectrometry by the PNACL, University of Leicester.

2.11. Yeast-Two Hybrid Screen

2.11.1. Constructs for Yeast two-hybrid screen

The CH1 domain of RaLP/ShcD cloned into pBTM116/PDGFR vector was generated previously in this lab. A mouse embryo cDNA library cloned into the pVP16 vector was provided by Dr. Stan Hollenberg. Vectors are illustrated in Figure 2.1.

2.11.2. Small-Scale Test Transformation

Before completing the large scale library screen, the bait protein was tested to determine whether it can activate the *HIS3* reporter gene on its own. The L40 yeast strain was

cultured on YPD plastes from a frozen stock stored at -80°C in 20% glycerol/YPD. Yeast cells were grown at 30°C for up to 72 hours. A single yeast colony was picked from a fresh YPD plate and inoculated into 5 ml of YPD broth, incubated at 30°C overnight at 220 rpm. The following day, 100 µl of the overnight yeast culture was transferred into 100 ml of YPD broth and incubated overnight at 30°C until the OD_{600} was between 1 and 2.

The 100 ml of yeast culture was split between two sterile 50 ml of Falcon tubes and centrifuged at 3,000 rpm for 5 minutes at room temperature. The pellet was washed once with 50 ml of 0.1 M Lithium acetate in TE. The cells were pelleted again and then resuspended in 1 ml of 0.1 M Lithium acetate in TE, and incubated in a shaking incubator for a further 1 hour at 30°C. Before competent yeast were dispensed (100 µl each) into fresh eppendorf tubes, 1 µg of pBTM116/PDGFR-RaLP/ShcD-CH1 construct (from now on referred to as LexA-ShcD-CH1) was premixed with either 1 µg of the pVP16 vector, or with 1 µg of Grb2 cDNA in the pVP16 vector as a positive control. As an additional positive control, 1 µg of LexA-ShcD-SH2 and 1 µg of Gab1 cDNA (encoding residue 124-217 of Gab1) in the pVP16 vector was premixed together and added to an aliquot of competent yeast. 400 µl of 50% PEG-3350 (Sigma P3640) in TE was transferred into each tube and mixed by inverting a few times. Transformation mixtures were incubated in a heating block for 30 minutes at 30°C and then incubated again in a water bath for 20 minutes at 42°C. After incubation, the mixtures were centrifuged for a few seconds at maximum speed and the supernatant was discarded. The tubes were centrifuged one more time and remaining PEG solution was aspirated. The yeast pellet was resuspended in 100 µl of sterile 1x PBS. All the transformation mixtures were plated onto plates lacking tryptophan and leucine and incubated in a

30°C incubator for two days.

2.11.3. Test HIS3 Transcriptional Activation using 3-AT

To check for the activation of *HIS3* reporter gene, two colonies from each plate from the small-scale test transformation were restreaked onto drop-out plates lacking uracil, leucine, tryptophan and histidine but containing 0 mM, 10 mM, 25 mM, 50 mM or 100mM 3-AT (3-Amino-1, 2, 4-Triazole).

2.11.4. Large-Scale Library Transformation

L40 yeast were transformed with LexA-ShcD-CH1 plasmid as described in *2.11.2* and plated onto yeast drop-out plates lacking uracil, leucine, histidine and tryptophan. A colony was picked and inoculated into 5 ml liquid drop-out medium lacking uracil, leucine, histidine and tryptophan and grown overnight until the OD_{600} ~ 1.

A couple of milliliters from the overnight culture was then inoculated into 100 ml of the same broth for each and incubated at 30°C overnight until the OD_{600} was more than 1.1 litre of YPAD medium (YPD containing 40 μg/ml adenine) was prepared and divided into two flasks. 50 ml of L40/LexA-ShcD-CH1 was added to each flask and grown at 30°C for about 4 hours to a final OD_{600} of 0.3 ~ 0.5. Yeast cell cultures were centrifuged for 5 minutes at 2,500 rpm at room temperature and the supernatant was removed and the pellet was resuspended in 500 ml of TE, and then centrifuged again, and the pellet was resuspened in 20 ml of 0.1 M Lithium acetate in TE and incubated for 10 minutes at room temperature.

1 ml of 10 mg/ml denatured herring sperm DNA and 500 μg of library plasmid DNA was added to the mixture. To the DNA mixture, 140 ml of 0.1 M Lithium acetate in TE with 40% PEG-3350 was added and mixed, then incubated at 30°C for 30 minutes. The mixture was then transferred to a sterile 2 litre flask (sealed using aluminium foil) and 17.6 ml of DMSO was added following by heat shock for 6 minutes at 42°C, by swirling occasionally to help heat transfer. Cells were cooled to room temperature in a water bath, and then centrifuged for 5 minutes at room temperature at 2,500 rpm. The pellet was washed with 500 ml of TE and resuspended in 1 litre of YPAD followed by incubating at 30°C for 1 hour with shaking. The centrifugation and resuspension steps were repeated once more. The pellet was resuspended in 1 litre of drop-out medium lacking uracil, leucine and tryptophan then incubated in a shaking incubator for approximately 16 hours at 30°C.

To determine the primary transformation efficiency, the overnight culture was centrifuged and washed, followed by plating out 100 μl of culture onto drop-out plate lacking uracil, leucine and tryptophan. The rest of the culture was centrifuged and washed two times with 500 ml of TE. The final pellet was resuspended in 10 ml of TE. The same amount of transformed yeast cells were plated onto drop-out plates lacking uracil, leucine, histidine and tryptophan but containing 5 mM or 10 mM 3-AT (30 plates for each) and incubated at 30°C for three days. Yeast colonies were selected and streaked onto drop-out plates lacking uracil, leucine and tryptophan. They were tested with the β-galactosidase Filter Assay as described in *2.11.5*.

2.11.5. β-Galactosidase Filter Assay

Whatman grade-50 filters were gently laid onto drop-out plates lacking uracil, leucine and tryptophan and allowed to absorb moisture, carefully removing any air bubbles trapped under the filter. The yeast colonies were then streaked onto filter papers and incubated overnight (or up to two days to grow) at 30°C along with a positive and negative control. When the yeast transformants had grown, the filters were immersed into Liquid nitrogen for 10 seconds to permeabilize cells. They were subsequently placed yeast-side up onto 10 cm Petri dishes, containing Whatman grade-3 filter paper soaked with Z-buffer/X-gal substrate. To assess β-galactosidase activity, the plates were then placed in a 30°C incubator for a few minutes for up to 24 hours to allow blue colour to form.

2.11.6. Library Plasmid Recovery from Positive Colony

From a positive colony patch, yeast were scraped off and transferred into a fresh eppendorf tube containing 100 µl of yeast lysis buffer. Yeast were resupended then 200µl of Phenol:Chloroform:Isoamyl alcohol (25:24:1) from Invitrogen, was added. To facilitate the lysis of yeast, glass beads (Sigma) were added using a small spatula. The contents of tubes were vortexed for 2 to 3 minutes at maximum speed and then centrifuged for 5 minutes at 12,000 rpm at room temperature.

The aqueous phase was removed to a fresh eppendorf tube. 2 volumes of 100% ethanol with 0.1 volume of 5 M potassium acetate were applied and subsequently left for 2 minutes at room temperature, and then centrifuged for 5 minutes at 12,000 rpm at room temperature. After the centrifugation, the supernatant was discarded and the pellet was washed once with pre-chilled 70% ethanol. The supernatant was removed and the pellet

was air-dried for 15 ~ 30 minutes at room temperature, then resuspended in 30 µl of sterile H_2O. From the purified yeast DNA, 1 µl was used for transformation into HB101 electrocompetent cells and plated onto M9 plates.

From each positive, 5 to 10 colonies were selected and inoculated in 5 ml of LB containing appropriate antibiotic, and incubated overnight at 37°C. The purification of library plasmid from the bacteria was performed using the alkaline lysis/LiCl method as described in *2.3.1f*.

2.11.7. Electroporation of HB101 (Leu-) electrocompetent cells

Initially the cuvettes and cuvette holder were placed for 10 minutes on ice before performing the electorporation and then the Bio-Rad Gene Pulser (electroporation device) was set to 2.5 k volts. Directly before electroporation, 1 µl of library plasmid sample was transferred to an aliquot of 50 µl HB101 electrocompetent cells and the mixture was kept on ice. The plasmid/HB101 mixture was subsequently transferred to the pre-chilled cuvette and electroporated for up to 10 seconds. Once electroporation was performed, 1 ml of SOC broth (pre-warmed at 37°C) was added immediately to the cuvette. The contents of cuvette were transferred to a pre-chilled eppendorf tube and incubated for 1 hour at 37°C with shaking. After incubation, the mixture was centrifuged for 1 minute at 2,500 rpm and 1 ml of 1x M9 medium was added and mixed by gently pipetting up and down. After centrifugation, the pellet was resuspended in 200µl of 1x M9 medium and plated onto M9 plates.

2.11.8. Quantitative assay for β-Galactosidase with ONPG substrate

A single colony was selected and inoculated in 5 ml of drop-out broth lacking tryptophan and leucine followed by incubation at 30°C overnight with shaking. From the overnight culture, the OD_{600} was determined, and the culture diluted to an OD_{600} of 0.2, and incubated at 30°C with shaking for 6 hours. The OD_{600} was then measured again.

Assays were performed in triplicate; 1 ml of culture for each transformant was transferred into 3 different fresh eppendorf tubes and pelleted at maximum speed for 1 minute. The pellet was washed and resuspended in 1 ml of Z-buffer, then 50 µl of suspension was transferred into a fresh eppendorf tube. To lyse the cells, the tube was immersed in liquid nitrogen, and then thawed quickly in a water bath at 30°C for 1 minute (or until fully thawed). For a blank, 50 µl of Z-buffer was added into a fresh tube. 700 µl of Z-buffer including β-mercaptoethanol was added for each sample, and also to the blank, and 160 µl of ONPG substrate was then added, and incubated at 30°C in a heating block and timing was started.

Once a distinctive yellow colour was observed (this could take between 5 minutes to several hours or overnight), 400 µl of 1 M Sodium Carbonate (Na_2CO_3) was added to each sample to stop the reaction, and the time of reaction was recorded in minutes. Subsequently the OD_{420} was determined. β-galactosidase units were calculated with the equation below:

$$\text{Miller units} = 1{,}000 \times OD_{420} / (t \times V \times OD_{600})$$

where t: elapsed time of incubation in minutes, OD_{420}: absorbance at 420 nm, V: used volume of cells, OD_{600}: Optical Density of culture at 600 nm

2.12. *Renilla* Luciferase Assay

Renilla Luciferase assays were performed using the *Renilla* Luciferase assay kit from Promega (E2810). HEK293 cells in 6-well plates were transfected with a CMV driven Luciferase reporter and plasmids of interest. After 24 hours, cells were washed 3 times with PBS, then lysed with 500 µl cell lysis buffer for 15 minutes at room temperature. The lysed cells were scraped off and transferred into eppendorf tubes. 100 µl of *Renilla* Luciferase Assay Reagent was added to fresh eppendorf tubes followed by 20 µl of cell lysate. The samples were then mixed quickly by vortexing for a few seconds. 100 µl of each sample was transferred to a 96-well plate and then the plate was placed in a luminometer, the activity of the *Renilla* luciferase was measured.

2.13. siRNA knock down experiments

To perform knock-down experiments, either INTERFERin^{TM} reagent (Polyplus) or Turbofect siRNA transfection reagent (Fermantas) was employed following the manufacturer's protocol. Oligonucleotides were designed to knock-down Gab1 (Invitrogen), or Lamin as a control provided by Dr. Sue Shackleton as indicated in Table 2.4 and Table 2.5, respectively.

Oligo Name	**Sequence (5'→3')**
Gab1 siRNA #1	CGG GUG GGA UCU UGC ACC UUU GAA A
Gab1 siRNA #2	CAG GUU UAG ACA AUG AGC UUU GGU U

Table 2.4. The sequence of Oligonucleotide primers for Gab1 siRNA.

Oligo Name	**Sequence (5'→3')**
Lamin A/C	CTG GAC TTC CAG AAG AAC A

Table 2.5. The sequence of Oligonucleotide primer for Lamin A/C siRNA.

Chapter 3

Investigation of the interaction between RaLP/ShcD and Gab1 in melanoma cell lines

3.1. Introduction

Each member of the Shc family of adaptor proteins mediates cellular responses following receptor tyrosine kinase (RTK) stimulation such as cell proliferation, invasion, survival, and migration via several signalling pathways. RaLP/ShcD is the most recent member of the Shc family to be identified. The biological roles of the RaLP/ShcD adaptor protein are poorly understood, however evidence exists for a role in regulating melanoma cell migration (Fagiani *et al.*, 2007). Since the function of Shc proteins depends on its ability to form protein complexes, it is likely that the unique role of RaLP/ShcD in melanoma migration depends on novel, as yet unidentified interaction with other proteins. Since the SH2 domain is a well-known mediator of interactions with tyrosine phosphorylated proteins, and important in the function of other Shc proteins, this domain was used in previous studies as a bait protein to screen a mouse embryo yeast two-hybrid library using a modification of the system designed to direct phospho-tyrosine dependent interactions. As a result of yeast two hybrid screens, Gab1 was found to be a novel potential binding partner of the SH2 domain of RaLP/ShcD.

Gab1 is a well characterised adaptor/scaffolding protein (Holgado-Madruga *et al*., 1996). So far, three Gab proteins have been identified; Gab1, Gab2, and Gab3. Gab1, unlike the other members of the Gab family of proteins, is a vital regulator of several biological responses including epithelial morphogenesis, cell invasion, and migration induced by the Met receptor (Lock *et al*., 2002). These proteins share a PH domain, and contain many tyrosine residues that can be phosphorylated by stimulation of cell surface receptors such as RTKs, G-coupled receptors and cytokine receptors. Consequently, it has been shown to associate with several signal transducer proteins containing the SH2

domain such as Shc and Grb2 via its phosphorylated tyrosine residues (Lehr *et al*., 2000; Nishida *et al*., 1999). Interestingly, it possesses a distinct c-Met Binding site (MBS) within the proline rich domain (PRD) that directly interacts with phosphorylated c-Met receptor and does not require other adaptor proteins such as Grb2 (Lock *et al*., 2002). It has previously been shown that the Gab1-PI3K complex is induced during cell migration upon EGF receptor activation (Schaeper *et al*., 2007).

In this chapter, we will investigate the interaction between RaLP/ShcD and Gab1 to determine whether the intact proteins can interact in mammalian cells. We will also determine the interaction site for RaLP/ShcD on Gab1 and attempt so explore the significance of the interaction.

3.2. Results

3.2.1. Association of RaLP/ShcD and Gab1

3.2.1.1. Demonstration of interaction between the SH2 domain of RaLP/ShcD and Gab1

Previously this lab identified that Gab1 is a novel interacting partner for RaLP/ShcD by performing a yeast-two hybrid screen, using the SH2 domain of RaLP/ShcD as bait protein (Prigent, unpublished data).

To confirm the specifically of the interaction between RaLP/ShcD and Gab1, a yeast two-hybrid assay was performed using the SH2 domain of RaLP/ShcD fused to the DNA-binding domain of LexA in the vector PBTM116/PDGFR (LexA-ShcD-SH2) and the region corresponding to amino acids 124-217 of Gab1 that had previously been identified in the library screen fused to VP16 activation domain (VP16-Gab1$^{(124-217)}$). For comparison, yeast were also transformed with the LexA-ShcD-SH2 construct together with pVP16 vector as a negative control and VP16-Gab1$^{(124-217)}$ together with the CH2 domain of RaLP/ShcD fused to LexA (LexA-ShcD-CH2). By performing β-galactosidase filter assays as shown in Figure 3.1, it is clearly shown that when L40 yeast are transformed with the LexA-ShcD-SH2 and VP16-Gab1$^{(124-217)}$ the reporter is active (blue colour) whereas no reporter activation was observed in the negative controls. This result confirms that the SH2 domain of RaLP/ShcD and Gab1$^{(124-217)}$ clearly associate in the yeast.

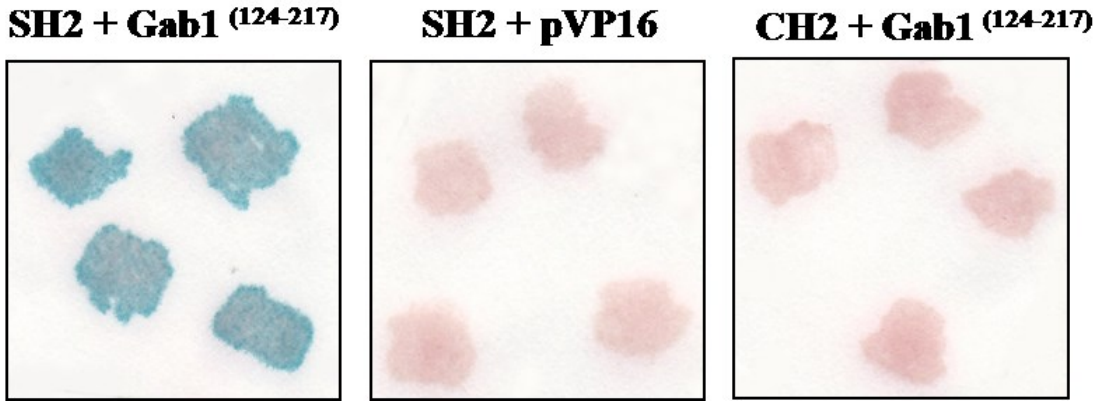

Figure 3.1. β-galactosidase filer assay to demonstrate interaction between RaLP/ShcD SH2 domain and wild-type Gab1. L40 yeast were transformed with LexA-ShcD-SH2 (SH2) together with Gab1$^{(124\text{-}217)}$ in pVP16 (Gab1) or pVP16 alone as a negative control. Gab1$^{(124\text{-}217)}$ in pVP16 was transformed together with the LexA-ShcD-CH2 (CH2). Yeast were grown onto plates lacking leucine and tryptopan. A β-galactosidase filter assay was performed to test for *LacZ* reporter activation.

3.2.1.2. Determination of Gab1 expression in Melanoma cell lines

Having established that Gab1 and RaLP/ShcD can interact in the yeast two-hybrid assay we wanted to determine whether this interaction occurs in cells. Since RaLP/ShcD is expressed in melanoma cells (Fagiani *et al*., 2007) it was decided to determine whether Gab1 and RaLP/ShcD interact in melanoma cell lines. The expression of Gab1 in seven melanoma cell lines was first examined by using immunoblot experiments using anti-Gab1 antibody as indicated in Figure 3.2A. A doublet of approximately 120 kDa in molecular weight corresponding to Gab1 was detected in all seven melanoma cell lines, although fainter bands were observed in Gerl43 melanoma cells. As a loading control, the blot was stripped and reprobed with anti-Vinculin antibody which is mainly used in this lab, as shown Figure 3.2B. The apparent lower level of vinculin in B16 cells may be accounted for as this is a mouse cell line, and the anti-Vinculin antibody interacts better with human vinculin. Further pull-down experiments were performed on melanoma cells by employing GST and GST-RaLP/ShcD-SH2 fusion proteins to verify their interaction. Seven melanoma cell lines were treated with 1 mM sodium orthovanadate (Na_3VO_4) to increase the amount of tyrosine phosphorylated protein, and then lysates were incubated with either GST, or GST-RaLP/ShcD-SH2 fusion proteins with tumbling overnight at 4ºC. Precipitated proteins were analysed by western blotting using an anti-Gab1 antibody and data are indicated in Figure 3.2C. In all seven melanoma cell lines tested, there is one major band of approximately 120 kDa corresponding to Gab1 consistently appearing in the GST-RaLP/ShcD-SH2 lanes, except in the Gerl43 cells (Figure 3.2C top), indicating that RaLP/ShcD clearly associates with Gab1 via its SH2 domain in this assay. To confirm that equal amounts of GST and GST-RaLP/ShcD-SH2 fusion proteins were used in the pull-down experiment, the blot was probed using anti-GST antibody (Figure 3.2C bottom).

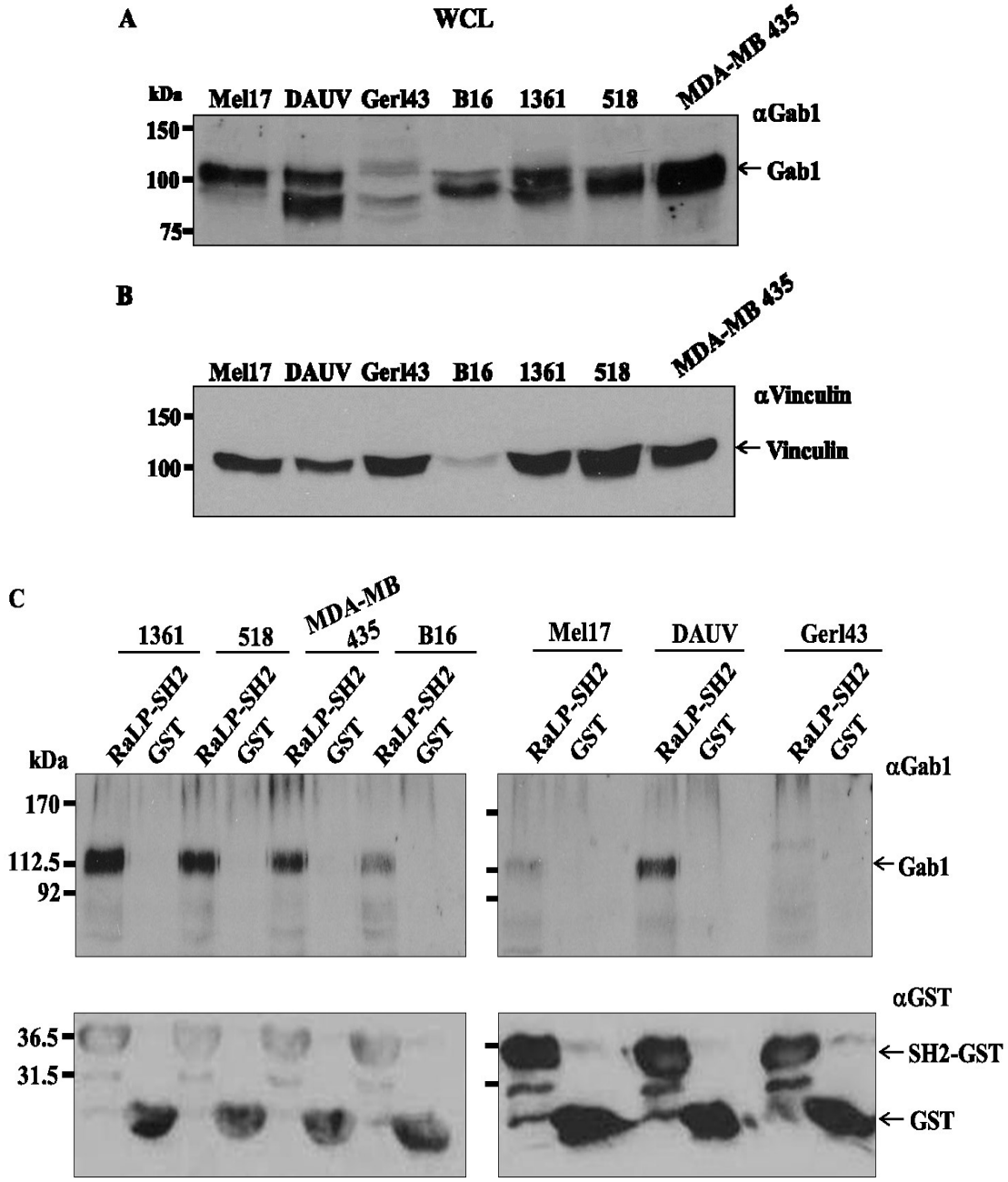

Figure 3.2. Precipitation of Gab1 from melanoma cell lines using GST-RaLP/ShcD-SH2 fusion protein. Whole cell lysates (WCL) from six human melanoma cell lines (Mel17, DAUV, Gerl43, 1361, 518 and MDA-MB 435) and one mouse melanoma cell line (B16) were analysed by western blotting for the expression of Gab1 (A). The blot was stripped and reprobed with anti-Vinculin antibody (B). Proteins were precipitated from the same cell lines with GST-RaLP/ShcD-SH2 or GST alone, and the precipitation of Gab1 was detected by immunoblotting with anti-Gab1 antibody (C). Blots were reprobed with anti-GST antibody.

3.2.1.3. Expression of Receptor Tyrosine Kinases in Melanoma cell lines

The yeast-two hybrid vector (pBTM116/PDGFR) encodes PDGFR kinase as described in Figure 2.1. Therefore, PDGFR can presumably phosphorylate Gab1 to permit interaction with RaLP/ShcD. In order to investigate whether Gab1 and RaLP/ShcD associate in a phosphorylation dependent manner in melanoma cell lines, it was first necessary to characterise the cells to determine which receptor tyrosine kinases they express. Six different human melanoma cell lines were initially characterised. The cells were lysed and analysed by immunoblotting using antibodies recognising EGFR, PDGFRβ and Met as shown in Figure 3.3. DAUV, 518 and 1361 melanoma cells express EGF receptor (Figure 3.3A) detected as a band at approximately 170 kDa. In addition, Gerl43 and 518 melanoma cells express PDGF receptor, at a molecular weight of around 180 kDa (Figure 3.3B), and MDA-MB 435 melanoma cells express Met receptor at a molecular weight of roughly 145 kDa (Figure 3.3C). The blot was reprobed and immunoblotted using anti-Vinculin antibody as a control (Figure 3.3D).

3.2.1.4. Co-immunoprecipitation of RaLP/ShcD and wild-type Gab1 from 518 melanoma cells

Since it was established that 518 melanoma cell lines possess both EGF and PDGF receptors as shown in *3.2.1c*, and it had also been confirmed that GST-RaLP/ShcD-SH2 could pull-down Gab1 from these cells, further co-immunoprecipitation assays were performed using these cells. Both wild-type GFP-RaLP/ShcD and GFP-Gab1 were co-transfected into 518 melanoma cells.

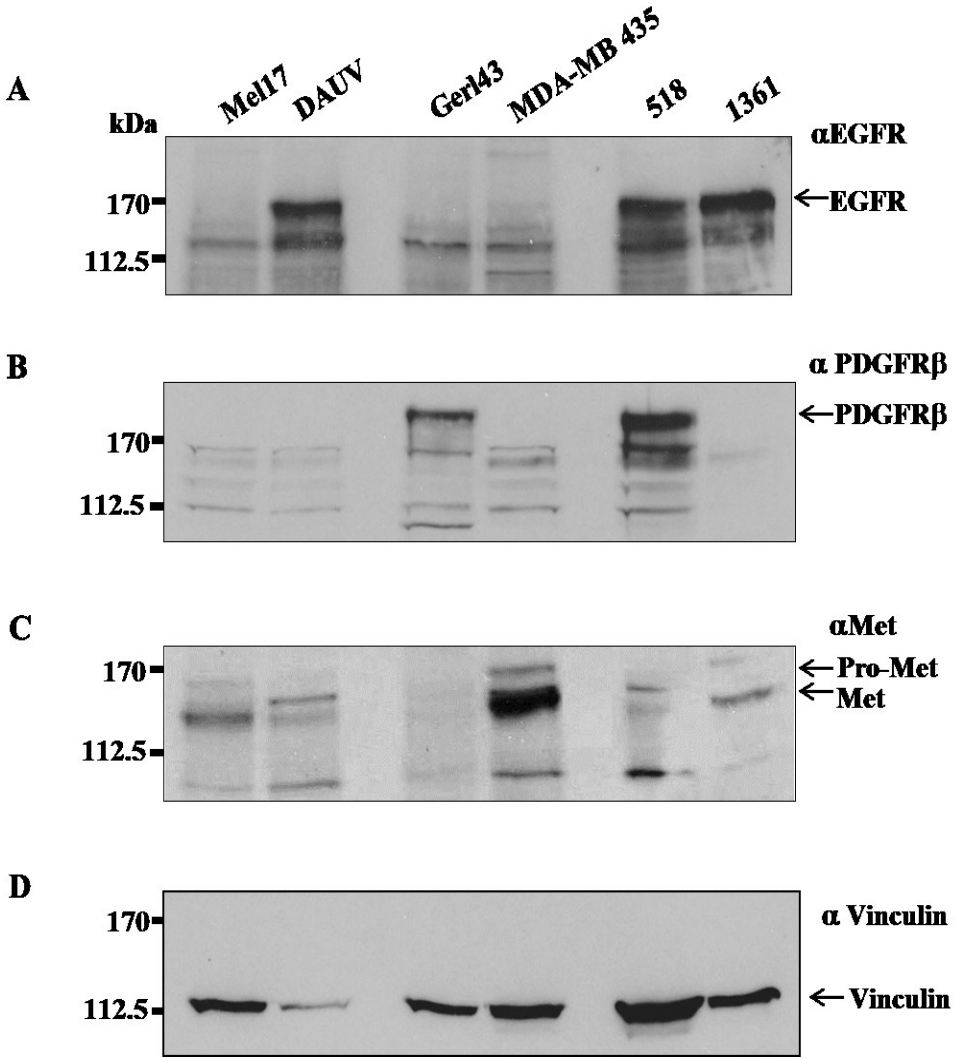

Figure 3.3. Expression of receptor tyrosine kinases (EGF receptor, PDGF receptor β, and Met receptor) in melanoma cell lines. Immunoblotting was performed with anti-EGF receptor (A), anti-PDGF receptor β (B), anti-Met receptor (C) and anti-vinculin (D) antibodies in six human melanoma cell lines.

To enhance phosphorylation-dependent interaction, transfected cells were treated with PDGF and the cells were lysed. Gab1 was immunoprecipitated using anti-Gab1 antibody and an unrelated protein was used as a negative control (anti-Flt1). Immunoblot analysis was then achieved using an anti-RaLP/ShcD antibody or anti-GFP antibody. As indicated in Figure 3.4A, a band at approximately 100 kDa molecular weight corresponding to GFP-RaLP/ShcD protein was observed in the whole cell lysates of the cells which were co-transfected with both GFP-RaLP/ShcD and GFP-Gab1 either without or with PDGF treatment.

Also, in the same panel, bands at roughly 90 kDa were detected in the whole cell lysates from transfected and untransfected cells. This could represent endogenous RaLP/ShcD but is larger than the predicted molecular weight of 69 kDa. Bands corresponding to GFP-Gab1 and GFP-RaLP/ShcD were detected in whole cell lysates from transfected cells (Figure 3.4B). In the immunoprecipitation experiments, GFP-RaLP/ShcD was only detected in the samples where Gab1 has been immunoprecipitated following PDGF treatment indicating that GFP-RaLP/ShcD can associate with Gab1 in a phosphorylation-dependent manner (Figure 3.4C). GFP-RaLP/ShcD was not present in samples where precipitations were performed using anti-Flt1 antibody as a negative control. To confirm that GFP-Gab1 has been precipitated equally from PDGF treated and untreated cells, blots were reprobed with an anti-GFP antibody (Figure 3.4D).

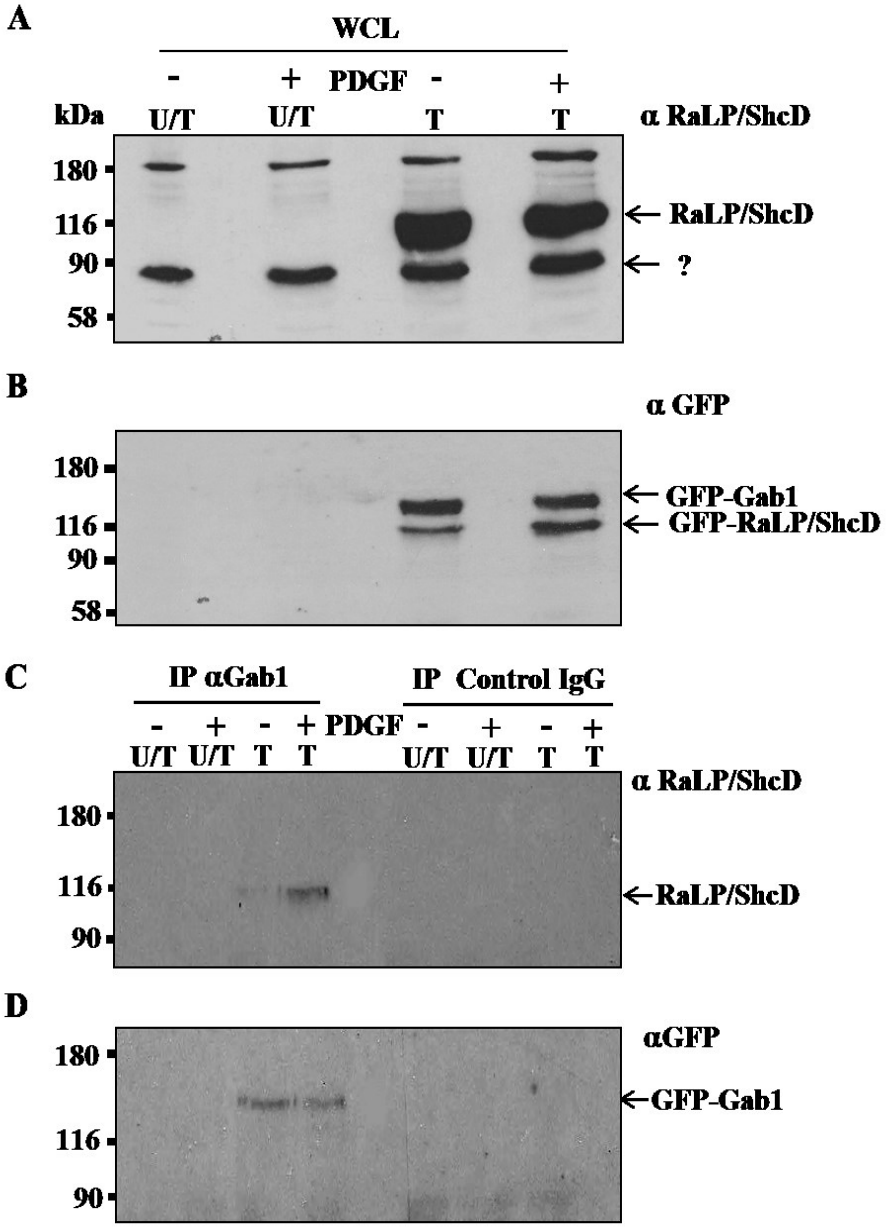

Figure 3.4. GFP-RaLP/ShcD can co-immunoprecipitate with GFP-Gab1 in 518 melanoma cells. 518 melanoma cells were co-transfected with GFP-RaLP/ShcD and GFP-Gab1 (T) or left untransfected (U/T). Cells were serum starved for 3 hours and then either treated with PDGF for 2 minutes (+) or left untreated (-). Immunoprecipitaiton (IP) was performed with anti-Gab1 or anti-Flt-1 (VEGF receptor 1) antibody as negative control. Bands at approximately 150 kDa represent GFP-Gab1 protein. Whole cell lysates (WCL) were analysed on an 8% SDS-PAGE gel followed by western blotting with anti-RaLP/ShcD (A) or anti-GFP antibody (B). Immunoprecipitates were analysed on 8% SDS-PAGE gel followed by western blotting with anti-RaLP/ShcD (C) or anti-Gab1 antibody (D).

To support the previous findings the experiment was repeated using a different RaLP/ShcD construct, and using EGF as a stimulus. 518 melanoma cells were transfected with mCherry-RaLP/ShcD and GFP-Gab1 and either stimulated with EGF or left unstimulated.

Whole cell lysates were analysed to test for expression of mCherry-RaLP/ShcD and GFP-Gab1 as indicated in Figure 3.5A and 3.5B. A band of approximately 100 kDa corresponding to RaLP/ShcD was only present in whole cell lysates of transfected 518 melanoma cells and not in the untransfected cells (Figure 3.5A). Similarly a band of approximately 150 kDa corresponding to GFP-Gab1 was present only in transfected cells (Figure 3.5B). mCherry-RaLP/ShcD was present only in samples where Gab1 had been immunoprecipitated from transfected cells following EGF-stimulation (Figure 3.5C). It did not co-precipitate with Gab1 from unstimulated cells, nor did it precipitated non-specifically with the control antibody.

In conclusion, EGF (also PDGF) promotes association between Gab1 and RaLP/ShcD in transfected melanoma cells. In addition, to test the efficiency of immunoprecipitation, the blot was probed with anti-GFP antibody as indicated in Figure 3.5D. Bands at approximately 150 kDa in molecular weight size represent GFP-Gab1 proteins.

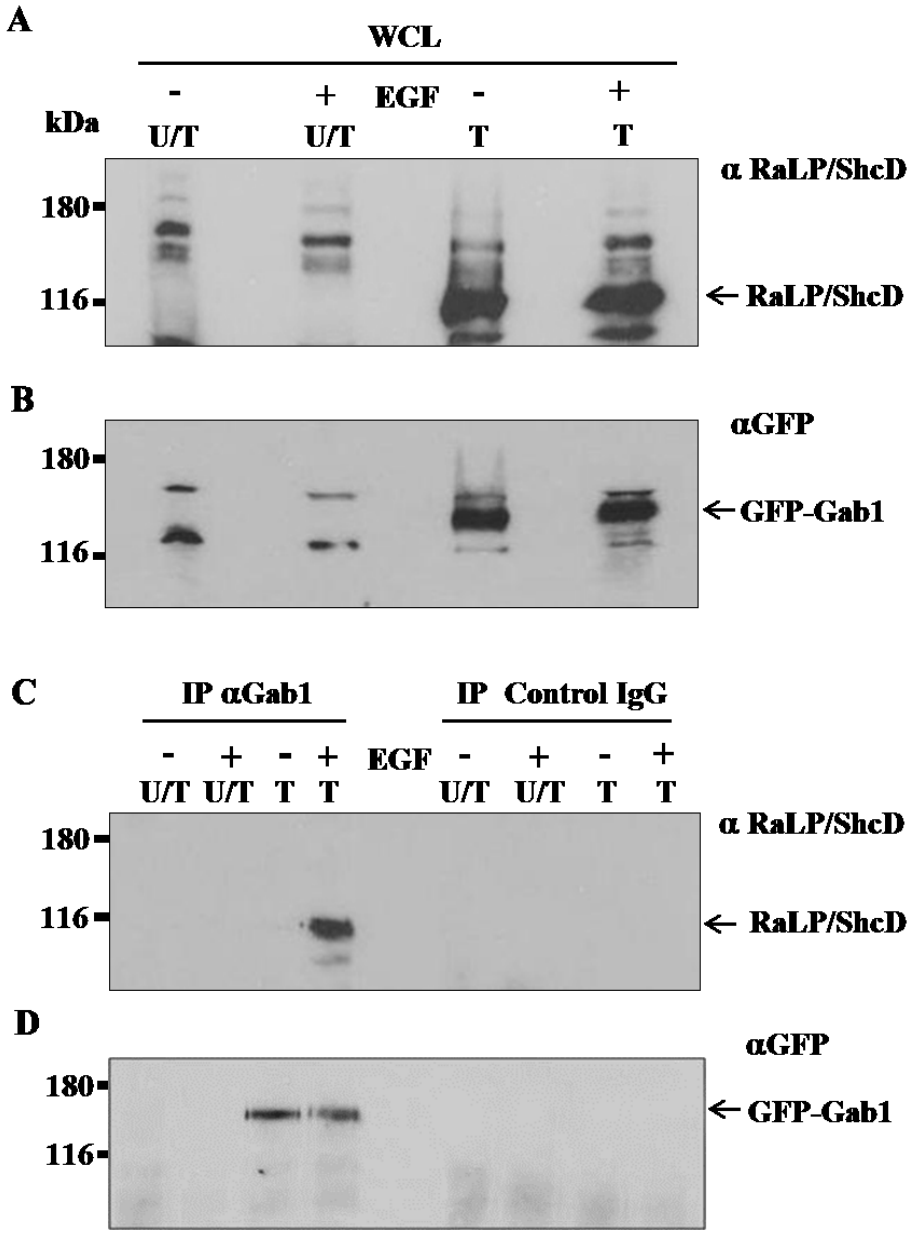

Figure 3.5. mCherry-RaLP/ShcD can co-immunoprecipitate with GFP-Gab1 in 518 melanoma cells. 518 melanoma cells were co-transfected with mCherry-RaLP/ShcD and GFP-Gab1. Cells were serum starved for 3 hours and then either treated with EGF for 5 mins (+) or left untreated (-). Immunoprecipitaiton (IP) was performed with anti-Gab1 or anti-caveolin antibody as a negative control. Whole cell lysates (WCL) were analysed on a 10% SDS-PAGE gel followed by western blotting with anti-RaLP/ShcD (A) or anti-GFP antibody (B). Immunoprecipitates were analysed on 10% SDS-PAGE gel followed by western blotting with anti-RaLP/ShcD (C) or anti-Gab1 antibody (D).

3.2.1.5. Determination of Subcellular Localisation of RaLP/ShcD and Gab1 in transfected Melanoma cells

RaLP/ShcD has previsously been reported to localise in the cytoplasm and with roughly 5% of the protein localised in the plasma membrane (Fagiani *et al*., 2007). Gab1 has been well studied, and is present largely in the cytoplasm, but interestingly, upon stimulation with growth factors, such as HGF, receptor tyrosine kinases (RTKs) are phosphorylated, resulting in the localisation of Gab1 to dorsal ruffles (Abella *et al*., 2010).

To investigate the subcellular localisation of RaLP/ShcD and Gab1 upon receptor tyrosine kinase stimulation, 518 melanoma cells were co-transfected with mCherry-RaLP/ShcD and GFP-Gab1 then the transfected cells were serum starved for 3 hours. Transfected cells were stimulated either with EGF or left unstimulated, and then fixed cells were visualised by confocal microscopy. As shown in Figure 3.6, both RaLP/ShcD and Gab1 seem to distribute mainly in the cytoplasm in the absence of growth factor stimulation. By contrast, RaLP/ShcD and Gab1 were found to be localised predominantly to the cytoplasm and nuclear with small portion co-localised to the plasma membrane (white arrows) after stimulation by EGF receptor as noted in Figure 3.6. Co-localisation was particularly evident at membrane ruffles.

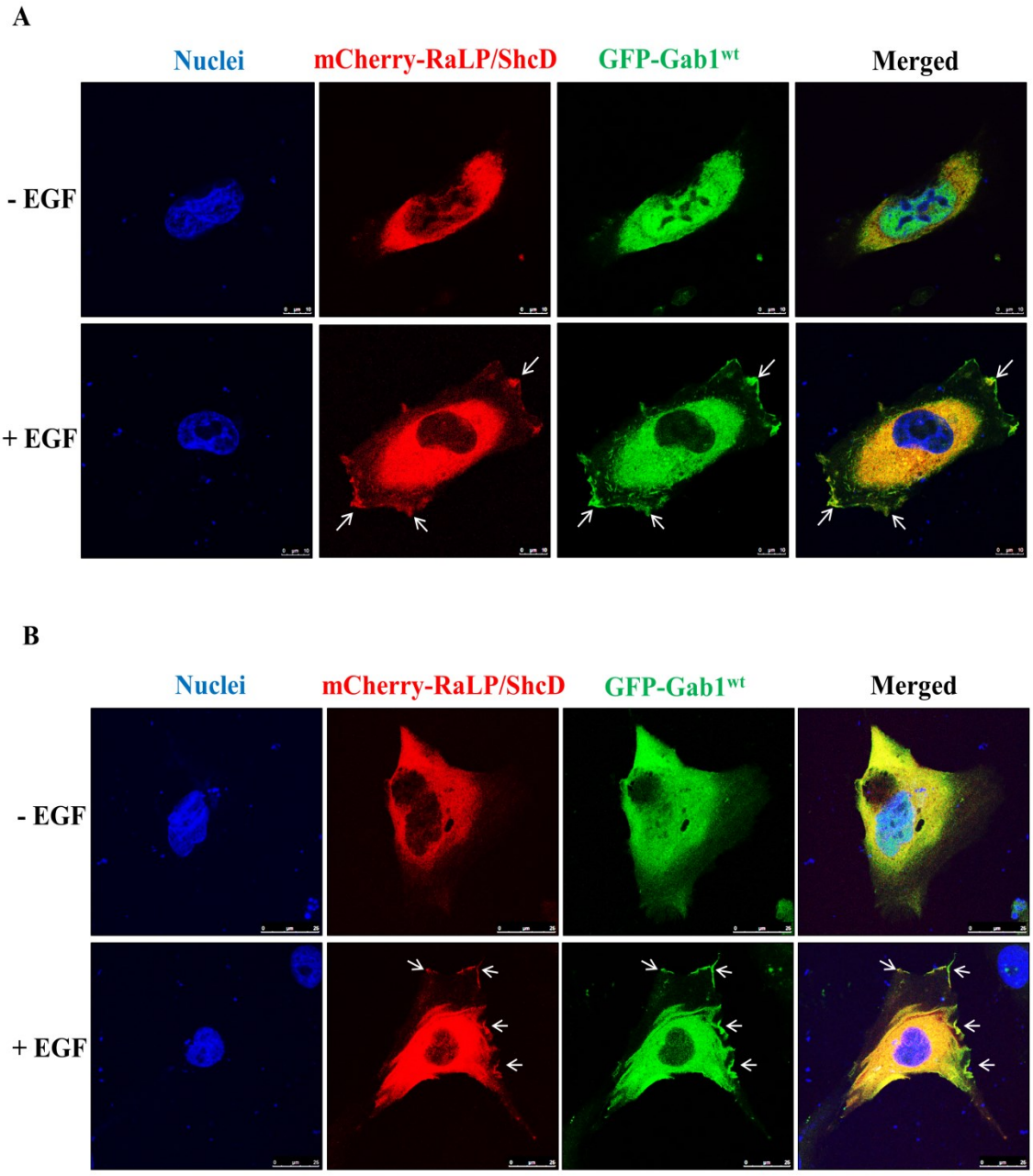

Figure 3.6. Determination of subcellular localisation of mCherry-RaLP/ShcD and GFP-Gab1 in 518 melanoma cells. To study RaLP/ShcD and Gab1 subcellular localisation, 518 melanoma cells were co-transfected with mCherry-RaLP/ShcD and GFP-Gab1 (A, B). After serum starvation for 3 hours, a set of cells were left untreated or treated with EGF for 5 minutes were then fixed and visualised using a Leica Confocal Laser Scanning Microscope. The white arrows indicate that wild-type GFP-Gab1 is present in the membrane ruffles along with mCherry-RaLP/ShcD. Scale bar represents 10 µm (A) and 25 µm (B).

3.2.2. Identification of the phosphorylation site on Gab1 responsible for the interaction with RaLP/ShcD

3.2.2.1. Demonstration of interaction between the SH2 domain of RaLP/ShcD and two Gab1 tyrosine mutants

The region of Gab1 identified in a yeast two hybrid screen as a binding partner for RaLP/ShcD possesses two potential tyrosine phosphorylation sites at tyrosine (Y) 162 and Y183 (Figure 3.7). Neither of these has previously been reported as a phosphorylation site. It was of interest to determine which (if either) of these sites represent the binding site for RaLP/ShcD. Using the Gab1 containing library plasmid identified in the yeast two-hybrid screen, two Gab1 mutants were generated: tyrosine (Y) 162 to phenylalanine (F), referred to Gab1Y162F mutant, and tyrosine (Y) 183 to phenylalanine (F), referred to Gab1Y183F mutant. These constructs were introduced into L40 yeast together with positive and negative controls in the following combinations; LexA-ShcD-SH2 and VP16-WT-Gab1$^{(124\text{-}217)}$, the LexA-ShcD-SH2 and VP16-Y162FGab1$^{(124\text{-}217)}$, and the LexA-ShcD-SH2 and VP16-Y183FGab1$^{(124\text{-}217)}$ plasmids, or negative controls corresponding to the LexA-ShcD-SH2 and VP16, and the LexA-ShcD-CH2 and VP16-WT-Gab1 (Figure 3.8). All the yeast transformants were grown onto plates lacking leucine and tryptopan for two days. β-galactosidase filer assays indicated that the Gab1Y183F mutant was no longer able to interact with RaLP/ShcD, whereas binding of RaLP/ShcD to Gab1Y162F mutant was not affected. This data obviously demonstrates that tyrosine 183 on Gab1 is the tyrosine responsible for interaction with the RaLP/ShcD-SH2 domain.

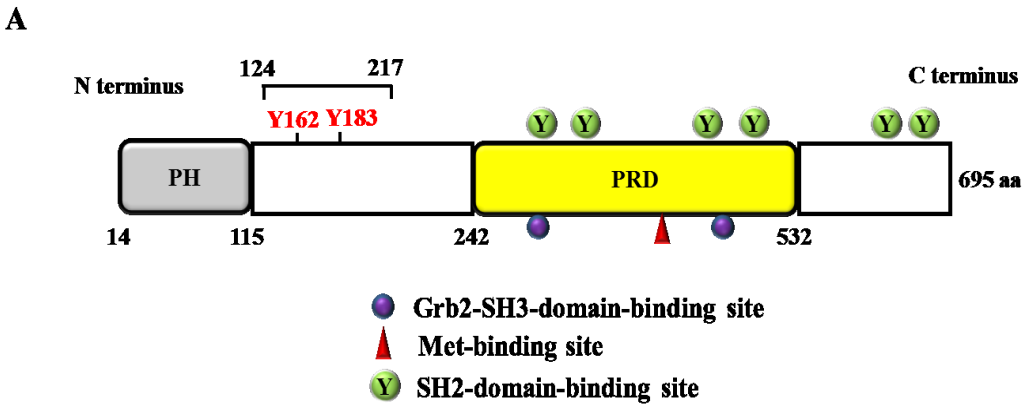

B

Protein sequence of Gab1 corresponding to the DNA insert in library plasmid translated using ExPASy Translate Tool

PVKPLTGSSQAPVDSPFAISTAPASSQMEASSVALPPPYQVISLPPHPDTLGLQ
DDPQDYLLLINCQSKKPEPNRTLFDSAKPTFSETDCNDNV

Figure 3.7. Schematic diagram indicating the domain structure of mammalian Gab1. A, Gab1 protein comprises a PH domain, a proline rich domain (PRD) domain in the middle and several tyrosines (Y) that have been reported to be phosphorylated in green dots. The binding sites for Met receptor and Grb2 are also shown as red triangle and purple dots, respectively. The region of Gab1 isolated in the library screen is indicated (124-217) on Gab1. B, The Two potential binding sites on Gab1 for RaLP/ShcD SH2 domain upon tyrosine phosphorylation are shown in red.

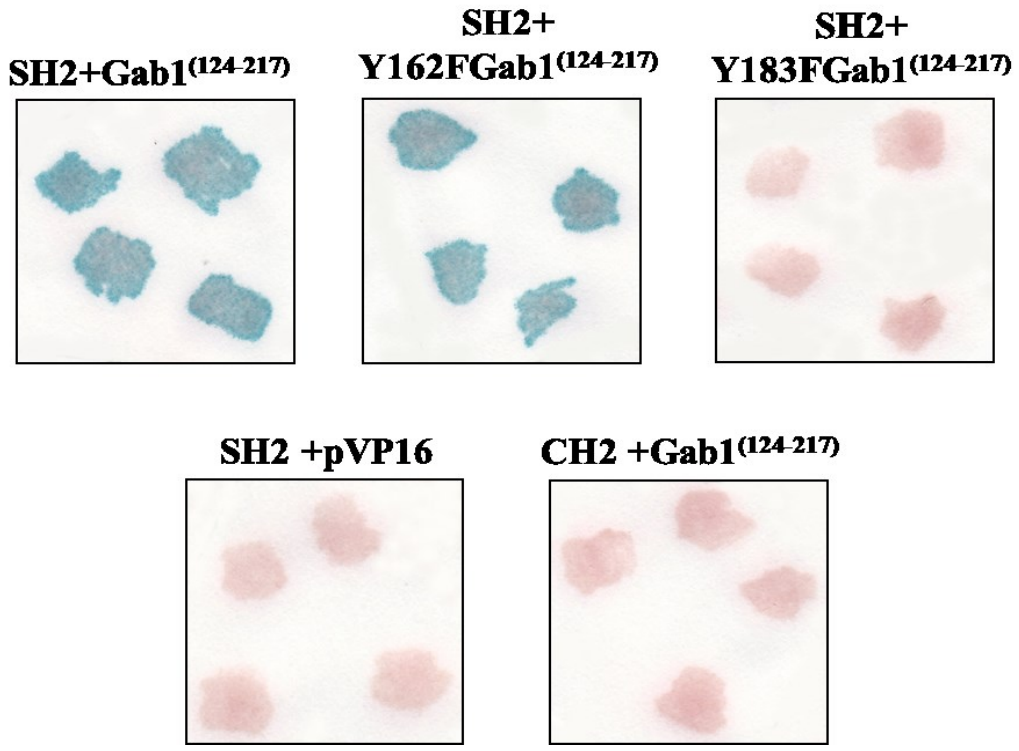

Figure 3.8. Y2H β-galactosidase filer assay to demonstrate interation between the SH2 domain of RaLP/ShcD and Y162F and Y183F mutant of Gab1. L40 yeast were transformed with the LexA-ShcD-SH2 (SH2) bait construct, together with VP16-Gab1$^{(124-217)}$, or Gab1 mutants VP16-Y162FGab1$^{(124-217)}$ or VP16-Y183FGab1$^{(124-217)}$, or pVP16 vector as indicated as a negative control. LexA-ShcD-CH2 was incubated with VP16-Gab1$^{(124-217)}$. Yeast were grown onto plate lacking leucine and tryptopan. A β-galactosidase filter assay was performed to test for *LacZ* reporter activation. The same experiment was repeated three times.

3.2.2.2. Co-immunoprecipitation of RaLP/ShcD and Y183F mutant expressed in 518 melanoma cells

Previously we have shown that RaLP/ShcD can co-precipitate with Gab1 in transfected 518 melanoma cells by employing immunoprecipitation experiments (Figure 3.4 and 3.5). Moreover, tyrosine 183 on Gab1 was identified as the phosphorylation responsible for the interaction with RaLP/ShcD in yeast two-hybrid assays (Figure 3.8).

In order to establish that this tyrosine residue (Y183) is responsible for the interaction in mammalian cells, wild-type GFP-Gab1, and a Gab1 mutant in which tyrosine 183 was mutated to phenylalanine were transfected into 518 melanoma cell lines together with wild-type mCherry-RaLP/ShcD. Co-immunoprecipitation experiments were carried out by using either anti-Gab1 antibody or anti-Caveolin antibody as a control. Transfected cells were treated either with EGF to enhance the tyrosine phosphorylation and therefore interaction, or left untreated. Immunoblot experiments were then achieved using an anti-RaLP/ShcD antibody.

Bands of approximately 100 kDa in molecular weight representing RaLP/ShcD protein were detected in whole cell lysates of the cells that were co-transfected with both mCherry-RaLP/ShcD and wild-type GFP-Gab1, or GFP-Gab1Y183F mutant either with or without EGF treatment, as shown in Figure 3.9A. Intriguingly, mCherry-RaLP/ShcD co-immunoprecipitated with wild-type GFP-Gab1 following EGF treatment, but not with the Y183F mutant of GFP-Gab1 as indicated by a band of approximately 100 kDa corresponding to mCherry-RaLP/ShcD was observed (Figure 3.9C).

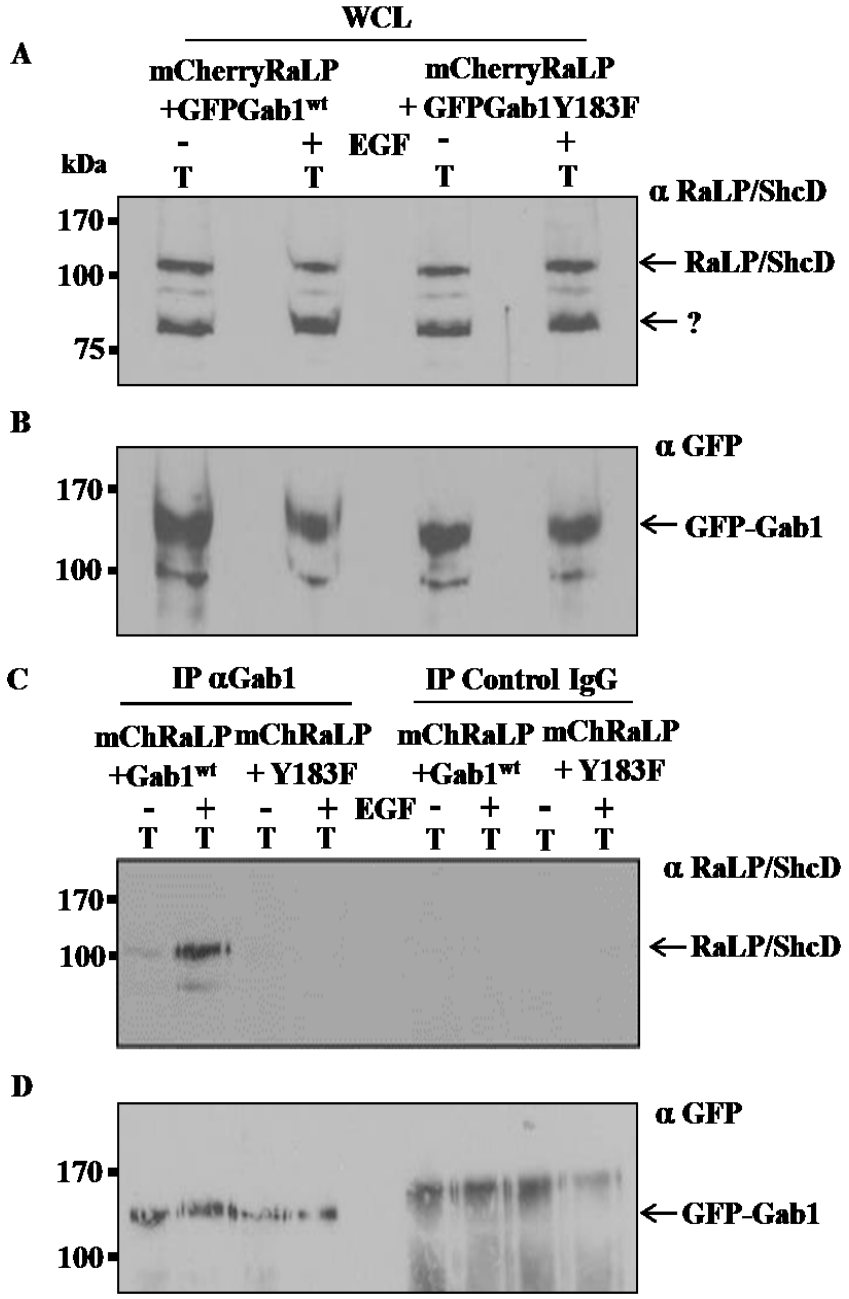

Figure 3.9. mCherry-RaLP/ShcD can only co-precipitate with wild-type GFP-Gab1 in 518 melanoma cells. 518 melanoma cells were co-transfected with mCherry-RaLP/ShcD and wild-type GFP-Gab1 (T) or GFP-Gab1Y183F (T). Cells were serum starved for 3 hours and then either treated with EGF for 5 minutes (+) or left untreated (-). Immunoprecipitaiton (IP) was performed with anti-Gab1 or anti-caveolin antibody as a negative control. Whole cell lysates (WCL) were analysed on a 10% SDS-PAGE gel followed by western blotting with anti-RaLP/ShcD (A) or anti-GFP antibodies (B). Immunoprecipitates were analysed on a 10% SDS-PAGE gel followed by western blotting with anti-RaLP/ShcD (C) or anti-GFP antibodies (D).

The blots were stripped and reprobed with anti-GFP antibody in order to demonstrate that both wild-type GFP-Gab1 and GFP-Gab1Y183F mutant were expressed at the same level and also equally immunoprecipitated (Figure 3.9B and Figure 3.9D). Bands around 150 kDa in molecular weight representing wild-type GFP-Gab1 or the Y183F mutant of GFP-Gab1 were observed. These results further suggest that Y183 is indeed the phosphorylation site present in the full-length protein that is required for RaLP/ShcD interaction.

3.2.2.3. Determination of the Subcellular localisation of RaLP/ShcD and Gab1Y183F mutant in 518 melanoma cells

Previously the subcellular localisation of RaLP/ShcD and wild-type Gab1 was found to be predominantly cytoplasmic with some apparent co-localisation at membrane ruffles following EGFR treatment (Figure 3.6). It was also demonstrated that the interaction between RaLP/ShcD depends on phosphorylation of tyrosine 183 on Gab1. To further investigate the subcellular localisation of RaLP/ShcD and wild-type Gab1 or Gab1Y183F upon receptor tyrosine kinase stimulation, 518 melanoma cells were co-transfected with wild-type mCherry-RaLP/ShcD and GFP-Gab1Y183F mutant, and either stimulated with EGF or left untreated.

After 24 hours transfection, transfected cells were serum starved for 3 hours and then either treated with EGF or left untreated. Transfected cells were fixed and visualised by confocal microscopy. Both RaLP/ShcD and Gab1Y183F mutant seemed to distribute mainly in the cytoplasm without activation of EGF receptor (Figure 3.10A and 3.10B).

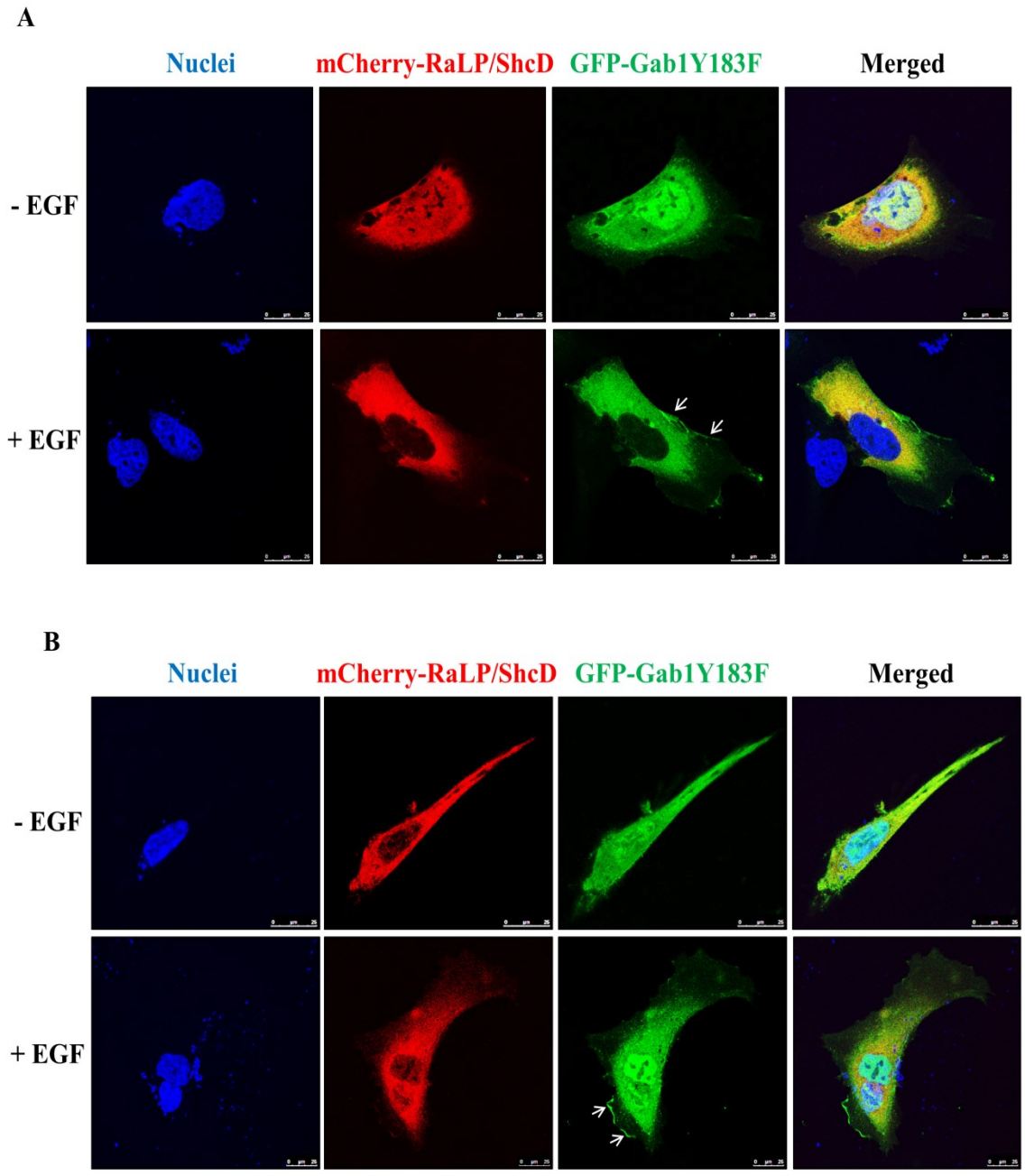

Figure 3.10. Determination of subcellular localisation of mCherry-RaLP/ShcD and GFP-Gab1Y183F in 518 melanoma cells. To study RaLP/ShcD and Gab1 subcellular localisation, 518 melanoma cells were co-transfected with mCherry-RaLP/ShcD and GFP-Gab1Y183F (A, B). After serum starvation for 3 hours, a set of cells left untreated or treated with EGF for 5 minutes, then fixed and visualised using a Leica Confocal Laser Scanning Microscope. The white arrows indicate that GFP-Gab1Y183F existence in the membrane ruffles. Scale bar represents 25 µm.

By contrast, a small portion of Gab1Y183F mutant was localised to membrane ruffles after activation with EGF whereas RaLP/ShcD did not appear to be present. This result suggests that RaLP/ShcD and Gab1Y183F mutant were not associated and that wild-type Gab1 may recruit a small proportion of RaLP/ShcD to membrane ruffles following EGF treatment.

3.2.2.4. Determination of Gab1 knock-down by siRNA

In order to investigate the role of Gab1 and RaLP/ShcD interaction in cell migration, we aimed to knock-down endogenous Gab1 in 518 melanoma cells, and replace it either will wild-type Gab1 or Gab1Y183F mutant. The motility of cells expressing either wild-type or mutant Gab1 could then be compared.

To examine the efficiency of RNAi knock-down, we developed two siRNAs targeting non-coding regions of Gab1. siRNA duplex targeting human Gab1 were transfected into 518 melanoma cells at concentration from 5 to 100 nM for 24 and 48 hours (data not shown). Despite repeated efforts, no knock down was ever observed.

We therefore attempted the knock-down on HeLa cells, as knock-down of expression of other proteins in these cells had already been established. HeLa cell lines were transfected with siRNAs at concentrations from 5 to 100 nM for 24 and 48 hours (Figure 3.11A and Figure 3.11B). Western blots of whole cell lysates were performed using anti-Gab1 antibody, or anti-Vinculin antibody as a loading control.

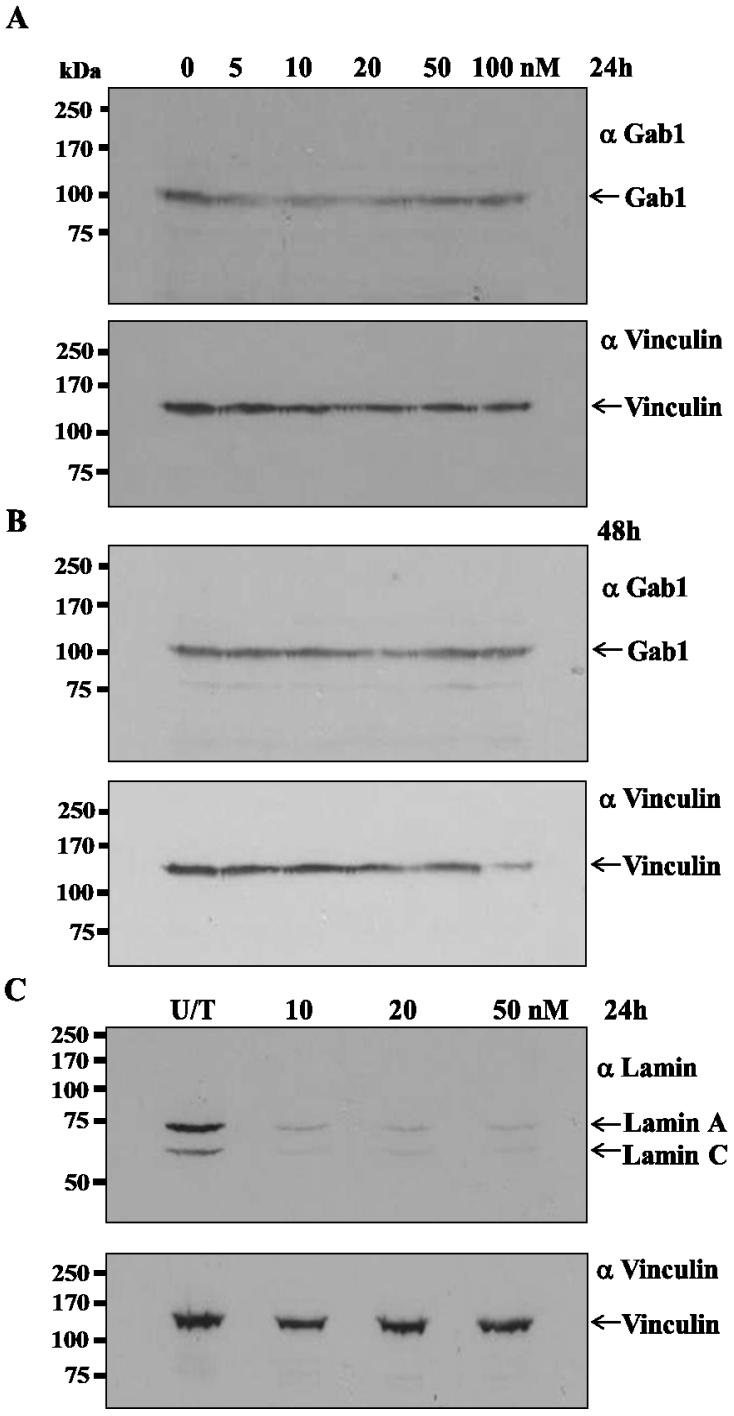

Figure 3.11. Attempted inhibition of Gab1 and Lamin expression by RNA interference in HeLa cells. Western blot analysis of Gab1 following treatment with siRNA for different times (A, B) at different concentrations. Lysates were extracted at 24 (A) and 48 (B) hours following siRNA duplex transfection, and western blots were probed with anti-Gab1 and anti-Vinculin antibodies. Western blot analysis of Lamin following treatment with siRNA at different concentrations. Lysates were extracted at 24 hours following siRNA duplex transfection, and western blots were probed with anti-Lamin (C) and anti-Vinculin antibodies.

As seen in Figure 3.11A and Figure 3.11B, neither siRNA has an effect on Gab1 expression. To determine the efficiency of siRNA transfection reagent, siRNAs targeting Lamin A/C were transfected into HeLa cells at different concentrations (0 nM, 20 nM, and 50 nM) for 24 hours as indicated in Figure 3.11C. Western blotting was performed using anti-Lamin A/C antibody, or anti-Vinculin antibody as a control.

To sum up, upon EGF (also PDGF) stimulation, RaLP/ShcD is able to directly interact with the SH2 domain of Gab1 adaptor protein. Furthermore, Gab1 recruitment to RaLP/ShcD promotes co-localisation to the cell membrane in ruffles in 518 melanoma cells following EGF treatment. Consequently, our data propose that the interaction between RaLP/ShcD and Gab1 is EGF (also PDGF) dependent manner. In addition, the isolated region of Gab1 possesses two potential tyrosine phosphorylation sites that RaLP/ShcD associate through its SH2 domain is responsible for tyrosine phosphorylation. Even if RaLP/ShcD and Gab1 interact, however the RaLP/ShcD and Gab1Y183F mutant association was failed following EGF treatment. Also, we provided that Gab1Y183F mutant was not abled to recruit RaLP/ShcD to the cell membrane in ruffles upon EGF treatment. Taken together, RaLP/ShcD and Gab1 association is growth factors such as EGF dependent and also Y183 on Gab1 is a novel binding site for RaLP/ShcD which is essential for EGF stimulation.

3.3. Discussion

3.3.1. RaLP/ShcD can directly associate with Gab1

It has recently been identified that the Gab1 adaptor protein is a novel interacting partner for the RaLP/ShcD-SH2 domain by performing a yeast two hybrid screen using the SH2 domain cloned into pBTM116-PDGFR (LexA-ShcD-SH2) as bait plasmids (Prigent, unpublished data). At the outset of this project it had not been shown that the interaction occurs in mammalian cells, and the stimuli promoting the association had not been determined, although in the yeast two-hybrid assay used it was PDGFR kinase that was responsible for Gab1 phosphorylation. Based on our findings, RaLP/ShcD and Gab1 are clearly associated, and tyrosine phosphorylation by RTKs such as EGF and PDGF receptors is required for their association. Also, based on our subcellular localisation data in melanoma cells, transfected RaLP/ShcD and Gab1 are co-localised upon stimulation with EGF at a small portion of the membrane in ruffles, but do not appear to co-localise without stimulation. This result suggests that upon growth factor stimulation, RaLP/ShcD associates with Gab1 to form a complex, although the consequence of this interaction remains to be determined.

Previous studies have shown that Shc/ShcA and Rai/ShcC proteins among the Shc family members can interact with Gab1. For instance, phosphorylated Shc/ShcA is able to recruit Gab1 via Grb2 and the complex can regulate formation of endothelial tumours (Ong *et al*., 2001) whereas activated Rai/ShcC may associate with Gab1, inducing thyroid tumours (De Falco *et al*., 2005) and cell survival (Troglio *et al*., 2004) via recruitment of the p85 subunit of PI3K, and activation of the AKT signalling pathway. Thus, the RaLP/ShcD could play a role as a linker for regulating the PI3K/AKT

signalling pathway, via direct binding of its SH2 domain to Gab1. Although the data was not presented, it was mentioned in a previous study that RaLP/ShcD was not able to recruit any signal transducer proteins, including Gab1 and IRS-1, or mediate activation of the AKT signalling pathway in metastatic melanoma cell lines overexpressing RaLP/ShcD upon EGF and IGF-1 treatment (Fagiani *et al.*, 2007). It might be a possibility that EGF and IGF-1 ligand stimulation could not induce the tyrosine phosphorylation of the appropriate residue on Gab1 in these cells, therefore the association between RaLP/ShcD and Gab1 did not occur. Also, it is interesting that c-Met is highly implicated in melanoma development, consequently RaLP/ShcD possibly may have a novel role in Gab1-mediated Met signalling pathways resulting in melanoma cell migration.

Interestingly, the portion of Gab1 that was isolated from the yeast two-hybrid screen using the SH2 domain of RaLP/ShcD possesses two possible tyrosine phosphorylation residues (Y162 and Y183), which have not been reported previously to be phosphorylation sites of Gab1 by RTKs. Yeast two-hybrid interaction assays and mutagenesis studies have confirmed that the mutant Y183F of Gab1 failed to associate with RaLP/ShcD, whereas the Y162F mutant interacted as well as the wild-type protein, indicating that tyrosine 183 on Gab1 has a significant role in binding RaLP/ShcD. Furthermore, subcellular co-localisation studies have shown that Gab1Y183F mutant was not able to recruit RaLP/ShcD, both with and without RTKs stimulation. Therefore, based on our results, we propose that the RaLP/ShcD and Gab1 complex is involved in RTKs signalling pathways leading to enhanced migration as illustrated in Figure 3.12.

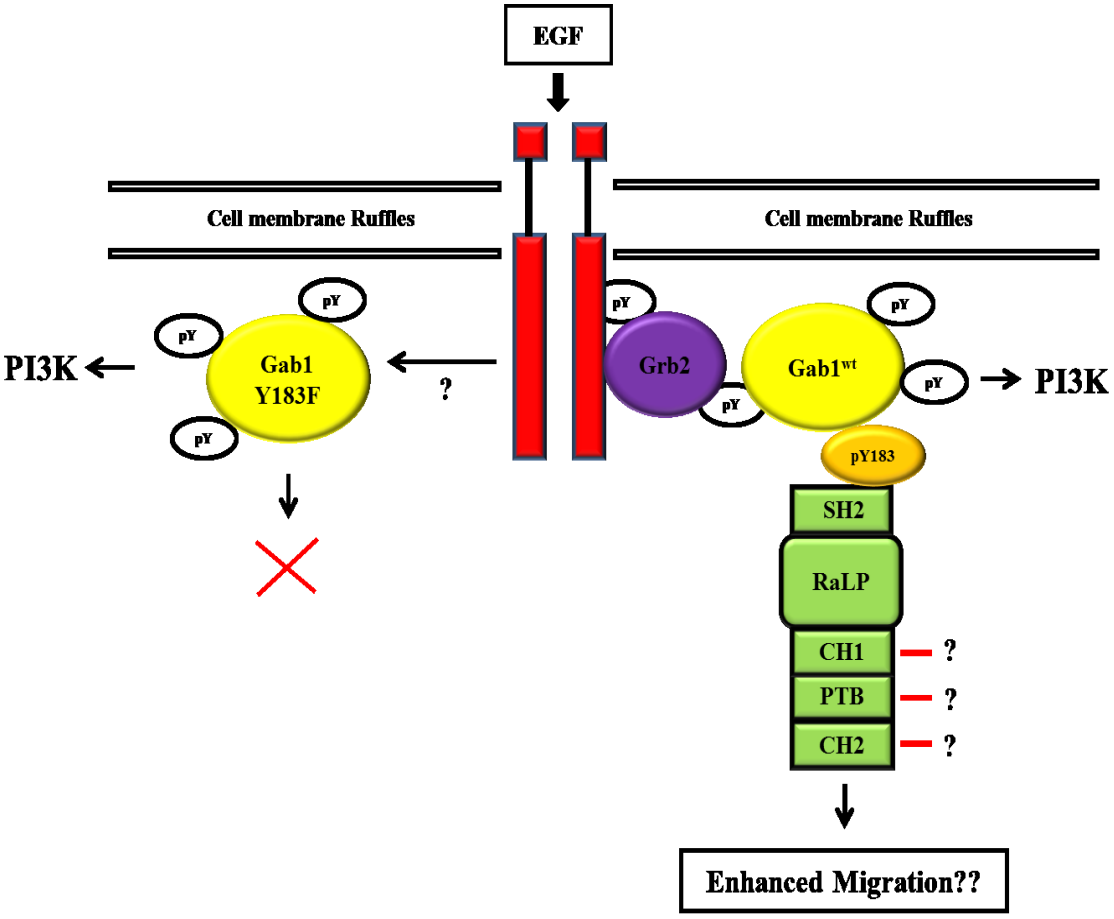

Figure 3.12. Model illustrating possible involvement of RaLP/ShcD and Gab1 in RTK signalling pathways. Gab1 can be phosphorylated upon EGF or PDGF stimulation, and directly recruits the SH2 domain of RaLP/ShcD via its tyrosine 183. Phosphorylation at Y472 recruits the p85 subunit of PI3 kinase. When RaLP/ShcD is recruited, it could bind to other proteins via its CH1, PTB and CH2 domains which may be involved in enhanced cell migration.

Gab1 can be phosphorylated by EGF or PDGF stimulation (Saito *et al*., 2002), and directly recruit the SH2 domain of RaLP/ShcD via tyrosine 183 on Gab1. While Gab1 phosphorylation results in activation of the PI3K/AKT signalling pathway, enhanced cell migration might be achieved by additional interactions with the PTB, CH1, and CH2 domains of RaLP/ShcD which remain free to associate with other signal transduction proteins. It would be very important to determine binding partners for the other domains of RaLP/ShcD to identify its biological roles.

3.3.2. Pak4 is a novel potential linker for the association between RaLP/ShcD and Gab1?

Interestingly, Pak4 was recently shown to interact with residues 116-234 of Gab1 upon HGF stimulation (Paliouras *et al*., 2009). This encompasses the region that we isolated from the yeast two-hybrid sereen (124-217) as a binding partner for the SH2 domain of RaLP/ShcD. To our knowledge this is the only other protein known to association with this region of Gab1.

p21-activated kinase 4 (Pak4) has been reported to modulate cell invasion and migration upon the Met receptor stimulation (Paliouras *et al*., 2009). The Pak family members are well characterised as key effectors of the Rho family members of the small GTPases, CDC42 and Rac1 (Jaffer and Chernoff, 2002) and act as mediators of actin cytoskeletal reorganisation (Abo *et al*., 1998; Ahmed *et al*., 2008). They also have been characterised in a variety of biological responses such as cell survival, motility and morphology. So far, six members of the Pak family have been identified and classified

into two groups; Group I (Pak1 to Pak3) and Group II (Pak4 to Pak6), based on their sequence similarities (Jaffer and Chernoff, 2002).

Pak4 protein was also previously reported to translocate to cell membrane ruffles upon HGF stimulation in MDCK cells (Wells *et al*., 2002). Upon HGF stimulation, the Pak4-Gab1 complex is able to induce Pak4 translocation to the edge of the cells, regulating biological activities, such as cell invasion. Pak4 was shown by co-immunoprecipitation experiments to interact only with Gab1, but not the other Gab proteins such as Gab2 and Gab3, following HGF stimulated Met activation. These results indicated that the Pak4 interaction with Gab1 following HGF stimulation is crucial for regulating of cell invasion, and migration (Lamorte *et al*., 2002; Maroun *et al*., 2000).

The fact that Pak4 interacts with exactly the same region on Gab1, as RaLP/ShcD is of great interest. In their studies Paliouras and co-workers showed that the interaction between Pak4 and Gab1 is phosphorylation dependent as it was abrogated by lambda phosphatase treatment which method may be worth to apply for RaLP/ShcD as well. Their studies suggested that tyrosine phosphorylation may be involved, although Pak4 does not contain known phosphotyrosine binding domains such as SH2 and PTB domains. There studies utilised co-immunoprecipitation of transfected deletion constructs to identify the interaction domain, therefore it is possible that the association was indirect. It would be interesting to determine whether RaLP/ShcD competes for binding of Pak4 to Gab1, or whether it acts and a linker between the two proteins. The

fact that RaLP/ShcD, Gab1 and Pak4 have all been implicated in cell migration makes them interesting targets for further investigation.

3.3.3. Future Investigations

Clearly it is important to investigate the functional consequence of the association between RaLP/ShcD and Gab1. In order to understand the biological function of RaLP/ShcD and Gab1 association, we tried to knock-down endogenous Gab1 in melanoma cell lines, with a view to reintroducing Gab1Y183F mutant and examining the effect on motility. To date we have not been able to knock-down Gab1 using siRNAs targeting its non-coding region. We have also tried using published siRNAs targeting the coding region of Gab1 (Jin *et al*., 2005), and have tried to obtain Gab1$^{-/-}$ mouse embryonic fibroblasts (MEFs). However, the siRNAs targeting the coding region of Gab1 did not affect Gab1 knock-down. We have not measured the half-life of Gab1. If very long, it may contribute to the difficulty in obtaining efficient knock-down. We could attempt alternative approaches such as the use of short hairpin RNAs (shRNAs) using lentiviral or non-viral vectors to improve efficiency of knock-down. It would be useful if we could establish a cell system such as the Boyden chamber assay where RaLP/ShcD expression may promote cell migration. We could then investigate whether mutant RaLP/ShcD that cannot associate with Gab1 shows an impaired ability to promote cell migration. Finally, since the association between Pak4 and Gab1 was recently reported and occurs in the same region of Gab1 as RaLP/ShcD, it would also be worthwhile to investigate the biological roles of RaLP/ShcD in the Pak4-Gab1 complex. Initially a yeast two hybrid assay could determine whether Pak4 and Gab1 interact directly. If not, RaLP/ShcD could act as an adaptor linking the two proteins.

Chapter 4

Identification and Characterisation of proteins interacting with the CH1 domain of RaLP/ShcD by using a Yeast-Two Hybrid system

4.1. Introduction

In the previous chapter the interaction of Gab1 with the SH2 domain of RaLP/ShcD was described. The CH1 domain of all Shc family members is well characterised as containing binding sites for Grb2 (Growth factor receptor-bound protein 2) when phosphorylated (Rozakis-Adcock *et al*., 1992). The CH1 domain of RaLP/ShcD has additional binding sites for Grb2 not present in other family members (Jones *et al*., 2007). The CH1 domain is the least conserved region of the protein and shares less than 24% sequence identity with ShcA protein. Among the other Shc-CH1 domains, only the CH1 domain of RaLP/ShcD is rich in cysteine and histidine residues in both mouse and human. This region could potentially bind metal ions such as Zinc, although the CH1 domain does not contain classical Zinc finger domains. Zinc finger-like domains are not only involved in the interaction between protein and protein, but also more notably the association between protein and DNA. Other Zinc containing domains also exist such as the LIM domain which is involved in protein-protein interactions (Yaden *et al*., 2005).

Basically, the SH2 domain of Grb2 binds a pYXN motif (where pY is a phosphotyrosine and N is an asparagine residue) (Songyang *et al.*, 1994) and it also can interact directly with RTKs when they are phosphorylated by growth factors. All Shc proteins have more than one pYXN motif within the CH1 domain.

Given the unique features of the CH1 domain of RaLP/ShcD, we speculated that interactions with this region of RaLP/ShcD may contribute to its unique role in melanoma cell migration and invasion. In order to look for protein-protien interactions, we used the yeast two-hybrid system. As mentioned in the previous chapter, the system is adapted from the original method developed by Stanley Fields, and is modified by inclusion of the PDGFR kinase in the bait vector to permit phosphorylation of proteins on tyrosine, as yeast do not express classical tyrosine kinases (Keegan and Cooper, 1996). Using this system we would expect to identify Grb2 in a library screen as well as other possible phosphorylation-dependent or independent interactions.

4.2. Results

4.2.1. A Yeast two Hybrid screen of mouse embryo library with CH1 domain of RaLP/ShcD as bait

4.2.1.1. Small-Scale Test transformation

Since it is known that the SH2 domain of Grb2 can interact with the CH1 domains of Shc family members through pYXN motif, we initially wanted to test it the SH2 domain of Grb2 would interact with the CH1 domain of RaLP/ShcD using the yeast two-hybird system degineded by Jonathan Cooper's lab. A small-scale yeast two-hybrid assay was performed using the CH1 domain of RaLP/ShcD cloned into pBTM116/PDGFR (LexA-ShcD-CH1) and the SH2 domain of Grb2 in pVP16 (VP16-Grb2-SH2). The LexA-ShcD-CH1 construct had been made previously in this lab by performing PCR amplification, gel purification, *SalI* digestion and ligation into the pBTM116/PDGFR vector using the *SalI* restriction site (data not shown). The Grb2-pVP16 construct was already available as it had previously been identified in a yeast two-hybrid screen with the CH1 domain of ShcA. LexA-ShcD-CH1 was transformed into yeast together with the VP16-Grb2-SH2 construct, or with the pVP16 vector as a negative control. The LexA-ShcD-SH2 domain construct was transformed together with VP16-Gab1$^{(124\text{-}217)}$ described in the previous chapter as a positive control (Figure 4.1). β-galactosidase filter assays revealed an interaction between RaLP/ShcD-CH1 and Grb2-SH2, and RaLP/ShcD-SH2 and Gab1$^{(124\text{-}217)}$ as expected (blue colour) and the negative control produced no change in colour (pink colour), indicating no non-specific reporter activation. These data proved that RaLP/ShcD-CH1 and Grb2 proteins can directly associate in this assay.

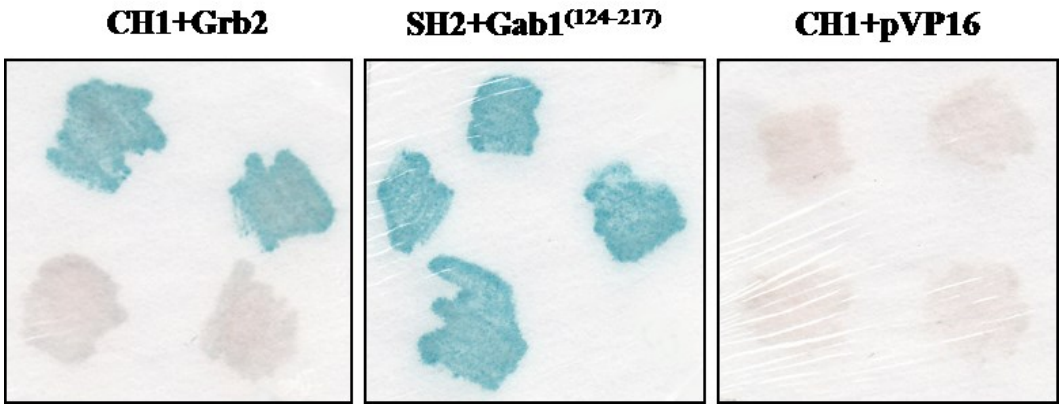

Figure 4.1. β-galactosidase filter assay to demonstrate interaction between RaLP/ShcD-CH1 domain and Grb2. Transformation of LexA-ShcD-CH1 (CH1) and VP16-Grb2-SH2 (Grb2) into L40 yeast. Transformation of LexA-ShcD-SH2 plasmid (SH2) and VP16-Gab1$^{(124-217)}$ into L40 yeast. Transformation of LexA-ShcD-CH1 plasmid (CH1) and pVP16 vector into L40 yeast. Yeast were grown on plates lacking leucine and tryptopan. A β-galactosidase filter assay was performed to test for *LacZ* reporter activation.

4.2.1.2. Suppression of background HIS3 Transcriptional Activation using 3-amino triazole (3-AT)

The preliminarily small-scale test transformation revealed that when the construct containing the RaLP/ShcD-CH1 cloned into the pBTM116/PDGFR plasmid was transformed into L40 yeast containing the *HIS3* reporter gene together with the pVP16 vector alone, some growth was observed on plates lacking, histidine indicating some activation of the *HIS3* reporter gene (data not shown). This could mean that the CH1 domain has some ability to activate transcriptional activities, which may be of interest, although no significant activation of the β-galatosidase reporter was observed. In order to perform a library screen with the LexA-ShcD-CH1 plasmid it was necessary to supress the basal activity of the *HIS3* gene caused by the LexA-ShcD-CH1 plasmid.

Basically, the *HIS3* gene endcodes an enzyme which is involved in the biosynthesis of histidine, and its product is generally generated even at a low level of activity of the *HIS3* reporter gene. 3-Amino-1,2,4-triazole (3-AT) is a well known inhibitor of the *HIS3* gene product. Therefore when included in medium at an appropriate dose it will inhibit the activity of the *HIS3* gene product, and prevent synthesis of histidine.

We needed to identify an appropriate concentration of 3-AT that would suppress the activity of the basal level of *HIS3* gene product, but would permit identification of interactions which promoted strong activation of the *HIS3* reporter gene. We used the LexA-ShcD-CH1 and VP16-Grb2-SH2 and LexA-ShcD-SH2 and PV16-Gab1$^{(124\text{-}217)}$ as

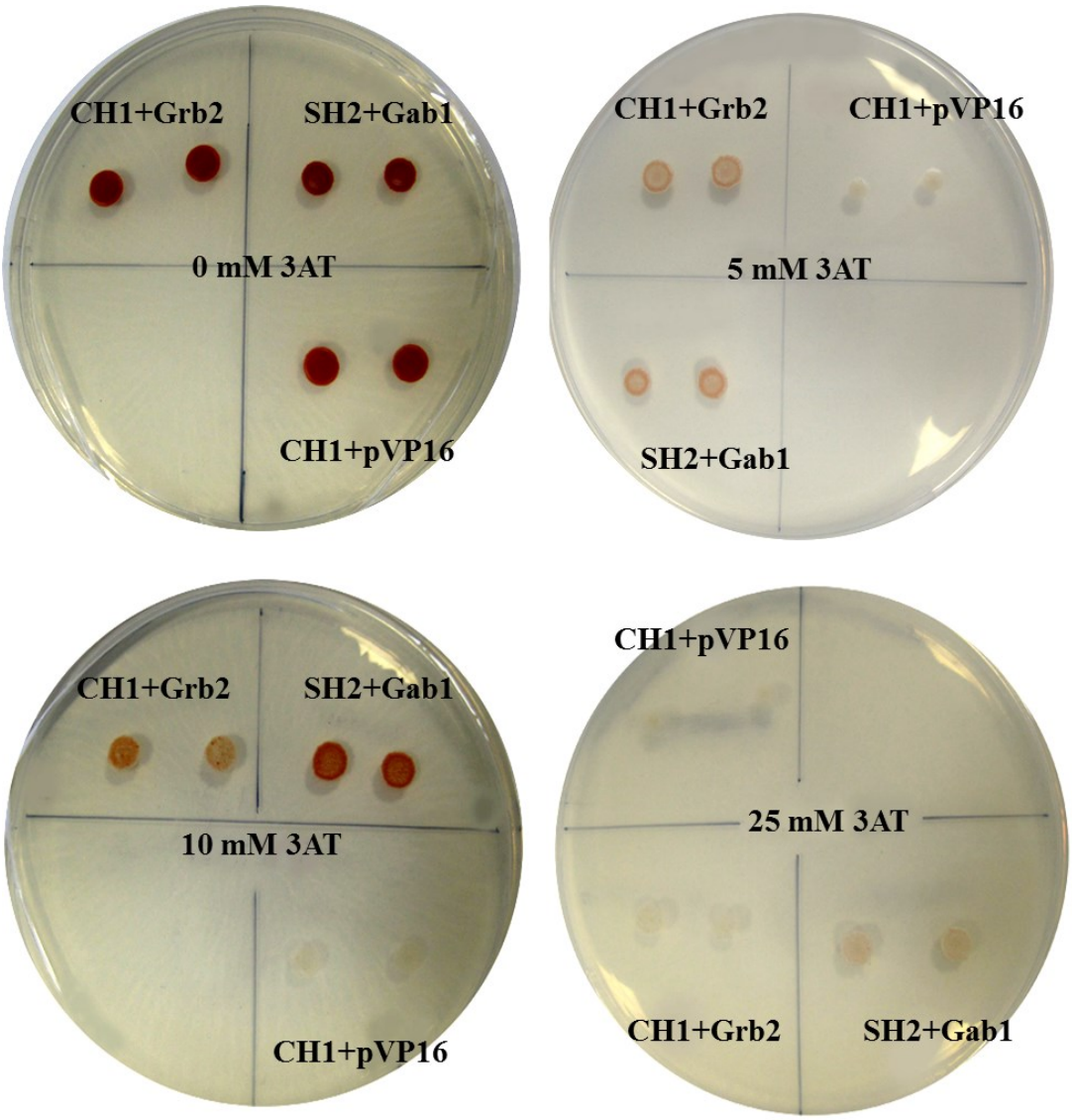

Figure 4.2. Test transformations to determine for the ability of bait plasmids to self-activate *HIS3* reporter gene. Yeast transformants containing LexA-ShcD-CH1 (CH1) + VP16-Grb2-SH2 (Grb2), LexA-ShcD-CH1 + pVP16 or LexA-ShcD-SH2 (SH2) + VP16-Gab1$^{(124\text{-}217)}$ (Gab1) were grown on selective medium lacking Histidine, Tryptophan, Leucine, Uracil with different concentrations of 3-AT (5 mM, 10 mM and 25 mM).

positive controls to determine the minimum dose of 3-AT that would prevent background growth of yeast containing the LexA-ShcD-CH1 plasmid with the pVP16 vector, but would not inhibit the grow of yeast containing plasmids encoding genuine interacting proteins. Yeast were transformed and grown for 3 days at 30°C on selective plates containing 0 mM, 5 mM, 10 mM or 25 mM 3-AT as indicated in Figure 4.2. In the presence of 25 mM 3-AT, the positive yeast strains were not capable of growing on histidine-lacking selective medium compared to 0 mM, 5 mM and 10 mM 3-AT concentrations. For the large-scale yeast library transformation selective plates containing either 5 mM or 10 mM 3-AT were used.

4.2.1.3. Large-Scale Library Transformation

The CH1 domain of RaLP/ShcD is poorly characterised compared to the other CH1 domains of Shc family members. To identify novel interacting partners for the CH1 domain of RaLP/ShcD, the large-scale yeast two-hybrid screen was employed. Principally, LexA-ShcD-CH1 plasmid was transformed into the L40 yeast strain with denatured herring sperm carrier DNA and the mouse embryo library (from Stan Hollenberg). Yeast were grown on drop-out plates lacking leucine, histidine, and tryptophan containing 5 mM or 10 mM 3-AT for three days. Roughly 10^5 yeast colonies were screened. Out of all the 135 colonies, 54 colonies were selected from the CH1 library screen as noted in Figure 4.3. To test the *LacZ* gene activation from the colonies identified, β-galactosidase filter assays were performed, resulting in 51 clones that turned blue out of 54 colonies. From all the positives, we had selected seventeen clones were selected in which yeast clones turned blue most rapidly (3, 7, 8, 11, 13, 15, 21, 28, 29, 31, 33, 36, 38, 43, 45, 48, 50, 52 and 54) as indicated by red arrows in Figure 4.3.

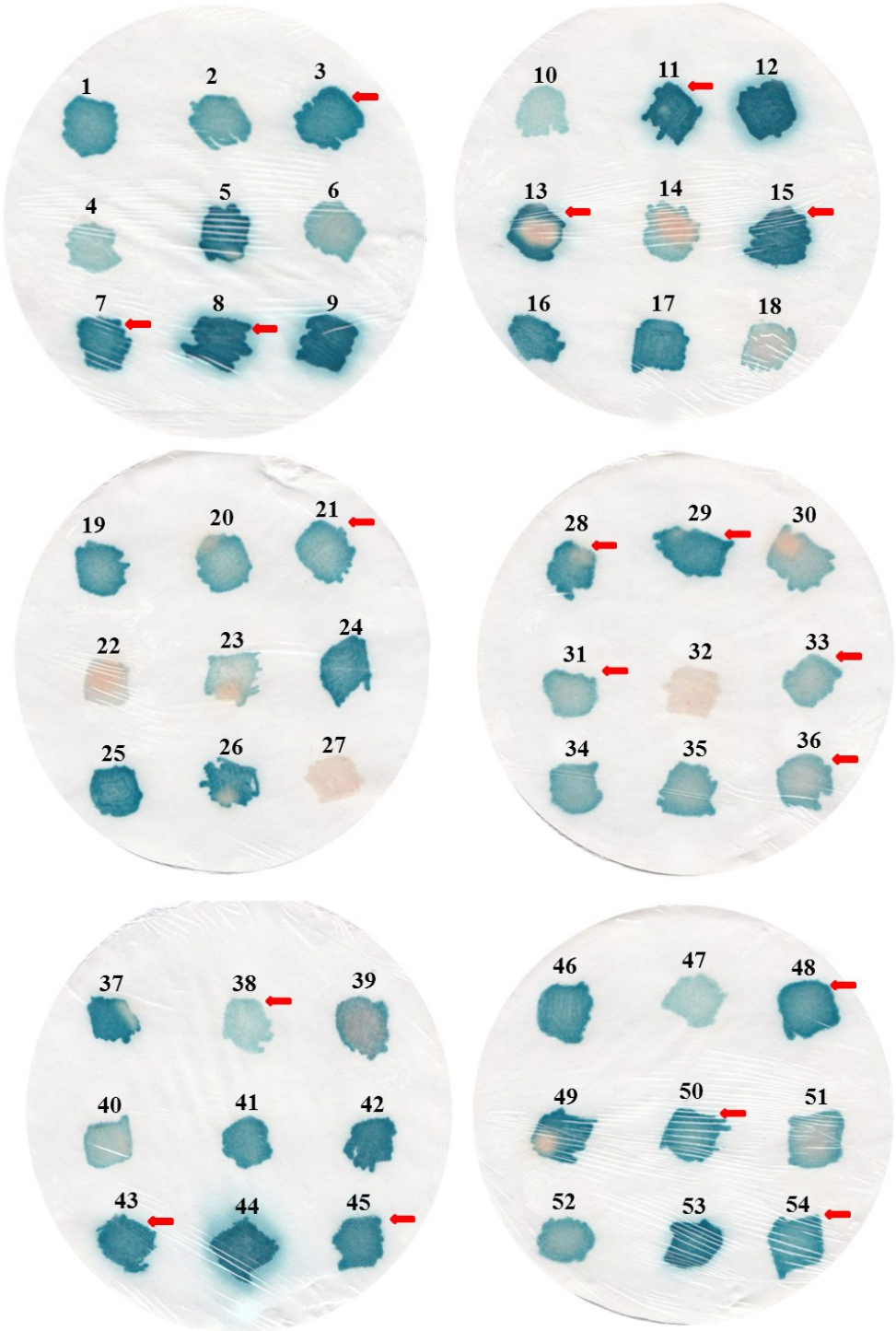

Figure 4.3. β-galactosidase filter assays on select yeast clones isolated from large-scale yeast library screen. β-galactosidase filter assays were carried out on positive clones identified from the library screen using the LexA-ShcD-CH1 plasmid. Clones indicated by red arrows were selected for further analysis.

4.2.1.4. Isolation and characterisation of library plasmids from positive yeast clones

Library plasmids were isolated from positive yeast clones and restriction digestion was performed by using *Not*I restriction enzyme to determine the size of the inserts. The positive clones possessed inserts ranging for 200 - 800 bp as shown in Figure 4.4. The library had been constructed intentionally with short inserts to favour production of protein domains. To further analyse, all the clones were sequenced by PNACL, University of Leicester.

4.2.1.5. BLAST analysis of Clones illustrates novel binding partners for the CH1 domain of RaLP/ShcD

All the positive yeast clones as noted in Figure 4.4 were analysed by the DNA sequencing technique by PNACL, University of Leicester. Sequences were translated using the ExPASy Translate Tool to ensure that inserts were in the correct reading frame to encode the identified proteins. As a result, several potential novel interacting partners for the CH1 domain of RaLP/ShcD were identified including Peg3/Pw1 (Paternally expressed gene 3) and HP1α (Heterochromatin protein 1) as shown in Figure 4.5 and Figure 4.6, respectively. Additionally, Grb2, Hipk2 (Homeodomain-interacting protein kinase 2), and Deubiquitinating protein Vcip135 were also identified as novel petential binding partners for the CH1 domain (see Appendix).

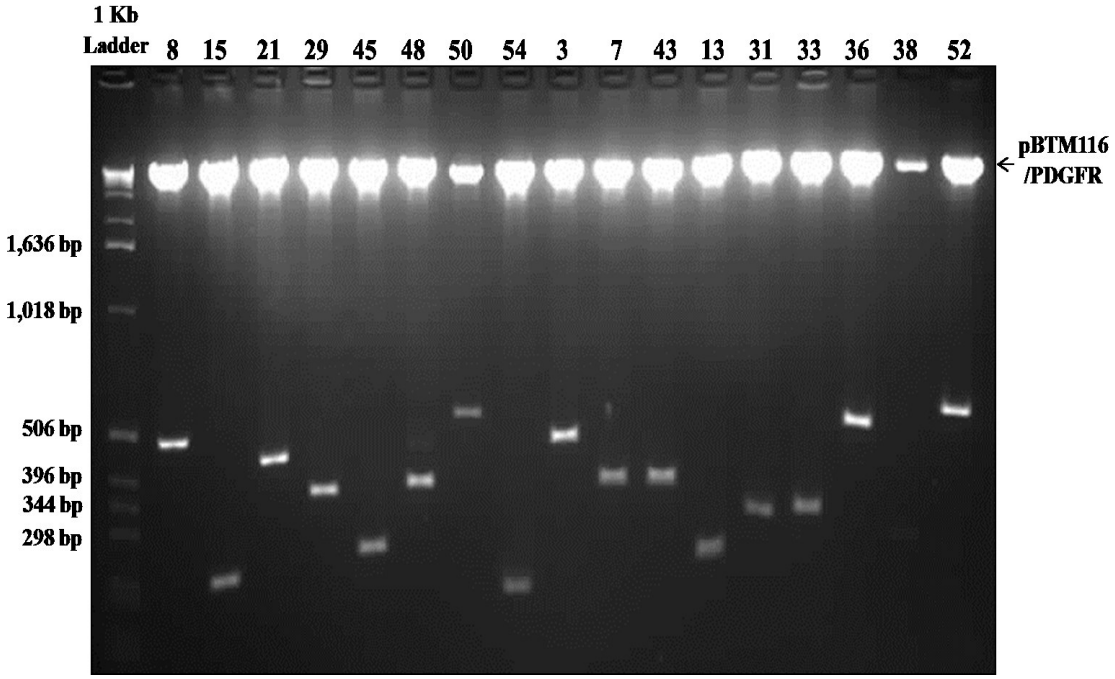

Figure 4.4. Digestion of plasmids isolated from positive yeast clones by *Not*I restriction enzyme. All the positive clones, 3, 7, 8, 11, 13, 15, 21, 28, 29, 31, 33, 36, 38, 43, 45, 48, 50, 52 and 54, were digested by *Not*I restriction enzyme. 1Kb DNA ladder was run alongside samples.

A. BLAST analysis of nucleotide sequence from Clones 7 and 29 isolated from library screen

>gb|BC085183.1| Mus musculus paternally expressed 3, mRNA (cDNA clone MGC:105241 IMAGE:30663888), complete cds Length=5914

GENE ID: 18616 Peg3 | paternally expressed 3 [Mus musculus]
(Over 10 PubMed links)

Score = 604 bits (327), Expect = 7e-170
Identities = 331/333 (99%), Gaps = 0/333 (0%)
Strand=Plus/Plus

```
Query  38    AGAAGATGTATGGCAAAGATAAGTTCTATGAGTGCAAGGTGTGCAAGGAGACCTTTCTGC  97
             ||||||||||||||||||||||||||||||||||||||||||||||||||||||||||||
Sbjct  1627  AGAAGATGTATGGCAAAGATAAGTTCTATGAGTGCAAGGTGTGCAAGGAGACCTTTCTGC 1686

Query  98    ACAGTTCCGCCCTGATTGAGCACCAGAAAATCCATGGTAGAGGCAACTCAGATGACAGAG  157
             ||||||||||||||||||||||||||||||||||||||||||||||||||||||||||||
Sbjct  1687  ACAGTTCCGCCCTGATTGAGCACCAGAAAATCCATGGTAGAGGCAACTCAGATGACAGAG 1746

Query  158   ATAATGAGCGTGAACGCGAACGTGATCGCCTACGTGCACGTGCACGAGAGCAGCGTGAGC  217
             |||||||||||||||||||||||||| ||||||||||||||||||||||||||||||||
Sbjct  1747  ATAATGAGCGTGAACGCGAACGTGATCGTCTACGTGCACGTGCACGAGAGCAGCGTGAGC 1806

Query  218   GCGAACGTGAACGGGAGCGTGAGCGTGAGCTTGGGGAACCCTTTCTGACCTGTCCAAACT  277
             ||||||||||||||||||||||||||||||||||||||||||||||||||||||||||||
Sbjct  1807  GCGAACGTGAACGGGAGCGTGAGCGTGAGCTTGGGGAACCCTTTCTGACCTGTCCAAACT 1866

Query  278   TCAATGAGTTTCGGAAGATGTACAGGAAAGACAAAATCTATGAGTGCAAAGTGTGTGGGG  337
             ||||||||||||||||||||||||||||||||||||||||||||||||||||||||||||
Sbjct  1867  TCAATGAGTTTCGGAAGATGTACAGGAAAGACAAAATCTATGAGTGCAAAGTGTGTGGGG 1926

Query  338   AGAGCTTTCTTCATCTCTCATCCCTGAGTGAGC  370
             |||||||||||||||||||||||||||| ||||
Sbjct  1927  AGAGCTTTCTTCATCTCTCATCCCTGAGGGAGC  1959
```

B. Protein sequence of Peg3/Pw1 translated using ExPASy Translate Tool

QIHAREYLAECRDQEDEETIMPSPTFSELQ**KMYGKDKFYECKVCKETFLHS SALIEHQKIHGRGNSDDRDNERERERDRLRARAREQRERERERERERERELL GEPFLTCPNFNEFRKMYRKDKIYECKVCGESFLHLSSL**REHQKIHTRGNPF ENKSRMCEETFVPSQSLRRRQKTYR

Figure 4.5. BLAST analysis of Clones 7 and 29 revealed that they encode Peg3/Pw1 protein. A, BLAST analysis of nucleotide sequence from clones 7 and 29. B, Protein sequence of Peg3/Pw1 translated using ExPASy Translate Tool. Matched protein sequences are shown in bold red.

A. BLAST analysis of nucleotide sequence from Clone 3 isolated from library screen

>ref|NM_001110216.1| Mus musculus chromobox homolog 5 (Drosophila HP1α) (Cbx5), transcript variant 3, mRNA Length=8902

GENE ID: 12419 Cbx5 | chromobox homolog 5 (Drosophila HP1α) [Mus musculus]
(Over 10 PubMed links)

Score = 793 bits (429), Expect = 0.0
Identities = 429/429 (100%), Gaps = 0/429 (0%)
Strand=Plus/Plus

```
Query  13   GGGGCAAGTGGAATATCTGTTGAAGTGGAAAGGCTTTTCTGAGGAGCACAATACTTGGGA  72
            ||||||||||||||||||||||||||||||||||||||||||||||||||||||||||||
Sbjct  327  GGGGCAAGTGGAATATCTGTTGAAGTGGAAAGGCTTTTCTGAGGAGCACAATACTTGGGA  386

Query  73   ACCTGAGAAGAACTTGGATTGTCCTGAACTAATTTCTGAGTTTATGAAAAAGTATAAGAA  132
            ||||||||||||||||||||||||||||||||||||||||||||||||||||||||||||
Sbjct  387  ACCTGAGAAGAACTTGGATTGTCCTGAACTAATTTCTGAGTTTATGAAAAAGTATAAGAA  446

Query  133  GATGAAGGAGGGTGAAAACAATAAGCCCAGGGAGAAATCAGAAGGAAACAAGAGGAAATC  192
            ||||||||||||||||||||||||||||||||||||||||||||||||||||||||||||
Sbjct  447  GATGAAGGAGGGTGAAAACAATAAGCCCAGGGAGAAATCAGAAGGAAACAAGAGGAAATC  506

Query  193  CAGTTTCTCCAACAGCGCTGATGATATTAAATCTaaaaaaaaGAGAGAGCAAAGCAATGA  252
            ||||||||||||||||||||||||||||||||||||||||||||||||||||||||||||
Sbjct  507  CAGTTTCTCCAACAGCGCTGATGATATTAAATCTAAAAAAAAAGAGAGAGCAAAGCAATGA  566

Query  253  TATCGCTCGGGGCTTTGAGAGAGGACTGGAACCAGAAAAGATCATCGGAGCAACAGATTC  312
            ||||||||||||||||||||||||||||||||||||||||||||||||||||||||||||
Sbjct  567  TATCGCTCGGGGCTTTGAGAGAGGACTGGAACCAGAAAAGATCATCGGAGCAACAGATTC  626

Query  313  CTGCGGTGACTTAATGTTCTTAATGAAATGGAAAGACACAGATGAAGCTGACCTGGTTCT  372
            ||||||||||||||||||||||||||||||||||||||||||||||||||||||||||||
Sbjct  627  CTGCGGTGACTTAATGTTCTTAATGAAATGGAAAGACACAGATGAAGCTGACCTGGTTCT  686

Query  373  TGCAAAAGAAGCTAACGTGAAGTGTCCACAGATTGTGATAGCATTTTATGAAGAGAGACT  432
            ||||||||||||||||||||||||||||||||||||||||||||||||||||||||||||
Sbjct  687  TGCAAAAGAAGCTAACGTGAAGTGTCCACAGATTGTGATAGCATTTTATGAAGAGAGACT  746

Query  433  GACGTGGCA  441
            |||||||||
Sbjct  747  GACGTGGCA  755
```

B. Protein sequence of HP1α translated using ExPASy Translate Tool

MGKKTKRTADSSSSEDEEEYVVEKVLDRRMVK**GQVEYLLKWKGFSEEHNTWEPE KNLDCPELISEFMKKYKKMKEGENNKPREKSEGNKRKSSFSNSADDIKSKKKRE QSNDIARGFERGLEPEKIIGATDSCGDLMFLMKWKDTDEADLVLAKEANVKCP QIVIAFYEERLTWH**AYPEDAENKEKESAKS

Figure 4.6. BLAST analysis of clone 3 indicates that it is a fragment of HP1α protein. A, BLAST analysis of nucleotide sequence from clone 3. B, Protein sequence of HP1α translated using ExPASy Translate Tool. Matched protein sequences are shown in bold red.

4.2.1.6. Confirmation that isolated library plasmids encode proteins that interact specifically with RaLP/ShcD

Isolated library plasmids were retransformed into L40 yeast together with a negative control bait plasmid LexA-Lamin, or the LexA-ShcD-CH1 plasmid, and subjected to a β-galatosidase assay (Figure 4.7A). In most cases, yeast containing isolated library plasmids together with LexA-ShcD-CH1 plasmid turned blue in 15 minutes to 1 hour; whereas yeast containing the LexA-Lamin negative control together with isolated library plasmid did not change colour. In the case of the Hipk2 clone a weak blue colour was observed in the negative control transformation, suggesting that this clone may be activating the β-galatosidase reporter independent of RaLP/ShcD interaction. Further negative controls were included using the CH1 domain, and Lamin bait plasmids together with the pVP16 vector as detailed in Figure 4.7B.

4.2.1.7. Quantitative Analysis of β-Galactosidase activity

The amount of β-galactosidase activity gives a crude indication of affinity of the bait and prey protein interaction in the yeast two-hybrid screen. β-galactosidase enzyme activity present in yeast cells can be determined using ortho-Nitrophenyl-β-galactoside (ONPG) as the substrate in liquid culture. Library plasmids encoding Peg3/Pw1, Hipk2, HP1α, Grb2 and Vcip135 were retransformed into yeast with the LexA-ShcD-CH1 (positive interactor), or LexA-ShcD-CH2 plasmid as a negative control and β-galactosidase solution assays were performed. In each case the interaction with the LexA-ShcD-CH1 plasmid was significantly greater than the negative control. In the case of Grb2, β-galactosidase activity was 637 fold greater when LexA-ShcD-CH1 was present than with the negative control.

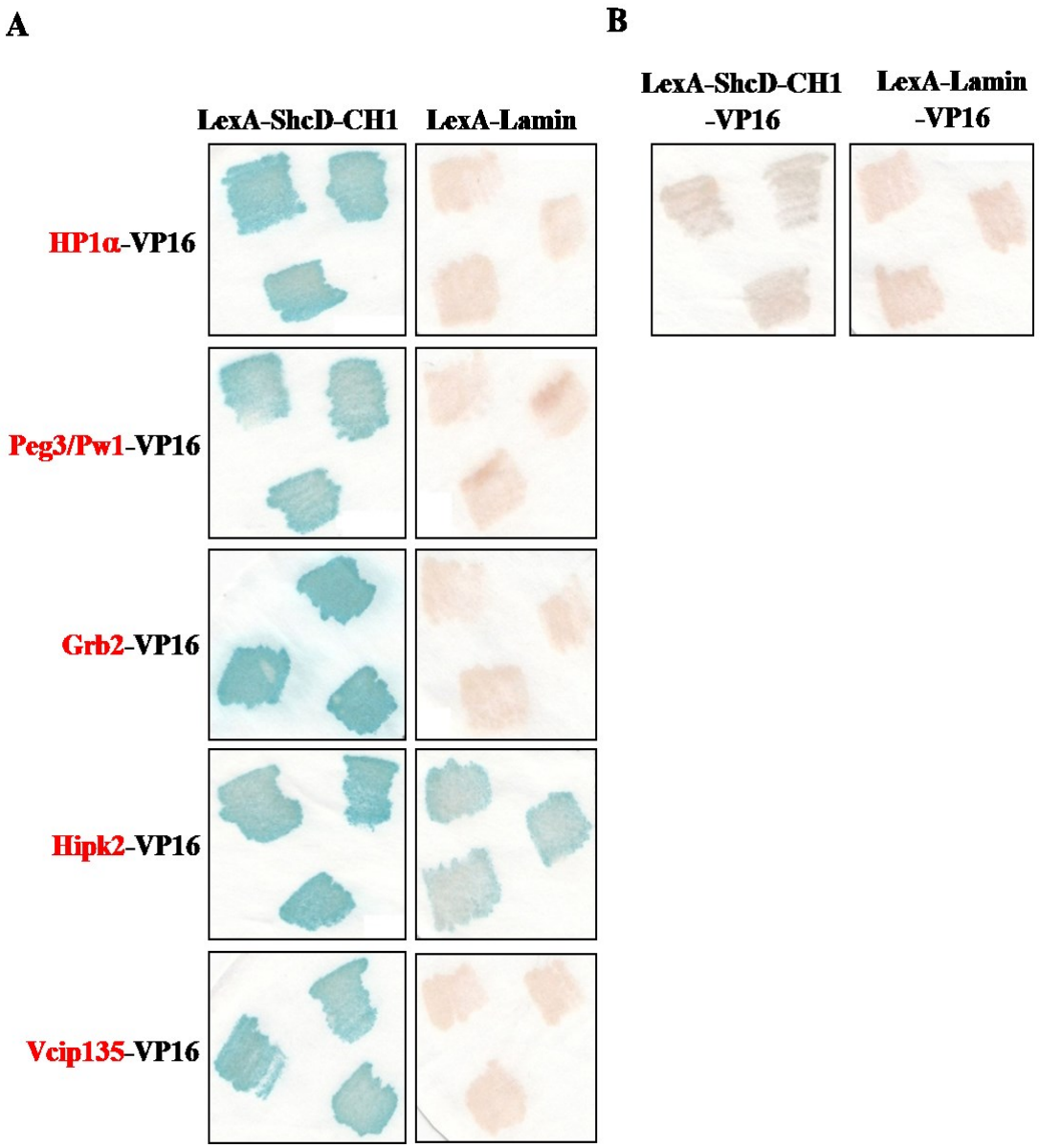

Figure 4.7. β-galactosidase filter assay on positive plasmids from library screen with negative controls. A, Library plasmids isolated from the yeast two-hybrid screen were retransformed into L40 yeast together with the LexA-ShcD-CH1 plasmid, or with negative controls corresponding to LexA-Lamin. B, Further negative controls were performed using the LexA-ShcD-CH1 plasmid, and LexA-Lamin plasmids together with pVP16.

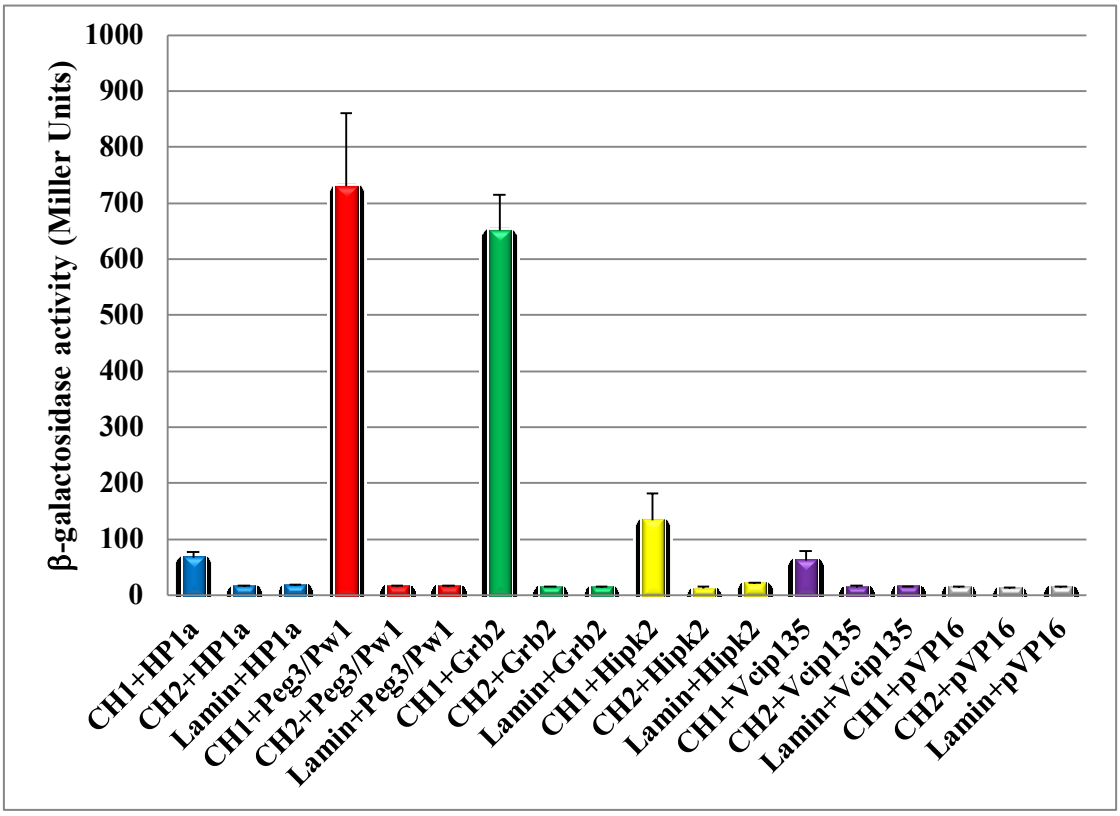

Figure 4.8. Quantitative assay of β-Galactosidase activity of yeast transformants. Yeast transformed with bait and library plasmids as indicated were analysed for β-galactosidase activity assay in liquid culture using ONPG as substrate. The β-galactosidase activities of three colonies were tested in each case and three independent experiments were performed. Final data are the mean ±s.d.

The interaction with Peg3/Pw1 was even stronger than the well characterised Grb2 showing a 715 fold increase in activity compared to the negative control containing LexA-ShcD-CH2. Interaction between the RaLP/ShcD-CH1 domain and the other proteins was apparently weaker, at least in this assay, but all were significantly different from corresponding negative controls. Given the apparent intensity of interaction, Peg3/Pw1 was selected for further study, along with HP1α.

4.2.2. The investigation of RaLP/ShcD and Peg3/Pw1 interaction

4.2.2.1. Precipitation of Peg3/Pw1 and Znic Finger domains using GST-RaLP/ShcD-CH1 fusion protein in HEK293 cells

Briefly, Peg3/Pw1 is a well-known imprinted gene which is mainly expressed in human brain, testis, and muscle (Yamaguchi *et al.*, 2002). In human Peg3/Pw1, a SCAN domain is present at the N-terminus. This protein comprises twelve Zinc-finger domains (from now on referred to as ZnF) at the C-terminus. The plasmid isolated in the library screen of Peg3/Pw1 encoded ZnF domains 2 - 3.

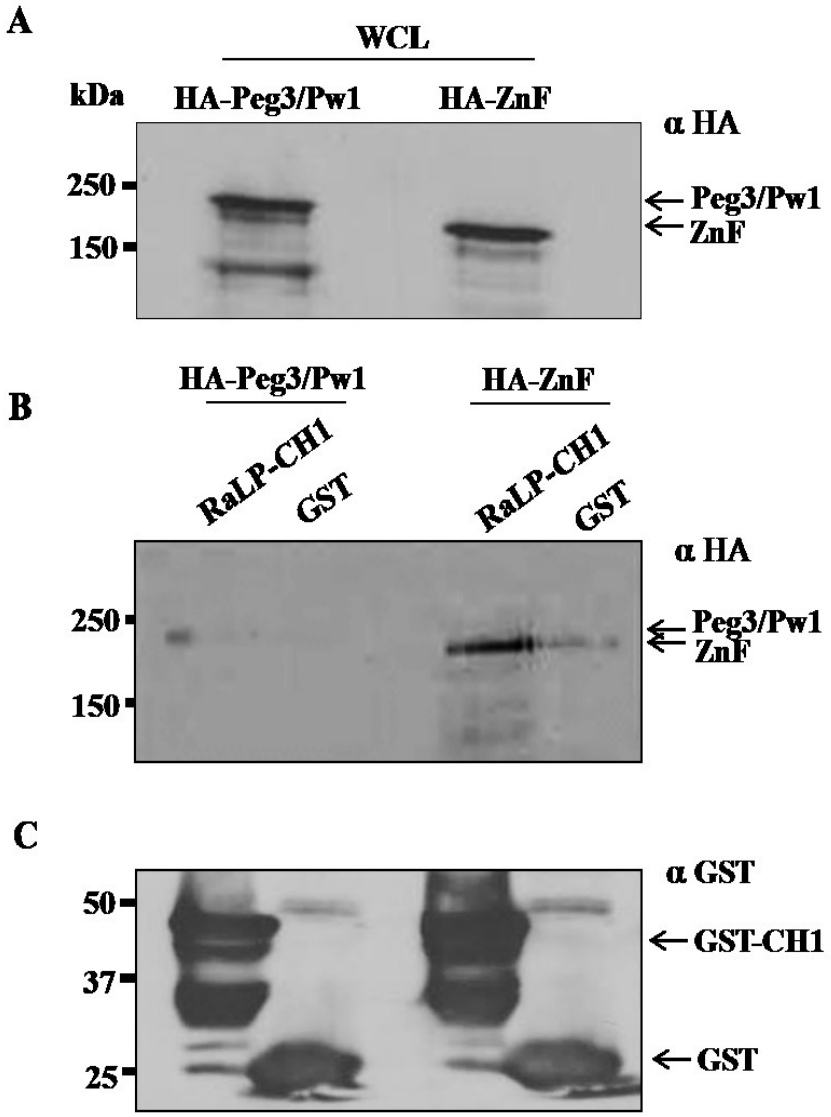

Figure 4.9. Precipitation of Peg3/Pw1 and a deletion encoding only the ZnF domains from transfected HEK293 cell lines using GST-RaLP/ShcD-CH1 fusion protein. HEK293 cells were transfected either with HA-Peg3/Pw1 or HA-ZnF. Cell lysates were incubated with GST-RaLP/ShcD-CH1 fusion protein or GST. Bands at approximately 230 kDa and 210 kDa represent Peg3/Pw1 and ZnF protein, respectively. Immunoblotting was performed with anti-HA antibody (A and B) and also anti-GST antibody as a control (C).

To further investigate the interaction between RaLP/ShcD and Peg3/Pw1, pull-down experiments were performed using GST or GST-RaLP/ShcD-CH1 fusion proteins to precipitate full-length Peg3/Pw1 or a deleted version encoding only ZnF domains 1 - 12 without the SCAN domain (HA-ZnF) using HEK293 cells transfected either with full-length HA-Peg3/Pw1 or HA-ZnF as shown in Figure 4.9. The cells were lysed and incubated either with GST or GST-RaLP/ShcD-CH1 fusion proteins at 4ºC with tumbling. In the whole cell lysates, two major bands of approximately 230 kDa and 210 kDa were observed corresponding to HA-Peg3/Pw1 and HA-ZnF, respectively (Figure 4.9A). Also, the same size bands were detected in samples where HA-Peg3/Pw1 and HA-ZnF had been immunoprecipitated with GST-RaLP/ShcD-CH1 (Figure 4.9B).

Intriguingly, the intensity of bands of full-length Peg3/Pw1 precipitating with RaLP/ShcD-CH1 domain was less than the ZnF shortened, suggesting that the CH1 domain of RaLP/ShcD may interact better with the Zinc finger region than full-length Peg3/Pw1 protein. In order to confirm that GST and GST-RaLP/ShcD-CH1 fusion proteins were present in equal amounts in the pull-down experiement, the blot was stripped and reprobed with anti-GST antibody as shown in Figure 4.9C.

4.2.2.2. Co-immunoprecipitation of RaLP/ShcD and Peg3/Pw1 expressed in HEK293 cells

To further confirm that the interaction between RaLP/ShcD and Peg3/Pw1 is significant, co-immunoprecipitation experiments were performed. HEK293 cells were co-transfected either with GFP-RaLP/ShcD and HA-Peg3/Pw1, or HA-ZnF. The cells were lysed and immunoprecipitation experiments were then completed using anti-HA or anti-Flotillin 2 antibodies as a negative control and immunoblotting was achieved using an anti-GFP antibody. Bands at around 100 kDa represent GFP-RaLP/ShcD protein in the whole cell lysates of the cells which were co-transfected together with GFP-RaLP/ShcD and HA-Peg3/Pw1, or HA-ZnF (Figure 4.10A). Also, approximately the same size band was observed in samples where GFP-RaLP/ShcD had been co-precipitated with HA-Peg3/Pw1 and HA-ZnF as shown in Figure 4.10C.

In order to verify the efficiency of immunoprecipitation of HA-Peg3/Pw1 and HA-ZnF, the blot was stripped and reprobed with anti-HA antibody (Figure 4.10B). As shown in Figure 4.10B and Figure 4.10D, bands of about 230 kDa and 210 kDa in the molecular weight corresponding to HA-Peg3/Pw1 and HA-ZnF, respectively were detected both in whole cell lysates and the anti-HA immunoprecipitations, confirming that Peg3/Pw1 and ZnF had been immunoprecipitated efficiently. This result confirmed that GFP-RaLP/ShcD can co-precipitate with HA-Peg3/Pw1 and HA-ZnF in HEK293 cells. Interestingly, the ZnF domains appeared to interact more efficiently than the full-length protein.

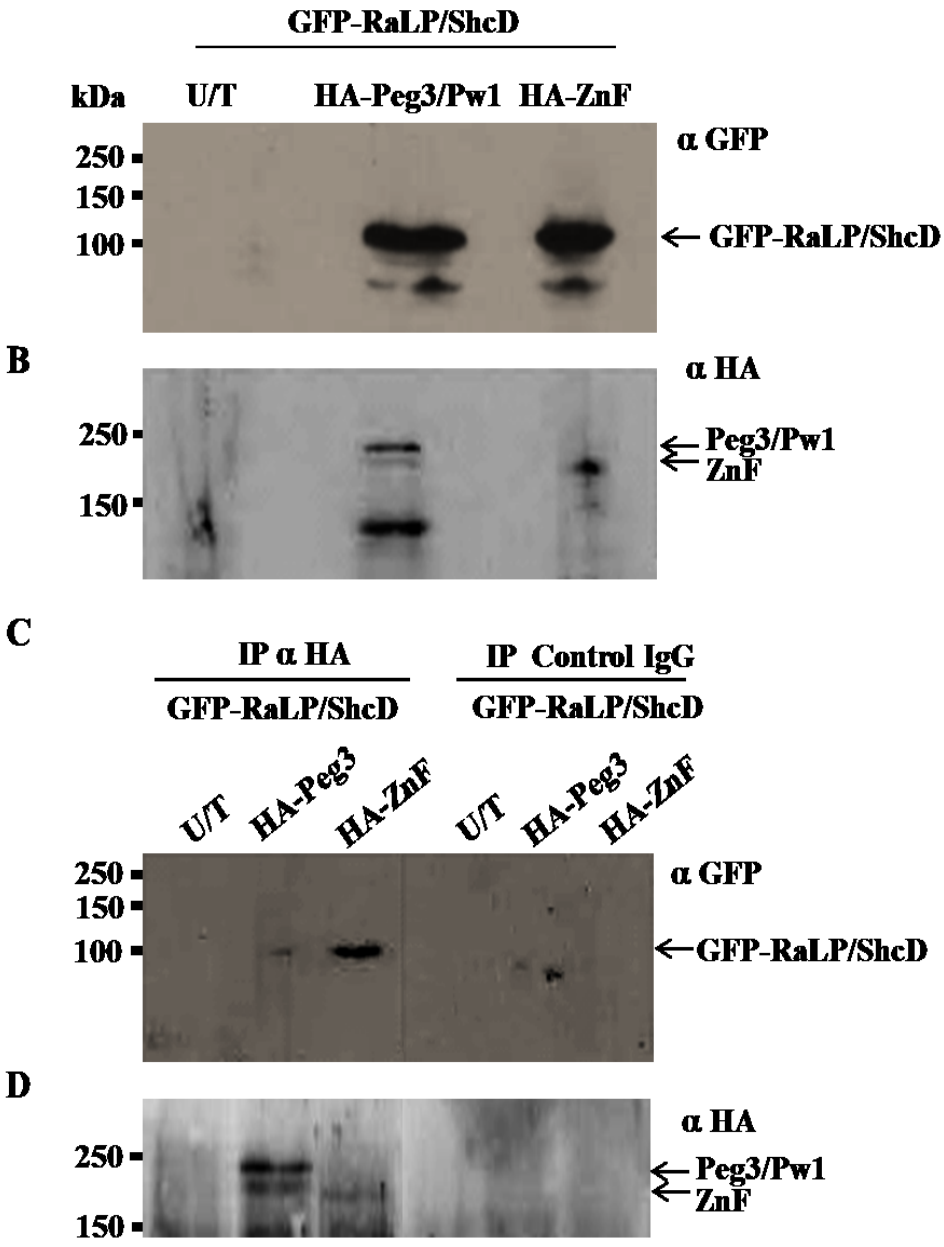

Figure 4.10. GFP-RaLP/ShcD can co-precipitate with HA-Peg3/Pw1 and HA-ZnF in HEK293 cells. HEK293 cells were either co-transfected with GFP-RaLP/ShcD and HA-Peg3/Pw1 or HA-ZnF (T) or left untransfected (U/T). Immunoprecipitation (IP) was performed with anti-HA antibody or anti-Flotillin 2 antibody as a negative control. Bands at approximately 100 kDa represent GFP-RaLP/ShcD in cells co-transfected with HA-Peg3/Pw1 and HA-ZnF protein. Whole cell lysates (WCL) were analysed on 10% SDS-PAGE gels followed by western blotting with anti-GFP (A) or anti-HA antibody (B). Immunoprecipitates were analysed on 10% SDS-PAGE gels followed by western blotting with anti-GFP (C) or anti-HA antibody (D).

4.2.2.3. Effect of Peg3/Pw1 and Camptothecin on RaLP/ShcD protein in HEK293 cells stably expressing FLAG-RaLP/ShcD (F4) or GFP-RaLP/ShcD (G5)

Our results suggested that a small proportion of Peg3/Pw1 and RaLP/ShcD can co-immunoprecipitate. Since Peg3/Pw1 has been shown to be involved in the cellular response to DNA damage, we speculated that maybe RaLP/ShcD association with Peg3/Pw1 could be enhanced upon DNA damage. For the following studies we used HEK293 cells that stably express either FLAG-RaLP/ShcD (F4) or GFP-RaLP/ShcD (G5). By using stable cells it was only necessary to introduce one plasmid, thereby reducing variation between experiments.

Initially, F4 cells were transfected with HA-Peg3/Pw1 and then DNA damage was induced by treatment with camptothecin (CPT) for 24 hours, or cells were left untreated. CPT is a well-known DNA damaging agent, inhibiting DNA religation by binding the topo I (DNA enzyme topoisomerase I) causing DNA damage to the cells. CPT treated cells were stained with anti-phospho H2A.X antibody alone using an appropriate secondary antibody as a control (data not shown). Immunoblotting was performed on whole cell lysates using anti-FLAG antibody. As shown in Figure 4.11A, a band of roughly 75 kDa representing FLAG-RaLP/ShcD was present in the untreated sample but at a reduced level in the CPT treated sample. The blot was stripped and reprobed with anti-HA antibody in order to confirm the equal level of HA-Peg3/Pw1 expression. In both CPT treated and untreated samples, bands of about 230 kDa were present corresponding to HA-Peg3/Pw1, although a slight reduction in levels was observed following CPT treatment. These initial results suggested that CPT was causing degradation of RaLP/ShcD, and to a lesser extent Peg3/Pw1.

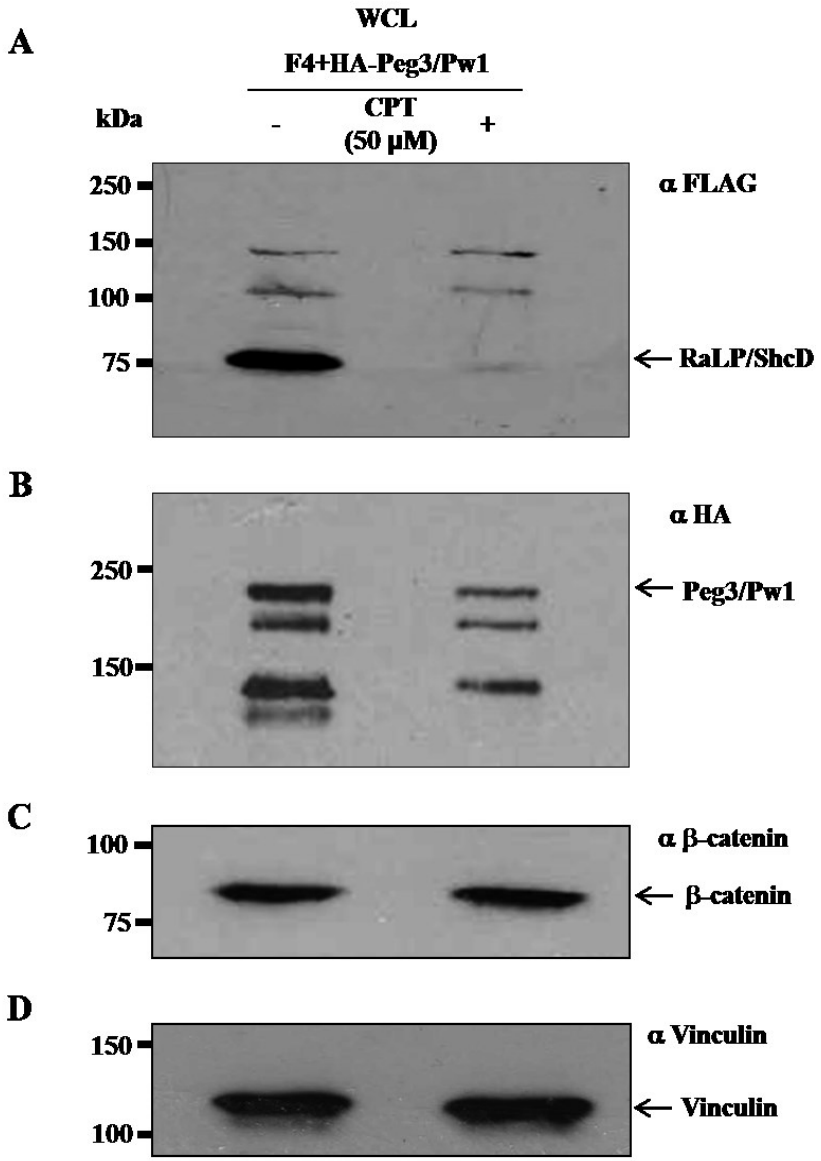

Figure 4.11. Effect of Peg3/Pw1 and Camptothecin on RaLP/ShcD protein in HEK293 cells stably expressing FLAG-RaLP/ShcD (F4). HEK293 cells stably expressing FLAG-RaLP/ShcD were transfected with HA-Peg3/Pw1. DNA damage was induced by treatment with camptothecin (50 µM) for 24 hours (+) or cells were left untreated (-). Whole cell lysates (WCL) were analysed on a 10% SDS-PAGE gel followed by western blotting with anti-FLAG (A) or anti-HA (B) or anti-β Catenin (C) antibodies. Also anti-vinculin antibody was used as loading control (D).

Intriguingly, a recent paper revealed that a decrease in Peg3/Pw1 protein expression levels resulted in increased levels of β-catenin, resulting in the inhibition of Wnt signalling (Jiang *et al*., 2010). Since the level of Peg3/Pw1 decreased slightly on CPT treatment we looked to see if this decrease level of Peg3/Pw1 resulted in an change in the level of β-catenin using β-catenin antibody. However, as seen in Figure 4.11C, the expression level of β-catenin in both CPT treated and untreated cells were almost the same. The blot was then stripped and reprobed with anti-Vinculin antibody as a loading control as shown in Figure 4.11D.

To confirm the intriguing finding in F4 cells, HEK293 cells stably expressing GFP-RaLP/ShcD (G5) were analysed similarly. Immunoblotting was performed using an anti-RaLP/ShcD antibody. As noted in Figure 4.12, bands of about 100 kDa representing GFP-RaLP/ShcD were detected in all the samples while the level of expression of RaLP/ShcD was greatly elevated only in Peg3/Pw1 transfected cells without CPT treatment. In this case, cells that had not been transfected with Peg3/Pw1 were also analysed by western blotting with or without CPT. Camptothecin treatment restored the level of GFP-RaLP/ShcD to the levels in the G5 cells that had not been transfected with Peg3/Pw1. This changes the interpretation of the previous figure as it appears the Peg3/Pw1 is inducing RaLP/ShcD expression, and camptothecin is preventing this induction. One possibility is that Peg3/Pw1 is acting as a transcription factor and inducing transcription of GFP-RaLP/ShcD which is driven by the CMV promoter, and that DNA damage causes a reduction in transcription. To test whether increased transcription was responsible for the dramatic effect on RaLP/ShcD protein levels in Peg3/Pw1 expressing cells, Luciferase assays were performed.

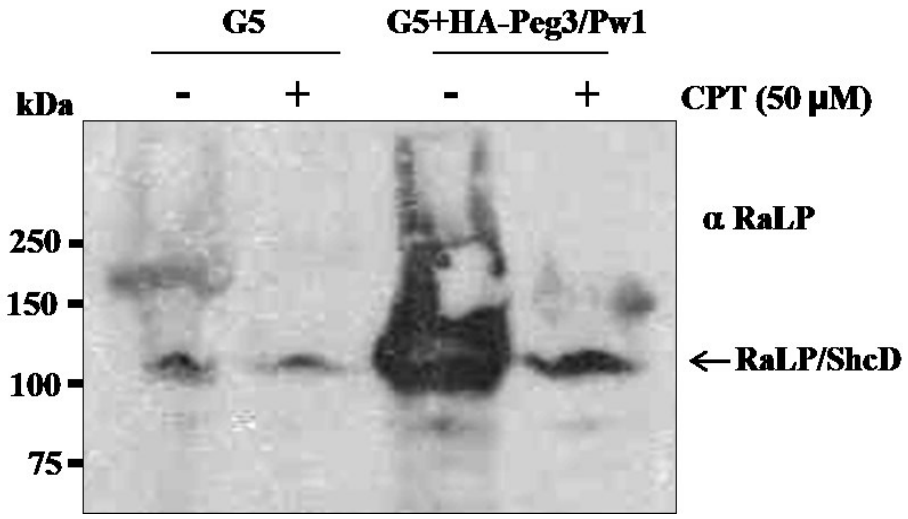

Figure 4.12. Effect of Peg3/Pw1 and Camptothecin on RaLP/ShcD protein in HEK293 cells stably expressing GFP-RaLP/ShcD (G5). HEK293 cells stably expressing GFP-RaLP/ShcD were either transfected with HA-Peg3/Pw1 or left untransfected. DNA damage was induced by either treating with camptothecin (CPT, 50 µM) for 24 hours (+) or cells were left untreated (-). Whole cell lysates were analysed on a 10% SDS-PAGE gel followed by western blotting with anti-RaLP antibody.

4.2.2.4. Renilla Luciferase Assay

To investigate whether Peg3/Pw1 was able to activate a CMV reporter or not, *Renilla* Luciferase assays were performed. HEK293 cells were co-transfected either with a CMV driven Luciferase reporter and HA-Peg3/Pw1, or FLAG-pCMV as a negative control. The measurement of *Renilla* Luciferase was achieved by using a luminometer. As seen in Figure 4.13, there is no significant difference in the luciferase activity of the cells expressing and Peg3/Pw1 compared to those transfected with a control vector. These findings suggest that Peg3/Pw1 is not activating the CMV promoter directly.

4.2.2.5. Determination of endogenous levels of RaLP/ShcD in B16-F10 Melanoma cells and the effect of Peg3/Pw1 transfection

Based on the previous investigations, the level of RaLP/ShcD expression was greatly elevated when the cells were transfected together with RaLP/ShcD and Peg3/Pw1 but this did not appear to be due to activation of the CMV promoter. To confirm that elevated levels of Peg3/Pw1 could similarly cause an increase in expression of endogenous RaLP/ShcD in cells, B16-F10 melanoma cells were transfected either with HA-Peg3/Pw1, or left untransfected. Immunoblotting was employed using anti-RaLP antibody. As shown in Figure 4.14A, the intensity of RaLP/ShcD was increased its expression when Peg3/Pw1 was overexpressed. To check the transfection efficiency of Peg3/Pw1, immunoblotting was performed using anti-HA antibody (Figure 4.14B). Also, immunobloting was performed using anti-Vinculin antibody as a loading control as shown in Figure 4.14C.

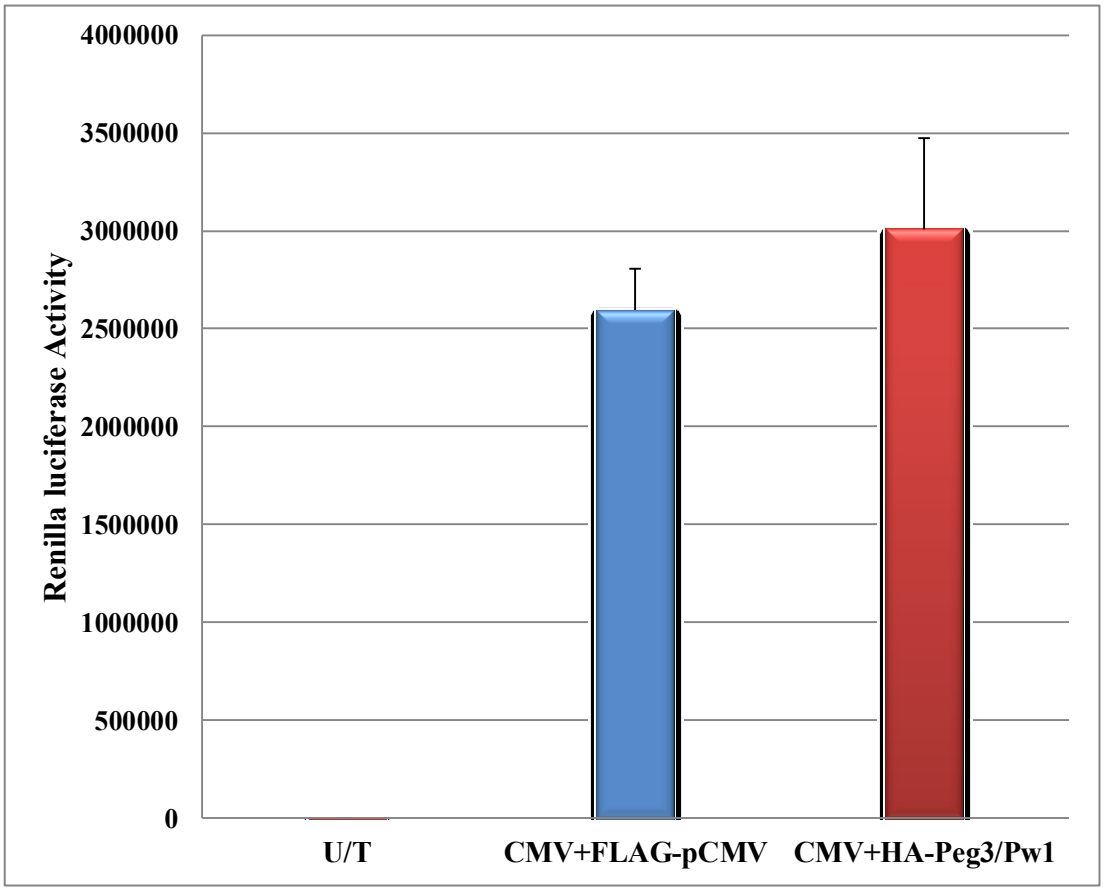

Figure 4.13. Determination of the activity of the CMV promoter by performing *Renilla* Luciferase assays in HEK293 cells. HEK293 cells were co-transfected either with the CMV driven luciferase reporter construct and HA-Peg3/Pw1, or the CMV driven reporter and FLAG-pCMV as a negative control. Luciferase activity was measured in untransfected cells (U/T) as a negative control. Three independent experiments were performed. *Renilla* luciferase was measured using a luciferase assay kit using a luminometer.

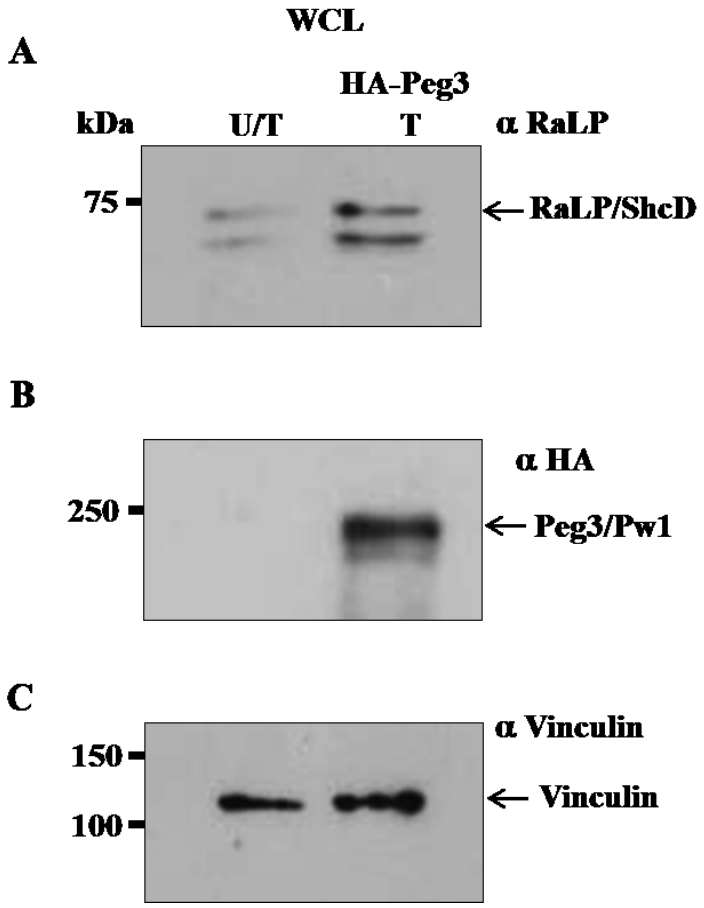

Figure 4.14. The endogenous level of RaLP/ShcD is increased following transfection with Peg3/Pw1 in B16-F10 melanoma cells. B16-F10 melanoma cells were either transfected with HA-Peg3/Pw1 or left untransfected. Whole cell lysates (WCL) were analysed on a 10% SDS-PAGE gel followed by western blotting with anti-RaLP (A) or anti-HA (B) antibodies. Also anti-Vinculin antibody was used as loading control (C).

This result illustrated that the endogenous expression of RaLP/ShcD was slightly elevated following transfection with Peg3/Pw1 in B16-F10 melanoma cells. Therefore it would seem that Peg3/Pw1 is affecting the RaLP/ShcD protein levels, possibly by stabilisation. Given the small amount of Peg3/Pw1 that binds directly to RaLP/ShcD, this may be via an indirect mechanism.

4.2.2.6. Determination of Subcellular localisation of RaLP/ShcD and Peg3/Pw1 in HEK293 cells

HEK293 cells were co-transfected with GFP-RaLP/ShcD and HA-Peg3/Pw1 and then analysed by immunocytochemistry using anti-HA antibody followed by an appropriate secondary antibody coupled to Alexa Fluor 594. HA-Peg3/Pw1 was mainly localised in the nucleus while GFP-RaLP/ShcD was predominantly localised in the cytoplasm (Figure 4.15A). This result revealed that there was no evidence that RaLP/ShcD and Peg3/Pw1 were associated in cells that had not been subjected to any treatments. Cells were stained with anti-HA antibody alone using the same secondary antibody as previously to test for specificity of staining. Although some background staining was observed in the cytoplasm, none was observed in the nucleus, suggesting that the anti-HA staining of HA-Peg3/Pw1 in the nucleus is specific (Figure 4.15B). We then examined the effect of camptothecin (CPT) on nuclear morphology.

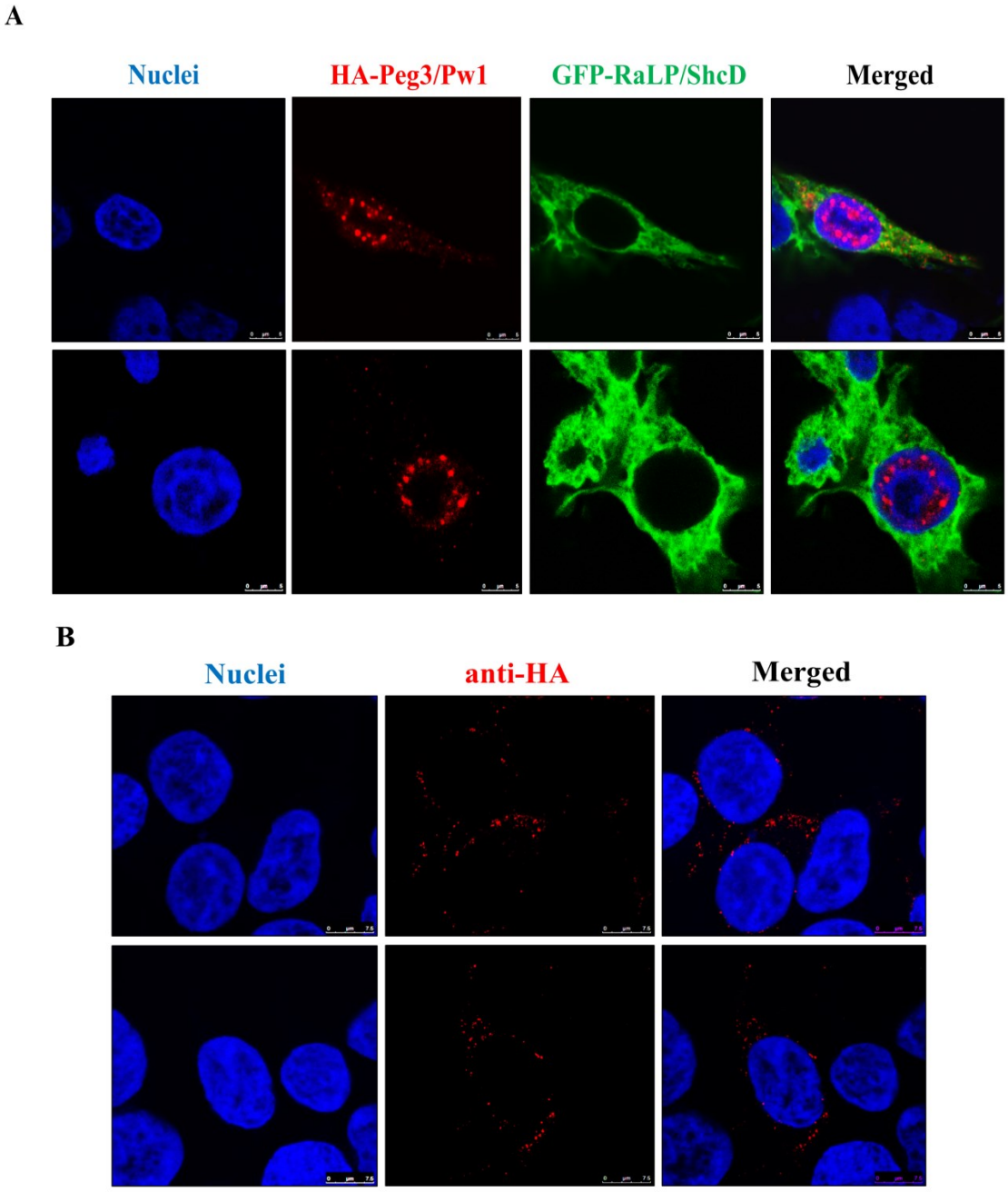

Figure 4.15. Determination of the subcellular localisation of HA-Peg3/Pw1 and GFP-RaLP/ShcD in HEK293 cells. A, HEK293 cells were co-transfected with HA-Peg3/Pw1 and GFP-RaLP/ShcD. The cells were stained with anti-HA antibody and Alexa Fluor 594 conjugated secondary antibody. B, HEK293 cells were stained with anti-HA antibody using secondary antibody coupled to Alexa Fluor 594. The cells were fixed and the visualised by confocal microscopy. Scale bar represents 5 µm (A) and 7.5 µm (B).

Following CPT treatment for 24 hours, nuclear morphology has changed compared to untreated sample, suggesting that DNA damage has induced chromatin margination and apoptosis in these cells (Figure 4.16A). HEK293 cells were transfected with HA-Peg3/Pw1, and either treated with CPT for 24 hours or left untreated, then the cells were stained with the secondary antibody as previously (Figure 4.16B and 4.16C). Transfected cells were fixed and visualised by confocal microscopy. Peg3/Pw1 was localised in the nucleus in both CPT treated and untreated samples. Many studies demonstrated that the Peg3/Pw1 is mainly localised in the nucleus (Relaix *et al*., 1996) whereas RaLP/ShcD is mainly localised in the cytoplasm.

Since Peg3/Pw1 has previously been implicated in DNA damage response we speculated that DNA damage may promote association with RaLP/ShcD. Previous studies in this lab have shown that a proportion of RaLP/ShcD can translocate the nucleus in response to stresses such as H_2O_2 treatment (Ahmed and Prigent, unpublished). Therefore nuclear translocation may have a role in protecting cells from cellular stress, or in inducing apoptosis. Although the p69-RaLP/ShcD isoform that has been used up until now in this thesis is the only one that has so far been reported in cells, the study by Jones *et al*., 2007, suggested that shorter isoforms p59-RaLP/ShcD and p49-RaLP/ShcD may arise as a result of alternative initiation codon usage. This would be similar to the situation with ShcA where three isoforms arise as a result of alternative splicing and initiation codon usage. Other work in this lab has shown that these shorter veriants p59-RaLP/ShcD and p49-RaLP/ShcD are predominantly present in the nucleus as they lack a nuclear export sequence (Ahmed and Prigent, unpublished).

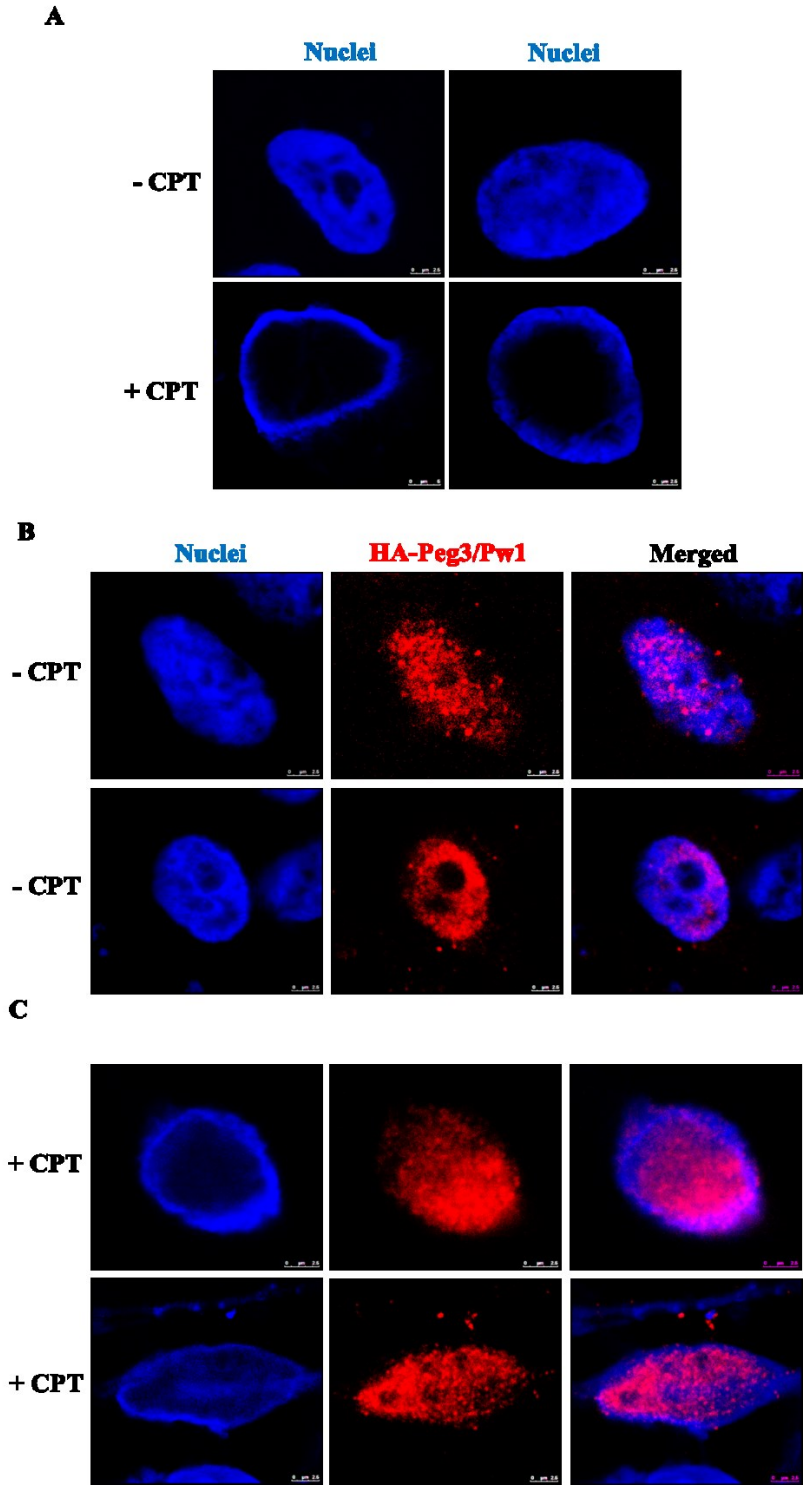

Figure 4.16. Determination of the efficiency of CPT treatment and anti-HA staining. The subcellular localisation of wild-type HA-Peg3/Pw1 with and without CPT treatment in HEK293 cells. A, HEK293 cells were either CPT treated (+CPT) for 24 hours or left untreated (-CPT). B and C, HEK293 cells were transfected with HA-Peg3/Pw1 and either treated with CPT (+CPT) for 24 hours or left untreated (-CPT). The cells were fixed and the visualised by confocal microscopy. Scale bar represents 5 µm (A) and 2.5 µm (B and C).

We hypothesised that maybe the shorter isoforms of RaLP/ShcD may show a more significant co-localisation with Peg3/Pw1 either in the presence or absence of DNA damage. Initially cells were transfected with GFP-p49RaLP/ShcD alone to see if CPT would affect its cellular localisation. No obvious difference was observed (Figure 4.17).

Cells were then cotransfected with HA-Peg3/Pw1 and GFP-p49RaLP/ShcD and subjected to the same treatment. RaLP/ShcD and Peg3/Pw1 were discovered to be predominantly localised to the nucleus, both in the presence and absence of CPT treatment, with a small proportion of RaLP/ShcD and Peg3/Pw1 apparently co-localising in discrete subcompartments within the nucleus (white arrows) as shown in Figure 4.18.

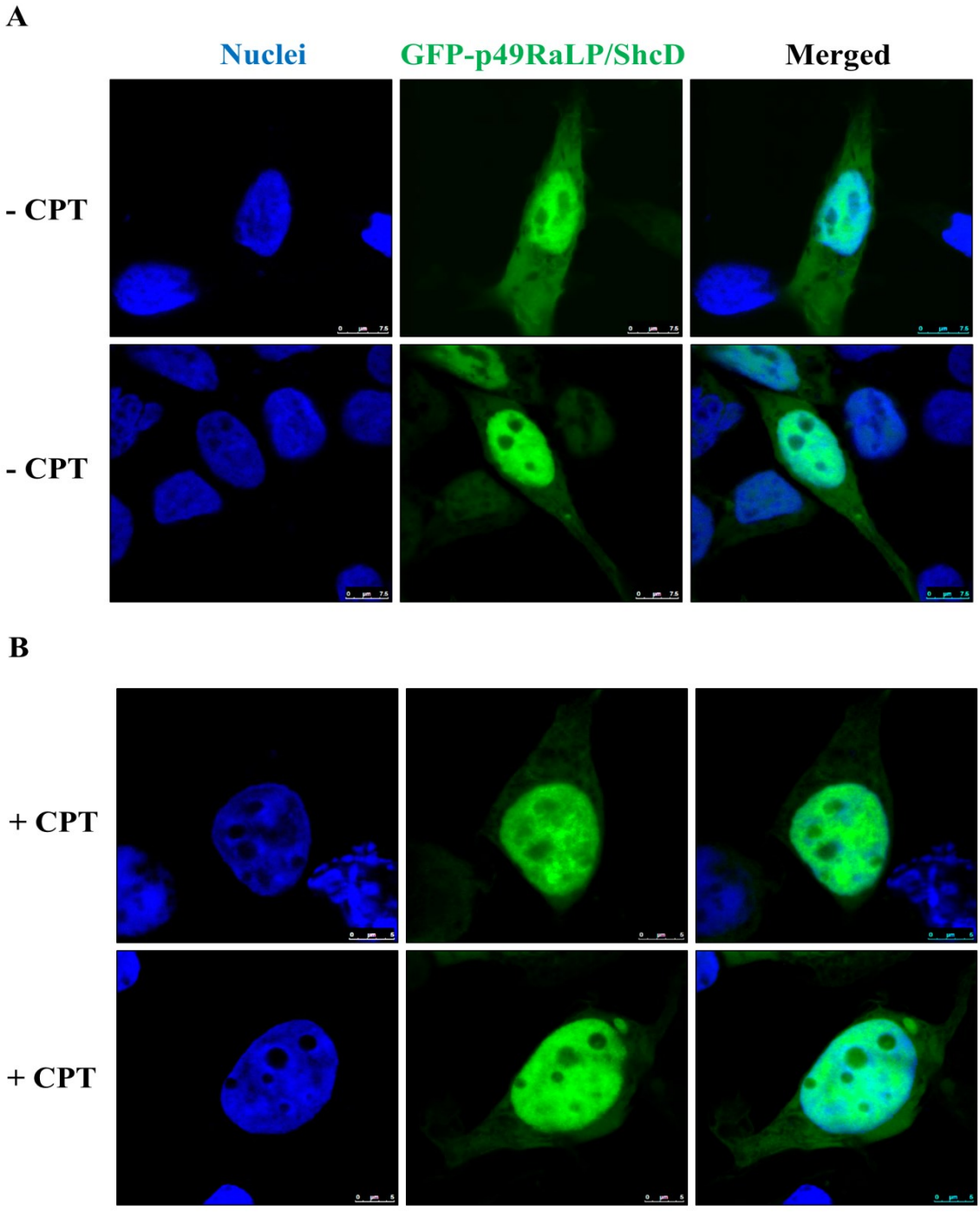

Figure 4.17. Determination of subcellular localisation of GFP-p49RaLP/ShcD in HEK293 cells with and without CPT treatment. HEK293 cells were transfected with GFP-p49RaLP/ShcD, and either treated for 24 hours with CPT (+CPT) or left untreated (-CPT). Cells were fixed and visualised by confocal microscope. Scale bars represent 7.5 µm (A) and 5 µm (B).

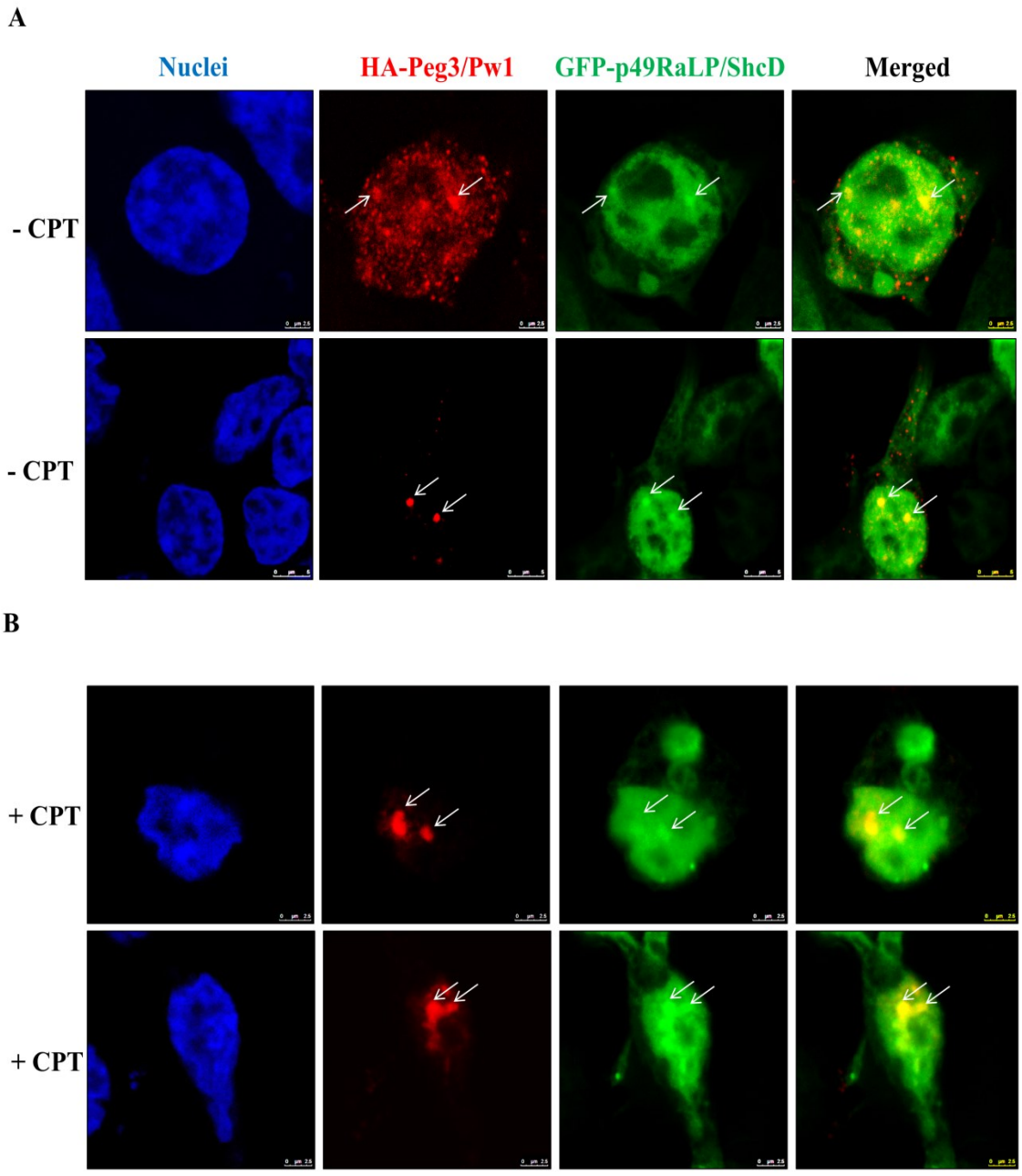

Figure 4.18. Determination of subcellular localisation of HA-Peg3/Pw1 and GFP-p49RaLP/ShcD in HEK293 cells with and without CPT treatment. HEK293 cells were co-transfected with HA-Peg3/Pw1 and GFP-p49RaLP/ShcD. The cells were treated with CPT for 24 hours (+CPT), while another set of cells were left untreated (-CPT) as a control. The cells were fixed and visualised by Confocal microscopy. Scale bar represents 2.5 µm.

4.2.3. Investigation of RaLP/ShcD and HP1α interaction

4.2.3.1. Precipitation of HP1α using GST-RaLP/ShcD-CH1 fusion protein in HEK293 cells

Since we identified HP1α as a novel interacting partner for RaLP/ShcD-CH1 in the yeast-two hybrid screen, we wanted to confirm that the interaction occur in human cells. HP1α is one of the families of HP1 adaptor proteins which may be involved in response to DNA damage (Dinant and Luijsterburg, 2009).

To confirm the interaction of RaLP/ShcD and HP1α, pull-down assays were firstly carried out by employing GST and GST-RaLP/ShcD-CH1 fusion proteins (Figure 4.19). HEK293 cells were either transfected with GFP-HP1α, or left untransfected. The cells were lysed and incubated either with GST or GST-RaLP/ShcD-CH1 fusion proteins bound to glutathione sepharose beads for 24 hours with tumbling at 4°C. Immunoblotting was then performed using an anti-GFP antibody. In whole cell lysates of the cells, one main band of around 55 kDa corresponding to GFP-HP1α was observed, which was not present in untransfected cells as seen in Figure 4.19A. This same size band was also observed in same samples from GFP-HP1α transfected cells that had been precipitated with GST-RaLP/ShcD-CH1 fusion protein. The blot was stripped and reprobed with anti-GST antibody to verify that similar amounts of GST and GST-RaLP/ShcD-CH1 fusion proteins were used for precipitation experiments (Figure 4.19B). This result showed that the CH1 domain of RaLP/ShcD can bind to full-length HP1α expressed in human cells.

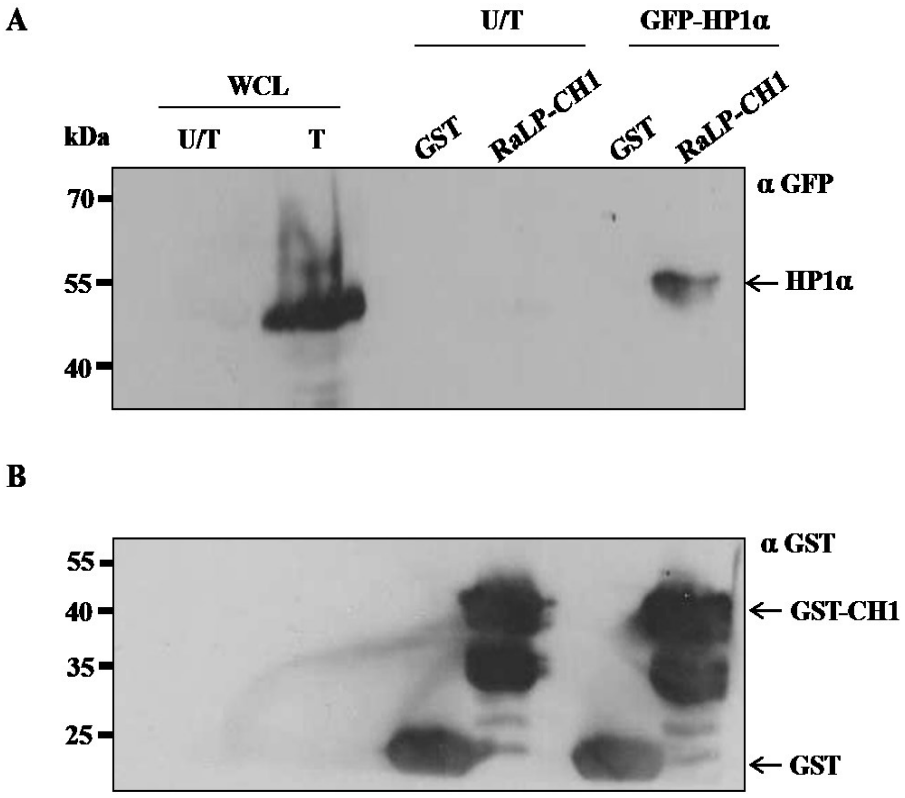

Figure 4.19. Precipitation of HP1α from transfected HEK293 cell lines using GST-RaLP/ShcD-CH1 fusion protein. HEK293 cells were transfected with GFP-HP1α. Cell lysates were incubated with GST or GST-RaLP/ShcD-CH1 fusion protein bound to glutathione sepharose beads. Bands at approximately 55 kDa represent HP1α protein. Immunoblotting was performed with anti-GFP antibody (A) and also anti-GST antibody was used as a control (B).

4.2.3.2. Co-immunoprecipitaion of RaLP/ShcD and HP1α expressed in HEK293 cells

Since RaLP/ShcD and HP1α interacted in pull-down assays, we decided to attempt co-immunoprecipitation assays. HEK293 cells were co-transfected with mCherry-RaLP/ShcD and GFP-HP1α. Transfected cells were lysed and immunoprecipitation was then carried out by anti-GFP-Trap (Chromotek). Immunoblot analysis was completed either using anti-GFP or anti-RaLP/ShcD antibodies as shown in Figure 4.20. A band of approximately 55 kDa of GFP-HP1α was presented in the whole cell lysates of transfected cells and the same band was precipitated by GFP-Trap (Figure 4.20A). A band of roughly 100 kDa corresponding to mCherry-RaLP/ShcD was detected in the whole cell lysates of transfected cells and was also present in the GFP-Trap immunoprecipitation (Figure 4.20B). This provides further evidence that full-length RaLP/ShcD is able to interact with full-length HP1α.

4.2.3.3. Determination of Subcellular localisation of RaLP/ShcD and HP1α in 518 melanoma cells

Given the positive results of association studies were interested to investigate co-localisation of RaLP/ShcD and HP1α in human cells. RaLP/ShcD is predominantly localised to the cytoplasm and HP1α is well-studied as a nuclear protein which mainly localises to heterochromatin in the nucleus (Cheutin *et al.*, 2003). This protein is also newly identified as being involved in the DNA damage response to Ultra-Violet (UV) irradiation (Luijsterburg *et al.*, 2009).

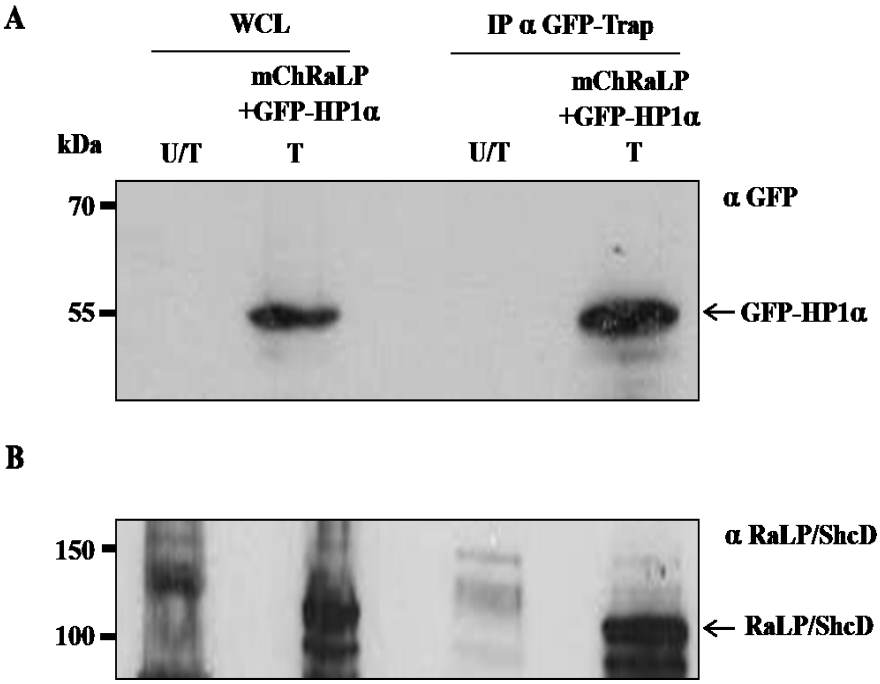

Figure 4.20. mCherry-RaLP/ShcD can precipitate with GFP-HP1α in HEK293 cells. HEK293 cells were co-transfected with mCherry-RaLP/ShcD and GFP-HP1α (T) or left untransfected (U/T). Immunoprecipitaiton (IP) was performed with anti-GFP-Trap. Bands at approximately 55 kDa represent GFP-HP1α and 100 kDa represent mCherry-RaLP/ShcD proteins, respectively. Whole cell lysates (WCL) of the cells were analysed on 10% SDS-PAGE gel followed by western blotting with anti-GFP (A) or anti-RaLP/ShcD (B) antibodies. Immunoprecipitates were analysed on a 10% SDS-PAGE gel followed by western blotting with anti-GFP (A) or anti-RaLP/ShcD (B) antibodies.

To determine subcellular localisation of RaLP/ShcD and HP1α, 518 melanoma cells were co-transfected with mCherry-RaLP/ShcD and GFP-HP1α followed by treatment either with cisplatin (CIS) to induce DNA damage, leptomycin B (LMB) to inhibit nuclear export or left untreated as a negative control. The reason for using LMB was that it had been observed that RaLP/ShcD possesses a functional nuclear export signal, and after addition of LMB, which is widely used as a suppressor of nuclear export, RaLP/ShcD accumulated in the nucleus (Ahmed and Prigent, unpublished).

It was hypothesized that by enhancing nuclear accumulation of RaLP/ShcD we may have a better chance of observing co-localisation. After the cells were treated with LMB, mCherry-RaLP/ShcD transfected cells displayed a predominantly nuclear distribution rather than cytoplasmic distribution, while in untreated cells mCherry-RaLP/ShcD was mainly in the cytoplasm (Figure 4.21). In addition, HP1α was mostly localised to the nucleus in cells treated with LMB or CIS and untreated cells. However, these results demonstrated that there was no obvious evidence that RaLP/ShcD and HP1α co-localise.

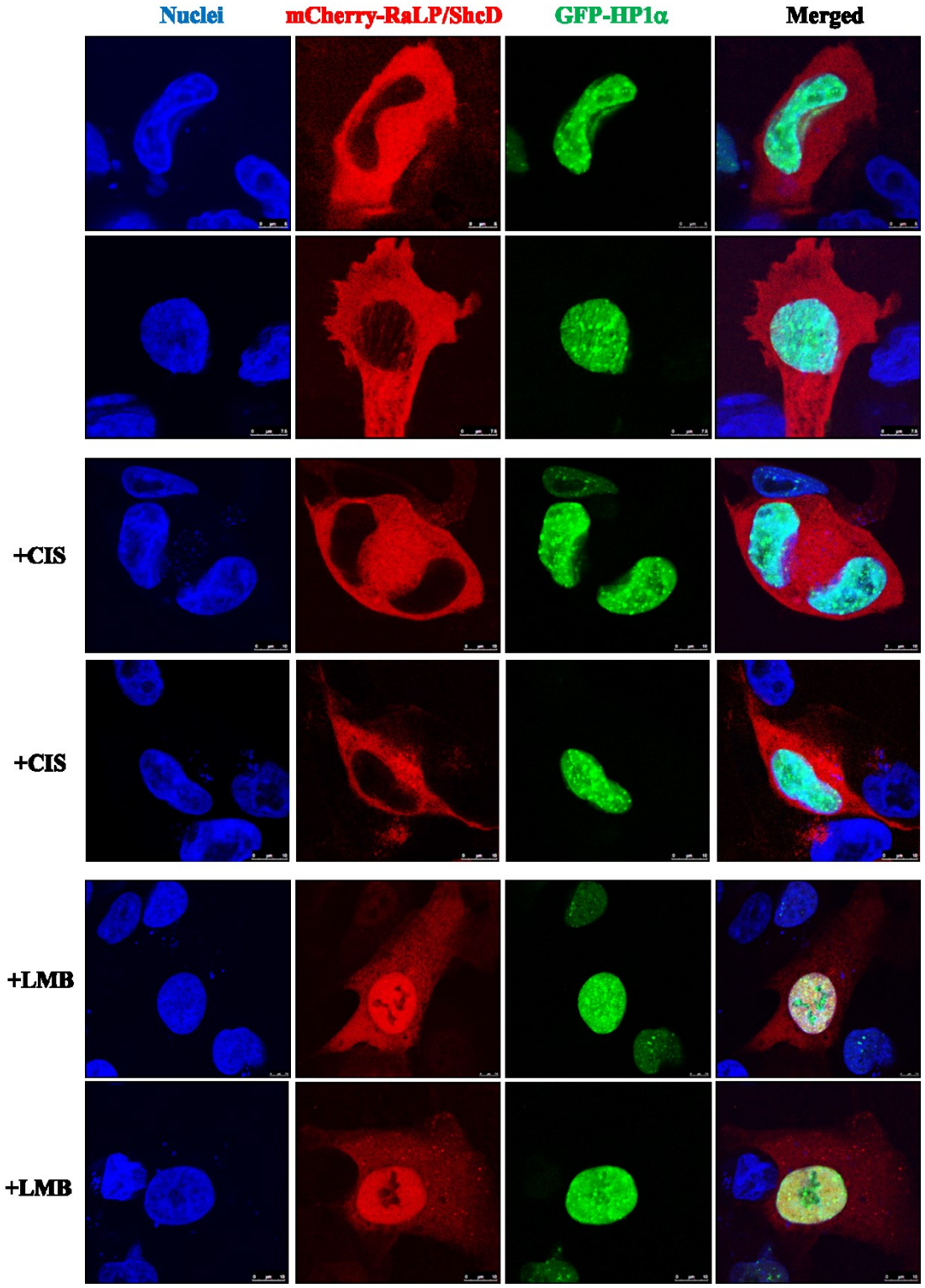

Figure 4.21. Determination of Subcellular localisation of mCherry-RaLP/ShcD and GFP-HP1α in 518 melanoma cells. 518 melanoma cells were cotransfected together with mCherry-RaLP/ShcD and GFP-HP1α followed by treatment with Cisplatin (+CIS) for 24 hours, or Leptomycin B (+LMB) for 2 hours, or left untreated. The cells were fixed and visualised by confocal microscopy. Scale bar represents 7.5 μm.

4.3. Discussion

Since the nuclear proteins Peg3/Pw1 and HP1α were isolated in the yeast two-hybrid screen using the CH1 domain of RaLP/ShcD as bait, it is interesting to speculate that RaLP/ShcD may have a function in the nuleus. Of the other Shc family members, p46-ShcA and p52-ShcA have been reported to interact with Ran (a Ras-like small GTPase) (George *et al*., 2009). Ran GTPases are involved in nuclear import and export. It was reported that these isoforms may directly associate with Ran via their SH2 domain mediating the translocation of Shc proteins into the nucleus. The SH2 domain of RaLP/ShcD, which shares a high degree of sequence homology with ShcA, may also associate with Ran to facilitate nuclear import.

4.3.1. A nuclear role for RaLP/ShcD

It has been characterised that RaLP/ShcD is predominantly localised in the cytoplasm of cells with only 5% of the protein found at the cell membrane (Fagiani *et al*., 2007). Interestingly, this lab has determined that RaLP/ShcD can localise in the nucleus of the cells when the protein is truncated within the N-terminal CH2 domain (Ahmed and Prigent, unpublished). Also, Jones and colleagues have previously reported that RaLP/ShcD possibly may have smaller isoforms due to the presence of several possible alternative initiation codons. Isoforms corresponding to the predicted p59 and p49 forms were observed when a construct encoding p69RaLP/ShcD was expressed in mammalian cells (Jones *et al*., 2007). This would parallel the situation with ShcA which exists at three different proteins of molecular weight 66, 52 and 46 kDa. This lab determined that RaLP/ShcD possesses a potential sequence within the CH2 domain at the N-terminus which can act as a nuclear export sequence (NES). RaLP/ShcD isoforms

p49-RaLP/ShcD and p59-RaLP/ShcD were observed predominantly in the nucleus when exogenously expressed in cells. So if these proteins exist naturally their role will reside within the nuclear compartment. Nuclear RaLP/ShcD could have significant biological functions, regulating transcriptional activity or associating with transcription regulatory molecules, leading to expression of proteins that mediate cell migration and invasion. It is of interest that the CH1 domain fused to LexA promoted activation of the *HIS3* reporter in L40 yeast. It is intriguing that almost all the proteins identified by the yeast two-hybrid screen studies using the CH1 domain of RaLP/ShcD are nuclear proteins such as Peg3/Pw1, HP1α and Hipk2. Having identified a number of proteins that interacted with the CH1 domain of RaLP/ShcD in the yeast two-hybrid assay, we focoused on the two nuclear proteins Peg3/Pw1 and HP1α for further evaluation.

4.3.2. Peg3/PW1 as a novel binding partner of RaLP/ShcD

Peg3/Pw1 (paternally expressed gene 3) was originally identified as one of the imprinted genes, containing twelve C2H2 (Cys-Cys-His-Cys) Zinc-finger (ZnF) domains in mouse (Kuroiwa *et al*., 1996). Human Peg3/Pw1 contains an additional SCAN domain at the N-terminus together with twelve Zinc-finger domains at the carboxy terminal (Figure 4.22). The SCAN domain is a subfamily of C2H2 type of Zinc finger in which involved in protein-protein associations and functions as a transcription factor (Edelstein and Collins, 2005).

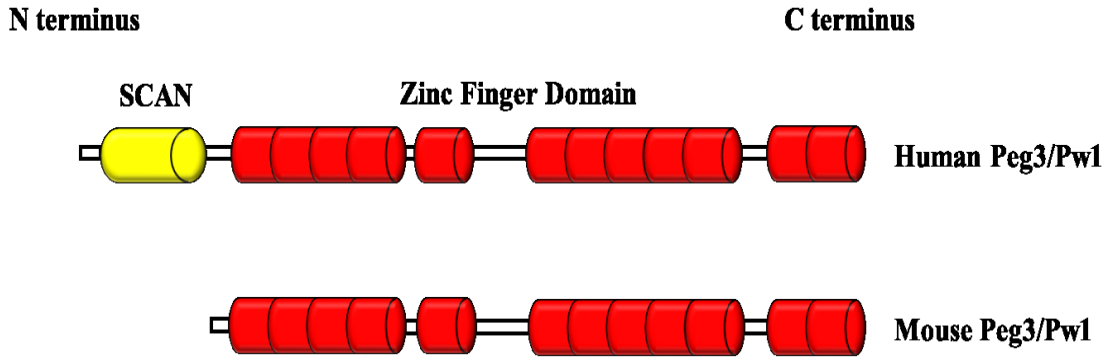

Figure 4.22. Schematic illustration of human and mouse Peg3/Pw1 protein. Human Peg3/Pw1 protein contains an N-terminal SCAN domain and twelve C2H2-type of Zinc-finger domains. The mouse protein lacks the SCAN domain.

These ZnF-like domains are able to mediate transcriptional activities, and can associate with proteins containing C2H2-type Zinc finger motifs (Pieler and Bellefroid, 1994). Peg3/Pw1 is generally expressed in brain, testis, embryo glial cells, and ovary in human. It has been reported to bind metal ions to have transcriptional activity, and to bind nucleic acids. The protein is predominantly localised in the nucleus and has been reported to be involved in mediating apoptosis, as well as cell proliferation under different situations (Deng and Wu, 2000). Also, it has been reported that the Siah (seven in absentia homology) family members, including Siah1a, interact with Peg3/Pw1 (Relaix *et al*., 2000). DNA damage induced p53 expression has been shown to initiate up-regulation of Peg3/Pw1 and its association with Siah1a. Interestingly, Siah1a has been documented as a significant regulator of p53-linked apoptosis (Amson *et al*., 1996; Nemani *et al*., 1996).

More intriguingly, it has been recently reported that overexpression of mRNA of Peg3/Pw1 resulted in decreased expression of β-catenin and prevention of the Wnt signalling pathway during embryo development of zebrafish (Jiang *et al*., 2010). Also, Peg3/Pw1 can bind to β-catenin and mediate its degradation through the complex of the p53 and the ubiquitinligase Siah1 protein, via a GSK3-independent proteasomal event, resulting in inhibiting the Wnt signalling cascade in human cell lines (Jiang *et al*., 2010). This suggests that Peg3/Pw1 may have a role as a tumour suppressor gene. Also it was observed that a decrease in Peg3/Pw1 expression resulted in increased expression of β-catenin, regulating cell proliferation, and also inhibiting p53-mediated apoptosis in human glioma cell lines. Hence, Peg3/Pw1 can manipulate the Wnt pathway.

Our results from pull-down and co-immunoprecipitation experiments confirmed that RaLP/ShcD can associate with Peg3/Pw1 when exogenously expressed in HEK293 cells. Interestingly, in both experiments full-length Peg3/Pw1 associated less efficiently with RaLP/ShcD than the Peg3/Pw1 protein lacking the SCAN domain but containing all twelve Znic finger domains (referred to as ZnF). This ZnF protein is similar to the mouse Peg3/Pw1 (Figure 4.9 and 4.10). It seems to be that RaLP/ShcD interacts directly with the ZnF region of Peg3/Pw1. It may be that human Peg3/Pw1 is folded such that the SCAN domain prevents access of RaLP/ShcD to its binding site. Opening up of the molecule, perhaps by interaction with another protein may make improve access to the RaLP/ShcD binding site. We investigated the RaLP/ShcD and Peg3/Pw1 association only in HEK293 cell lines as it was never possible to achieve Peg3/Pw1 expression in melanoma cell lines such as 518 and DAUV. It is possible that Peg3/Pw1 transfected melanoma cells may undergo apoptosis as these cells are readily transfected by most constructs we have used. Future investigations could use B16-F10 melanoma cell lines, in which exogenous Peg3/Pw1 expression has been achieved in preliminary experiments.

Peg3/Pw1 protein is predominantly localised in the nucleus (Deng and Wu, 2000), our findings also support its nuclear localisation. A small fraction of Peg3/Pw1 can co-localise with p49-RaLP/ShcD in the presence or absence of CPT treatment in the nucleus in HEK293 cell lines (Figure 4.18). This may suggest that RaLP/ShcD could act as a linker protein of Peg3/Pw1 mediated signalling events. Interestingly, in preliminary experiments, cells were transfected p49-RaLP/ShcD together with Peg3/Pw1 showed reduced apoptosis in response to CPT treatment when compared to those expressing

Pwg3/Pw1 alone, suggesting RaLP/ShcD in the nucleus may have a protective effect either reducing apoptosis or stimulating DNA damage (data not shown). These experiments need to be repeated with appropriate controls.

Furthermore, in Peg3/Pw1 and RaLP/ShcD co-transfected cells, Peg3/Pw1 led to increased expression of RaLP/ShcD. Given the dramatic effect of Peg3/Pw1 and camptothecin on expression levels of RaLP/ShcD in this system, we did not continue to perform co-immunoprecipitation experiments, as the results would be difficult to interpret. Further investigations need to be performed to determine whether Peg3/Pw1 and RaLP/ShcD interaction has a biological role, especially in the nucleus by using other stimuli. Also, RaLP/ShcD phosphorylation can be induced by growth factors such as EGF and IGF-1 in metastatic melanoma cells and this may lead to association (Fagiani *et al*., 2007).

4.3.3. HP1α (heterochromatin protein 1) is a novel binding partner for RaLP/ShcD

The heterochromatin protein 1 (HP1) family was initially isolated as a heterochromatin regulated gene silencing protein in Drosophila melanogaster, although this protein is not a histone chromosomal protein (Eissenberg *et al*., 1990). HP1 proteins contain two conserved domains including the chromo domain (CD) at the N-terminus, and the chromo shadow domain (CSD) at the C-terminus, which are separated by the hinge domain (HD) as illustrated in Figure 4.23. The CD domain can directly associate with methylated Histone H3-Lysine 9 (H3K9), and this interaction has a significant role in heterochromatin maintenance (Maison and Almouzni, 2004). Also, the HD region is able to associate either with DNA or RNA, and the CSD domain is involved in various protein-protein interactions (Eskeland *et al*., 2007).

So far, three members of the HP1 protein family have been characterised including HP1α, HP1β, and HP1γ (Maison and Almouzni, 2004). It is interesting that these members display a different subcellular localisation although they share the comparable domain structures and share similar amino-acid sequences. Both HP1α and -β predominantly interact with heterochromatin. In addition, HP1β is also found in nucleoplasm, while HP1γ is associated with a number of euchromatic organelles (Minc *et al*., 2000; Nielsen *et al*., 2001). HP1α can also associate with linker histones such as H1 and H5, and DNA via its HD domain (Meehan *et al*., 2003).

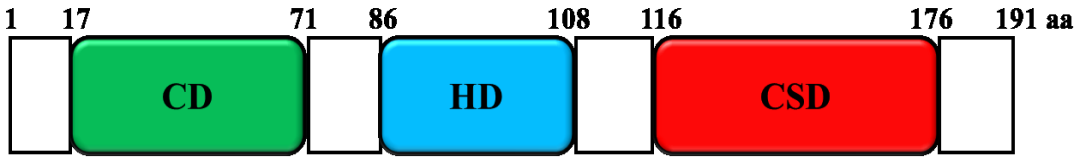

Figure 4.23. Schematic illustration of domain structure of HP1α. HP1α is shown with the N-terminal chromo domain (CD) and the C-terminal chromo shadow domain (CSD) separated by the hinge domain (HD). Each of the domains of HP1α can interact with particular molecules which are theoretically significant for the heterochromatin maintenance. Notably, the CD domain is able to bind methylated histone H3 lysine 9, and the HD domain can associate with chromatin, DNA and RNA.

Since HP1α has been identified, several roles of the protein have been reported as it is involved in DNA replication and repair, and interacts with a variety of proteins and nuclear envelope components such as the nuclear membranes, and nuclear pore proteins (Lomberk *et al*., 2006; Fanti and Pimpinelli, 2008). HP1α is able to associate with various nuclear proteins (Fuks *et al*., 2003) and its roles are primarily in heterochromatin organisation and association with transcriptional activator proteins in the nucleus of cells. However, a recent finding has indicated that HP1α protein might be implicated in the DNA damage response upon UV stimulation (Luijsterburg *et al*., 2009).

Our results have shown that RaLP/ShcD can interact with HP1α as revealed in both pull-down and co-immunoprecipitation experiments. Therefore, we sought to investigate their subcellular localisation. However, there was no evidence of co-localisation of RaLP/ShcD and HP1α before and after CIS and LMB treatment in 518 melanoma cells. It is possible that a different stimulus may promote association. It should be noted that all the expression studies were formed in transfected cells expressing vey high levels of HP1α and RaLP/ShcD. High expression may mask any evidence of association of a small amount of the proteins. It may be worth using Triton X-100 to wash away soluble nuclear proteins prior to fixing so that proteins associating with chromatin may become more evident. Ideally we would like to visulaise the endogenous proteins.

These proteins described in this chapter were all identified using the yeast two-hybrid system. The yeast two-hybrid system is a well-established technique which provides an easy way to investigate protein-protein interactions. One advantage of the yeast two-hybrid system is that interactions occur in the living cell. It allows determination of even weak interactions due to the sensitive reporter gene, and weak protein interactions can be very significant in signalling pathways. On the other hand, a critical disadvange of this system is that bait and/or prey fusion proteins may have an altered conformation resulting in changes in binding abilities. Consequently, a misfolded bait protein may not be able to provide binding sites for interacting proteins or have alterned binding properties. Since bait and prey constructs are engineered to contain nuclear localisation sequences, it is possible that interactions will be detected between proteins that would not normally meet in their normal environment. Clearly we cannot rule out the possibility that the interactions that we have detected would not occur when the proteins are expressed at their natural levels in mammalian cells.

Chapter 5

Characterisation of the CH1 domain of RaLP/ShcD

5.1. Introduction

Although the Shc family of adaptor proteins share the CH2-PTB-CH1-SH2 domain structure from the N- to C-terminus, the CH1 domains are poorly conserved. The CH1 domain of RaLP/ShcD has not been characterised, but it contains 6 cysteine and 2 histidine residues not present in other Shc family members using a protein structure prediction package this region has very weak homology to a Zinc finger domain (Figure 1.6).

Due to its unusual sequence (6 cysteines, 2 histidines) we speculated that the CH1 domain of RaLP/ShcD could be acting as a metal-binding or Zinc finger-like domain. Various zinc finger domains have been identified including Cys_2His_2 (C2H2) and Cys_4. These histidine and/or cysteine rich motifs usually require zinc binding to acquire the stability of their folds (Berg and Godwin 1997; Coleman, 1992). The C2H2 type is the classic form of zinc finger, in which the sequence motif present is: Cys-$X_{2,4}$-Cys-X_{12}-His-$X_{3,4,5}$-His. These have been found in transcription factors such as Transcription Factor for polymerase III A (TFIIIA) from *Xenopus laevis*, and functions as a DNA-binding domain (Miller *et al*., 1985; Hanas *et al*., 1983). Proteins containing C2H2 zinc fingers have been shown to be involved in mediating DNA-protein, RNA-protein and protein-protein associations (Mackay and Crossley, 1998).

Furthermore, the LIM domains are well characterised metal binding domains which are found in the euaryotes. In terms of name, LIM stands for the first letters of three proteins Linl-1, Isl-1 and Mec-3, in which this domain was initially identified (Way and

Chalfie, 1988; Karlsson *et al*., 1990). Generally, these domains possess two zinc finger-like domains which are rich in cysteines and histidines. These residues allow co-ordinate bond formation zinc atoms. LIM domains are able to bind DNA and act as transcription factors, and are also involved in protein-protein interactions (Yaden *et al*., 2005). Also, many proteins containing LIM domains a shuttle between the cytoplasm and the nucleus although some of them have limited functions either in the cytoplasm or the nucleus. For example, several focal-adhesion proteins containing LIM domains including zyxin (Cattaruzza *et al*., 2004) and FHL2 (Müller *et al*., 2002) have been reported that are able to translocate to the nucleus, and these may have different functions in the two cellular compartments.

Therefore, in this chapter, we aimed to purify the CH1 domain of RaLP/ShcD, to determine whether this domain binds metal ions, and whether it has any structrure, using NMR spectroscopy. We also aimed to use the purified CH1 domain to generate an affinity column to purify binding partners from cell extracts.

5.2. Results

5.2.1. Expression and Purification of GST-RaLP/ShcD-CH1domain

A construct encoding GST fused at the N-terminus of the RaLP/ShcD-CH1 domain was generated by ProTex (Department of Biochemistry, University of Leicester). Preliminary studies were carried out to test the solubility of the fusion protein. The GST-RaLP/ShcD-CH1 construct was transformed into BL21(DE3) competent cells.

A small-scale protein preparation was attempted to examine the solubility of the protein and optimal induction conditions. The protein expression was induced with IPTG in 10ml cultures for different times, and bacteria were then pelleted and resuspended in 200µl lysis buffer. Sonication was used to break open cells. Insoluble product was pelleted by centrifugation. In parallel total bacterial pellets were analysed after IPTG induction for different times by solubilising bacterial pellets in SDS-PAGE sample buffer (Figure 5.1A). Following induction by IPTG, a band of 34 kDa was observed in both soluble and insoluble fractions (Figure 5.1B and 5.1C). 4 hour stimulation with IPTG promoted maximal induction of GST-RaLP/ShcD-CH1.

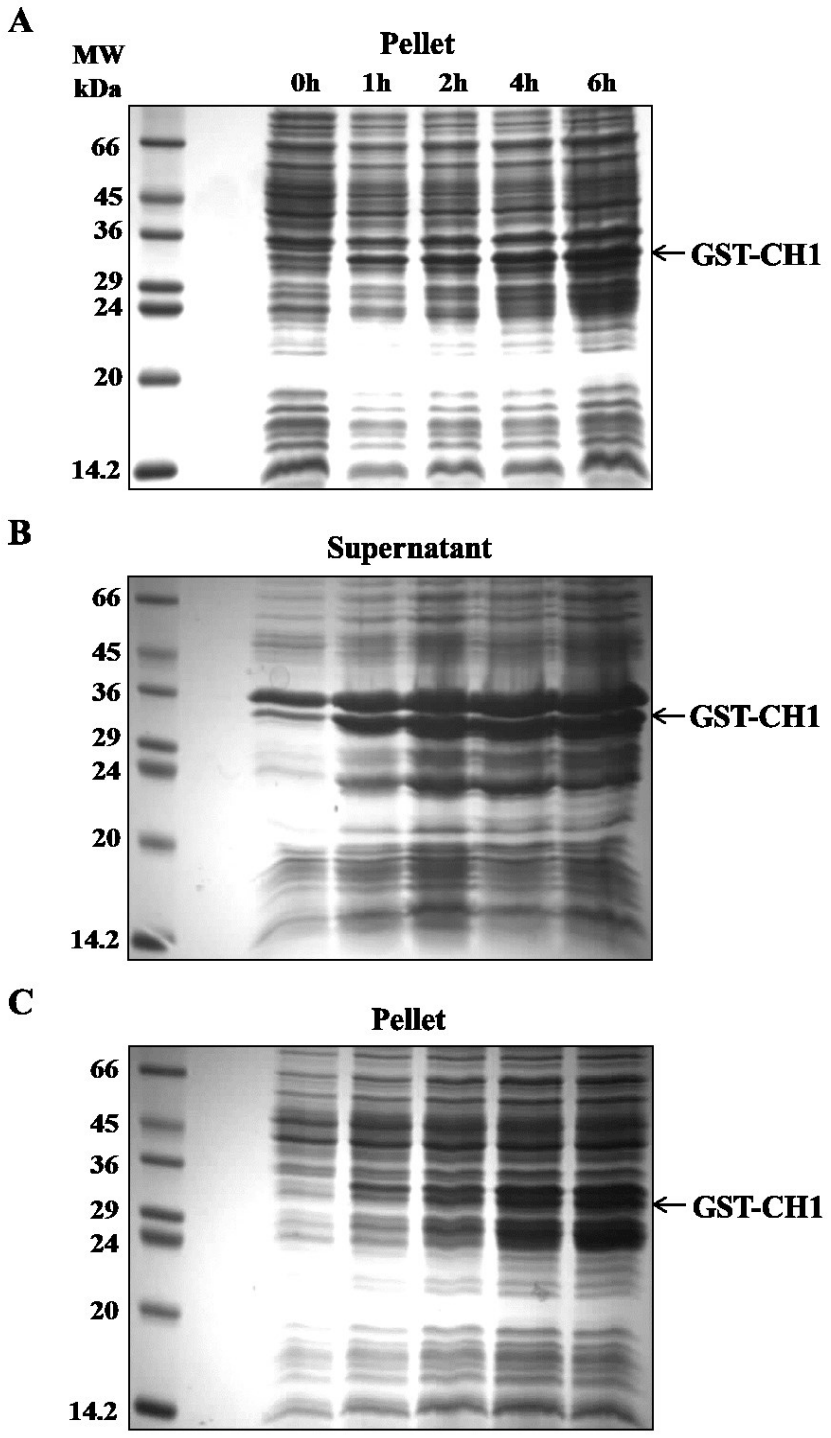

Figure 5.1. Expression of GST-RaLP/ShcD-CH1 in the soluble or insoluble fraction of BL21(DE3). *E.coli* were stimulated with IPTG for the indicated times. Total bacterial pellets (A) were analysed on 15% SDS-PAGE gels as well as soluble (B) and insoluble fractions (C).

5.2.2. Purification of GST-RaLP/ShcD CH1 domain

Having performed preliminary expressing studies to test the solubility of the GST-RaLP/ShcD-CH1 region, a large scale protein preparation was performed. 6 litres of bacterial culture were grown to an OD_{550} of 0.6 to 0.8 at 37°C and the GST-CH1 expression was induced with IPTG at 15°C overnight.

Bacteria were pelleted and disrupted using the French press. The GST-CH1 containing supernatant was bound to glutathione sepharose beads for 4 hours at 4°C with tumbling. Soluble GST-RaLP/ShcD-CH1 fusion protein was then eluted with reduced glutathione from a glutathione sepharose column (Figure 5.2A).

Bands at approximately 34 kDa in molecular weight corresponding to the GST-RaLP/ShcD-CH1 domain were observed. Protein was combined from the elution fractions (3 - 7) and then it was dialysed to remove the reduced glutathione, and treated with GST-TEV protease to cleave the GST from the fusion protein. The GST fusion protein was successfully cleaved yielding a band of approximately 17 kDa in molecular weight corresponding to the CH1 domain (Figure 5.2B).

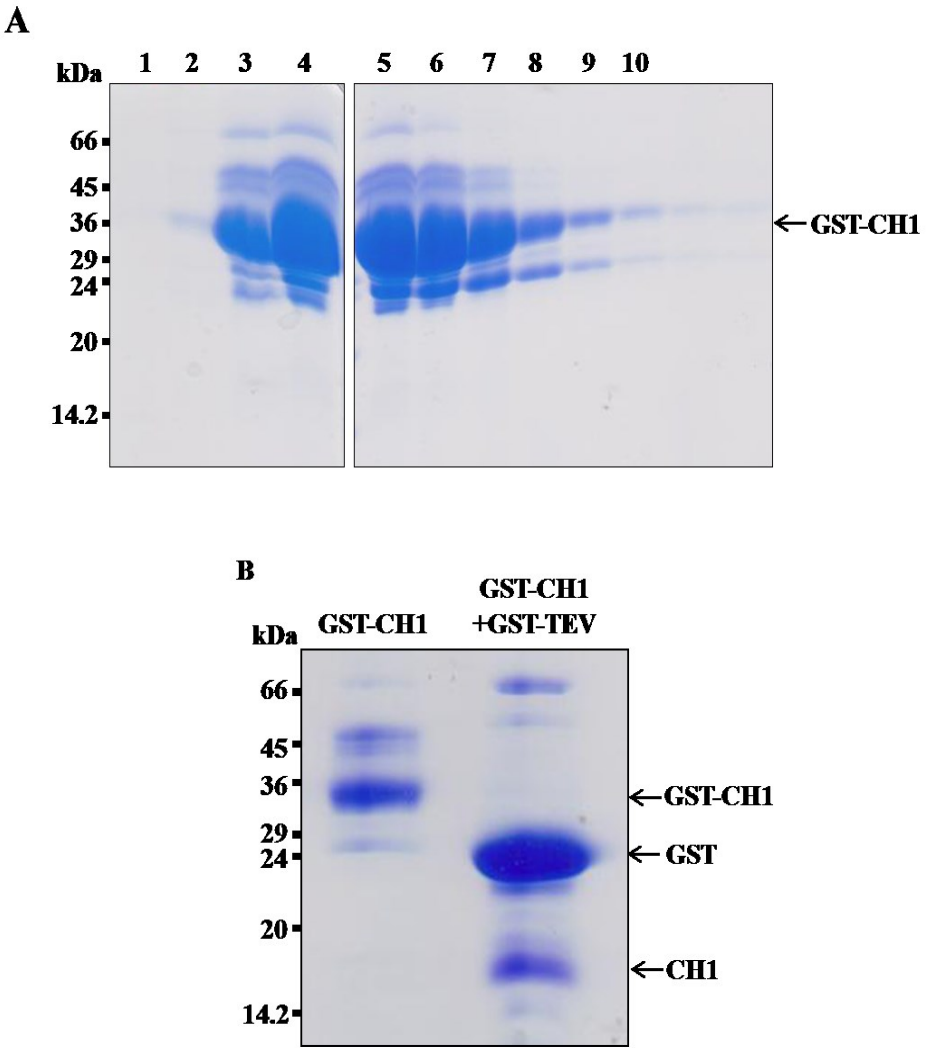

Figure 5.2. Purification of the GST-RaLP/ShcD-CH1 domain. A, Elution of the GST-RaLP/ShcD-CH1 fractions from glutathione sepharose column. Protein was eluted with elution buffer containing 20 mM reduced glutathione. B, The GST-RaLP/ShcD-CH1 cleavage by adding GST-TEV protease. Lane 1: before adding GST-TEV protease (GST-CH1), Lane 2: Cleaved form of the RaLP/ShcD-CH1 protein (GST-CH1+GST-TEV). The purity of the protein was assessed by SDS-PAGE on 15% gels under reducing conditions followed by staining with Coomassie blue stain.

5.2.3. Further Purification by Gel-filtration chromatography

Further purification was employed to remove the GST from the CH1 domain protein and other contaminants using gel filtration chromatography as shown in Figure 5.3. Column fractions were analysed at OD_{280} for total protein, and by SDS-PAGE to identify fractions containing the 17 kDa CH1 domain (Figure 5.3). Fractions B12, C1 and C2 containing the desired product were pooled and the concentration of the protein was measured by using the BCA protein assay.

6 ml of protein solution was obtained at a concentration of 40 µM. The purified CH1 domain was concentrated to 120 µM and subjected to the 1D NMR. However, the results indicated that the protein was unstructured. Also, we tried to add $ZnCl_2$ at a final concentration of 500 µM to the purified CH1 domain, but the result suggests that Zinc did not cause the CH1 domain of RaLP/ShcD to fold (data not shown).

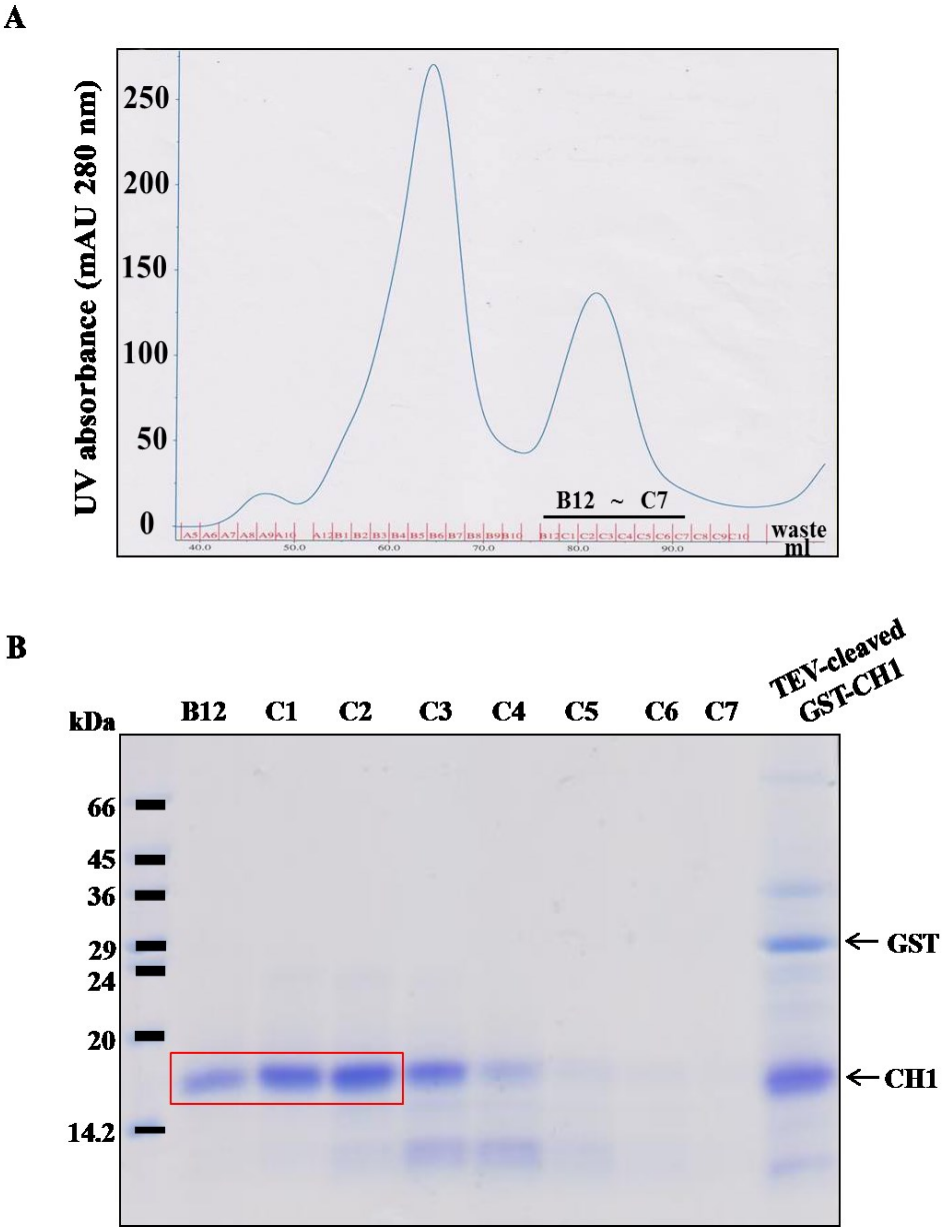

Figure 5.3. Purification of GST-RaLP/ShcD-CH1 domain by Gel-filtration chromatography. A, Elution profile of proteins from gel-filtration column (OD_{280}). B, RaLP/ShcD-CH1 was purified using gel filtration chromatography. B12, C1-C7, refer to elution fractions of RaLP/ShcD-CH1 domain from the gel filtration column, RaLP/ShcD-CH1 domain, prior to gel filtration, was loaded as a control. The purity of the protein was assessed by SDS-PAGE on a 15% gel under reducing conditions followed by staining with Coomassie blue.

5.2.4. Investigation of the CH1 domain of RaLP/ShcD as a metal binding domain

Since we were able to purifiy the CH1 domain, we carried out a simple experiment to determine if it has the potential to bind metal ions. Purified CH1 domain was incubated with Nickel bound chelating sepharose beads for 6 hours with tumbling at 4ºC. After incubation, the supernatant was removed into a fresh eppendorf tube and the beads were washed 3 times with wash buffer. Proteins bound to the beads were eluted in SDS-PAGE sample buffer and were analysed alongside the flow through by SDS-PAGE and Coomassie blue staining for the presence of the CH1 domain.

As shown in Figure 5.4, the 17 kDa protein corresponding to the CH1 domain was present in the sample eluted from the nickel beads but not in the supernatant. The purified CH1 domain, prior to binding the nickel beads, was also loaded as a control. This finding revealed that the CH1 domain could have a function as metal binding domain.

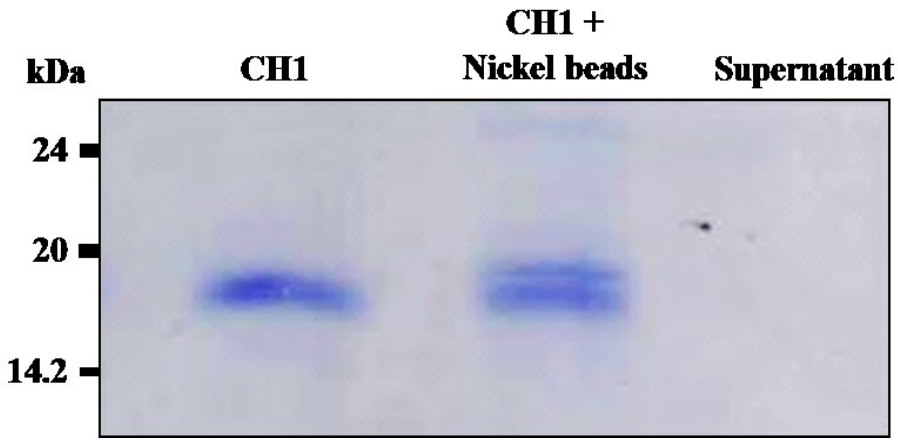

Figure 5.4. Preliminary characterisation of the CH1 domain as a metal binding domain. The purified CH1 domain was incubated with Nickel chelating sepharose beads with tumbling for 6 hours at 4 ºC. Lane 1, the purified CH1 domain, prior to incubation with the Nickel beads as a control. Lane 2, the purified CH1 domain was incubated with Nickel beads. Beads were washed and proteins bound to beads eluted with SDS-PAGE sample buffer, Lane 3, Proteins remaining in the supernatant after incubation with Nickel beads. The samples were analysed on a 15% SDS-PAGE gel under reducing conditions followed by staining with Coomassie blue.

5.2.5. Further investigation of the CH1 domain as a Metal binding domain using Cobalt ions

Since the preliminary studies showed that the purified CH1 domain of RaLP/ShcD could bind to Nickel-sepharose, we sought to further investigate the metal binding properties of RaLP/ShcD.

In a previous study to investigate the metal ion binding properties of the 18 amino acid peptide (Asp-Gln-**Cys**-Ala-Tyr-**Cys**-Lys-Glu-Lys-Gly-**His**-Trp-Ala-Lys-Asp-**Cys**-Pro-Lys) from Rauscher murine leukemia virus, an assay was employed which measured the shift in absorbance at 314 nm on cobalt binding. This happened due to the peptide coordinating with Co^{2+} through three cysteines and one histidine, forming a tetrahedral conformation (Green and Berg, 1989).

The CH1 domain of reduced protein was incubated in buffer containing 20 mM of Tris (pH 7.4) with 100 mM of NaCl. The protein was then treated with an increasing concentration of $CoCl_2$ up to 1 mM. The absorbance of the protein was monitored over the range 250 to 800 nm by employing a spectrophotometer. As shown in Figure 5.5, the spectrum of the CH1 protein revealed no obvious shift in absorbance on the addition of $CoCl_2$, suggesting no binding of cobalt to the CH1 domain had occured.

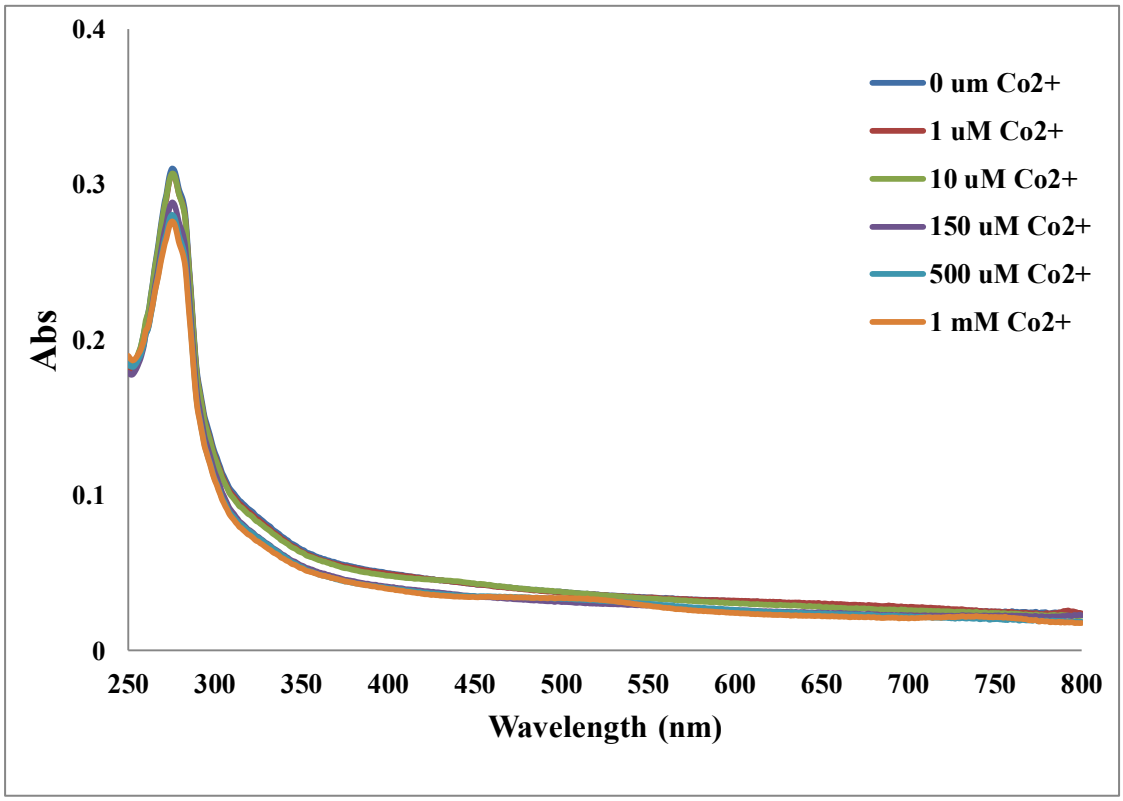

Figure 5.5. Assay to measure Co^{2+} binding to the CH1 domain of RaLP/ShcD. A solution of the reduced protein in 20 mM Tris, 100 mM NaCl, pH 7.4, buffer was treated with an increasing concentration of $CoCl_2$ and the absorbance of the solution was monitored over the range 250-800 nm.

5.2.6. Affinity purification of proteins interacting with the CH1 domain of RaLP/ShcD and identification by Mass Spectrometry

Having purified 3.4 mg of CH1 domain protein that was apparently unstructured, we decided to generate an affinity column to attempt to purifiy other proteins which could interact with the CH1 domain of RaLP/ShcD. These studies complement the yeast two-hybrid experments. Purified CH1 domain protein (3.4 mg) was coupled to NHS-activated beads (100 µl). CH1 bound beads were incubated with cell lysates from twenty 10 cm tissue culture dishes of 518 melanoma cells. NHS-activated beads that had been quenched with sodium acetate and glycine were used as a negative control. Bound proteins were eluted with elution buffer containing sodium acetate with glycine and analysed by SDS-PAGE and staining with Instant Blue solution.

Four distinct protein bands of about 56 kDa, 54 kDa, 45 kDa and 25 kDa were observed in samples precipitated with the CH1 protein (Figure 5.6A). These were cut out and analysed by Mass Spectrometry (Figure 5.6B). The MASCOT search tool was used to isolate to the excised bands. Vimentin was identified as the main protein in the first sample (~ 56 kDa). The matched peptides are illustrated in red in Figure 5.6B. The other bands were also identified, but contained contaminants such as skin keratin and bacterial proteins (data not shown). To confirm the interaction between RaLP/ShcD-CH1 and vimentin, immnunoblot analysis was carried out using an anti-Vimentin antibody and the same sample that was analysed by Mass Spectrometry. As shown in Figure 5.6C, a band of 56 kDa corresponding to vimentin was only present in the precipitates using CH1 protein coupled to NHS-activated beads, but not in the precipitation from uncoupled beads. These findings suggested that the CH1 domain of RaLP/ShcD can bind to vimentin.

A

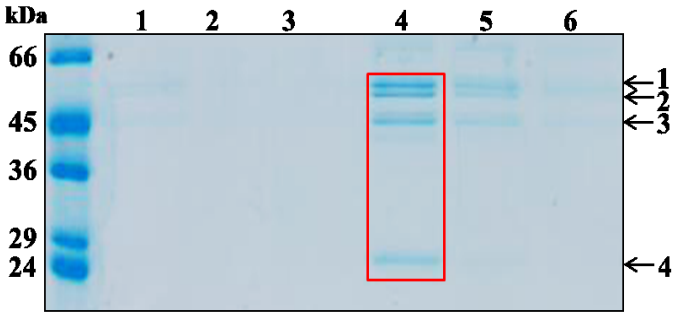

B

Matched peptides shown in **Bold Red**

```
  1 MSTRSVSSSS YRRMFGGPGT ASRPSSSRSY VTTSTRTYSL GSALRPSTSR
 51 SLYASSPGGV YATRSSAVRL RSSVPGVRLL QDSVDFSLAD AINTEFKNTR
101 TNEKVELQEL NDRFANYIDK VRFLEQQNKI LLAELEQLKG QGKSRLGDLY
151 EEEMRELRRQ VDQLTNDKAR VEVERDNLAE DIMRLREKLQ EEMLQREEAE
201 NTLQSFRQDV DNASLARLDL ERKVESLQEE IAFLKKLHEE EIQELQAQIQ
251 EQHVQIDVDV SKPDLTAALR DVRQQYESVA AKNLQEAEEW YKSKFADLSE
301 AANRNNDALR QAKQESTEYR RQVQSLTCEV DALKGTNESL ERQMREMEEN
351 FAVEAANYQD TIGRLQDEIQ NMKEEMARHL REYQDLLNVK MALDIEIATY
401 RKLLEGEESR ISLPLPNFSS LNLRETNLDS LPLVDTHSKR TLLIKTVETR
451 DGQVINETSQ HHDDLE
```

C

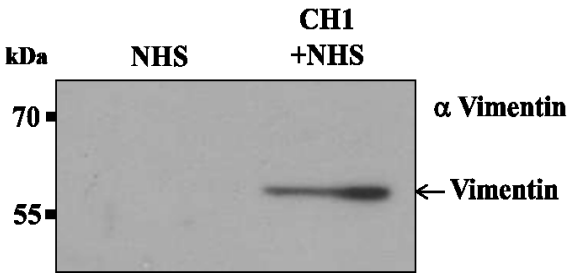

Figure 5.6. Large-scale *in vitro* pull-down assay using the CH1 domain of RaLP/ShcD and 518 melanoma cell extracts. A, Protein was precipitated from cell lysates of 518 melanoma cells with the CH1 protein coupled to NHS-activated beads. Eluted fractions were analysed (Lane 4-6); proteins precipitates from whole cell lysates with NHS-activated beads as a negative control. Eluted fractions were analysed (Lane 1-3). Four specific bands were extracted and isolated for Mass Spectrometry (1, 2, 3 and 4). B, The peptide sequences with homology ($p<0.05$) were achieved by Mass Spectrometry from band 1. Matched peptides (from the MASCOT search results) are shown in bold red. C, Immunoboltting was performed using anti-vimentin antibody. lane 1; NHS-activated beads were incubated with cell lysates from 518 melanoma cells as a negative control, lane 2; the cell lysates were incubated with the CH1 protein conjugated to NHS-activated beads. Immunoboltting was performed using anti-Vimentin antibody. A band of about 56 kDa corresponding to vimentin was observed.

5.2.7. Determination of Subcellular localisation of RaLP/ShcD and Vimentin

Since we found an association between RaLP/ShcD and vimentin, we aimed to determine whether the subcellular localisation of RaLP/ShcD and vimentin overlap. Briefly, vimentin is widely known as an intermediate filament (IF) protein which is mainly expressed in mesenchymal cells. Vimentin expression was observed in 518 melanoma cells using immunocytochemistry using an anti-Vimentin antibody to detect endogenous vimentin protein. Cells were visualised by confocal microscopy. As seen in Figure 5.7, vimentin was predominantly localised to the cytoplasm and nuclear as filaments in the cells.

Co-localisation studies were performed to determine the subcellular localisation of RaLP/ShcD and Vimentin. GFP-RaLP/ShcD was transfected into 518 melanoma cells followed by immunocytochemical staining using an anti-Vimentin antibody and Alexa Fluor 594 coupled secondary antibody. Wild-type GFP-RaLP/ShcD is mainly localised in the cytoplasm. Vimentin was also localised to the cytoplasm as filaments although these were not distributed evenly throughout the cytoplasm. However there was no obvious co-localisation of RaLP/ShcD and vimentin (Figure 5.8A). As a negative control, 518 melanoma cells were transfected with GFP-RaLP/ShcD and immunostained with Alexa Fluor 594 antibody as seen Figure 5.8B. No staining was observed indicating that the vimentin staining was specific.

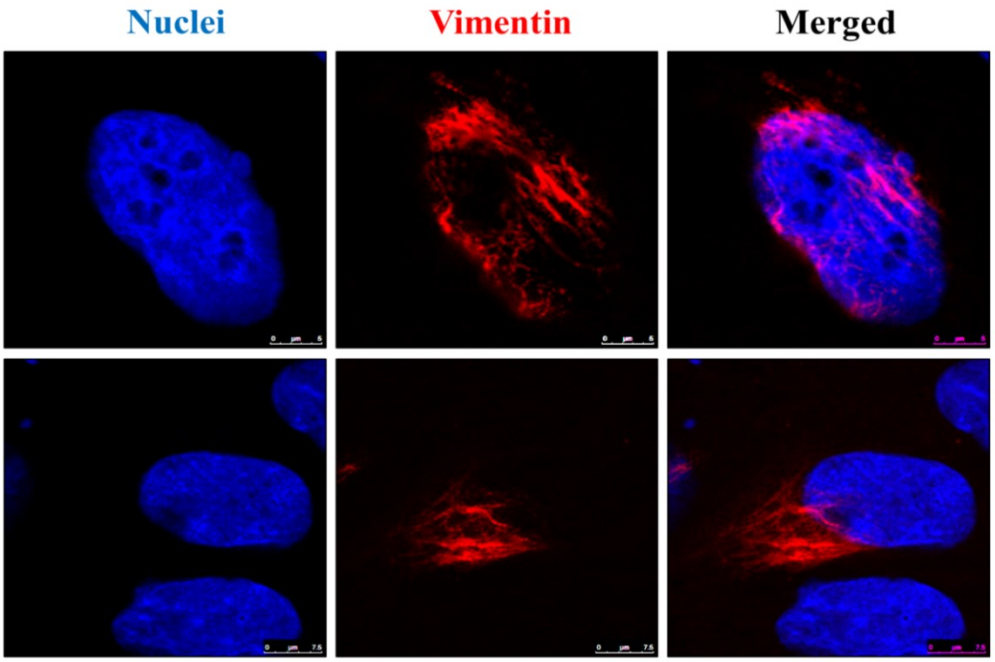

Figure 5.7. Determination of cellular localisation of Vimentin in 518 melanoma cells. 518 melanoma cells were stained with anti-Vimentin antibody and secondary antibody coupled to Alexa Fluor 594. The cells were fixed and visualised by confocal microscopy. Scale bar represents 5 µm.

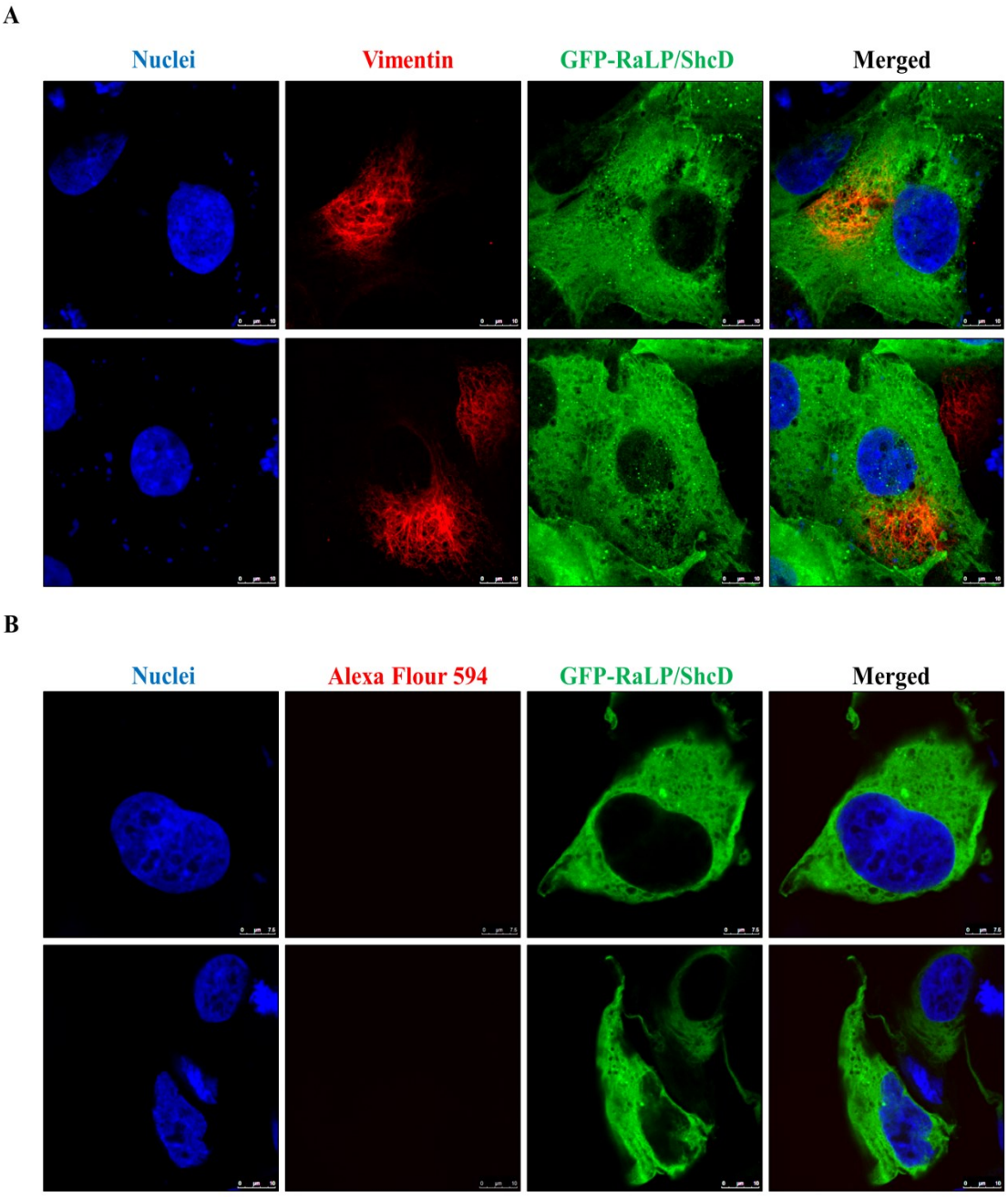

Figure 5.8. Determination of cellular localisation of RaLP/ShcD and Vimentin in 518 melanoma cells. Wild-type GFP-RaLP/ShcD was transfected into 518 melanoma cells and cells were immunocytochemically stained with anti-vimentin antibody and secondary antibody coupled to Alexa Fluor 594 (A). 518 melanoma cells were transfected with GFP-RaLP/ShcD and stained with Alexa Fluor 594 secondary antibody in the absence of primary antibody (B). The cells were fixed and visualised by confocal microscopy. Scale bars represent 10 µm (A) and 7.5 µm (B).

5.3. Discussion

5.3.1. The interaction between RaLP/ShcD and Vimentin which may have migratory functions

From our affinity purification experiment using the CH1 protein of RaLP/ShcD the cytoskeletal proteins, vimentin was identified as a potential interacting protein. To confirm that vimentin specifically associates with the CH1 domain, and was not an artefact, we performed a western blot on the same samples analysed by SDS-PAGE and mass spectrometry using anti-Vimentin antibody. Vimentin was clearly absent in the precipitation from uncoupled beads.

The microtubules, microfilaments, and intermediate filaments (IFs) are three main classes of cytoskeletal filaments. There are, so far, six main groups of IFs classified according to their protein structure and amino acid sequences, i.e. type I to type VI (Fuchs and Weber 1994; Niki *et al*., 1999). For example, type I (acidic keratin) and type II (basic keratin) are discovered primarily in epithelial cells; type III - vimentin and desmin are found in mesenchymal and muscle cells, respectively; type IV - neurofilaments are expressed in neurons; type V - lamins are found in the nucleus; type VI - nestin is expressed in embryonic neurons.

Vimemtin has been well characterised as a member of the IF proteins which is involved in mediating cell transformation in many types of human cancers, including metastatic melanoma (Kokkinos *et al*., 2007; Li *et al*., 2010). Also, this protein is now commonly used as a biological marker for epithelial-mesenchymal transition (EMT), and is able to bind to focal adhesions and regulate cell migration. A major function of the protein in

the cytoskeleton is to support the structure of the cell, and it is also bound to mitochondria, the nucleus as well as endoplasmic reticulum (ER) (Katsumoto *et al*., 1990).

Vimentin contains a central α-helical domain alongside two specialised non-α-helical domains including the N-terminal head domain and the tail domain at the C-terminus. Both head and tail domains are able to associate with many signalling and structural proteins (Goldie *et al*., 2007). In addition, phosphorylation regulates its organisatoin, dynamics, and subcellular localisation (Omary *et al*., 2006). The phosphorylation sites of vimentin could be regulated by various cellular events such as cell signalling, adhesion, and cell migration (Ivaska *et al*., 2007). However, the biological roles of vimentin are not yet fully understood.

Based on our hypothesis, their association may be involved in the migratory function of RaLP/ShcD in a direct or indirect manner. A very recent paper demonstrated that vimentin is a novel interacting partner for one of the AKT family, AKT1, and revealed that this complex can mediate cell migration and invasion (Zhu *et al*., 2011). We determined the subcellular localisation of RaLP/ShcD and vimentin in 518 melanoma cell lines, however, there was no obvious evidence of co-localisation between RaLP/ShcD and vimentin. These results are very preliminary and need repeating in different cell lines. Ideally we would like to examine the endogenous localisation of RaLP/ShcD adaptor protein. It would be worth preforming further experiments to visulalise focal adhesion proteins such as integrin β1 which has previously been reported to co-localise with vimentin in the region of focal adhesions (Kreis *et al*., 2005)

and also possibly paxillin.

Also, our studies so far have been carried out in the 518 melanoma cell line without ligand stimulation. Since the phosphorylation of vimentin has been identified as a key aspect for mediating many cellular signalling pathways, the RaLP/ShcD interaction with vimentin could be enhanced by ligand stimulation. Therefore, to further analyse the RaLP/ShcD and vimentin association, stimulation by different growth factors in different cell lines should be performed.

5.3.2. Is the CH1 domain of RaLP/ShcD a Metal-binding or Zinc finger-like domain?

Our findings suggest that the purified CH1 domain is unfolded. Although it binds to a nickel column, the cobalt binding experiment did not suggest any interaction. However, this experiment lacked a positive control, so we cannot be sure that it was performed correctly. Ideally we should synthesise the cobalt-binding peptide used in the original study as a positive control, but this would be costly.

Although the CH1 domain in its current form is unfolded, it is possible that it is induced to fold when Zinc or another metal ion is correctly bound. We attempted 1D NMR in samples to which Zinc had been added to look for changes in the spectra. Although there were slight changes of the amide/aromatic signals, there was no dramatic effect to suggest folding.

It is noteworthy that the CH1 domain showed a strong tendency to precipitate when Zinc was added to the soluble protein suggesting that it is affecting the protein. It may be that we would need to purify the full-length protein, or at least a version including a flanking N-terminal PTB domain and C-terminal SH2 domain in order for the CH1 domain to form its correct conformation.

Chapter 6

Discussion

6.1. Discussion

Signalling through RTKs mediates the formation of many protein complexes containing proteins with SH2 and/or PTB domain such as Shc adaptor proteins. RaLP/ShcD is the latest member of the Shc family to be identified and its biological functions have not been well established. The major purpose of this project was to investigate novel binding partners for RaLP/ShcD, with a view to understanding its involvement in signalling pathways in cells.

Based on the findings of this study, together with other on-going work in the lab, and published data, many proteins have been suggested to form a complex with RaLP/ShcD as indicated in Figure 6.1. This lab has newly found that nischarin is a novel binding partner for the CH2 domain. This protein is an invasion suppressor and may be important in the migratory function of RaLP/ShcD. Also, interstingly a NES was identified in this region. The PTB domain of RaLP/ShcD interacts with MuSK, EGFR, IGF-1R, and TrkB (Jones *et al*., 2007; Fagiani *et al*., 2007; You *et al*., 2010). Both the SH2 domain and CH1 domain of RaLP/ShcD to date are poorly studied. The SH2 domain can bind to Gab1 and TrkB. Proteins binding to the CH1 domain of RaLP/ShcD may include Grb2 and Peg3/Pw1, HP1α, vimentin and may be metal ions.

The fact that RaLP/ShcD accumulates in the nucleus when nuclear export is chemically inhibited suggests that the protein is able to shuttle between the cytoplasm and nucleus. Interestingly, the p52-ShcA isoform can interact with Ran-GTPase. This compelx may permit Ran-mediated ShcA translocation to the nucleus (George *et al*., 2009).

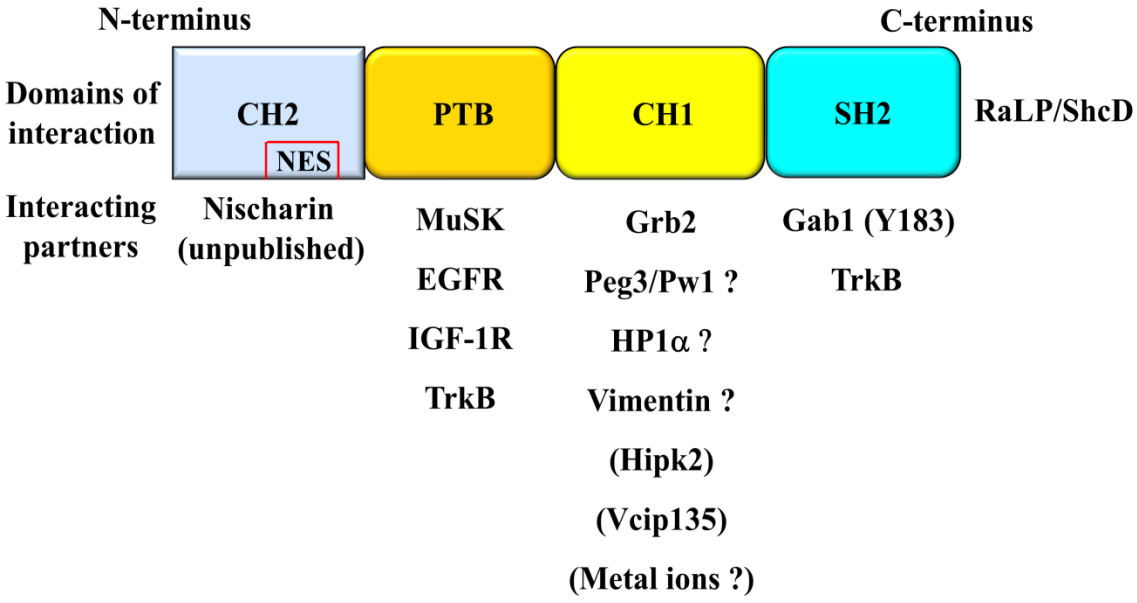

Figure 6.1. A diagram illustrating the possible interaction partners for different domains of RaLP/ShcD. Nischarin has been shown to be a novel binding partner for the CH2 domain and interstingly a NES was identified within the CH2 domain (Ahmed and Prigent, unpublished). The PTB domain of RaLP/ShcD interacts with MuSK, EGFR, IGF-1R, and TrkB. The SH2 domain binds Gab1 and TrkB. The CH1 domain of RaLP/ShcD can interact with Grb2 and Peg3/Pw1, HP1α, vimentin and may act as a metal binding domain. Other potential interacting proteins from the yeast two-hybrid screen Hipk2 and Vcip135, have not been further investigated.

A NES has been identified within the CH2 domain of RaLP/ShcD by other members of the lab which when mutated causes nuclear accumulation of RaLP/ShcD. It is quite possible that RaLP/ShcD possesses shorter isoforms with non-redundant roles in cells, due to the presence of several potential ATG (initiation codons) in the CH2 domain (Jones *et al*., 2007). Also, this lab showed that p49- and p59-RaLP/ShcD isoforms, which lack the NES, are predominantly present within the nucleus of transfected cells (Ahmed and Prigent unpublished). Alterative forms of ShcA have very different functions such as p66-ShcA which is involved in apoptosis and p52-ShcA which is involved predominantly in proliferation therefore it is possible that p49 and p59-RaLP/ShcD will have different fuction to p69-RaLP/ShcD due to this nuclear localisation. The CH1 domain of RaLP/ShcD fused to LexA DNA binding domain revealed self-acvtivation of the *HIS3* suggesting that this domain may have the ability to activate transcription. Isolated proteins from the yeast two-hybird screen with this domain were almost all nuclear proteins. Therefore, shorter isoforms of RaLP/ShcD may be nuclear proteins with a role in regulating gene transcription.

Affinity purification combined with mass spectrometry offers a number of advantages over the yeast two-hybrid library screen, but also disadvantages. For instance, this technique is fast and extracts can be readily prepared from any desired cell type without need for library preparation. Contaminants are a common problem due to the presence of proteins such as skin keratin in the lab, and the sensitivity of mass spectrometry. Also, the interactions that are detected are not happening in the cells and the high concentration of protein on the column may permit binding of proteins that would not usually interact. Vimentin was the only protein identified in the purification. The

interaction appears to be specific as no binding of vimentin was observed with the uncoupled beads as shown by western blotting (Figure 5.6). A recent paper described vimentin as a novel associator for AKT1, and showed that the complex regulates cell migration and invasion (Zhu *et al*., 2011). RaLP/ShcD may associate either directly or indirectly with vimentin and recruit other proteins to the complex (e.g. Gab1) to enhance cell migration. Clearly the association between RaLP/ShcD and vimentin warrants further investigation in different cell lines, using different stimuli.

The yeast two-hybrid technique is a valuable *in vivo* system which has advantage that it enables identification of interactions in living yeast. However, this system is well known for isolating artefects proteins might be identified that would normally be in a different cellular compartment, as all the fusion proteins are targeted to the nucleus in yeast. The library in this study was designed to generate small folding domains which might show better interactions than full-length proteins. We have confirmed many of the interactions identified using biochemical assays and full-length proteins, suggesting that the interactions between RaLP/ShcD, Gab1, Peg3/Pw1 and HP1α are real interaction.

RaLP/ShcD can directly associate with the Gab1 adaptor protein through its SH2 domain upon both PDGF and EGF stimulation. We identified that Y183 is the tyrosine which when phosphorylated is able to bind RaLP/ShcD (Figure 3.9). We also showed that Gab1Y183F mutant was unable to recruit RaLP/ShcD to the cell membrane in ruffles upon EGF stimulation (Figure 3.10).

The interaction between Peg3/Pw1 and RaLP/ShcD was confirmed by pull-down and co-immunoprecipitation experiments (Figure 4.9 and 4.10). We revealed that a small portion of RaLP/ShcD can co-localise with Peg3/Pw1 in the nucleus in HEK293 cells (Figure 4.18). HP1α also interacts with RaLP/ShcD. Their association was also demonstrated by pull-down and co-immunoprecipitation experiments (Figure 4.19 and 4.20). However, there was no evidence of co-localisation of RaLP/ShcD and HP1α in transfected cells (Figure 4.21). Interestingly in preliminary experiments cells expressing the nuclear p49-RaLP/ShcD isoform together with Peg3/Pw1 showed reduced apoptosis in response to camptothecin (CPT) as compared to cells expressing only Peg3/Pw1 (data not shown).

In conclusion, although we have identified several novel binding partners in this study which suggest novel roles for RaLP/ShcD in processes not previously thought to involve Shc proteins, further studies should focus on determining the functional significance of these interactions.

References

References

Abella, J.V., Vaillancourt, R., Frigault, M.M., Ponzo, M.G., Zuo, D., Sangwan, V., Larose, L. and Park, M. (2010) The Gab1 scaffold regulates RTK-dependent dorsal ruffle formation through the adaptor Nck. *J. Cell. Sci.* **15**: 123: 1306-19.

Abo, A., Qu, J., Cammarano, M. S., Dan, C., Fritsch, A., Baud, V., Belisle, B., and Minden, A. (1998) PAK4, a novel effector for Cdc42Hs, is implicated in the reorganization of the actin cytoskeleton and in the formation of filopodia. *EMBO J.* **17**: 6527-6540.

Ahmed, T., Shea, K., Masters, J. R., Jones, G. E., and Wells, C. M. (2008) A PAK4-LIMK1 pathway drives prostate cancer cell migration downstream of HGF. *Cell. Signal.* **20**: 1320-1328.

Agazie, Y. M., and Hayman, M. J. (2003) Molecular mechanism for a role of SHP2 in epidermal growth factor receptor signalling. *Mol. Cell. Biol.* **23:** 7875-7886.

Amson, R.B., Nemani, M., Roperch, J.P., Israeli, D., Bougueleret, L., Le Gall, I., Medhioub, M., Linares-Cruz, G., Lethrosne, F., Pasturaud, P., Piouffre, L., Prieur, S., Susini, L., Alvaro, V., Millasseau, P., Guidicelli, C., Bui, H., Massart, C., Cazes, L., Dufour, F., Bruzzoni-Giovanelli, H., Owadi, H., Hennion, C., Charpak, G., Telerman, A., et al. (1996) Isolation of 10 differentially expressed cDNAs in p53-induced apoptosis: activation of the vertebrate homologue of the drosophila seven in absentia gene. *Proc. Natl. Acad. Sci. USA* **93**(9): 3953-7.

Bardelli, A., Longati, P., Gramaglia, D., Stella, M.C. and Comoglio, P.M. (1997) Gab1 coupling to the HGF/Met receptor multifunctional docking site requires binding of Grb2 and correlates with the transforming potential. *Oncogene* **15**: 3103-3111.

Bennett, D.C. (2008) How to make a melanoma: what do we know of the primary clonal events? *Pigment cell melanoma res.* **21**(1): 27-38.

Blake, R.A., Broome, M.A., Liu, X., Wu, J., Gishizky, M., Sun, L., and Courtneidge, S.A. (2000) SU6656, a selective src family kinase inhibitor, used to probe growth factor signalling. *Mol. Cell. Biol.* **20**: 9018-9027.

Borg, J.P. and Margolis, B. (1998) Function of PTB domains. *Curr. Top. Microbiol. Immunol.* **228**: 23-38.

Cattaneo, F. and Pelicci, P.G. (1998) Emerging roles for SH2/PTB-containing Shc adaptor proteins in the developing mammalian brain. *Trends Neurosci.* **21**(11): 476-81.

Cattaruzza, M., Lattrich, C. and Hecker, M. (2004) Focal adhesion protein zyxin is a mechanosensitive modulator of gene expression in vascular smooth muscle cells. *Hypertension* 4: 726-730.

Cheng, A. M., Saxton, T. M., Sakai, R., Kulkarni, S., Mbamalu, G., Vogel, W., Tortorice, C. G., Cardiff, R. D., Cross, J. C., Muller, W. J., and Pawson, T. (1998) Mammalian Grb2 regulates multiple steps in embryonic development and malignant transformation. *Cell* **95**: 793-803.

Cheutin, T., McNairn, A. J., Jenuwein, T., Gilbert, D. M., Singh, P. B. and Misteli, T. (2003) Maintenance of stable heterochromatin domains by dynamic HP1 binding. *Science* **299**: 721-725.

Chudnovsky, Y., Khavari, P.A., Adams, A.E. (2005) Melanoma genetics and the development of rational therapeutics. *J. Clin. Invest.* **115**(4): 813-824.

Cullen, P. J. (2001) Ras effectors: buying shares in Ras plc. *Curr. Biol.* **11**: R342-R344.

Deng, Y. and Wu, X. (2000) Peg3/Pw1 promotes p53-mediated apoptosis by inducing Bax translocation from cytosol to mitochondria. *Proc. Natl. Acad. Sci. USA* **97**(22): 12050-12055.

De Falco, V., Guarino, V., Malorni, L., Cirafici, A.M., Troglio, F., Erreni, M., Pelicci, G., Santoro, M., Melillo, R.M. (2005) RAI(ShcC/N-Shc)-dependent recruitment of GAB 1 to RET oncoproteins potentiates PI3-K signalling in thyroid tumors. *Oncogene* **24**(41): 6303-13.

Desgrosellier, J.S. and Cheresh, D.A. (2010) Integrins in cancer: biological implications and therapeutic opportunities. *Nat. Rev. Cancer* **10**(1): 9-22.

Dhe-Paganon, S., Ottinger, E.A., Nolte, R.T., Eck, M.J., and Shoelson, S.E. (1999) Crystal structure of the pleckstrin homology-phosphotyrosine binding (PH-PTB) targeting region of insulin receptor substrate 1. *Proc. Natl. Acad. Sci. USA* **96**: 8378-8383.

Di Cristofano, A. and Pandolfi, P.P. (2000) The multiple roles of PTEN in tumor suppression. *Cell* **100**: 387-390.

Dunnion, D.J., Cywinski, A.L., Tucker, V.C., Murray, A.K., Rickinson, A.B., Coulie, P., Browning, M.J. (1999) Human antigen-presenting cell/tumour cell hybrids stimulate strong allogeneic responses and present tumour-associated antigens to cytotoxic T cells in vitro. *Immunology* **98**(4): 541-50.

Dinant, C. and Luijsterburg, M.S. (2009) The Emerging Role of HP1 in the DNA damage Response. *Mol. Cell. Biol.* **29**(24): 6335-40.

Eck, M.J., Dhe-Paganon, S., Trub, T., Nolte, R.T. and Shoelson, S.E. (1996) Structure of the IRS-1 PTB domain bound to the juxtamembrane region of the insulin receptor. *Cell* **85**: 695-705.

Edelstein, L.C. and Collins, T. (2005) The SCAN domain family of zinc finger transcription factors. *Gene* **359:** 1-17.

Eissenberg, J.C., James, T.C., Foster-Hartnett, D.M., Hartnett, T., Ngan, V. and Elgin, S.C.R. (1990) Mutation in a heterochromatin-specific chromosomal protein is associated with suppression of position-effect variegation in Drosophila melanogaster. *Proc. Natl. Acad. Sci. USA* **87:** 9923-9927.

Eliceiri, B.P. and Cheresh, D.A. (2001) Adhesion events in angiogenesis. *Curr. Opin. Cell Biol.* **13**(5): 563-8.

Ellis, C., Moran, M., McCormick, F. and Pawson, T. (1990) Phosphorylation of GAP and GAP-associated proteins by transforming and mitogenic tyrosine kinases. *Nature* **343**: 377-381.

Eskeland, R., Eberharter, A., and Imhof, A. (2007) HP1 binding to chromatin methylated at H3K9 is enhanced by auxiliary factors. *Mol. Cell. Biol.* **27**: 453-465.

Eulenfeld, R. and Schaper, F. (2009) A new mechanism for the regulation of Gab1 recruitment to the plasma membrane. *J. Cell Sci.* **122**: 55-64

Fagiani, E., Giardina, G., Luzi, L., Cesaroni, M., Quarto, M., Capra, M., Germano, G., Bono, M., Capillo, M., Pelicci, P., Lanfrancone, L. (2007) RaLP, a new member of the Src homology and collagen family, regulates cell migration and tumour growth of metastatic melanomas. *Cancer Res.* **67**(7): 3064-73.

Fargnoli, M.C., Argenziano, G., Zalaudek, I., Peris, K. (2006) High- and low-penetrance cutaneous melanoma susceptibility genes. *Expert Rev. Anticancer Ther.* **6**(5): 657-670.

Fecher, L.A., Amarabvadi, R.K., Flaherty, K.T. (2008) The MAPK pathway in melanoma. *Curr. opin. Oncol.* **20**(2): 183-9.

Felder, S., Zhou, M., Hu, P., Urena, J., Ullrich, A., Chaudhuri, M., White, M., Shoelson, S. E., Schlessinger, J. (1993) SH2 domains exhibit high-affinity binding to tyrosine-phosphorylated peptides yet also exhibit rapid dissociation and exchange. *Mol. Cell. Biol.* **13**: 1449-1455.

Feng, S., Chen, J.K., Yu, H., Simon, J.A. and Schreiber, S.L. (1994) Two binding orientations for peptides to the Src SH3 domain: development of a general model for SH3-ligand interactions. *Science* **266**: 1241-1247.

Fuchs, E. and Weber, K. (1994) Intermediate filaments: structure, dynamics, function, and disease. *Annu. Rev. Biochem.* **63**: 345-382.

Fuks, F., Hurd, P.J., Deplus, R. and Kouzarides, T. (2003) The DNA methyltransferases associate with HP1 and the SUV39H1 histone methyltransferase. *Nucleic Acids Res.* **31**: 2305-2312.

George, R., Chan, H.L., Ahmed, Z., Suen, K.M., Stevens, C.N., Levitt, J.A., Suhling, K., Timms, J., Ladbury, J.E. (2009) A complex of Shc and Ran-GTPase localises to the cell nucleus. *Cell. Mol. Life Sci.* **66**(4): 711-20.

Giacinti, C. and Giordano, A. (2006) RB and cell cycle progression. *Oncogene* **25**(38): 5220-5227.

Giorgio, M., Migliaccio, E., Orsini, F., Paolucci, D., Moroni, M., Contursi, C., Pelliccia, G., Luzi, L., Minucci, S., Marcaccio, M., Pinton, P., Rizzuto, R., Bernardi, P., Paolucci, F., Pelicci, P.G. (2005) Electron transfer bwteen cytochrome c and p66Shc generates reactive oxygen species that trigger mitochondrial apoptosis. *Cell* **122**(2): 221-33.

Giorgio, M., Trinei, M., Migliaccio, E. and Pelicci, P.G. (2007) Hydrogen peroxide: a metabolic by-product or a common mediator of ageing signals? *Nat. Rev. Mol. Cell. Biol.* **8**(9): 722-8.

Glass, D.J., Apel, E.D., Shah, S., Bowen, D.C., DeChiara, T.M., Stitt, T.N., Sanes, J.R., Yancopoulos, G.D. (1997) Kinase domain of the muscle-specific receptor tyrosine kinase (MuSK) is sufficient for phosphorylation but not clustering of acetylcholine receptors: required role for the MuSK ectodomain? *Proc. Natl. Acad. Sci. USA* **94**(16): 8848-53.

Gogas, H.J., Kirkwood, J.M., Sondak, V. (2007) Chemotherapy for metastatic melanoma: time for a change? *Cancer* **109**(3): 455-464.

Goldie, K.N., Wedig, T., Mitra, A.K., Aebi, U., Herrmann, H., Hoenger, A. (2007) Dissecting the 3D structure of vimentin intermediate filaments by cryo-electron tomography. *J. Struct. Biol.* **158**: 378-385.

Gotoh, N., Toyoda, M., and Shibuya, M. (1997) Tyrosine phosphorylation sites at amino acids 239 and 240 of Shc are involved in epidermal growth factor-induced mitogenic signaling that is distinct from Ras/mitogen-activated protein kinase activation. *Mol. Cell. Biol.* **17**: 1824-1831.

Green, L.M. and Berg, J.M. (1989) A retroviral Cys-Xaa2-Cys-Xaa4-His-Xaa4-Cys peptide binds metal ions: spectroscopic studies and a proposed three-dimensional structure. *Proc. Natl. Acad. Sci. USA* **86**(11): 4047-51.

Gu, H., Pratt, J.C., Burakoff, S.J. and Neel, B.G. (1998) Cloning of p97/Gab2, the major SHP2-binding protein in hematopoietic cells, reveals a novel pathway for cytokine-induced gene activation. *Mol. Cell.* **2**: 729-740.

Gu, J., Tamura, M., Yamada, K.M. (1998) Tumor suppressor PTEN inhibits integrin- and growth factor-mediated mitogen activated protein (MAP) kinase signaling pathways. *J. Cell. Biol.* **143**: 1375-1383.

Gual, P., Giordano, S., Williams, T.A., Rocchi, S., Van Obberghen, E. and Comoglio, P.M. (2000) Sustained recruitment of phospholipase C-gamma to Gab1 is required for HGF-induced branching tubulogenesis. *Oncogene* **19**: 1509-1518.

Guo, W. and Giancotti, F.G. (2004) Integrin signalling during tumour progression. *Nat. Rev. Mol. Cell. Biol.* **5**(10): 816-26.

Haluska, F., Pemberton, T., Ibrahim, N., Kalinsky, K. (2007) The RTK/RAS/BRAF/PI3K pathways in melanoma: biology, small molecule inhibitors, and potential applications. *Sem. in Oncol.* **34**(6): 546-54.

Haugh, J. M. and Lauffenburger, D. A. (1997) Physical modulation of intracellular signaling processes by locational regulation. *Biophys. J.* **72**: 2014-2031.

Hawley, S.P., Wills, M.K., Rabalski, A.J., Bendall, A.J., Jones, N. (2011) Expression patterns of ShcD and Shc family adaptor proteins during mouse embryonic development. *Dev. Dyn.* **240**: 221-231.

Hayward, N.K. (2003) Genetics of melanoma predisposition. *Oncogene* **22**(20): 3053-3062.

Hennessy, B.T., Smith, D.L., Ram, P.T., et al (2005) Exploiting the PI3K/AKT pathway for cancer drug discovery. *Nat. Rev. Drug Discov.* **4**: 988-1004.

Hollenberg, S., Sternglanz, R., Cheng, P. and Weintraub, H. (1995) Identification of a new family of tissue specific basic helix-loop-helix proteins with a two-hybrid system. *Mol. Cell. Biol.* **15**: 3813-3822.

Holgado-Madruga, M., Emlet, D.R., Moscatello, D.K., Godwin, A.K. and Wong, A.J. (1996) A Grb2-associated docking protein in EGF- and insulin -receptor signalling. *Nature* **379**: 560-564.

Howell, B.W., Lanier, L.M., Frank, R., Gertler, F.B., Cooper, J.A. (1999) The disabled 1 phosphotyrosine-binding domain binds to the internalization signals of transmembrane glycoproteins and to phospholipids. *Mol. Cell. Biol.* **19**(7): 5179-88.

Hunter, T. (2000) Signaling-2000 and beyond. *Cell* **100**: 113-127.

Huveneers, S., Truong, H. and Danen, H. J. (2007) Integrins: Signaling, disease, and therapy. *Int. J. Radiat. Biol.* **83**(11-12): 743-751.

Hynes, R.O. (1992) Integrins: Versatility, modulation, and signalling in cell adhesion. *Cell* **69**: 11-25.

Hynes, R.O. (1999) Cell adhesion: old and new questions. *Trends Cell Biol.* **9**: 33-37.
Hubbard, S.R. and Miller, W.T. (2007) Receptor tyrosine kinases: mechanisms of activation and signalling. *Curr. Opin. Cell Biol.* **19**(2): 117-23.

Ivaska, J., Pallari, H.M., Nevo, J., Eriksson, J.E. (2007) Novel functions of vimentin in cell adhesion, migration, and signalling. *Exp. Cell Res.* **313**(10): 2050-62.

Jemal, A., Siegel, R., Ward, H., et al. (2008) Cancer statistics. *Cancer J. Clin.* **58**(2): 71-96.

Jiang, X., Yu, Y., Yang, H.W., Agar, N.Y.R., Frado, L. and Johnson, M.D. (2010) The Imprinted Gene PEG3 Inhibits Wnt Signalling and Regulates Glioma Growth. *J. Biol. Chem.* **285**: 8472-8480

Jin, Z.G., Wong, C., Wu, J., Berk, B.C. (2005) Flow shear stress stimulates Gab1 tyrosine phosphorylation to mediate protein kinase B and endothelial nitric-oxide synthase activation in endothelial cells. *J. Biol. Chem*. **280**(13): 12305-12309.

Jones, N., Hardy, W.R., Friese, M.B., Jorgensen, C., Smith, M.J., Woody, N.M., Burden, S.J., Pawson, T. (2007) Analysis of a Shc family adaptor protein, ShcD/Shc4, that associates with muscle-specific kinase. *Mol. Cell. Biol.* **27**(13): 4759-73.

Karlsson, O., Thor, S., Norberg, T., Ohlsson, H. and Edlund, T. (1990) Insulin gene enhancer binding protein Isl-1 is a member of a novel class of proteins containing both a homeo- and a Cys-His domain. *Nature* **344**: 879-882.

Katsumoto, T., Mitsushima, A. and Kurimura, T. (1990) The role of the vimentin intermediate filaments in rat 3Y1 cells elucidated by immunoelectron microscopy and computer-graphic reconstruction. *Biol. Cell* **68**(2): 139-46.

Kavanaugh, W.M. and Williams, L.T. (1994). An alternative to SH2 domains for binding tyrosine-phosphorylated proteins. *Science* **266**: 1862-1865.

Keegan, K. and Cooper, J.A. (1996) Use of the two hybrid system to detect the association of the protein-tyrosine-phosphatase, SHPTP2, with another SH2-containing protein, Grb7. *Oncogene* **12**(7): 1537-44.

Kholodenko, B. N., Hoek, J. B., and Westerhoff, H. V. (2000) Why cytoplasmic signalling proteins should be recruited to cell membranes. *Trends Cell Biol.* **10**: 173-178.

Kojima, T., Yoshikawa, Y., Takada, S., et al. (2001) Genomic organization of the Shc-related phosphotyrosine adapters and characterization of the full-length Sck/ShcB: specific with pp135. *Biochem. Biophys. Res. Commum.* **284**(4): 1039-47.

Kokkinos, M.I., Wafai, R., Wong, M.K., Newgreen, D.F., Thompson, E.W., Waltham, M. (2007) Vimentin and epithelial-mesenchymal transition in human breast cancer-observations in vitro and in vivo. *Cells Tissues Organs* **185**(1-3): 191-203.

Kreis, S., Schönfeld, H.J., Melchior, C., Steiner, B., Kieffer, N. (2005) The intermediate filament protein vimentin binds specifically to a recombinant integrin alpha2/beta1 cytoplasmic tail complex and co-localizes with native alpha2/beta1 in endothelial cell focal adhesions. *Exp. Cell. Res.* **305**(1): 110-21.

Kuphal, S., Bauer, R., Bosserhoff, A.K. (2005) Integrin signalling in malignant melanoma. *Cancer Metastasis Rev.* **24**(2): 195-222.

Kuroiwa, Y., T. Kaneko-Ishino, F. Kagitani, T. Kohda, L.-L. Li, M. Tada, R. Suzuki, M. Yokoyama, T. Shiroishi, S. Wakana, S.C. Barton, F. Ishino, and M.A. Surani. (1996) *Peg3* imprinted gene on proximal chromosome 7 encodes for a zinc finger protein. *Nature Genet.* **12:** 186-190.

Laemmli, U. K. (1970) *Nature* **227:**680-685

Laffargue, M., Raynal, P., Yart, A., Peres, C., Wetzker, R., Roche, S., Payrastre, B., Chap, H. (1999) An epidermal growth factor receptor/Gab1 signalling pathway is required for activation of phosphoinositide 3-kinase by lysophosphatidic acid. *J. Biol. Chem.* **274**: 32835-41.

Lai, K.M. and Pawson, T. (2000) The ShcA phosphotyrosine docking protein sensitizes cardiovascular signaling in the mouse embryo. *Genes Dev.* **14**(9): 1132-45.

Lamorte, L., Rodrigues, S., Naujokas, M., and Park, M. (2002) Crk synergizes with epidermal growth factor for epithelial invasion and morphogenesis and is required for the Met morphogenic program. *J. Biol. Chem.* **277**: 37904-37911.

Lehr, S., Kotzka, J., Herkner, A., Sikmann, A., Meyer, H.E., Krone, W., Müller-Wieland, D. (2000) Identification of major tyrosine phosphorylation sites in the human insulin receptor substrate Gab-1 by insulin receptor kinase in vitro. *Biochemistry* **39**(35): 10898-907.

Lewitzky, M., Kardinal, C., Gehring, N.H., Schmidt, E.K., Konkol, B., Eulitz, M., Birchmeier, W., Schaeper, U., Feller, S.M. (2001) The C-terminal SH3 domain of the adapter protein Grb2 binds with high affinity to sequences in Gab1 and SLP-76 which lack the SH3-typical P-x-x-P core motif. *Oncogene* **20**: 1052-1062.

Li, M., Zhang, B., Sun, B., Wang, X., Ban, X., Sun, T., Liu, Z., Zhao, X. (2010) A novel function for vimentin: the potential biomarker for predicting melanoma hematogenous metastasis. *J. Exp. Clin. Cancer Res.* **29**: 109.

Lioubin, M.N., Algate, P.A., Tsai, S., Carlberg, K., Aebersold, A., Rohrschneider, L.R. (1996) p150Ship, a signal transduction molecule with inositol polyphosphate-5-phosphatase activity. *Genes Dev*. **10**(9): 1084-95.

Liu, Y. and Rohrschneider, L.R. (2002) The gift of Gab. *FEBS Lett.* **515**(1-3): 1-7.

Liu, V. and Mihm, M.C. (2003) Pathology of malignant melanoma. *Surg. Clin. North Am*. **83**(1): 31-60.

Lock, L.S., Maroun, C.R., Naujokas, M.A., Park, M. (2002) Distinct recruitment and function of Gab1 and Gab2 in Met receptor-mediated epithelial morphogenesis. *Mol. Biol. Cell* **13**(6): 2132-46.

Lock, L.S., Royal, I., Naujokas, M.A. and Park, M. (2000) Identification of an atypical Grb2 carboxyl-terminal SH3 domain binding site in Gab docking proteins reveals Grb2-dependent and -independent recruitment of Gab1 to receptor tyrosine kinases. *J. Biol. Chem*. **275**: 31536-31545.

Lomberk, G., Wallrath, L., and Urrutia, R. (2006) The heterochromatin protein 1 family. *Genome Biol.* **7**(7): 228.

Luijsterburg, M. S., Dinant, C., Lans, H., Stap, J., Wiernasz, E., Lagerwerf, S., Warmerdam, D. O., Lindh, M., Brink, M. C., Dobrucki, J. W., Aten, J. A., Fousteri, M. I., Jansen, G., Dantuma, N. P., Vermeulen, W., Mullenders, L. H., Houtsmuller, A. B., Verschure, P. J. and van Driel, R. (2009) Heterochromatin protein 1 is recruited to various types of DNA damage. *J. Cell Biol*. **185**: 577-86.

Luzi, L., Confalonieri, S., Di Fiore, P.P. and Pelicci, P.G. (2000) Evolution of Shc functions from nematode to human. *Curr. Opin. Genet. Dev.* **10**(6): 668-74.

Margolis, B., Li, N., Koch, A., Mohammadi, M., Hurwitz, D. R., Zilberstein, A., Ullrich, A., Pawson, T., Schlessinger, J. (1990) The tyrosine phosphorylated carboxyterminus of the EGF receptor is a binding site for GAP and PLC-γ. *EMBO J.* **9**: 4375-4380.

Maison, C. and Almouzni, G. (2004) HP1 and the dynamics of heterochromatin maintenance. *Nat. Rev. Mol. Cell. Biol.* **5**: 296-304.

Margolis, B., Borg, J.P., Straight, S. and Meyer, D. (1999). The function of PTB domain proteins. *Kidney Int.* **56**: 1230-1237.

Markevich, N. I., Moehren, G., Demin, O., Kiyatkin, A., Hoek, J. B. and Kholodenko, B. N. (2004) Signal processing at the Ras circuit: what shapes Ras activation patterns? *IEE Systems Biol.* **1**: 104-113

Maroun, C.R., Holgado-Madruga, M., Royal, I., Naujokas, M.A., Fournier, T.M., Wong, A.J. and Park, M. (1999) The Gab1 PH domain is required for localization of Gab1 at sites of cell-cell contact and epithelial morphogenesis downstream from the Met receptor tyrosine kinase. *Mol. Cell.Biol.* **19**: 1784-1799.

Maroun, C. R., Naujokas, M. A., Holgado-Madruga, M., Wong, A. J. and Park, M. (2000) The tyrosine phosphatase SHP-2 is required for sustained activation of extracellular signal-regulated kinase and epithelial morphogenesis downstream from the Met receptor tyrosine kinase. *Mol. Cell. Biol.* **20**: 8513-8525.

Mattoon, D. R., Lamothe, B., Lax, I. and Schlessinger, J. (2004) The docking protein Gab1 is the primary mediator of EGF-stimulated activation of the PI-3K/Akt cell survival pathway. *BMC Biol.* **2**: 24.

Mc Kay, M.M. and Morrison, D.K. (2007) Integrating signals from RTKs to ERK/MAPK. *Oncogene* **26**(22): 3113-21.

Meehan, R.R., Kao, C-F. and Pennings, S. (2003) HP1 binding to native chromatin in vitro is determined by the hinge region and not by the chromodomain. *EMBO J.* **22**: 3164-3174.

Migliaccio, E., Giorgio, M., Mele, S., Pelicci, G., Reboldi, P., Pandolfi, P.P., Lanfrancone, L., Pelicci, P.G. (1999) The p66shc adaptor protein controls oxidative stress response and life span in mammals. *Nature* **402**(6759): 309-13.

Migliaccio, E., Mele, S., Salcini, A.E., Pelicci, G., Lai, K.M., Superti-Furga, G., Pawson, T., Di Fiore, P.P., Lanfrancone, L., Pelicci, P.G. (1997) Opposite effects of the p52shc/p46shc and p66shc splicing isoforms on the EGF receptor-MAP kinase-fos signalling pathway. *EMBO J.* **16** (4): 706-16.

Mikol, V., Baumann, G., Zurini, M.G., Hommel, U. (1995) Crystal structure of the SH2 domain from the adaptor protein SHC: a model for peptide binding based on X-ray and NMR data. *J. Mol. Biol.* **254**(1): 86-95.

Millar, A.J. and Mihm, M.C. (2006) Melanoma. *N. Eng. J. Med.* **355**(1): 51-65.

Minc, E., Courvalin, J. C. and Buendia, B. (2000) HP1γ associates with euchromatin and heterochromatin in mammalian nuclei and chromosomes. *Cytogenet. Cell Genet.* **90**: 279-284.

Montagner, A., Yart, A., Dance, M., Perret, B., Salles, J. P., and Raynal, P. (2005) A novel role for Gab1 and SHP2 in epidermal growth factor-induced Ras activation. *J. Biol. Chem.* **280**: 5350-5360.

Moran, M. F., Koch, C. A., Anderson, D., Ellis, C., England, L., Martin, G. S., Pawson, T. (1990) Src homology region 2 domains direct protein-protein interactions in signal transduction. *Proc. Natl. Acad. Sci. USA* **87**: 8622- 8626.

Moreau-Aubry, A., Le Guiner, S., Labarrière, N., Gesnel, M.C., Jotereau, F., Breathnach, R. (2000) A processed pseudogene codes for a new antigen recognized by a CD8(+) T cell clone on melanoma. *J. Exp. Med.***191**(9): 1617-24.

Müller, J.M., Metzger, E., Greschik, H., Bosserhoff, A.K., Mercep, L., Buettner, R., Schüle, R. (2002) The transcriptional coactivator FHL2 transmits Rho signals from the cell membrane into the nucleus. *EMBO J.* **21**: 736-748.

Nakamura, T., Muraoka, S., Sanokawa, R., Mori, N. (1998) N-Shc and Sck, two neuronally expressed Shc adapter homologs. Their differential regional expression in the brain and roles in neurotrophin and Src signalling. *J. Biol. Chem.* **273**(12): 6960-7.

Nielsen, A.L., Oulad-Abdelghani, M., Ortiz, J.A., Remboutsika, E., Chambon, P., Losson, R. (2001) Heterochromatin formation in mammalian cells: interaction between histones and HP1 proteins. *Mol. Cell* **7**, 729-739.

Niki, T., Pekny, M., Hellemans, K., Bleser, P.D., Berg, K.V., Vaeyens, F., Quartier, E., Schuit, F., Geerts, A. (1999) Class VI intermediate filament protein nestin is induced during activation of rat hepatic stellate cells. *Hepatology* **29**: 520-527.

Nemani, M., Linares-Cruz, G., Bruzzoni-Giovanelli, H., Roperch, J.P., Tuynder, M., Bougueleret, L., Cherif, D., Medhioub, M., Pasturaud, P., Alvaro, V., der Sarkissan, H., Cazes, L., Le Paslier, D., Le Gall, I., Israeli, D., Dausset, J., Sigaux, F., Chumakov, I., Oren, M., Calvo, F., Amson, R.B., Cohen, D., Telerman, A. (1996) Activation of the human homologue of the Drosophila sina gene in apoptosis and tumor suppression. *Proc. Natl. Acad. Sci. USA* **93**(17): 9039-42.

Nguyen, L., Holgado-Madruga, M., Maroun, C., Fixman, E.D., Kamikura, D., Fournier, T., Charest, A., Tremblay, M., Wong, A.J. and Park, M. (1997) Association of the multisubstrate docking protein Gab1 with the hepatocyte growth factor receptor requires a functional Grb2 binding site involving tyrosine 1356. *J. Biol. Chem.* **272**: 20811-20819.

Niemann, C., Brinkmann, V., Spitzer, E., Hartman, G., Sachs, M., Naudorf, H. and Bircheier, W. (1998) Reconstitution of mammary gland development in vitro: requirement of c-met and c-erbB2 signaling for branching and alveolar morphogenesis. *J. Cell. Biol.* **143**: 533-545.

Nishida, K., Yoshida, Y., Itoh, M., Fukada, T., Ohtani, T., Shirogane, T., Atsumi, T., Marika, T., Katsuhika, I., Masahiko, H. and Hirano, T. (1999) Gab-family adapter proteins act downstream of cytokine and growth factor receptors and T- and B-cell antigen receptors. *Blood* **93**: 1809-1816.

Omary, M.B., Ku, N.O., Tao, G.Z., Toivola, D.M., Liao, J. (2006) "Heads and tails" of intermediate filament phosphorylation: multiple sites and functional insights. *Trends Biochem. Sci.* **31**: 383-394.

Ong, S.H., Dilworth, S., Hauck-Schmalenberger, I., Pawson, T., Kiefer, F. (2001) ShcA and Grb2 mediate polyoma middle T antigen-induced endothelial transformation and Gab1 tyrosine phosphorylation. *EMBO J.* **20**(22): 6327-36.

Paliouras, G.N., Naujokas, M.A., Park, M. (2009) Pak4, a novel Gab1 binding partner, modulates cell migration and invasion by the Met receptor. *Mol. Cell. Biol.* **29**(11): 3018-32.

Pascal, S.M., Singer, A.U., Gish, G., Yamazaki, T., Shoelson, S.E., Pawson, T., Kay, L.E., Forman-Kay, J.D. (1994) Nuclear magnetic resonance structure of an SH2 domain of phospholipase C-gamma 1 complexed with a high affinity binding peptide. *Cell* **77**(3): 461-72.

Pasini, L., Turco, M.Y., Luzi, L., Aladowicz, E., Fagiani, E., Lanfrancone, L. (2009) Melanoma: targeting signaling pathways and RaLP. *Expert Opin. Ther. Targets* **13**(1): 93-104.

Pelicci, G., Lanfrancone, L., Grignani, F., McGlade, J., Cavallo, F., Forni, G., Nicoletti, I., Pawson, T. and Pelicci, P.G. (1992) A novel transforming protein (SHC) with an SH2 domain is implicated in mitogenic signal transduction. *Cell* **70**: 93-104.

Pelicci, G., Troglio, F., Bodini, A., Melillo, R.M., Pettirossi, V., Coda, L., De Giuseppe, A., Santoro, M., Pelicci, P.G. (2002) The neuron-specific Rai (ShcC) adaptor protein inhibits apoptosis by coupling Ret to the phosphatidylinositol 3-kinase/Akt signaling pathway. *Mol. Cell. Biol.* **22**(20): 7351-63.

Pellegrini, M., Pacini, S. and Baldari, C.T. (2005) p66SHC: the apoptotic side of Shc proteins. *Apoptosis* **10**(1): 13-8.

Pieler, T. and Bellefroid, E. (1994) Perspectives on zinc finger protein function and evolution-An update. *Mol. Biol. Rep.* **20:** 1-8.

Polsky, D. and Cordon-Cardo, C. (2003) Oncogenes in melanoma. *Oncogene* **22**(20): 3087-3091.

Ponzetto, C., Bardelli, A., Zhen, Z., Maina, F., dalla Zonca, P., Giordano, S., Graziani, A., Panayotou, G. and Comoglio, P.M. (1994) A multifunctional docking site mediates signaling and transformation by the hepatocyte growth factor/scatter factor receptor family. *Cell* **77**: 261-271.

Pratt, J.C., van den Brink, M.R., Igras, V.E., Walk, S.F., Ravichandran, K.S., and Burakoff, S.J. (1999) Requirement for Shc in TCR-mediated activation of a T cell hybridoma. *J. Immunol.* **163**: 2586-2591.

Raabe, T., Olivier, J. P., Dickson, B., Liu, X., Gish, G. D., Pawson, T. and Hafen, E. (1995) Biochemical and genetic analysis of the Drk SH2/SH3 adaptor protein of Drosophila. *EMBO J.* **14**: 2509-2518.

Rameh, L.E., Arvidsson, A., Carraway, K.L. 3rd, Couvillon, A.D., Rathbun, G., Crompton, A., VanRenterghem, B., Czech, M.P., Ravichandran, K.S., Burakoff, S.J., Wang, D.S., Chen, C.S., Cantley, L.C. (1997) A comparative analysis of the phosphoinositide binding specificity of pleckstrin homology domains. *J. Biol. Chem.* **272** (35): 22059-66.

Rass, K. and Reichrath, J. (2008) UV damaging and DNA repair in malignant melanoma and nonmelanoma skin cancer. *Adv. Exp. Med. Biol*. **624**: 162-178.

Ravichandran, K.S. (2001) Signaling via Shc family adapter proteins. *Oncogene* **20**(44): 6322-30.

Ravichandran, K.S., Zhou, M.M., Pratt, J.C., Harlan, J.E., Walk, S.F., Fesik, S.W., Burakoff, S.J. (1997) Evidence for a requirement for both phospholipid and phosphotyrosine binding via the Shc phosphotyrosine-binding domain in vivo. *Mol. Cell. Biol.* **17** (9): 5540-9.

Reichardt, L. F. (2006) Neurotrophin-regulated signalling pathways, *Philos. Trans. R. Soc. Lond. B. Biol. Sci.* **361**: 1545-1564.

Relaix, F., Wei, X., Li, W., Pan, J., Lin, Y., Bowtell, D.D., Sassoon, D.A., Wu, X. (2000) Pw1/Peg3 is a potential cell death mediator and cooperates with Siah1a in p53-mediated apoptosis. *Proc. Natl. Acad. Sci. USA* **97** (5): 2105-10.

Relaix, F., Weng, X., Marazzi, G., Yang, E., Copeland, N., Jenkins, N., Spence, S. E., and Sassoon, D. (1996) Pw1, a novel zinc finger gene implicated in the myogenic and neuronal lineages. *Dev. Biol*. **177**: 383-398

Rodrigues, G.A., Falasca, M., Zhang, Z., Ong, S.H. and Schlessinger, J. (2000) A novel positive feedback loop mediated by the docking protein Gab1 and phosphatidylinositol 3-kinase in epidermal growth factor receptor signaling. *Mol. Cell. Biol.* **20**: 1448-1459.

Royal, I. and Park, M. (1995) Hepatocyte growth factor-induced scatter of Madin-Darby canine kidney cells requires phosphatidylinositol 3-kinase. *J. Biol. Chem.* **270**: 27780-27787.

Rozakis-Adcock, M., McGlade, J., Mbamalu, G., Pelicci, G., Daly, R., Li, W., Batzer, A., Thomas, S., Brugge, J., Pelicci, PG., et al. (1992) Association of the Shc and Grb2/Sem5 SH2-containing proteins is implicated in activation of the Ras pathway by tyrosine kinases. *Nature* **360**: 689-692.

Saito, Y., Hojo, Y., Tanimoto, T., Abe, J., Berk, B.C. (2002) Protein kinase C-alpha and protein kinase C-epsilon are required for Grb2-associated binder-1 tyrosine phosphorylation in response to platelet-derived growth factor. *J. Biol. Chem*. **277**(26): 23216-22.

Sakai, R., Henderson, J.T., O'Bryan, J.P., Elia, A.J., Saxton, T.M., Pawson, T. (2000) The mammalian ShcB and ShcC phosphotyrosine docking proteins function in the maturation of sensory and sympathetic neurons. *Neuron* **28**(3): 819-33.

Sampaio, C., Dance, M., Montagner, A., Edouard, T., Malet, N., Perret, B., Yart, A., Salles, J. P. and Raynal, P. (2007) Signal strength dictates PI3K contribution to Ras/ERK1-2 activation via differential Gab1/Shp2 recruitment: consequences for resistance to EGFR inhibition. *Mol. Cell. Biol.* **285**: 587-600.

Sasaoka, T., Rose, D.W., Jhun, B.H., Saltiel, A.R., Draznin, B., Olefsky, J.M. (1994) Evidence for a functional role of Shc proteins in mitogenic signaling induced by insulin, insulin-like growth factor-1, and epidermal growth factor. *J. Biol. Chem.* **269**: 13689-13694.

Saxton, T.M., Cheng, A.M., Ong, S.H., Lu, Y., Sakai, R., Cross, J.C. and Pawson, T. (2001) Gene dosage-dependent functions for phosphotyrosine-Grb2 signaling during mammalian tissue morphogenesis. *Curr. Biol.* **11**: 662-670.

Schaeper, U., Gehring, N.H., Fuchs, K.P., Sachs, M., Kempkes, B. and Birchmeier, W. (2000) Coupling of Gab1 to c-Met, Grb2, and Shp2 mediates biological responses. *J. Cell. Biol.* **149**: 1419-1432.

Schaeper, U., Vogel, R., Chmielowiec, J., Huelsken, J., Rosario, M., Birchmeier, W. (2007) Distinct requirements for Gab1 in Met and EGF receptor signaling in vivo. *Proc. Natl. Acad. Sci. USA* **104**(39): 15376-81.

Schlessinger, J. (2000) Cell signaling by receptor tyrosine kinases. *Cell* **103**: 211-225.

Schlessinger, J. (2004) Common and distinct elements in cellular signaling via EGF and FGF receptors. *Science* **306**: 1506-1507.

Schlessinger, J. and Lemmon, M.A. (2003) SH2 and PTB domains in tyrosine kinase signalling. *Sci. STKE* (191): RE12.

Simpson, L. and Parsons, R. (2001) PTEN: life as a tumor suppressor. *Exp. Cell. Res.* **264**: 29-41.

Skolnik, E.Y., Margolis, B., Mohammadi, M., Lowenstein, E., Fischer, R., Drepps, A., Ullrich, A., Schlessinger, J. (1991) Cloning of PI3 kinase-associated p85 utilizing a novel method for expression/cloning of target proteins for receptor tyrosine kinases. *Cell* **65**: 83-90.

Smith, M. J., Hardy, W. R., Murphy, J. M., Jones, N. and Pawson, T. (2006) Screening for PTB domain binding partners and ligand specificity using proteome-derived NPXY peptide arrays. *Mol. Cell. Biol.* **26**: 8461-8474.

Songyang, Z., Shoelson, S.E., McGlade, J., Olivier, P., Pawson, T., Bustelo, X.R., Barbacid, M., Sabe, H., Hanafusa, H. and Yi, T. (1994) Specific motifs recognized by the SH2 domains of Csk, 3BP2, fps/fes, GRB-2, HCP, SHC, Syk, and Vav. *Mol. Cell. Biol.* **14**: 2777-2785.

Stahl, J.M., Sharma, A., Cheung, M., et al. (2004) Deregulated Akt3 activity promotes development of malignant melanoma. *Cancer Res.* **64**: 7002-7010.

Stambolic, V., Suzuki, A., de la Pompa, J.L., Brothers, G.M., Mirtsos, C., Sasaki, T., Ruland, J., Penninger, J.M., Siderovski, D.P., Mak, T.W. (1998) Negative regulation of PKB/Akt-dependent cell survival by the tumour suppressor PTEN. *Cell* **95**: 29-39.

Takahashi-Tezuka, M., Yoshida, Y., Fukada, T., Ohtani, T., Yamanaka, Y., Nishida, K., Nakajima, K., Hibi, M and Hirano, T. (1998) Gab1 Acts as an Adapter Molecule Linking the Cytokine Receptor gp130 to ERK Mitogen-Activated Protein Kinase. *Mol. Cell. Biol.* **18**: 4109-17.

Tawbi, H.A. and Kirkwood, J.M. (2007) Management of metastatic melanoma. *Semin. Oncol.* **34**(6): 532-545.

Turco, M.Y., Furia, L., Dietze, A., Fernandez Diaz, L., Ronzoni, S., Sciullo, A., Simeone, A., Constam, D., Faretta, M., Lanfrancone, L. (2012) Cellular Heterogeneity During Embryonic Stem Cell Differentiation to Epiblast Stem Cells Is Revealed by the ShcD/RaLP Adaptor Protein. *Stem Cells* **30**(11): 2423-36

Trinei, M., Giorgio, M., Cicalese, A., Barozzi, S., Ventura, A., Migliaccio, E., Milia, E., Padura, I.M., Raker, V.A., Maccarana, M., Petronilli, V., Minucci, S., Bernardi, P., Lanfrancone, L., Pelicci, P.G. (2002) A p53-p66Shc signalling pathway controls intracellular redox status, level of oxidation-damaged DNA and oxidative stress-induced apoptosis. *Oncogene* **21**(24): 3872-8.

Troglio, F., Echart, C., Gobbi, A., Pawson, T., Pelicci, P.G., De Simoni, M.G., Pelicci, G. (2004) The Rai (Shc C) adaptor protein regulates the neuronal stress response and protects against cerebral ischemia. *Proc. Natl. Acad. Sci. USA* **101**(43): 15476-81.

Ursini-Siegel, J. and Muller, W.J. (2008) The ShcA adaptor protein is a critical regulator of breast cancer progression. *Cell Cycle* **7**(13): 1936-43.

Van der Geer, P., Wiley, S., Gish, G.D. and Pawson, T. (1996) The Shc adaptor protein is highly phosphorylated at conserved, twin tyrosine residues (Y239/240) that mediate protein-protein interactions. *Curr. Biol.* **6**: 1435-1444.

Velazquez, L., Gish, G.D., van Der Geer, P., Taylor, L., Shulman, J. and Pawson, T. (2000) The shc adaptor protein forms interdependent phosphotyrosine-mediated protein complexes in mast cells stimulated with interleukin 3. *Blood* **96**: 132-138.

Walk, S.F., March, M.E. and Ravichandran, K.S. (1998) Roles of Lck, Syk and ZAP-70 tyrosine kinases in TCR-mediated phosphorylation of the adapter protein Shc. *Eur. J. Immunol.* **28**: 2265-2275.

Way, J.C. and Chalfie, M. (1988) Mec-3, a homeobox-containing gene that specifies differentiation of the touch receptor neurons in C. elegans. *Cell* **54**: 5-16.

Weidner, K.M., Di Cesare, S., Sachs, M., Brinkmann, V., Behrens, J. and Birchmeier, W. (1996) Interaction between Gab1 and the c-Met receptor tyrosine kinase is responsible for epithelial morphogenesis. *Nature* **384**: 173-176.

Weisner, S., Legate, K.R. and Fässler, R. (2005) Integrin-actin interactions. *Cell. Mol. Life Sci.* **62**: 1081-1099.

Wells, C. M., Abo, A. and Ridley, A. J. (2002) PAK4 is activated via PI3K in HGF-stimulated epithelial cells. *J. Cell Sci.* **115:** 3947-3956.

Weng, Z., Thomas, S.M., Rickles, R.J., Taylor, J.A., Brauer, A.W., Seidel-Dugan, C., Michael, W.M., Dreyfuss, G., and Brugge, J.S. (1994) Identification of Src, Fyn, and Lyn SH3-binding proteins: implications for a function of SH3 domains. *Mol. Cell. Biol.* **14**: 4509-4521.

White, M. F., Livingston, J. N., Backer, J. M., Lauris, V., Dull, T. J., Ullrich, A., Kahn, C. R. (1988) Mutation of the insulin receptor at tyrosine 960 inhibits signal transmission but does not affect its tyrosine kinase activity. *Cell* **54**: 641-649.

Wills, M.K. and Jones, N. (2012) Teaching an old dogma new tricks: twenty years of Shc adaptor signalling. *Biochem. J.* **447**(1): 1-16.

Wolf, I., Jenkins, B., Liu, Y., Seiffert, M., Custodio, J.M., Young, D. and Rohrschneider, L. (2002) Gab3, a new DOS/Gab family member, facilitates macrophage differentiation. *Mol. Cell. Biol.* **22**: 231-244.

Wu, H., Goel, V., Haluska, F.G. (2003) PTEN signalling pathways in melanoma. *Oncogene* **22**: 3113-3122.

Wulf, G., Finn, G., Suizu, F. and Lu, K.P. (2005) Phosphorylation specific prolyl isomerization: Is there an underlying theme? *Nat. Cell. Biol.* **7**: 435-441.

Yaden, B.C., Savage, J.J., Hunter, C.S. and Rhodes, S.J. (2005) DNA recognition properties of the LHX3b LIM homeodomain transcription factor. *Mol. Biol. Rep*. **32**: 1-6.

Yamaguchi, A., Taniguchi, M., Hori, O., Ogawa, S., Tojo, N., Matsuoka, N., Miyake, S., Kasai, K., Sugimoto, H., Tamatani, M., Yamashita, T., and Tohyama, M. (2002) Peg3/Pw1 is involved in p53-mediated cell death pathway in brain ischemia/hypoxia. *J. Biol. Chem.* **277**: 623-629.

Yoon, S. and Seger, R. (2006) The extracellular signal-regulated kinase: multiple substrates regulate diverse cellular functions. *Growth Factors* **24**(1): 21-44.

You, Y., Li, W., Gong, Y., Yin, B., Qiang, B., Yuan, J., Peng, X. (2010) ShcD interacts with TrkB via its PTB and SH2 domains and regulates BDNF-induced MAPK activation. *BMB Rep.* **43**(7): 485-90.

Zhou, M. M., Huang, B., Olejniczak, E. T., Meadows, R. P., Shuker, S. B., Miyazaki, M., Trub, T., Shoelson, S. E., Fesik, S. W. (1996) Structural basis for IL-4 receptor phosphopeptide recognition by the IRS-1 PTB domain. *Nat. Struct. Biol.* **3**: 388-393.

Zhu, Q.S., Rosenblatt, K., Huang, K.L., Lahat, G., Brobey, R., Bolshakov, S., Nguyen, T., Ding, Z., Belousov, R., Bill, K., et al. (2011) Vimentin is a novel AKT1 target mediating motility and invasion. *Oncogene* **30**: 457-470.

Appendix

Results

A. BLAST analysis of nucleotide sequence from Clones 8 and 28 isolated from library screen

> ref|NM_008163.3| Mus musculus growth factor receptor bound protein 2 (Grb2), mRNA Length=2624

GENE ID: 14784 Grb2 | growth factor receptor bound protein 2 [Mus musculus] (Over 100 PubMed links)

Score = 876 bits (474), Expect = 0.0
Identities = 476/477 (99%), Gaps = 0/477 (0%)
Strand=Plus/Plus

```
Query  12   ACATCCTTAAGGTTTTGAATGAAGAATGTGACCAGAACTGGTATAAGGCAGAACTCAATG  71
            ||||||||||||||||||||||||||||||||||||||||||||||||||||||||||||
Sbjct  399  ACATCCTTAAGGTTTTGAATGAAGAATGTGACCAGAACTGGTATAAGGCAGAACTCAATG  458

Query  72   GGAAAGATGGCTTCATCCCCAAGAATTACATAGAAATGAAACCACATCCGTGGTTTTTTG  131
            ||||||||||||||||||||||||||||||||||||||||||||||||||||||||||||
Sbjct  459  GGAAAGATGGCTTCATCCCCAAGAATTACATAGAAATGAAACCACATCCGTGGTTTTTTG  518

Query  132  GCAAAATCCCCAGAGCCAAGGCAGAAGAAATGCTCAGCAAACAGCGGCATGACGGGGCCT  191
            ||||||||||||||||||||||||||||||||||||||||||||||||||||||||||||
Sbjct  519  GCAAAATCCCCAGAGCCAAGGCAGAAGAAATGCTCAGCAAACAGCGGCATGACGGGGCCT  578

Query  192  TCCTGATCCGAGAGAGCGAGAGCGCTCCTGGGGACTTCTCCCTGTCCGTCAAGTTTGGAA  251
            ||||||||||||||||||||||||||||||||||||||||||||||||||||||||||||
Sbjct  579  TCCTGATCCGAGAGAGCGAGAGCGCTCCTGGGGACTTCTCCCTGTCCGTCAAGTTTGGAA  638

Query  252  ATGATGTGCAGCACTTCAAGGTGCTCCGCGACGGAGCCGGGAAGTATTTCCTGTGGGTGG  311
            ||||||||||||||||||||||||||||||||||||||||||||||||||||||||||||
Sbjct  639  ATGATGTGCAGCACTTCAAGGTGCTCCGCGACGGAGCCGGGAAGTATTTCCTGTGGGTGG  698

Query  312  TGAAGTTTAATTCTTTGAATGAGCTGGTGGATTACCACAGATCAACATCCGTGTCCAGGA  371
            |||||||||||||||||||||||||| ||||||||||||||||||||||||||||||||
Sbjct  699  TGAAGTTTAATTCTTTGAATGAGCTGGTAGATTACCACAGATCAACATCCGTGTCCAGGA  758

Query  372  ACCAGCAGATATTCTTACGGGACATAGAACAGATGCCACAGCAGCCAACCTACGTCCAGG  431
            ||||||||||||||||||||||||||||||||||||||||||||||||||||||||||||
Sbjct  759  ACCAGCAGATATTCTTACGGGACATAGAACAGATGCCACAGCAGCCAACCTACGTCCAGG  818

Query  432  CGCTCTTTGACTTTGACCCCCAGGAGGATGGCGAGCTGGGCTTTCGCAGAGGAGACT  488
            ||||||||||||||||||||||||||||||||||||||||||||||||||||||||||
Sbjct  819  CGCTCTTTGACTTTGACCCCCAGGAGGATGGCGAGCTGGGCTTTCGCAGAGGAGACT  875
```

B. Protein sequence of Grb2 translated using ExPASy Translate Tool

YDFKATADDELSFKRGD**ILKVLNEECDQNWYKAELNGKDGFIPKNYIEM KPHPWFFGKIPRAKAEEMLSKQRHDGAFLIRESESAPGDFSLSVKFGNDV QHFKVLRDGAGKYFLWVVKFNSLNELVDYHRSTSVSRNQQIFLRDIEQM PQQPTYVQALFDFDPQEDGELGFRRGD**FIHVMDNSDPNW

Figure A1. BLAST analysis of Clones 8 and 28 revealed that they encode Grb2 protein. A, BLAST analysis of nucleotide sequence from clones 8 and 28. B, Protein sequence of Grb2 translated using ExPASy Translate Tool. Matched protein sequences are shown in bold red.

A. BLAST analysis of nucleotide sequence from Clone 48 isolated from library screen

> ref|NM_010433.2| Mus musculus homeodomain interacting protein kinase 2 (Hipk2), transcript variant 2, mRNA Length=4259

GENE ID: 15258 Hipk2 | homeodomain interacting protein kinase 2 [Mus musculus]
(Over 10 PubMed links)

Score = 599 bits (324), Expect = 3e-168
Identities = 329/331 (99%), Gaps = 2/331 (0%)
Strand=Plus/Plus

```
Query  11    AATGTCTCCACCTGTGAGGTGACCTCTTCACAGGCTATCAGCTCCCCTCAGCGATCCAAG  70
             ||||||||||||||||||||||||||||||||||||||||||||||||||||||||||||
Sbjct  2810  AATGTCTCCACCTGTGAGGTGACCTCTTCACAGGCTATCAGCTCCCCTCAGCGATCCAAG  2869

Query  71    CGTGTCAAGGAGAACACTCCCCCACGGTGCGCCATGGTACACAGCAGCCCAGCTTGCAGC  130
             ||||||||||||||||||||||||||||||||||||||||||||||||||||||||||||
Sbjct  2870  CGTGTCAAGGAGAACACTCCCCCACGGTGCGCCATGGTACACAGCAGCCCAGCTTGCAGC  2929

Query  131   ACCTCAGTCACCTGTGGGTGGGGCGACGTGGCCTCCAGCACCACCCGGGAGCGACAGCGG  190
             ||||||||||||||||||||||||||||||||||||||||||||||||||||||||||||
Sbjct  2930  ACCTCAGTCACCTGTGGGTGGGGCGACGTGGCCTCCAGCACCACCCGGGAGCGACAGCGG  2989

Query  191   CAGACGATTGTCATCCCCGACACCCCGAGCCCCACAGTCAGTGTCATCACCATCAGCAGT  250
             ||||||||||||||||||||||||||||||||||||||||||||||||||||||||||||
Sbjct  2990  CAGACGATTGTCATCCCCGACACCCCGAGCCCCACAGTCAGTGTCATCACCATCAGCAGT  3049

Query  251   GACACCGATGAAGAAGAGGAGCAGAAGCACGCCCC-ACCAGCACAGTCTCCAAGCAAAGa  309
             |||||||||||||||||||||||||||||||||| |||||||||||||||||||||||||
Sbjct  3050  GACACCGATGAAGAAGAGGAGCAGAAGCACGCCCCCACCAGCACAGTCTCCAAGCAAAGA  3109

Query  310   aaaaaaTGTCATCAGCTGTGTCACCGTCCAC  340
             ||||| ||||||||||||||||||||||||
Sbjct  3110  AAAAA-TGTCATCAGCTGTGTCACCGTCCAC  3139
```

B. Protein sequence of Hipk2 translated using ExPASy Translate Tool

HVMRQQPTSTTSSRKSKQHQSSVR**NVSTCEVTSSQAISSPQRSKRVKENTPP RCAMVHSSPACSTSVTCGWGDVASSTTRERQRQTIVIPDTPSPTVSVITISS DTDEEEEQKHAPTSTVSKQRKNVISCVTVH**DSPYSDSSSNTSPYSVQQRT

Figure A2. BLAST analysis of Clone 48 revealed that it encodes Hipk2 protein. A, BLAST analysis of nucleotide sequence from clone 48. B, Protein sequence of Hipk2 translated using ExPASy Translate Tool. Matched protein sequences are shown in bold red.

A. BLAST analysis of nucleotide sequence from Clone 50 isolated from library screen

> ref|NM_173443.2| Mus musculus valosin containing protein (p97)/p47 complex interacting protein 1 (Vcpip1), mRNA

gb|BC059209.1| Mus musculus valosin containing protein (p97)/p47 complex interacting protein 1, mRNA (cDNA clone MGC:66512 IMAGE:6406239), complete cds
Length=5192

GENE ID: 70675 Vcpip1 | valosin containing protein (p97)/p47 complex interacting protein 1 [Mus musculus] (Over 10 PubMed links)

Score = 909 bits (492), Expect = 0.0
Identities = 492/492 (100%), Gaps = 0/492 (0%)
Strand=Plus/Plus

```
Query  14    GCCCACACTGTGAAACAAGAAGAGATTGCTGTTACTGGTAAACTGTCATCTAAGGAACTT  73
             ||||||||||||||||||||||||||||||||||||||||||||||||||||||||||||
Sbjct  2819  GCCCACACTGTGAAACAAGAAGAGATTGCTGTTACTGGTAAACTGTCATCTAAGGAACTT  2878

Query  74    CAGGAGCAAGCTGACAAAGAAATGTACTCCTTGTGTCTTTTAGCTACATTAATGGGAGAA  133
             ||||||||||||||||||||||||||||||||||||||||||||||||||||||||||||
Sbjct  2879  CAGGAGCAAGCTGACAAAGAAATGTACTCCTTGTGTCTTTTAGCTACATTAATGGGAGAA  2938

Query  134   GACGTGTGGTCTTATGCAAAGGGACTTCCTCACATGTTCCAGCAGGGTGGTGTATTCTAC  193
             ||||||||||||||||||||||||||||||||||||||||||||||||||||||||||||
Sbjct  2939  GACGTGTGGTCTTATGCAAAGGGACTTCCTCACATGTTCCAGCAGGGTGGTGTATTCTAC  2998

Query  194   AATATTATGAAGAAAACTATGGGCATGGCTGATGGCAAACATTGTACTTTTCCACATCTA  253
             ||||||||||||||||||||||||||||||||||||||||||||||||||||||||||||
Sbjct  2999  AATATTATGAAGAAAACTATGGGCATGGCTGATGGCAAACATTGTACTTTTCCACATCTA  3058

Query  254   CCTGGCAAAACCTTTGTTTATAATGCTTCTGAAGATAGACTGGAGTTGTGTGTCGATGCT  313
             ||||||||||||||||||||||||||||||||||||||||||||||||||||||||||||
Sbjct  3059  CCTGGCAAAACCTTTGTTTATAATGCTTCTGAAGATAGACTGGAGTTGTGTGTCGATGCT  3118

Query  314   GCAGGACATTTCCCCATTGGTCCTGATGTTGAAGATTTAGTTAAAGAGGCTGTAAGTCAG  373
             ||||||||||||||||||||||||||||||||||||||||||||||||||||||||||||
Sbjct  3119  GCAGGACATTTCCCCATTGGTCCTGATGTTGAAGATTTAGTTAAAGAGGCTGTAAGTCAG  3178

Query  374   GTGCGAGCAGAGGCTACTACAAGAAGTAGGGAATCAAGCCCTTCACATGGGTTATTAAAA  433
             ||||||||||||||||||||||||||||||||||||||||||||||||||||||||||||
Sbjct  3179  GTGCGAGCAGAGGCTACTACAAGAAGTAGGGAATCAAGCCCTTCACATGGGTTATTAAAA  3238

Query  434   CTAGGTAGTGGTGGAGTAGTGAAAAAGAAATCTGAGCAACTTCACAATGTAACTGCCTTT  493
             ||||||||||||||||||||||||||||||||||||||||||||||||||||||||||||
Sbjct  3239  CTAGGTAGTGGTGGAGTAGTGAAAAAGAAATCTGAGCAACTTCACAATGTAACTGCCTTT  3298

Query  494   CAGGGGAAGGGC  505
             ||||||||||||
Sbjct  3299  CAGGGGAAGGGC  3310
```

B. Protein sequence of Vcip135 translated using ExPASy Translate Tool

EKEPVPLQHGDRITIEILKGRAEGGPSTAAHS**AHTVKQEEIAVTGKLSSKELQEQAD KEMYSLCLLATLMGEDVWSYAKGLPHMFQQGGVFYNIMKKTMGMADGKHC TFPHLPGKTFVYNASEDRLELCVDAAGHFPIGPDVEDLVKEAVSQVRAEATTRS RESSPSHGLLKLGSGGVVKKKSEQLHNVTAFQGKG**HSLGTASSHPHIDPRARETL AVRKHNTGTDFSNS

Figure A3. BLAST analysis of Clone 50 revealed that it encodes Vcip135 protein. A, BLAST analysis of nucleotide sequence from clone 50. B, Protein sequence of Vcip135 translated using ExPASy Translate Tool. Matched protein sequences are shown in bold red.